ASSESSING THE COLLAPSE RISK OF CALIFORNIA'S EXISTING REINFORCED CONCRETE FRAME STRUCTURES: METRICS FOR SEISMIC SAFETY DECISIONS

A DISSERTATION
SUBMITTED TO THE DEPARTMENT OF
CIVIL AND ENVIRONMENTAL ENGINEERING
AND THE COMMITTEE ON GRADUATE STUDIES
OF STANFORD UNIVERSITY
IN PARTIAL FULFILLMENT OF THE REQUIREMENTS
FOR THE DEGREE OF
DOCTOR OF PHILOSOPHY

Abbie B. Liel
June, 2008

Abstract

The emerging field of performance-based earthquake engineering enables the evaluation of seismic performance of building structures. In this study, performance-based earthquake engineering tools are applied to a potential seismic safety problem: older non-ductile reinforced concrete frame structures. Because these buildings were constructed before significant advancements in building code provisions for reinforced concrete were instituted in the mid-1970s, they may be vulnerable to earthquake-induced collapse, posing a threat to public safety in future earthquakes. Assessment of collapse risk for non-ductile reinforced frame structures is examined here to quantify differences in safety between existing and modern structures and to investigate the effectiveness of mitigation strategies, providing much-needed data for the ongoing discussion of seismic safety in California.

A central component of this work involves assessing collapse risk of non-ductile reinforced concrete frame structures through dynamic analysis of nonlinear simulation models. Collapse performance assessments are conducted for a group of structures, varying in height, framing system and other design and detailing characteristics, which represents older reinforced concrete frame structures of the type constructed in California between 1950 and 1975. Nonlinear analysis models are constructed that are capable of capturing the effects of critical design and detailing features on structural behavior. Important aspects of the assessment procedure – such as propagation of sources of uncertainty, incorporation of non-simulated failure modes, and adjustments for appropriate spectral shape of input ground motions – are treated systematically such that collapse assessment results for different structures and structural systems can be compared. These evaluations are used to discover trends in performance associated with design variability in non-ductile reinforced concrete frame structures and to show how much more likely these structures are to collapse than their modern, code-conforming counterparts. Assessments of collapse performance provide one possible metric of life safety of building structures.

Structural modeling uncertainties, including those associated with component strength, stiffness, deformation capacity and cyclic deterioration, are incorporated in structural

performance predictions. The effect of modeling uncertainties was investigated by conducting sensitivity analyses to probe the relationship between model random variables and structural response, and then fitting a response surface to sensitivity analysis results. The response surface is a functional relationship between the input random variables and the limit state criterion for structural response, such as collapse capacity of the structure. Monte Carlo simulation, together with the response surface prediction of structural response, is used to propagate modeling uncertainties through the structural performance assessment. These uncertainties may have a significant impact on the structural performance predictions, particularly in cases where the underlying model random variables are characterized by large dispersion (high coefficient of variation) or where structural response is very nonlinear.

Even when they do not collapse, non-ductile reinforced concrete frame structures may also incur significant damage in future earthquakes, forcing building owners to invest in costly repairs. The cost of repairing earthquake damage is assessed, using data from previous researchers relating structural response to damage in non-structural and structural components and the cost of related repairs. These losses are shown to be more significant for owners of non-ductile reinforced concrete frame structures than those of newer code-conforming structures. The collapse assessments are also extended to provide estimations of earthquake-related fatalities in existing and modern reinforced concrete frame structures.

These metrics of earthquake-induced collapse, losses and fatalities are used to evaluate the effectiveness of replacement and retrofit strategies for mitigating hazards posed by non-ductile reinforced concrete frame structures. The effectiveness of policies for seismic strengthening is measured in terms of costs and benefits, where the benefits include reduced economic losses and fatalities. The cost-benefit assessment is used to develop recommendations to enhance the efficiency and equity of policies for seismic safety in California.

Acknowledgments

My studies and research at Stanford have been primarily funded by a National Science Foundation Graduate Research Fellowship and a Stanford Graduate Fellowship. Additional support was provided by the Applied Technology Council (through funding from FEMA), the Pacific Earthquake Engineering Research Center and the East Asia and Pacific Summer Institutes (through the Japan Society for the Promotion of Science and the National Science Foundation). This support is greatly appreciated.

A number of individuals have contributed significantly to the research described in this dissertation. Most importantly, I would like to thank my advisor, Professor Greg Deierlein, for sharing with me his insights into and enthusiasm for structural engineering. I am continually inspired by his commitment to his research and his students. I am very fortunate to have spent my time at Stanford as his student.

I would also like to thank Professors Eduardo Miranda, Helmut Krawinkler, and Jack Baker, for their thoughtful comments on my research, models and results during my time at Stanford. I am grateful for the opportunity to work closely with former and current Blume Center students, especially Curt Haselton and Marc Ramirez. This research has benefited significantly from our collaboration. Additionally, master's students, Steve Cranford and Brian Dean, and undergraduate research interns, Sarah Taylor Lange, Ashley Spear and Jackie Steiner, contributed to parts of the research. I am very appreciative of their contributions, and enjoyed working with each of them. I also thank administrative associates Racquel Hagen and Kim Vonner for their support to Blume Center students. The atmosphere of collegiality and friendship at the Blume Center is a delight to work in.

I have had the opportunity to work closely with a number of people outside Stanford. Charlie Kircher, Technical Director of the ATC-63 Project, was a frequent visitor to Stanford, and his suggestions have been very helpful in the development of this work. Other members of the ATC-63 Project Management Committee, particularly Bob Hanson and Jon Heintz, served as a valuable sounding board for research developments. I have also benefited from discussions with Peter May and Mary Comerio on aspects of seismic safety policy,

Judith Mitrani-Reiser, who graciously provided her MDLA toolbox for use in quantifying economic losses, and Christine Goulet, who conducted the necessary probabilistic seismic hazard analysis. Evan Reis, Joe Maffei, John Hooper, John Harris and Bill Holmes are always willing to provide feedback from the practitioner perspective. Professor Toshimi Kabeyasawa was a gracious host during my summer in Japan.

Above all, I would like to thank my parents, Meghan, Rose, Jackson, and my dear friends, who have supported and loved me throughout.

Contents

List of Tables

List of Figures

Chapter 1

Introduction

1.1 Applications of Performance-Based Earthquake Engineering

Performance-based earthquake engineering methods for evaluating the seismic performance of building and bridge structures have emerged in the past decade or so, through the combined efforts of earthquake engineering researchers and practitioners. The Pacific Earthquake Engineering Research (PEER) Center has developed a framework for performance-based earthquake engineering, which relies on integrating models and knowledge from seismology, structural engineering, and the social sciences to obtain probabilistic predictions of seismic hazard, structural response, damage, economic losses, and casualties (e.g. Deierlein (2004), Krawinkler and Miranda (2004)). Recent research has improved the data and technology related to each component of this methodology, including ground motion attenuation relationships (e.g. Abrahamson and Silva (2008), Boore and Atkinson (2007), Campbell and Bozorgnia (2006)) and selection of ground motion intensity measures (e.g. Baker and Cornell (2005), Tothong and Cornell (2006)), nonlinear simulation models (e.g. Lowes and Altoontash (2003), Elwood (2004), Sezen and Moehle (2002), Ibarra et al. (2005), Haselton et al. (2007)), analytical capabilities (e.g. PEER (2006)) and analysis techniques (e.g. Vamvatsikos and Cornell (2002)), fragility functions relating seismic demands on structures to damage and repair costs (e.g. Porter et al. (2002), Comerio and Stallmeyer (2003), Aslani (2005), Mitrani-Reiser (2007)), and descriptions of the uncertainty inherent in these models (e.g. Porter et al. (2002), Baker and Cornell (2007), Haselton and Deierlein (2007). May (2001; 2002; 2004), Comerio (1992; 2006) and others have explored organizational considerations for implementing performance-based regulations and the economic and societal implications of seismic performance. The upshot of these efforts is that it is now possible to quantify the seismic performance of new and existing structures in a more rigorous manner than had previously been possible.

Performance-based earthquake engineering provides a wealth of information for decisions about seismic performance. In the design of new buildings, these tools allow engineers and owners to assess the differences in seismic performance associated with the choice of alternative structural designs. These assessments may justify improvements on code-minimum design or employment of innovative structural systems that reduce building owners' susceptibility to losses or business interruption in future earthquakes. For older existing buildings, these techniques can be used to identify structures that pose a considerable threat to the life safety of their occupants, to develop designs for seismic retrofit, or to assess the costs and benefits associated with various seismic upgrading options. In short, performance-based earthquake engineering provides a framework through which owners and other government or institutional decision makers can explicitly manage seismic risk, using quantifiable, probabilistic metrics. These tools are especially useful in addressing the difficult question of which older structures pose a significant life safety hazard, necessitating mitigation.

1.2 Motivation and Objectives

Non-ductile reinforced concrete (RC) frame structures constructed in California prior to about 1975 lack important features of good seismic design and detailing. Design deficiencies such as widely spaced shear reinforcement, weak columns, inadequate confinement of columns and joints, and short lap-splices, etc., may lead to poor seismic performance. Motivated by a few high-profile failures of newly constructed RC structures in California's 1971 San Fernando Earthquake, modifications to building code provisions making ductile detailing for RC frame structures compulsory were adopted throughout California by the mid- to late 1970s.

It is widely acknowledged that some of California's estimated 40,000 non-ductile RC structures are at significant risk of earthquake-induced collapse, endangering life safety due to their deficient design (e.g. ATC (2003), Kircher et al. (2006)). This viewpoint was expressed in a recent article in the *Los Angeles Times*, which quoted an expert who asserted, "It's well recognized within the engineering professional community that many California non-ductile buildings are *at unacceptable risk of collapse* in moderately strong shaking" (Bernstein 2005) [Emphasis added]. Yet, it is equally clear that other non-ductile RC frame structures do not represent a serious public safety threat, because their design or construction

quality is above average, or because they are located in parts of the state where severe ground shaking is less likely. Building owners and businesses, who are worried about costs associated with seismic upgrading, "have long fought efforts to require retrofits, arguing *the risk is overstated"* (Bernstein 2005) [Emphasis added]. As a result of the large number of structures involved, and the substantial variation in structural design, maintenance, site conditions and seismic hazard throughout the state, state and local government have been unable to systematically mitigate the potential collapse hazard of non-ductile RC frame structures.

The central objective of this research is to apply the framework and technologies of performance-based earthquake engineering to assess what is potentially one of the most pressing seismic safety concerns in California, existing non-ductile RC frame structures. Performance-based collapse analysis of non-ductile RC frame structures is used to predict earthquake-induced collapse, fatalities and economic losses, which are critical measures for evaluating the safety of existing non-ductile structures, for identifying particularly hazardous structures and for assessing the effectiveness of mitigation through seismic retrofit or replacement. In particular, this study examines relative differences in collapse safety between older, 1960s-era non-ductile RC buildings and modern ductile RC frame buildings, by comparing their assessed seismic collapse risk at a typical high seismic site in southern California. The variability in seismic performance of California's existing non-ductile RC frame structures is investigated by assessing the collapse safety of a group of representative structures varying in height and other design characteristics. To evaluate differences in life safety, this study also obtains predictions of seismic fatality rates and economic losses in non-ductile RC frame structures, again in comparison to the performance predicted for ductile RC frame structures. Estimates of economic losses associated with repairing seismic damage quantify the economic costs of existing non-ductile RC buildings in the building stock. Data on collapse risk, fatality rates and economic losses can be used to assess the impact of strengthening or replacing vulnerable RC buildings.

1.3 Scope and Organization

This dissertation deals with the evaluation of the seismic collapse risk of non-ductile RC frame structures and examines the implications of this assessment, in terms of casualties and economic losses, for investigating the effectiveness of mitigation strategies such as retrofit or

replacement. A set of 26 characteristic structures is selected to be representative of office building RC construction California in the late 1960s, ranging in height from 2 to 12 stories and consisting of both space and perimeter framing systems. Seismic collapse risk of these structures is assessed using nonlinear simulation models subjected to incremental dynamic analyses. The analysis models are developed in the OpenSees software platform and are capable of simulating structural behavior under seismic shaking up to the onset of structural collapse. Collapse performance assessments are probabilistic, accounting for uncertainties in ground motions and structural modeling. Structural response predictions are used for predicting economic losses (costs associated with repairing seismic damage) and fatalities in non-ductile RC buildings. To quantify relative differences in safety, seismic performance predictions for the older non-ductile structures are compared to a set of modern code-conforming special moment frame structures, also ranging in height from 2 to 12 stories. Cost-benefit assessment is used to evaluate options for mitigating the seismic risks associated with non-ductile RC frame structures.

Chapter 2 identifies key characteristics of RC frame structures constructed in California between 1950 and 1975. Important parameters include structural geometry, engineering detailing, and occupancy that were representative of construction during that period. It is presumed that all structures met the requirements of the governing building code at the time of their design, but there is significant variation associated with size, function and design. Chapter 2 also reports examples of collapses or partial collapses observed in RC frame structures in past California earthquakes to illustrate their seismic vulnerabilities and motivate examination of their seismic performance. Policy options for mitigating the risks posed by non-ductile RC structures are introduced by exploring lessons learned in previous attempts to legislate improvement of existing buildings for seismic safety.

Chapter 3 provides an overview of the collapse assessment procedure including ground motion selection, nonlinear modeling and incremental dynamic analysis procedures. The focus of the chapter is on aspects of collapse assessment that relate particularly to non-ductile RC frame structures, including calibration of inelastic material/element models, appropriate treatment of spectral shape, and methods for incorporating failure modes that cannot be directly simulated. Results are compared to a codified first-generation performance-based earthquake engineering procedure, the ASCE/SEI 41 Standard for *Seismic Rehabilitation of Existing Buildings*.

Chapter 4 investigates a critical component of the probabilistic collapse assessment procedure: the treatment of uncertainties in structural modeling. Variability in modeling parameters associated with material, loading and system behavior may have a significant effect on the predicted collapse behavior of the structure. Chapter 4 proposes a method using response surface analysis and Monte Carlo simulation to quantify the effects of modeling uncertainties on predictions of structural performance, and demonstrates its application to both ductile and non-ductile RC frame structures. These results are compared to other approaches, and a generalized simplified procedure is presented.

The collapse assessment procedure is applied to a group of non-ductile RC frame structures in **Chapter 5**. A set of 26 archetypical frames is investigated, chosen to be representative of structures constructed between 1950 and 1975 in California. These structures vary in height (2 to 12 stories) and framing system (space and perimeter frames) and are designed to meet all the requirements of the 1967 Uniform Building Code. The outcome of the assessment process is a family of performance metrics associated with the collapse safety of these structures, which are used to quantify risks for different types of structures and to compare the collapse safety of older non-ductile and new code-conforming RC buildings.

Chapter 6 extends predictions of earthquake-induced collapse to assess economic losses and fatalities in non-ductile RC frame structures in future earthquakes. Economic losses are seismic repair costs incurred by building owners. Estimations of earthquake-related casualties provide an explicit measure of the life safety threat posed by non-ductile RC frame structures. The impact of four decades of changes to building code provisions are examined by comparing losses and fatalities predicted for non-ductile and ductile RC frame structures.

Chapter 7 explores the costs and benefits of retrofitting or replacing potentially vulnerable structures for the purpose of mitigating seismic collapse risk. The benefits of seismic strengthening of non-ductile RC frame structures include reduced fatalities and economic losses, but the costs of retrofit or replacement can be substantial. This assessment is used to investigate the implications of seismic safety policy decisions for California's existing non-ductile concrete building stock. Various policy options, including maintaining the status quo and mandatory and voluntary retrofit or replacement policies, are compared in terms of their potential to reduce the likelihood of collapse and potential fatalities.

Finally, **Chapter 8** summarizes the important contributions and findings of this research. These findings include metrics of seismic performance (in terms of collapse risk, economic

losses and fatality rate) for a set of 26 typical existing non-ductile RC frame structures ranging from 2 to 12 stories and including space and perimeter frame lateral resisting systems. The safety of existing non-ductile RC frame structures is judged through comparison with the seismic performance of modern RC frame buildings. Other key findings relate to the quantification of benefits and costs associated with mitigating vulnerable buildings through seismic strengthening or replacement. On the basis of the performance-based earthquake engineering assessment, recommendations for seismic safety policy are also presented.

Several chapters in this thesis contain repetition of background material and discussion of motivation. This repetition occurs because some of the chapters have been or will be published as individual journal articles. Some differences in terminology and notation may also exist between chapters. Apologies are made to those reading the thesis chapters together.

Chapter 2

Seismic Vulnerabilities of Existing Non-Ductile Reinforced Concrete Frame Structures in California

2.1 Overview

Reinforced concrete (RC) frame structures rely on beam and column elements, constructed from cast-in-place concrete reinforced with steel bars, to resist both seismic and gravity loads. Early RC frame structures, constructed in the 1920s and 1930s, often had infill masonry walls between frame elements, which provided substantial additional strength and stiffness. During the 1950s and 1960s, the characteristics of RC frame structures changed. While older structures had considerable strength and rigidity associated with the un-engineered filler walls and partitions, the newer buildings relied more on the framing system to resist lateral forces alone, requiring explicit considerations of necessary forces, material properties and allowable deflections. By the late 1960s, technological advancements in design and construction made it possible to construct RC frames of up to approximately 20 stories in height without any infill wall (CA Seismic Safety Commission 1985; Degenkolb 1994). These structures have been widely used for commercial, industrial and multi-family residential construction in California.

Based on the damage these structures experienced in past earthquakes and a growing understanding of inelastic behavior of reinforced concrete, RC frames constructed before 1975 are known to have deficient seismic resistance.[1] This chapter focuses first on characterizing these non-ductile pre-1975 RC frame structures, and how they differ from modern, code-conforming RC frame structures (Section 2.2). The existing inventory of these structures in California today, including the typical occupancy and function, is also considered. Observed damage to RC frames in past California earthquakes (Section 2.3) reveals the major problems in design of RC frames before significant building code changes

[1] RC shear wall buildings also were constructed with non-ductile detailing. These structures are thought to be less risky because of their higher overstrength and are outside the scope of this thesis.

in the 1970s were instituted. Given these apparent inadequacies, mechanisms for improving seismic safety of existing non-ductile RC frame buildings are discussed in Section 2.4, focusing on lessons learned from previous state and local government programs to improve seismic safety of existing buildings. These considerations provide the motivation for using performance-based earthquake engineering methods to evaluate the collapse risk of non-ductile RC frame structures. These methods provide quantitative measures of seismic safety, which can be used to evaluate seismic performance and the potential impact of proposals to retrofit or replace these structures.

2.2 Design Features of Non-Ductile Reinforced Concrete Frame Structures

2.2.1 Evolution of Building Code Seismic Provisions for Reinforced Concrete

Building codes are the primary means of governing earthquake design of new structures. First adopted state-wide in 1933, after the Long Beach Earthquake, California's early provisions for seismic design mandated that all new structures in the state be designed to withstand a (rather low) horizontal acceleration of 0.02g, and that local governments create building departments for the purpose of inspecting new construction to ensure that these requirements were met (Geschwind 2001). These provisions have been significantly modified since 1933 to incorporate improvements in earthquake engineering and seismic hazard analysis, especially in response to experience in major California earthquakes, such as the San Fernando (1971), Loma Prieta (1989) and Northridge (1994) Earthquakes. Seismic code requirements grew to include not only minimum lateral force requirements, but also other design and detailing provisions to improve seismic resistance. These changes in building code requirements over time account for the significant differences in seismic resistance that may exist between older structures and modern ones. The California Building Code was formerly an amended version of the Uniform Building Code, which was adopted by local governments as updated versions became available. The International Building Code has now replaced the three national codes (UBC, BOCA, Southern Building Code), and is used as the basis for the California Building Code.

Improved understanding of behavior of reinforced concrete subjected to cyclic loading led to significant changes to building code requirements for reinforced concrete in the 1960s and 1970s. The engineering community focused on design and detailing of RC structures to undergo significant deformations without collapsing, expanding the traditional concept of

force-based design. These considerations were described by Blume, Newmark and Corning, in their landmark 1961 report on reinforced concrete structures:

> The modern type building, without any appreciable lateral resistance except in the frame proper, will be subject to possibly large story distortions even in moderate earthquakes in spite of meeting present-day seismic requirements… All brittle elements should either be permitted to move freely within the structure or should be expected to fail, in which case they should be designed and detailed to protect building occupants and people on the street. (Blume et al. 1961)

This report illustrated that that reinforced concrete, like steel, could exhibit significant ductility if designed properly (Blume et al. 1961; Blume 1994). The report also encouraged thinking beyond elastic behavior in design, recommending methods of avoiding brittle failures by designing structures for plastic hinging to occur first in the girders. Experienced engineers gradually incorporated these concepts into their designs of RC frame structures in the 1960s (Degenkolb 1994). Modifications to building code provisions followed from these advancements in the profession.

The design of non-ductile RC frames that exist in California today were likely based on design requirements similar to those in the 1967 Uniform Building Code (ICBO 1967). This code is therefore used as the basis for this study. The 1967 UBC, which included relevant ACI provisions now published as separate documents, recognized the relationship between ductile detailing of RC elements and ductility. However, ductile detailing and design was not required for RC structures in California, except those exceeding 160 feet in height (ICBO 1967; Berg 1983; California Seismic Safety Commission 1999). Under the 1967 UBC requirements, the design base shear (V) for a structure is computed from $V = CKW$, where W is the weight of the structure, and C is the base shear coefficient, based on seismic zone 3 for most of California, the highest seismic zone at the time, as shown in Figure 2.1. Although in earlier code editions C varied with soil conditions, in the 1967 UBC provision it depended only on the period of the structure. The consideration of the period of the structure in computing the design base shear was a relatively new addition to code provisions at that time. K was introduced in the 1950s to increase or decrease the design base shear based on the estimated ductility and reserve capacity/redundancies of the structure. K varied from 0.67 to 1.33, depending on the structural framing system. For RC frame structures, K was based on a distinction between ductile ($K = 0.67$) and non-ductile ($K = 1$) moment resisting frames. In order to qualify as a ductile frame and achieve a corresponding reduction in design loads, the code required more detailing and other design requirements. Design of the structure is based

on application of the design base shear, distributed over the height of the structure. The 1967 requirements incorporate a design force distribution based on both story height and weight.

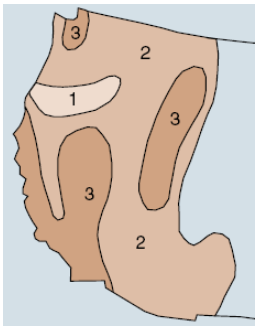

Figure 2.1 Seismic zones in the Western United States, as defined by the 1967 UBC.[2]

Substantial changes in building code provisions for reinforced concrete, implemented in the 1970s, represent the dividing line between the non-ductile potentially vulnerable structures that are the focus of this thesis and the ductile detailing and design that characterize modern RC frames. The most significant changes related to requirements for ductile detailing. In the 1967 UBC, ductile detailing of RC elements was only required where a low value of K was used to reduce design seismic forces (ICBO 1967). By the 1973 edition of the UBC, all RC frame structures in seismic zones 2 and 3, mapped as shown in Figure 2.1, had to meet specifications for ductile detailing (ICBO 1973). These specifications included strong column-weak beam provisions, limitations on splice locations, minimum shear stirrup/confinement requirements, and a specification that the ultimate strength design method must be used. In addition, the 1973 UBC instituted more stringent regulations on spacing and hook specifications for transverse column ties and incorporated the concept of development length in determining the necessary splice length and end-anchorage of reinforcing bars.

2.2.2 Engineering Details of Non-Ductile Reinforced Concrete Structures

This study is concerned with RC frame buildings constructed in California before significant modifications were made to building code requirements in the 1970s. Because these structures were constructed before seismic detailing was required by governing code

[2] Characterization of seismic hazard in building codes has undergone significant changes in the last 40 years. Until 1985, seismicity was defined by three seismic zones, which were used to determine equivalent seismic forces for design. A fourth seismic zone was added, recognizing the higher seismicity of California, in 1985. Today, maps of the maximum considered earthquake (MCE) developed by the USGS define earthquake design forces at a site.

provisions, they frequently had characteristics of non-ductile detailing, which are described below. RC frame structures with non-ductile detailing are still constructed in parts of the country with lower seismicity in the central and eastern U.S. Though not discussed here, older RC bridge structures (in California and elsewhere) also frequently had non-ductile detailing. Non-ductile RC frames remain a prevalent form of construction outside the U.S., as made evident in recent earthquakes in Turkey (1999) (Aschheim et al. 2000), Pakistan (2005) and China (2008), among others.

Typical characteristics of non-ductile RC frame structures are described in Table 2.1, which also highlights differences between design and detailing features of older RC frame elements and more modern design (Moehle 1998; ACI 2002). Standard non-ductile detailing of reinforcement is illustrated in Figure 2.2, and in comparison to ductile RC frames in Figure 2.3. One important distinction between designs of older and newer RC frame elements is the amount and detailing of shear (transverse) reinforcement in beams, columns and joints, making non-ductile RC frames more susceptible to brittle shear failure of these elements. Poor confinement of the concrete core of RC elements decreases deformation capacity. Other differences relate to the detailing of longitudinal reinforcement. Non-ductile RC frames sometimes have insufficient overlap of reinforcing bars to prevent lap-splice failure or pull-out of discontinuous bottom beam bars. These structures also had no requirements governing the relative strength of structural elements, such that there is no particular hierarchy of failure modes in beams, columns and joints is likely in earthquakes. This is in contrast to modern RC frames, which are designed to promote yielding first in the beams.

Table 2.2 lists key design parameters for three representative RC frame buildings constructed in California in the 1960s for which original structural drawings were obtained, including data on the lateral resisting system, member sizes and reinforcement detailing. One of these structures, Van Nuys, is a hotel built in Southern California in 1966 and the other two, Durand and Mitchell, are educational (office/library) buildings on the Stanford University campus. These structures are included here to provide real-world examples of the type of structure of interest, and to characterize representative building design for later purposes in this study. (Some of these structures have been retrofitted. Table 2.2 describes each structure's design, as originally constructed). Both perimeter and space frame buildings were constructed between 1950 and 1975, though space frame systems, like the Durand and Mitchell buildings, are more prevalent. Typical span lengths (column spacing) ranged from

18 to 30 feet. The provision of ductile detailing varied; some structures had all the characteristics of non-ductile detailing described in Table 2.1, while others had detailing that exceeded code minimum requirements in some instances. The Durand and Mitchell buildings, for example, have closely spaced transverse reinforcement in the hinge region of columns exceeding code-minimum requirements and all three structures specify 135º hooks on some stirrups. Other studies have documented examples of pre-1975 California RC frame buildings whose design and detailing went far beyond code-minimum requirements, especially in spacing of transverse reinforcement, lap-splice length and other design details (Miranda 1991; ATC 1996).

Table 2.1 Design and detailing features of non-ductile and ductile RC components.

	Non-Ductile	Ductile
Reinforced Concrete Beams	**Longitudinal Reinforcement**: bottom bars discontinuous in beam-column joints; top reinforcement not extended sufficiently past inflection points and not provided in mid-span	**Longitudinal Reinforcement**: longer development length requirements; a specified quantity of bottom reinforcement must be continuous through beam-column joint
	Transverse Reinforcement: relatively sparse transverse reinforcement is provided, sometimes only at the ends of beams; hoops inadequately sized for shear forces developed if beam yields; hoops typically have standard hooks of 90º (Figure 2.2)	**Transverse Reinforcement:** transverse reinforcement governed by capacity design provisions to provide adequate shear strength; closed (135º) hoops provide greater confinement
Reinforced Concrete Columns	**Weak Columns-Strong Beams:** no requirement regarding relative strength of columns and beams, such that flexural hinges may form first in columns	**Strong Columns-Weak Beams:** column strength often governed by strong column-weak beam requirement
	Splices: longitudinal reinforcement typically spliced just above joints for ease of construction; specified lap lengths were typically 20 or 24 bar diameters	**Splices:** splices must be located away from critical sections (ie. at mid-column height) and sized for transfer of tention forces
	Transverse Reinforcement: widely spaced transverse reinforcement is provided; reinforcement inadequately sized for shear forces developed if column yields; hoops typically have standard hooks of 90º	**Transverse Reinforcement:** governed by shear capacity design requirements, and maximum spacing requirements in order to confine the concrete core; hoops have 135º hooks
Reinforced Concrete Beam-Column Joints	**Transverse Reinforcement:** minimal, if any, transverse reinforcement is provided; no consideration of shear strength of joint	**Transverse Reinforcement:** joint shear strength is computed, and transverse reinforcement provided within joint
	Longitudinal Reinforcement: beam longitudinal reinforcment may terminate a short distance into the joint and be inadequately anchored	**Longitudinal Reinforcement:** column and beam reinforcement must be continuous through joint
	Geometry: beams may frame eccentrically into the column	**Geometry:** alignment of beams and columns within a single plane
Reinforced Concrete Slab-Column Connections	**Slab Reinforcement:** designed for flexure	**Slab Reinforcement:** some slab bottom reinforcement must be provided continuously through column connection;flat slabs are not permitted to resist lateral forces

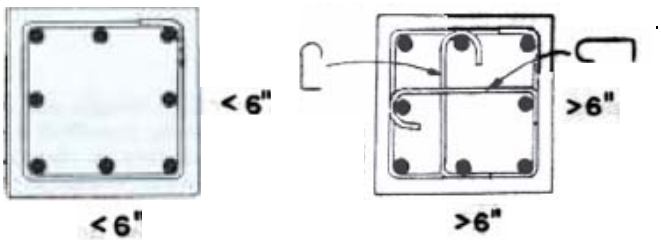

Figure 2.2 Standard practice for reinforcement detailing of reinforcement in RC columns, 1970 (Concrete Reinforcing Steel Institute 1970).

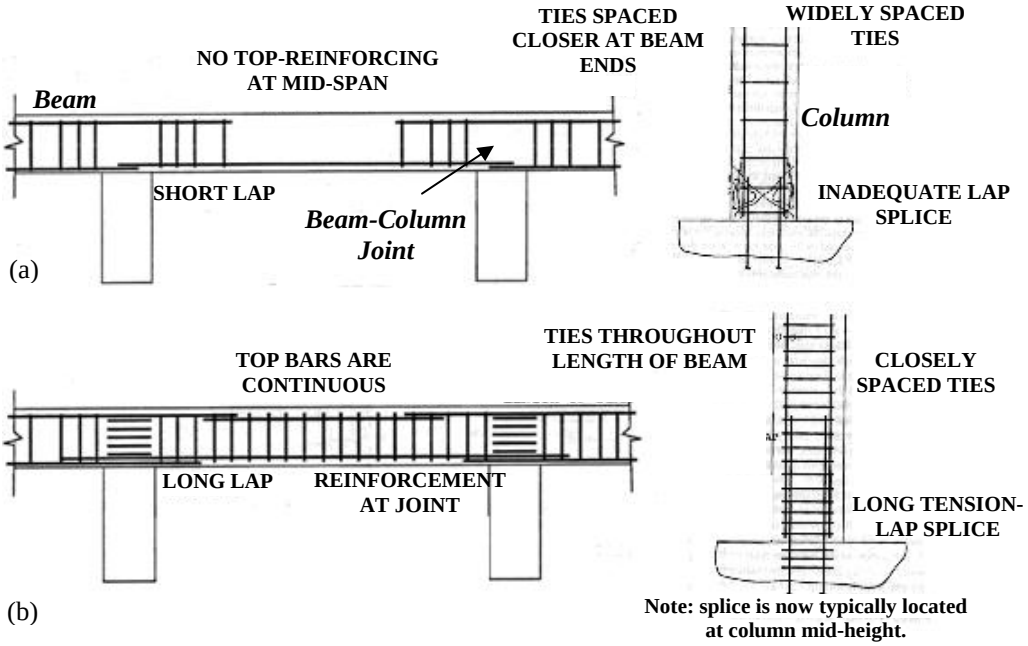

Figure 2.3 Typical detailing of (a) non-ductile and (b) ductile RC frames, based on Thiel et al. (1991).

Table 2.2 Design characteristics of selected RC frame buildings constructed in California in the 1960s.

	Van Nuys (Holiday Inn)[1]	Durand[2]	Mitchell[3]
Year of Completion	1966	1970	1968
Location	Van Nuys, California	Stanford, California	Stanford, California
Lateral Resisting System	Reinforced concrete perimeter frames	Reinforced concrete space frames	Reinforced concrete space frames
Floor System	Flat slab (8 to 10" depending on location)	RC joists with slab of varying thicknesses	RC joists with slab of varying thicknesses
Num. of Stories	7	5	5
Column Spacing	18.75 to 20 ft.	33 ft.	24 ft.
Beam Size	Beam height (h): 22 - 30 inches; beam width (b): 14 - 16 inches	h: 17 - 32 in.; b: 14 - 24 in.	h: 14 - 30 in.; b: 14 - 24 in.
Beam Transverse Reinforcement	No. 3 ties spaced at 3 in. and 5 in. near ends, spacing of 10 in. at midspan	Spacing of beam stirrups between 4 in. and 16 in. depending on location within span	Similar stirrup requirements to Durand
Notes on Beam Detailing	135º hooks specified	All beams have stirrups throughout the entire length; some specified for 90º hooks, but others have 135º hooks	Similar stirrup requirements to Durand
Column Size	Exterior columns: 14 in. x 20 in.	Column size ranges between 24 in. x 24 in. and 36 in. x 36 in.	Similar to Durand with some square columns and some rectangular columns
Column Transverse Reinforcement	No. 2 or No. 3 ties spaced at 12 in. on center; in some cases No. 4 ties are used	No. 4 ties spaced at 3 in. for 18. in from joint; others at 9 in.	Similar transverse reinforcement provided to Durand
Notes on Column Detailing	Spliced just above floor level	Spliced just above floor level	Spliced just above floor level
Joint Detailing	Drawings give column stirrups in joint, but may not be present in as built structure	No ties in joint	No ties in joint
Material Properties	f'_c = 3 to 6 ksi (depending on location in building); Grade 60 deformed bars used in columns, Grade 40 bars deformed bars used in slab and beams	f'_c = 5 ksi; Grade 60 deformed bars used in columns	f'_c = 5 ksi; Grade 60 deformed bars used in columns

[1](Krawinkler 2005), and original building drawings
[2,3] Drawings obtained from Stanford University

2.2.3 Inventory of Non-Ductile Reinforced Concrete Frame Structures in California

California has no state-wide inventory of RC buildings, and it is uncertain how many RC frames with non-ductile characteristics like those described above exist and for what purpose they are most typically used. Available estimates of the number of non-ductile RC structures are based on data gathered by local jurisdictions. For example, the City of San Francisco estimates that 2% of its construction is non-ductile reinforced concrete, based on census data, information from the Assessor's office, field investigations and feedback from local structural engineers (ATC 2003). From this and other local inventory data, the California hazard mitigation plan estimates that 65% of structures in the state were built before the late 1970s, and approximately 40,000 of these structures are non-ductile reinforced concrete (California Office of Emergency Services 2004). Many of these non-ductile RC frame buildings are used as warehouses and office buildings. The state of California, which has inventoried state-owned buildings, reports that 22% of state office buildings are non-ductile RC frame structures with curtain walls, and another 31% are non-ductile RC frame/shear wall buildings (CA Seismic Safety Commission 1985). In San Francisco, the largest number of these RC frames is thought to be in commercial districts, such as Downtown and Mission Bay, industrial areas (Western Addition), and some of the neighborhoods with a large number of multi-family residences (ATC 2003). It is unknown how many non-ductile RC frame structures in the state have been seismically retrofitted.

General data about the age of structures in California, and the prevalence of low-, mid- and high-rise construction is obtained from databases created for HAZUS (FEMA 2003) and updated by Kircher et al. (2006).[3] This information is used to obtain an estimate of the percentage of non-ductile RC frames in the existing building stock and of the height distribution of these structures. Since the HAZUS database is deliberately general, these estimates should be updated as more data specifically related to RC frame structures becomes available.

The fraction of California's buildings constructed between 1950 and 1974, the years of interest, are illustrated in Figure 2.4 for three California counties. These Bay Area counties are representative of different eras of development in California. San Francisco has older,

[3] The HAZUS database is based on Census Data, Department of Energy documentation on housing and commercial building characteristics, and the Dun & Bradsheet Business Population Report (FEMA 2003). Updates by Kircher et al. (2006) were based on the San Francisco study (ATC 2003) and other newly available data.

pre-World War II construction, while San Mateo and Santa Clara counties are assumed to have a large number of post-World War II and newer construction (Kircher et al. 2006). As shown in Figure 2.4, California experienced significant growth in the 1950s and 1960s, so a large number of buildings were constructed at that time. The percentage of the building stock used for various occupancy types is shown in Figure 2.5 (ATC 2003; FEMA 2003). The majority of structures in the state are used as single-family dwellings. Throughout California, most structures are low-rise structures (1 to 3 stories), and the number of mid-rise (4 to 7 stories) and high rise structures (8+ stories) depends on the population density of the region of interest (Kircher et al. 2006). These distributions are illustrated for selected California counties in Figure 2.6.

In order to identify the percentage of structures that are RC frame structures, according to occupancy type and height category, HAZUS default values for 1950 to 1970 West Coast construction are employed. It is estimated that 13% of high-rise multi-family residential construction, 9% of mid-rise commercial construction, 7% of high-rise commercial construction, 7% of low-rise industrial construction and 4% of mid-rise multi-family residential construction are RC frame structures. Based on this information, combined with estimates for what portion of California buildings were constructed between 1950 and 1975, it is observed that non-ductile RC frame structures likely make up a significant portion of the building stock in some categories including approximately 10% of mid-rise and 20% of high-rise apartment and hotel structures. Many mid-rise industrial buildings are also older RC frame structures.

These estimates of the number of non-ductile RC frames of varying heights and their functionality are approximate, but they are provided here to get a sense of how vulnerable California is if these structures perform poorly in earthquakes and who is at risk. How many people live and work in this type of structure and what kinds of businesses utilize this space affect predictions of economic losses and fatalities in future earthquakes. These data are important considerations in evaluating the economics, efficiency, and equity of any proposed retrofit policy. The improvement of this inventory data is currently under investigation by the Concrete Coalition (www.concretecoalition.org), sponsored by EERI, PEER and ATC.

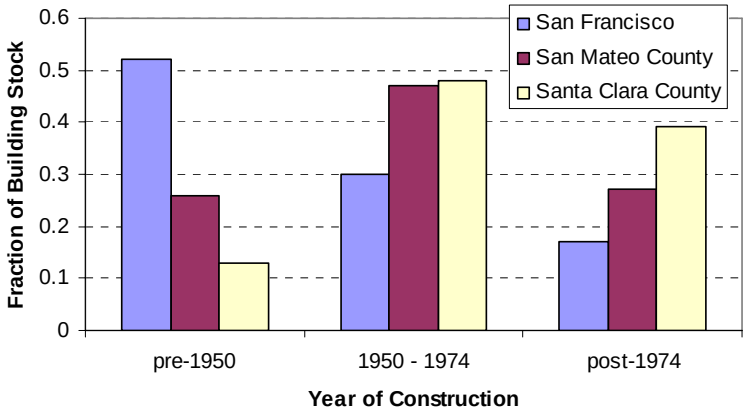

Figure 2.4 Assumed age distribution of building stock in selected California counties.

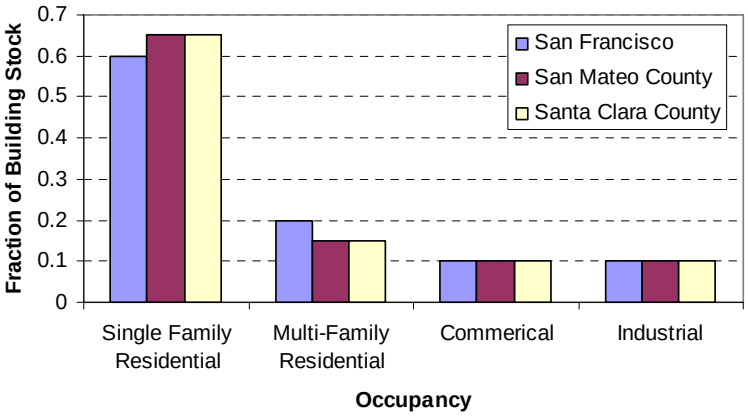

Figure 2.5 Assumed occupancy of building stock in selected California counties.

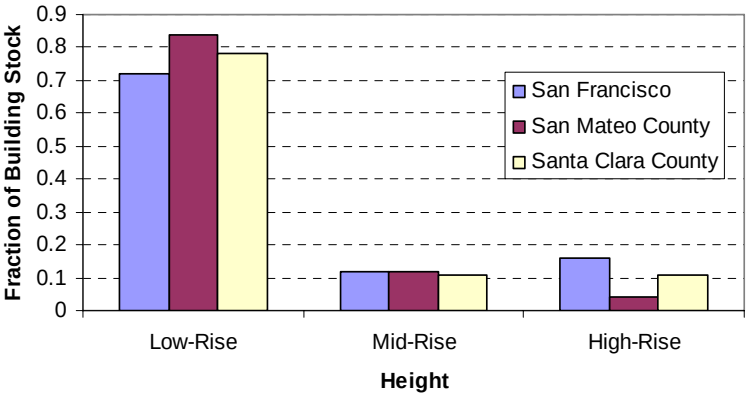

Figure 2.6 Assumed distribution of building heights in selected California counties.

2.3 Observed Damage to Reinforced Concrete Frames in California Earthquakes

2.3.1 Survey of Collapsed and Damaged Reinforced Concrete Frame Buildings in post-1950 California Earthquakes

Experience of how non-ductile RC frame structures have fared in past California earthquakes is reported in this section. This survey highlights some the effects of non-ductile detailing on earthquake performance and, at the same time, emphasizes the variability in

performance of non-ductile RC frame structures associated with differences in design and detailing and ground shaking at different sites. The discussion is limited to earthquakes that have occurred since 1950 in California, when non-ductile RC frames without masonry infill began to emerge as a common type of construction.

Table 2.3 summarizes the damage to building structures experienced in major California earthquakes since 1950, including those that caused fatalities and widespread damage to building structures. Some earthquake events were excluded from Table 2.3 due to the sparsely populated area affected or the scarcity of available data about earthquake-induced damage. The damage reported in Table 2.3 is based on reconnaissance reports conducted by engineers shortly following the earthquake. For those earthquakes that were followed by one or more aftershocks, the damage described includes damage from both the mainshock and aftershocks. Damage descriptions focus on failures in non-ductile RC buildings, but destruction in other types of structures is described for context. Damage to wood-frame single family dwellings, unreinforced masonry construction and, in more recent earthquakes, low-rise RC tilt-up construction significantly exceeded that in other types of building structures due to the large numbers of these structures in California.

Collapses, near-collapses, and significant damage have been reported in engineered RC buildings designed and constructed between 1950 and 1975, particularly in earthquakes that struck populated urban areas. Some of the failures in engineered RC structures constructed between 1950 and 1975 in past California earthquakes are described and illustrated in Figure 2.7. Failures of non-ductile bridge and transportation structures, not discussed here, corroborate and provide further evidence for failure modes in non-ductile RC elements. Damage to non-ductile RC structures in the 1971 San Fernando Earthquake provided a major impetus to modifications of building codes for reinforced concrete in the early 1970s.

Evidence from these earthquakes, as well as similar damage observed in earthquakes around the world, have demonstrated the potential problems in non-ductile RC frame structures of the type constructed in California between 1950 and 1975. Much of the damage described in Figure 2.7 made apparent inadequacies in detailing of reinforcement. For example, the Olive View Hospital Medical Treatment Building, which nearly collapsed in the 1971 San Fernando Earthquake had some columns with spiral reinforcement and some with widely spaced ties. Although both types of columns were significantly damaged in the earthquake, the spiral-wrapped columns provided more confinement to the concrete core and retained their capacity to carry gravity loads. Column failures due to insufficient

confinement and poor ductility and also occurred in the Santa Rosa Social Services Building, Imperial County Service Building, Olive View Psychiatric Building and many of the other structures described in Figure 2.7. Insufficient transverse reinforcement in beam-column joints contributed to the collapse of the Kaiser Permanente structure in the 1994 Northridge Earthquake. Likewise, the importance of provision of continuous reinforcement in slab-column connections was exemplified by the collapse of Bullock's Department Store, in the Northridge Earthquake. Continuous longitudinal bottom reinforcing bars in the slab-column connection probably could have prevented collapse of the floor slab. Lack of adequate reinforcement in connections between structural elements also played a role in the damage sustained at the Holy Cross Hospital and the CSU LA administration building, and the collapse of the Kaiser Permanente structure.

Damage to RC frames in past earthquakes also shows flaws in design of RC elements in older buildings for shear. Columns frequently experience larger shear forces than they are designed for due to overstrength in floor system (beams and slabs), the presence of nonstructural components or torsional effects. Deep spandrel beams in the Barrington building increased shear forces in RC columns, causing the X-cracking illustrated in Figure 2.7. The Olive View Psychiatric Building, and others, show the effect of flexure-shear or shear failure as columns experience shear failure and then collapse due to vertical loads.

Problems associated with irregularities in strength and stiffness in non-ductile RC frames, either in elevation or in plan, have recurred in California earthquakes. Many of the case studies in Figure 2.7 are soft-story collapses, where structural or non-structural shear walls were discontinued in the bottom story for architectural reasons. This soft-story, which is less strong and less stiff than those above, provide a fuse for earthquake failure, such as in the Olive View Medical Building, Imperial County Services buildings, and others. Soft-stories may also occur when beams are stronger than columns, as in the May Company Garage collapse. The detriments of weak columns and strong beams are not unique to reinforced concrete structures, but non-ductile RC frames tend to be especially vulnerable to this collapse mode. Structural and non-structural walls that are asymmetrically distributed can also create additional shear forces due to torsion. This behavior played a role in the collapse of the Olive View Hospital Psychiatric Building. Certain plan layouts tend to be particularly problematic, such as the L-shape of the May Company Garage.

Table 2.3 Major California earthquakes since 1950.

Year	Earthquake	Magnitude[1]	Num. of Fatalities[1]	Damage in Building Structures[2]
1952	Kern County	7.3	12	Damage in reinforced concrete primarily limited to older structures (1920s), which exhibited spalling and failure around construction joints and discontinuous walls. Significant damage to unreinforced masonry structures, wood frame construction, and adobe houses.
1969	Santa Rosa	5.7	1	No collapsed structures, but damage in unreinforced masonry, brick chimneys, some older buildings with RC walls. An RC Frame, the Social Service Building, was also damaged, as described below.
1971	San Fernando	6.6	65	Significant damage to wood frame and unreinforced masonry construction. In general, engineered steel and reinforced concrete structures had less damage, though there were a few notable exceptions including both the Medical Treatment and Psychiatric Buildings at the newly completed Olive View Hospital. Other damaged non-ductile RC structures included the Holy Cross Hospital, the Union Bank Building, the Bank of California Building and the Holiday Inn. A large number of people were killed in the Veterans Administration Hospital. This structure was a very early RC frame (constructed in 1925) with hollow-tile interior and exterior walls.
1979	Imperial Valley	6.4	none	No collapses in reinforced concrete, but a couple of RC frames exhibited significant damage. See Imperial County Services Building below. Other damage to homes and commercial buildings also occurred.
1983	Coalinga	6.4	none	Most engineered reinforced concrete structures performed well. Significant damage to unreinforced masonry structures; wood frame single family dwellings fell off foundations; chimneys damaged and toppled.
1987	Whittier Narrows	5.9	8	There was wide disparity in performance of non-ductile RC frame structures. Some buildings exhibited shear distress and significant hinging (e.g. May Company Parking Garage, described below), while others designed and constructed at the same time had very little damage. Other damage concentrated in the old Whittier business district and surrounding residential areas, affecting wood frame and unreinforced masonry construction.
1989	Loma Prieta	6.9	63	Spectacular failures in non-ductile RC bridge structures, but limited damage to non-ductile RC buildings. Damage in engineered non-ductile RC buildings was caused primarily by pounding and irregular shear walls. Tilt-up, wood frame and unreinforced masonry construction did not fare as well.
1992	Cape Mendocino	7.2	none	Sparsely populated region - most damage in older houses, wood frame commercial buildings and unreinforced masonry structures.
1992	Landers	7.3	3	Damage to water storage tanks, some older reinforced concrete/masonry construction and wood frame structures.
1994	Northridge	6.7	60	Non-ductile RC structures exhibited column failures, shear distress and other non-ductile failures, see particularly the Barrington Building and the Kaiser Permanente Office Building. Damage to single family wood frame houses, multi-family wood frame construction, unreinforced masonry construction and tilt-up structures.

[1](USGS 2008)

[2]Sources: Kern County- (Steinbrugge and Moran 1954; SEAONC 1955); Santa Rosa- (Steinbrugge et al. 1970); San Fernando- (Jennings 1971; Lew et al. 1971; Johnson 1972; Steinbrugge et al. 1975); Imperial Valley- (Wosser et al. 1982); Coalinga- (Poland et al. 1983; Messinger et al. 1984); Whittier Narrows- (Degenkolb et al. 1987; EQE Incorporated 1987; Miranda and Bertero 1996); Loma Prieta- (Benuska 1990; Meehan and Cole 1991); Cape Mendocino- (NOAA 1993); Landers- (NOAA 1993); Northridge- (CA Seismic Safety Commission 1995; Mitchell et al. 1995; Youssef 1995)

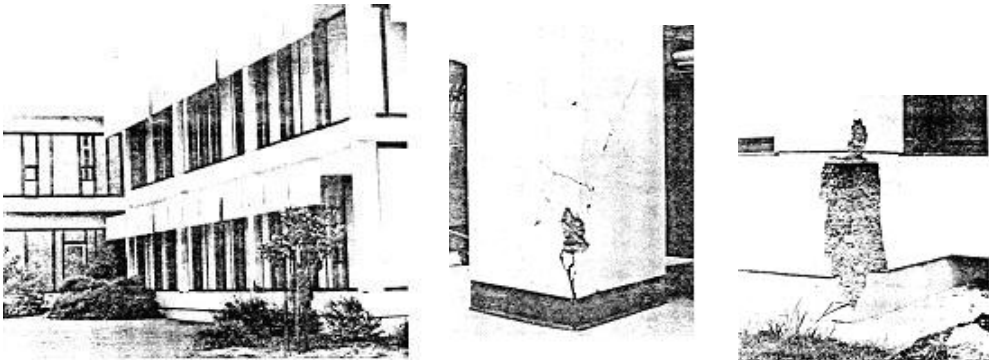

(a) **Social Service Building**, *1969 Santa Rosa Earthquake.* Description of Structure: 2-story RC frame structure, designed according to the 1964 UBC. Damage Incurred: Cracking and spalling in almost all 1st story columns. Cracks in walls around elevator core and 2nd story columns. Some nonstructural damage. Columns were repaired with epoxy and total repairs cost approximately 8% of the total value of the building. Source: (Steinbrugge et al. 1970) Photo Credit: (Steinbrugge et al. 1970)

(b) **Olive View Hospital Medical Treatment Building**, *1971 San Fernando Earthquake*. Description of Structure: 5-story building with lateral system consisting of RC Frames and shear walls, completed in 1970. Structure was very close to the epicenter of the earthquake and peak ground accelerations at the site probably exceeded 0.6g. Damage Incurred: Extensive damage in 1st story and basement due to discontinuous walls and soft-story effect. Failure in columns occurred due to lack of confinement. Pounding occurred with neighboring buildings. Building was replaced following the earthquake (100% loss). Source: (Frazier et al. 1971; Jennings 1971; Lew et al. 1971; Murphy 1973; Steinbrugge et al. 1975) Photo Credit: USGS Photographic Library

(c) **Olive View Hospital Psychiatric Building**, *1971 San Fernando Earthquake*. Description of Structure: 2-story RC frame structure designed in 1965/1966; T-shaped configuration in plan. Damage Incurred: Entire 1st story collapsed when columns failed in flexure-shear and then lost ability to carry gravity loads.

Damage was exacerbated by irregularities in plan due to masonry walls. Source: (Frazier et al. 1971; Jennings 1971; Lew et al. 1971; Murphy 1973; Steinbrugge et al. 1975) Photo Credit: USGS Photographic Library

(d) **Holy Cross Hospital**, *1971 San Fernando Earthquake*. Description of Structure: 7-story RC structure with RC frame lateral resisting system and shear walls in transverse direction, completed in 1961. Damage Incurred: Failure in beam-column joints and connection between framing, floor and wall systems. Source: (Frazier et al. 1971; Jennings 1971; Lew et al. 1971; Murphy 1973; Steinbrugge et al. 1975) Photo Credit: EERC Online Archive

(e) **Union Bank Building**, *1971 San Fernando Earthquake*. Description of Structure: 13-story RC frame structure. Damage Incurred: Cracks in columns in lower levels and damage to corner columns due to over-turning effects. This structure was damaged again in the Northridge Earthquake. Source: (Frazier et al. 1971; Jennings 1971; Lew et al. 1971; Murphy 1973; Steinbrugge et al. 1975) Photo Credit: (Lew et al. 1971)

(f) **Imperial County Services Building**, *1979 Imperial Valley Earthquake.* Description of Structure: 6-story RC frame building designed in 1968, with some discontinuous shear walls in upper stories. Structure

had some ductile detailing characteristics, including column bars spliced at mid-height, continuous steel in girders, and a small amount of transverse reinforcement in beam-column joints. Damage Incurred: 1st story columns experienced flexure-shear failure, hinging and then losing their ability to bear gravity loads. Structure was replaced following the earthquake (100% loss). Source: (Wosser et al. 1982) Photo Credit: USGS Photographic Library

(g) **May Company Garage**, *1987 Whittier Narrows Earthquake*. Description of Structure: 2-story parking garage structure, designed in 1964. Lateral resisting system was RC frame, in L-shaped configuration. Damage Incurred: Collapse of 2nd story and partial collapse of 1st story. RC columns experienced both flexural hinging and shear failures, due to lack of confinement, widely spaced transverse reinforcement, and weak columns (compared to beams). Source: (Degenkolb et al. 1987; EQE Incorporated 1987) Photo Credit: EERC Online Archive

(h) **CSU LA Administration Building**, *1987 Whittier Narrows Earthquake*. Description of Structure: 8-story RC moment resisting frame, with discontinuous shear walls, designed in 1967. Damage Incurred: Minor soft-story damage and cracking in 1st-story columns and 2nd story slab-wall connections. Source: (Degenkolb et al. 1987; EQE Incorporated 1987) Photo Credit: (Degenkolb et al. 1987)

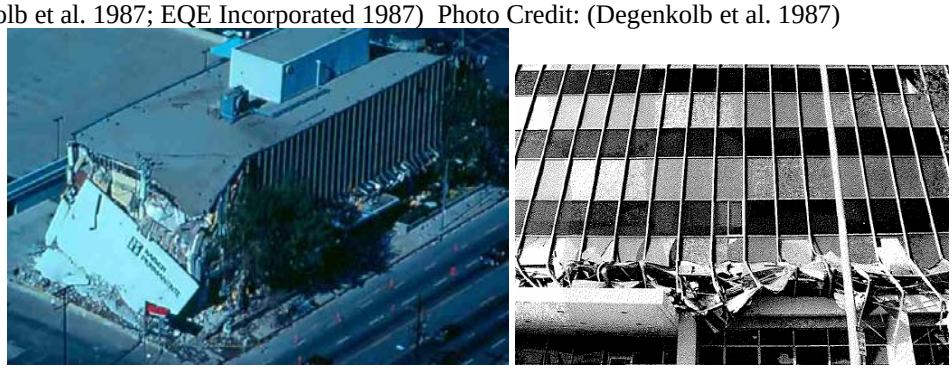

(i) **Kaiser Permanente Granada Hills Office Building**, *1994 Northridge Earthquake*. Description of Structure: Non-ductile RC frame structure, constructed in the 1960s. Damage Incurred: Entire 2nd story collapsed, as well as the end bays over the height of the building. Exterior walls were not adequately tied to the structure. Joints and columns failed due to lack of confinement of reinforcement. Source: (Mitchell et al. 1995; Youssef 1995) Photo Credit: EERC Online Archive, Mitchell et al.

(j) **Barrington Building**, *1994 Northridge Earthquake*. Description of Structure: 7-story non-ductile RC frame with discontinuous shear walls. Damage Incurred: Shear failure of most columns in 5 lower stories, due to spandrel beams that shortened columns, irregularity of shear walls and torsional effects. Columns did not lose their capacity to carry gravity loads. Source: (Mitchell et al. 1995; Youssef 1995) Photo Credit: EERC Online Archive

(k) **Bullock's Department Store**, *1994 Northridge Earthquake*. Description of Structure: Waffle-slab floor-system supported on circular columns; opened in 1971. Damage Incurred: Punching shear failure of slab-column connections, followed by vertical collapse. Source: (Mitchell et al. 1995). Photo Credit: EERC Online Archive

Figure 2.7 Notable collapses, near-collapses and damage in non-ductile RC frame structures in past California earthquakes.

In addition to these specific observations, the damage experienced by non-ductile RC frames in past California earthquakes is notable for its diversity. Of the structures included in Figure 2.7, some of the non-ductile RC frames collapsed, while others experienced only limited damage. Other non-ductile RC frame structures saw little to no damage in the same earthquakes. For example, in the Whittier Narrows earthquake, the Hinshaw Parking Garage, which is located close to the May Parking Garage and constructed around the same time, experienced only minor damage at expansion joints (Degenkolb et al. 1987). Many factors may explain these differences: design and detailing features, construction quality, level of ground-shaking experienced at the site, or pounding from nearby buildings.

2.3.2 Experimental Testing

The limited data on the performance of non-ductile RC frames in major California earthquakes has been augmented by numerous researchers, who have conducted experimental tests of RC components in their laboratories. These tests have typically aimed to examine the

effect of non-ductile detailing of components and to quantify their impact on seismic performance. A complete review of this research is outside the scope of this thesis. Many of the tests done on RC columns have been assembled into a database by PEER researchers (Berry et al. 2004), and these columns include those with both ductile and non-ductile detailing features. Mitra and Lowes (2007) have reviewed many of the experiments related to beam-column joints. In addition to component tests, researchers have tested reduced-scale non-ductile RC frames in the lab and, more recently, a few full-scale tests of RC frame buildings have also been conducted or planned, notably at the E-Defense testing facility near Kobe, Japan (Kabeyasawa et al. 2005). This body of data has been used to qualitatively and quantitatively describe the behavior of non-ductile RC elements in earthquakes and to validate analytical simulation models, as described in Chapter 3.

2.4 Mechanisms for Improving Seismic Safety in Existing Buildings

2.4.1 California's Seismic Safety Goals

California's principal objectives for seismic hazard mitigation are articulated in the state's Multi-Hazard Mitigation Plan: "to save lives and reduce injuries" and "to avoid damages to property" (California Office of Emergency Services 2004). Similar objectives have been expressed by many of California's local governments, e.g. (Assoc. of Bay Area Govts. 2005). The state plan identifies critical milestones that are associated with meeting these seismic safety goals. These milestones include identifying and prioritizing "all seismically vulnerable public and private buildings" and establishing a plan to reduce the risks posed by these buildings. Through the Multi-Hazard Mitigation Plan, California establishes a mandate for mitigating hazards from existing building stock including, potentially, non-ductile reinforced concrete frame structures. It does not, however, establish quantifiable safety goals.

2.4.2 Legislation for Seismic Safety in California

Reduction of collapse risk for public safety represents the most significant motivation for government intervention in the seismic safety of existing buildings. The seismic safety of new buildings in California is vetted through the established process of creation and modification of the seismic provisions of building codes, which are regularly updated to incorporate advances in design and construction. Compared to modern construction, existing

buildings, such as non-ductile RC frame structures, may be less safe, because they were designed under earlier, now sub-standard building code provisions. The primary avenue for improving the safety of these structures is through the creation of legislation or regulations requiring retrofit of unsafe structures at either the state or local government level. Without this legislation, individual owners may choose to seismically strengthen their structures, but they are not obligated to do so.

Legislative Precedents

Three major pieces of legislation regulate the seismic safety of existing structures in California: the Field Act, the Hospital Safety Act and the Un-reinforced Masonry (URM) Act. Each aims to protect public safety by instituting regulations designed to reduce the likelihood of earthquake-induced collapse for a specific group of existing buildings. In considering proposals for improving seismic safety of non-ductile reinforced concrete structures that are not currently covered by this legislation, these legislative precedents serve to illustrate successes and failures of past legislation.

Hospitals and schools were singled out for legislative attention based on their poor performance in the 1971 San Fernando and 1933 Long Beach Earthquakes, respectively, and their special status as places that house the sick, the injured and children. The 1933 Field Act regulates the safety of public school buildings in California. Initially applying only to new school buildings, more stringent requirements have been placed on the safety of existing school buildings over time. The 1939 Garrison Act legislated that if a structural engineer found a pre-1933 school building to be unsafe the structure needed to be upgraded to Field Act standards. In 1968, the Garrison Act was amended, mandating inspection of all pre-1933 school structures and requiring that all school buildings not meeting Field Act standards be abandoned by 1975. Further legislation in 1999 instituted plans to evaluate and rehabilitate non-wood frame school buildings that do not meet the requirements of the 1976 UBC. Under this legislation, the Office of the State Architect has inventoried non-ductile reinforced concrete school buildings and nonstructural seismic hazards have also been investigated (Jephcott 1986; Geschwind 2001; California Dept. of General Services 2002; California Office of Emergency Services 2003; Olson 2003).

The 1973 Alquist Hospital Safety Act mandates that hospitals, which provide critical post-earthquake services, achieve a superior level of seismic performance:

> It is the intent of the Legislature that hospitals, which house patients who have less than the capacity of normal healthy persons to protect themselves, and which must be reasonably capable of providing services to the public after a disaster, shall be designed and constructed to resist, insofar as practical, forces generated by earthquakes, gravity and wind.

Like the Field Act, the Hospital Safety Act originally applied only to new construction, but it was amended by Senate Bill 1953 in 1994 to require that acute care facilities built before 1973 be evaluated and, if needed, upgraded. The Bill requires that by 2008, hospitals should not pose a significant threat to life safety and, by 2030, hospital buildings should be capable of providing services to the public following an earthquake. A large number of hospital buildings must be retrofitted or replaced to meet this criteria; in San Francisco alone, data assembled by the Office of Statewide Health and Planning in 2001 found that 61% of hospital buildings needed to be retrofitted to meet the first deadline. The 2008 deadline has been delayed until 2013, due to slow compliance by financially-strained health care providers, both public and private (Geschwind 2001; Russell 2001; Alesch and Petak 2004; CA Office of Emergency Services 2004).

The Un-reinforced Masonry (URM) Buildings Act aims to mitigate the hazards posed by a particular structural system that has experienced disproportionate damage in past earthquakes, as described by Table 2.3. An early example of regulation of this type is the 1947 City of Los Angeles Parapet Correction Ordinance which required parapets of buildings facing streets, sidewalks, or exit paths to be removed or braced, to reduce the falling hazard in future earthquakes (Murphy 1973; Green 1993). Several cities, most notably Long Beach and Los Angeles, began requiring mitigation of unreinforced masonry structures in the late 1960s and early 1970s. Under the 1986 State law, all local governments in Seismic Zone 4 (most of California) were required to establish a risk reduction program for URM structures by 1990. The law recommends, but does not require, that local governments adopt mandatory strengthening programs, establish seismic retrofit standards and enact measures to reduce the number of occupants in URM buildings. Each local government has since adopted its own URM mitigation program. Some local governments (including 52% of municipalities) require that owners retrofit or demolish vulnerable structures, others use incentives to induce building owner participation in a voluntary strengthening program, and others merely have a notification system (approximately 18% of municipalities), alerting owners and the general public of the potential seismic risk of their structures. A sample public notification placard for a URM building is included as Figure 2.8. Compliance rates

vary according to the type of regulation instituted in each municipality (Macleod and Scott 1987; Comerio 1992; Green 1993; CA Seismic Safety Commission 2003).

Figure 2.8 Example of warning placard posted on unreinforced masonry construction in California located at 740 Valencia in San Francisco. (Photo: Jackson Reed)

Lessons Learned

The Field, Hospital Safety and Un-reinforced Masonry Building Acts each mandated a targeted examination of the seismic safety of a particular type of existing structure, resulting in many cases in retrofit or demolition of identified risky structures. The primary motivation has been to reduce the threat to life safety and not to decrease damage and economic losses (with the exception of the post-earthquake operability requirement for hospitals).

Though the evaluation and enforcement methods of these three laws differ, their histories illustrate the common barriers to successful seismic safety legislation. Once adopted, a central challenge is the definition of seismic performance standards for a class of structures, and how these standards should be evaluated. Seismic safety goals are qualitatively described in the legislation, but tend not to be explicitly linked to implementation or engineering requirements. The Hospital Safety Act includes the vague language that requirements should be met "insofar as practical." Many blame the slow progress of the Hospital Safety Act on overly stringent standards and poorly distinguishing evaluation methods, which have identified a large number of deficient structures without prioritizing the worst buildings. The revisions of the Field and Garrison Acts over the seventy years since first enacted reflect the changing knowledge and standards of seismic risk for public school buildings. In the case of the decentralized URM Act, the lack of a state-wide mitigation program or seismic safety standards has led to inconsistent improvements in seismic safety around the state, as each jurisdiction instituted different requirements.

A second challenge is the significant opposition seismic safety proposals face from building owners, due to the high costs and uncertainty involved in seismic rehabilitation or replacement. For each piece of legislation discussed above, major earthquakes - notably the

1933 Long Beach Earthquake, the 1971 San Fernando Earthquake and the 1994 Northridge Earthquake - provided the political impetus needed. Without the focusing effect of catastrophic damage, seismic safety often fails to attract attention from legislators and their constituents. In this sense, hospitals, schools and essential public service buildings, many of which are publicly owned and which invoke special societal sympathy, represent perhaps the easiest cases in developing momentum to develop and enforce the legislation. Even so, implementation of the Hospital Safety Act has been delayed as owners struggle to meet the financial burden of seismic upgrading.

Legislation mitigating seismic hazards in non-ductile RC frame structures would likely face similar obstacles. In order for non-ductile reinforced concrete to become the focus of legislative action, it is clear that there are several critical steps needed: (1) to convince the public and their legislators of the vulnerability of these structures (characterizing the problem), (2) to demonstrate the potential improvement in public safety if these structures were replaced or retrofitted (identifying a possible solution), (3) to clearly articulate the desired safety goals, (4) to develop a sufficiently discerning evaluation method such that the most deficient structures can be prioritized, and (5) to generate policies that have regulatory, financial or other incentives to encourage building owners compliance. Performance-based earthquake engineering is an important tool in this process.

2.4.3 Mitigation by Building Owners

Even without a legislative mandate, some building owners may choose to upgrade their structures. These efforts are motivated by a variety of factors, including the protection of life safety of employees or tenants and the reduction in business interruption or economic losses in future earthquakes, which are used to justify the expense of evaluating and upgrading buildings.

Several large institution or corporate owners that own a portfolio of structures have strategic plans to mitigate seismic risk. The University of California at Berkeley owns a large number of structures in close proximity to the Hayward Fault. Under the SAFER program begun in 1997, all existing structures on the Berkeley campus were evaluated to see if they meet life safety requirements to protect students, faculty and staff. Beyond the life safety objective, the University wants to limit closure time following a major earthquake event to less than 30 days, such that the essential teaching and research activities will not be significantly interrupted. Prioritization of funding for retrofit over the 20 year life-span of

the program is based on the seismic rating given to each structure and certain vital laboratory and teaching spaces are given additional priority (Comerio 2000; May 2001; Comerio 2006). Stanford University instituted a seismic risk management program following the 1989 Loma Prieta Earthquake, which led to the closure of 8% of the total campus building square footage (Comerio 2006). Like Berkeley, Stanford's seismic performance goals are designed to protect the protection of life safety of the Stanford community and to ensure the University's economic and intellectual resilience following a future seismic event (May 2001; Stanford University 2002). Studies showed that the University could not afford lose more than 23% of their teaching space. Prioritization for seismic retrofit and investment in new design is based on an established ratings system to meet these goals. In the corporate sector, Hewlett Packard, a major technology company with more than 300 structures located in high seismic areas around the world, instituted a seismic risk reduction policy in 1988. Hewlett Packard's program reflects similar goals to the policies of Berkeley and Stanford, by aiming to "reduce their earthquake risk related to both life safety and business operations" (Bonneville and Lanning 1996; May 2001).

The experiences of U.C. Berkeley, Hewlett Packard, and Stanford indicate that some proactive owners find it worthwhile and economically feasible to invest in retrofit, both to improve seismic safety and to reduce losses and business interruption in earthquakes. These motivations are particularly compelling for these institutions because of their large size, and their significant socioeconomic roles in society (May 2001). Similarly, public owners such as Caltrans, the California State government, and the U.S. General Services Administrations have conducted significant upgrading efforts (U.S. General Services Administration 2005). However, the costs of seismic upgrading are a significant inhibitor to widespread improvement of seismic safety by building owners. The challenge of funding seismic retrofitting is even more significant for smaller business owners with fewer resources and a shorter time frame of building ownership to motivate mitigation of future uncertain losses. In evaluating seismic safety decisions, accurate predictions of structural performance are needed for assessing deficiencies and for developing cost-effective retrofit strategies.

2.5 Using Performance-Based Earthquake Engineering to Frame Seismic Safety Decisions

In this study, performance-based earthquake engineering methods are used to evaluate the seismic safety of the diverse inventory of California's non-ductile RC frame structures. Quantifiable assessment of the life safety risks of non-ductile RC frame structures is an essential pre-requisite to any proposal, policy or other action to improve building safety. Evaluations of life safety require, first, quantifying the risk of earthquake-induced collapse and, second, relating the collapse risk to injuries and fatalities. Once the risk is identified, then performance-based earthquake engineering provides tools to apply in developing economical and practical retrofit techniques and evaluating the effectiveness of various seismic safety policies that could be pursued at the state or local government level. Data generated by performance-based earthquake engineering studies is useful for characterizing the problem of non-ductile RC structures, identifying the most vulnerable buildings and developing technical requirements for a policy solution.

Chapter 3

Collapse Assessment and Modeling of Non-Ductile Reinforced Concrete Frame Structures

3.1 Overview of Collapse Performance Assessment Methodology

3.1.1 Performance-Based Earthquake Engineering

Evaluation of the risk of earthquake-induced collapse in non-ductile RC frame structures in this study utilizes the framework of performance-based earthquake engineering developed by the Pacific Earthquake Engineering Research Center, which has been described in detail elsewhere (Deierlein 2004; Krawinkler and Miranda 2004). Performance-based earthquake engineering methods combine analysis of the ground-shaking hazard at a particular site and the expected structural response, obtained though nonlinear dynamic analysis, to probabilistically predict the occurrence of structural damage, economic losses or collapse. The ground motion hazard is typically represented by a hazard curve, which describes how a frequently a ground motion of a specified intensity (IM) is exceeded at a particular site. Structural response is predicted in terms of engineering demand parameters (EDPs), which are obtained from structural analysis results. Response parameters of interest may include interstory drift ratios, floor accelerations or residual drifts. These predictions of structural response can then be used to assess damage measures (DM) or decision variables (DV), which may describe the amount of repairs needed following an earthquake, the likelihood of collapse or other important measures of structural performance. The PEER performance-based earthquake engineering methodology can be represented mathematically as in Equation (3.1):

$$\lambda(DV) = \iiint G < DV \mid DM > dG < DM \mid EDP > dG < EDP \mid IM > d\lambda(IM) \qquad (3.1).$$

λ(DV) is a probabilistic description of the seismic performance in terms of mean annual frequency of exceedance, e.g. the mean annual frequency Y that repair costs will exceed X% of the building replacement cost: Y = λ(Repair Costs > X% Replacement Cost). λ(IM) represents the mean annual frequencies of exceedance for the ground motion intensity (IM),

and the intermediate terms $G\langle A|B\rangle$ are conditional probabilities for the methodology components EDP, DM, and DV.

Performance-based earthquake engineering assessments in this thesis provide metrics of seismic performance for evaluating the seismic safety of non-ductile RC frames structures, and for comparing these results with the seismic safety of other buildings, including modern code-conforming RC frame structures. In Chapters 3, 4, and 5, the performance-based earthquake engineering framework is used to predict the mean annual frequency of collapse and conditional probabilities of collapse of potentially vulnerable non-ductile RC frame structures in California. In Chapter 6, the same framework is applied to estimate earthquake-induced economic losses and fatalities in these structures. These predictions account for many of the possible sources of uncertainty in the assessment process, including uncertainties in the characteristics of future ground motions, uncertainties in how faithfully the nonlinear analysis model reflects the true properties of the structure, and uncertainty in damage generated in nonstructural or structural components.

Implementation of the performance-based earthquake engineering framework for assessing the collapse risk of existing non-ductile RC frame structures is presented in Section 3.1. The collapse assessment procedure begins by identifying characteristics of archetypical non-ductile RC structures, in order to obtain a finite set of structures that is representative of the structural system of interest (Section 3.1.2). These structures are then idealized in nonlinear simulation models (Section 3.1.3) that capture the critical failure modes of the system. Incremental dynamic analysis of the nonlinear model is used for predicting structural behavior up to and including structural collapse, as described in Section 3.1.4. Related issues regarding selection and scaling of ground motions, incorporation of non-simulated failure modes and structural modeling uncertainties are discussed in Sections 3.1.5 – 3.1.7. Following this overview, aspects of creating analysis models for RC frame structures are discussed in detail in Section 3.2. Section 3.3 illustrates the collapse assessment procedure for a case study structure, an 8-story non-ductile RC frame designed according to the 1967 Uniform Building Code. This assessment is compared to the results of ASCE/SEI 41 guidelines for *Seismic Rehabilitation of Existing Buildings*.

3.1.2 Archetypical Non-Ductile Reinforced Concrete Frame Structures

For the purposes of assessing seismic performance, the class of older, non-ductile RC frame structures is characterized using the concept of archetypical buildings. Archetype structures are a group of structures that are envisaged to represent the variety in design and performance possible among structures of the same building type. The ATC-63 project has employed the concept of archetypical structures to evaluate the performance of structural systems for the purpose of quantifying building response and performance factors in building code seismic provisions (ATC 2007).

Within the classification of non-ductile RC frame structures, there is significant variability related to structural geometry, building system configuration, and detailing decisions. For the purposes of collapse performance assessment, the critical design parameters are those that have a significant effect on component and system deterioration and structural collapse mechanisms. These design parameters are then used to guide the selection of archetypical structures for evaluation. For non-ductile RC moment frames, we identify the key design parameters based on previous studies by the author and colleagues (Haselton 2006; Haselton et al. 2007), as well as work by others documenting observed damage in past earthquakes, experimental data, and analytical results, e.g. (Kunnath et al. 1995; Kunnath et al. 1995; Filiatrault et al. 1998; Filiatrault et al. 1998; Fardis and Biskinis 2003). For example, the level of column axial compressive stresses, a byproduct of choices regarding system configuration and geometry, has a significant impact on column deformation capacity, which has been shown to be an important predictor for collapse performance (Ibarra 2003; Haselton et al. 2007). As a result, the archetype assessment should consider design factors that affect the column axial loads, such as gravity load intensity, building height, and column spacing. It is also necessary to establish the bounds for critical design variables, based on governing design provisions and commonly expected structural design practice, which may limit, for example, the range of building heights or framing span lengths that are considered. A set of building designs is then identified to interrogate the archetype design space that describes the range of possible building configurations (e.g. height, layout, and so forth) for the building class of interest.

Based on these considerations, non-ductile RC frame structures are represented in this study by archetype structures of 2, 4, 8 and 12 stories, and consisting of both perimeter and space frame systems, as illustrated in Figure 3.1. In addition, other variations in design and detailing are also considered, and discussed in more detail in Chapter 5. This set of buildings

is expected to capture critical aspects of seismic performance for the purpose of evaluating in a general sense non-ductile RC frame structures that are common to California. The archetype structures are then modeled and analyzed using the collapse performance assessment methodology described in the following sections.

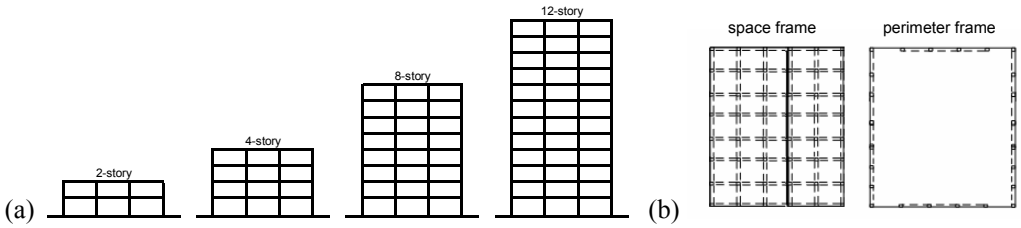

Figure 3.1 Archetype non-ductile RC frame structures illustrating (a) frame elevations and (b) frame plans.

3.1.3 Nonlinear Analysis Models

Assessment of a structure's seismic performance requires development of a nonlinear analysis model of the structure, which is then subjected to dynamic analysis to evaluate structural response. Each of the archetypical structures is idealized and analyzed. The analyses are conducted using a two-dimensional, three-bay frames in OpenSees, an open-source, object-oriented software platform developed by researchers at PEER (PEER 2006). For simplicity, only the lateral resisting system is modeled, neglecting the contributions of elements designed primarily for gravity loads or nonstructural elements.

Significant aspects of the analysis model are illustrated in Figure 3.2. A three-bay model is the minimum number of bays deemed necessary to capture behavior of interior and exterior columns and joints in structures that may have a larger number of bays. To ensure that the model faithfully represents the structure and possible failure modes, accurate representation of material properties and deterioration of beam-columns and joints is needed. As part of a companion effort to this study, nonlinear element models for RC beam-columns were calibrated to capture the yielding, strain hardening, and spalling and rebar buckling that leads to degradation of strength and stiffness in the structure, as described in Section 3.2.2. Modeling of possible joint shear failure in beam-column joints is the focus of Section 3.2.3.

The effect of foundation flexibility is incorporated using elastic, semi-rigid rotational springs at the base of each column (not shown in Figure 3.2). For structures with fewer than four stories, the stiffness of the rotational springs is determined from assumed grade beam stiffness and soil stiffness. For taller buildings, the computed rotational stiffnesses account for the presence of a basement wall (assumed rigid).

All model parameters account for expected rather than nominal values of material strength. The nominal f_y= 60 ksi for rebar is modeled with expected f_y = 67 ksi ((Melchers 1999). Expected levels of gravity loading are applied to the model, including 1.05 times the computed dead load and 12 psf for live load (25% of the design office loading of 50 psf) (Ellingwood et al. 1980). These expected gravity loads are also used in defining seismic masses, which are assigned at each floor of the building. The tributary width used in determining the seismic mass is equal to the bay width for space frame structures and half the total width of the building, for perimeter frame structures. Slab contributions to beam strength and stiffness are accounted for using an effective width. The effective width for strength is based on guidelines in ACI 318 (ACI 2002). The effective width for stiffness is one-third of the bay width, following suggestions from Robertson (2002). Five percent Rayleigh damping is applied to the first and third mode of elastic response. To account for the degradation of strength and stiffness associated with large deformations, the analysis utilizes suitable geometric transformations and a leaning (P-Δ) column. Robust convergence algorithms for solving simultaneous equations when strength and stiffness is degrading are implemented in OpenSees.

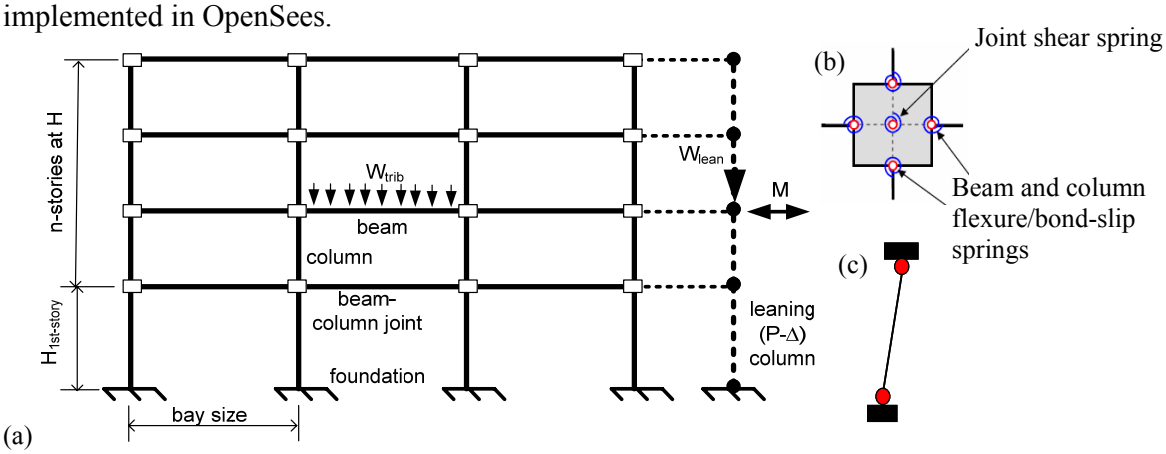

Figure 3.2 Key elements of nonlinear frame model, showing (a) archetype analysis model, (b) schematic of beam-column and joint material nonlinearities and (c) illustration of lumped plasticity beam-column elements.

3.1.4 Incremental Dynamic Analysis

Nonlinear simulations for predicting collapse are conducted using the incremental dynamic analysis technique (Vamvatsikos and Cornell 2002). In incremental dynamic analysis, illustrated in Figure 3.3, a recorded or synthetic ground motion is selected, applied to the nonlinear analysis model of the structure, and structural time-history response is computed. The peak interstory drift in the structure is an important parameter for predicting collapse, but other engineering demand parameters, such as plastic rotations and floor

accelerations may also be critical. Once this analysis is completed, the ground motion record is multiplied by a scale factor, and the simulation model is analyzed again. The ground motion is then scaled to increasing intensity, repeating the dynamic analysis until the structure has collapsed, as indicated by runaway interstory drifts, i.e. dynamic instability. Due to differences in frequency content, duration and other characteristics, different ground motion records do not give the same response, even when they are scaled to the same intensity. Therefore, the collapse prediction is repeated for a suite of ground motion records, in order to capture record-to-record variability in the response. Depending on the computational power available and complexity of nonlinear analysis models, the computer time required to complete incremental dynamic analysis, like the results shown in Figure 3.3, could be as much as 20 hours. The outcome of this assessment is a prediction of the probability the structure collapses, as a function of ground motion intensity. This method has been used for predicting collapse by a number of researchers including Ibarra (2003), Zariean (2006), and Haselton (2006), among others.

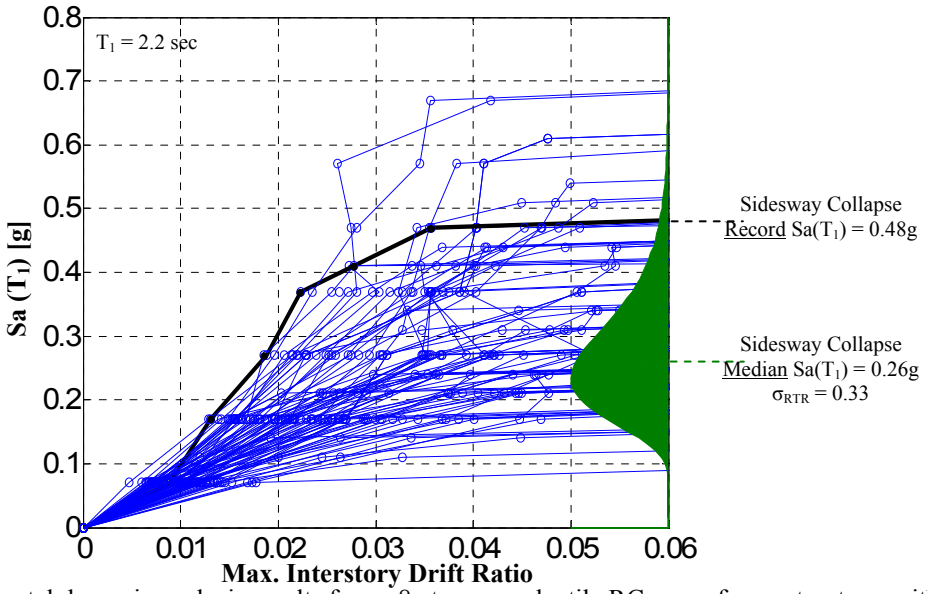

Figure 3.3 Incremental dynamic analysis results for an 8-story non-ductile RC space frame structure, with results blackened for one selected earthquake record. A lognormal probability distribution, representing the probability of collapse as a function of ground motion intensity is superimposed. The dispersion ($\sigma_{ln,RTR}$) of the probability distribution represents record-to-record uncertainty in the prediction of collapse.

A subtlety of the incremental dynamic analysis in this study is the treatment of pairs of ground motion records, recorded at the same site in two orthogonal directions. Each of these components is applied separately to the two-dimensional model of the structure. However, only the component of the pair of records that causes the structure to collapse first (i.e. at a lower ground motion intensity) is used in calculating the collapse probability distribution. By

basing the collapse predictions on the lower 'controlling' component of a pair of records, the three-dimensional collapse capacity of the structure can be approximated using a two-dimensional model. This approximation relies on the assumption that the structure has equivalent lateral resistance in its two orthogonal directions, and does not account for biaxial bending or torsional effects (See Section 3.2.5). Each structure is designed and analyzed as a two-dimensional frame, without consideration of bi-directional loading in either design or collapse assessment.

3.1.5 Ground Motion Selection, Scaling and Spectral Shape

A set of 22 pairs of recorded ground motion records is used in incremental dynamic analysis in this study. Many ground motion records are needed to account for uncertainty in the characteristics of the ground motions, such as frequency content, which are not fully captured by the ground motion intensity parameter (e.g. spectral acceleration). The set of ground motions used in the collapse assessment here are the far-field ground motions selected for the ATC-63 project (ATC 2007). The ground motion acceleration records were obtained from the PEER Next Generation Attenuation (NGA) database (PEER 2006). Selected records are the largest ground motions (PGA > 0.2g and PGV > 15 cm/sec) from large magnitude earthquakes ($M_w \geq 6.5$) that have been recorded in past seismic events. All ground motions were recorded at least 10 km from the fault, so that they reflect far-field ground motion characteristics without near-fault directivity effects. The ground motions included were recorded at soft rock or stiff soil sites. Selection also ensured that the filter frequencies were such that ground motion energy was retained up to at least 4 seconds. So as not to bias the results, the record set does not include more than two records from any one earthquake event.

In incremental dynamic analysis, ground motion records are scaled by the intensity of the records. Scaling is needed because there are few recorded ground motions that are strong enough to collapse a structure. Instead, the intensity of recorded ground motions is increased, until the structure collapses. The intensity measure used in this study is the geometric mean of the spectral acceleration of the pair of records at the fundamental (first mode) period of the structure of interest, denoted $Sa(T_1)$ (Baker and Cornell 2005).

The ground motion selection process described above is deliberately general so the set is applicable to many buildings with varying structural performance characteristics, and so does not account for characteristics of ground motion spectral shape. Previous studies have shown

that rare ground motions in California (e.g. ground motions with a 2500 year return period at a particular site), have a characteristic spectral shape that is significantly different from the shape of the code-design spectrum or uniform hazard spectrum (Baker and Cornell 2005). Compared to more frequent ground motions, the spectral intensity of rare ground motions is likely to be significantly larger in a small period range, and only somewhat larger at other periods, resulting in a 'peaked' spectral shape. This peaked shape occurs because, in California, these rare ground motions are uncharacteristically large ground motions (e.g. 2500 year return period) from relatively frequent earthquake events (e.g. 500 year return period). In California, the more rare the ground motion, the more peaked the spectral shape. Spectral shape can be quantified in terms of epsilon (ε), or the number of logarithmic standard deviations between the observed spectral value of the ground motion record and the median prediction from an attenuation function (based on the structure's period, magnitude and distance from the site).[1] Spectral shape must be explicitly considered in this analysis because the intensity measure used in this assessment, the spectral acceleration at the first mode period, is insufficient to characterize spectral shape.[2]

Since these large rare ground motions are typically those that will cause collapse of the California structures of interest, the effect of spectral shape should be considered in the collapse assessment procedure. Previous research has shown that the predicted collapse capacity of a structure subjected to a ground motion characterized by a 'peaked' spectrum ($\varepsilon > 0$) is higher than the collapse capacity of the same structure subjected to a record of the same intensity with average spectral shape (ε-neutral) (Baker and Cornell 2005; Haselton 2006; Haselton and Baker 2006; Goulet et al. 2007). This difference results from structural ductility and higher mode effects (ATC 2007). Provided that a structure is not brittle, its fundamental period will tend to elongate as its stiffness deteriorates before collapse and, if the structure is subjected to a 'peaked' record, this period increase tends to move the structure away from the most intense region of the spectrum. Likewise, higher modes are excited by a less damaging region of the spectrum. By not appropriately accounting for the spectral shape

[1]Computed using Abrahamson and Silva's (1997) attenuation relationship. In practice, any attenuation relationship could be used.

[2] Other intensity measures could also be used. Some of these, including the inelastic spectral displacement (S_{di}, Tothong et al. 2007), an average of spectral accelerations ($Sa_{avg,}$ Baker 2008), or a vector valued intensity measure ($<S_a, \varepsilon>$, Baker and Cornell 2005) already account for spectral shape, so other adjustments are not needed. $S_a(T_1)$ is used here despite this deficiency, because it is commonly used in practice, and because the site hazard information for this intensity measure is readily available.

of rare ground motions, the median collapse capacity of the structure may be under-predicted by 15 to 80%, depending on the ductility of the structure (Haselton 2006; Zareian 2006).

A variety of methods can be used to account for spectral shape (ε) of rare ground motions in California and their effect on median collapse prediction. One option is to select ground motions that have the 'peaked' shape and epsilon values consistent with those expected for the site, hazard level and period of interest (Baker and Cornell 2005; Goulet et al. 2006; Haselton et al. 2008). This method is impractical for this study, because it would require selecting a different set of ground motions for each archetype structure. Instead, the approach utilized here uses a general ground motion set selected without regard to epsilon or spectral shape, as described above, and then corrects the predicted collapse capacity distribution to account for the expected epsilon at the site and hazard level of interest (Haselton et al. 2008). Data from the generalized ground motion set is used to predict the relationship, using regression analysis, between the shape of a ground motion record, $\varepsilon(T_1)$, and the collapse capacity of a record, $Sa(T_1)$. The regression analysis, shown in Figure 3.4, depends on the structure, due to differences in ductility and fundamental period among different buildings. Accordingly, the mean collapse capacity can be adjusted to reflect the expected epsilon at a particular site. Haselton et al. (2008) has shown that this approach provides similar results to a method that selectively chooses records based on the site, hazard and structure.[3]

The effect of spectral shape on the predicted collapse capacity of the structure depends on the ductility of the building and the level of hazard or rarity of ground motions that cause collapse. 'Peaked' spectral shape has a less significant effect on non-ductile structures than ductile structures, because the period elongation preceding collapse is less significant, but any non-brittle structure is impacted. The expected epsilon depends on the rarity (and by extension spectral shape) of the ground motion expected to collapse the structure. Non-ductile RC structures collapse at intensities close to the 2% in 50 year ground motion of highly seismic sites in California. Disaggregation data from the USGS reveals that these rare ground motions have $\varepsilon = 1.2$, on average (ATC 2007; Haselton et al. 2008). Therefore, the expected $\varepsilon = 1.2$ is used in post-processing adjustment for appropriate spectral shape.

[3] Haselton et al. (2008) also finds that the variability in the collapse fragility is reduced when ground motions records with appropriate spectral shape are used. However, this effect is small, and is neglected here for simplicity.

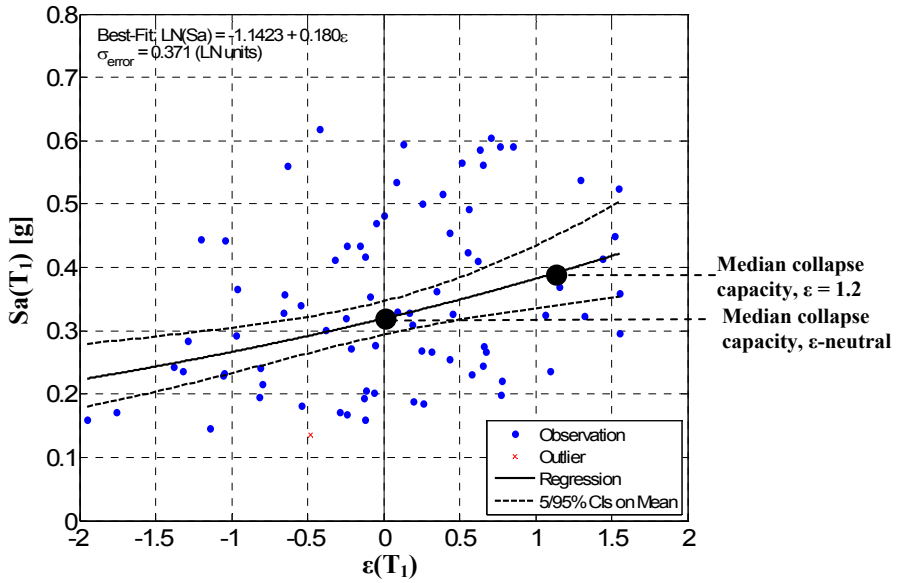

Figure 3.4 Relationship between collapse capacity and ε (spectral shape), showing results of regression analysis for the 8-story non-ductile RC frame structure.[4]

3.1.6 Assessment of Non-Simulated Failure Modes

Despite the care taken in developing nonlinear analysis models, the simulation model may not be able to capture all possible collapse modes, due to limitations in model technologies or available data for model validation. To avoid non-conservative under-prediction of collapse probabilities, these non-simulated failure modes should be incorporated by back-checking dynamic analysis results to determine whether these failure modes may have occurred before the sidesway collapse that was simulated. In the non-ductile RC frame structures, columns are potentially vulnerable to brittle shear failure, a failure that may eventually cause collapse of a portion of the structure when the column loses its ability to carry its gravity loads. For the columns in this study, which are expected to yield before failing in shear, the models described in Section 3.1.3 capture the important aspects of strength and stiffness deterioration as the column yields and, subjected to increasing deformations, fails in shear. However, the model cannot capture the subsequent axial collapse of column, because the column model does not incorporate axial-shear interaction. Post-processing for identifying this non-simulated failure mode and adjusting the resulting collapse fragility is discussed in detail in Section 3.2.4.

[4] A t-test was used to identify outliers, based on whether each residual has the same variance as the other residuals. Outliers were removed when the t-test showed a 5% or lower significance level.

3.1.7 Incorporating Uncertainties in Structural Modeling

Performance-based earthquake engineering enables probabilistic prediction of structural response, incorporating key sources of uncertainty in the process. By using a suite of earthquake records, incremental dynamic analysis directly incorporates information about variability in ground motions in the collapse performance assessment. However, incremental dynamic analysis alone does not account for how well the nonlinear simulation model represents the real building. These modeling uncertainties are especially important in predicting collapse, because of the high degree of empiricism and uncertainty in predicting deformation capacity and other critical parameters for modeling collapse. In this study, first order-second moment methods from structural reliability are used to approximate the effects of modeling uncertainties by increasing the dispersion in the collapse fragility. Analysis of the effect of modeling uncertainties on the collapse assessment process and an investigation of the appropriateness of FOSM assumptions are the focus of Chapter 4.

3.1.8 Outcome of Collapse Performance Assessment

The outcome of the collapse assessment procedure when applied to a particular structure is a probability distribution representing the cumulative probability of collapse, P[Collapse] = P[$Sa_{collapse}$ <Sa] as a function of the ground motion intensity, as illustrated in Figure 3.5. This collapse fragility curve is obtained by creating nonlinear analysis models of non-ductile RC frames (Section 3.1.3) and conducting incremental dynamic analysis (Section 3.1.4) with post-processing to account for the possible occurrence of non-simulated failure modes (Sections 3.1.6 and 3.2.4). The collapse fragility is adjusted for the expected spectral shape of rare ground motions in California (Section 3.1.5) and the increased variability associated with uncertainty in structural modeling (Section 3.1.7 and Chapter 4).

Important metrics for quantifying collapse resistance of structures are defined and illustrated in Figure 3.5, including the median collapse capacity, obtained directly from the collapse assessment procedure and given in terms of $Sa(T_1)$, and the conditional probability of collapse at an intensity level of interest. The ground motion intensity of interest depends on the ground-shaking hazard at the location of the structure. The ground motion that has a 2% likelihood of being exceeded in 50 years ($Sa_{2/50}$) at a particular site is frequently considered, which is typically consistent with the code-defined Maximum Considered Earthquake (MCE). Figure 3.5 also shows the Collapse Margin Ratio (CMR), a ratio of the median collapse capacity to $Sa_{2/50}$. This metric can be interpreted as a safety factor at the

ground motion intensity of interest. Ground motion hazard curves for a typical highly seismic, but not near field site in Los Angeles are illustrated in Figure 3.6. The hazard curve defines the mean annual frequency of exceeding a specified ground motion intensity at the site. When the collapse fragility curve and the hazard curve are integrated together, another possible metric for collapse performance, the mean annual frequency of collapse, is obtained, which describes how likely collapses are to occur, given the collapse capacity of the structure and the ground-shaking hazard at the site (Krawinkler and Miranda 2004).

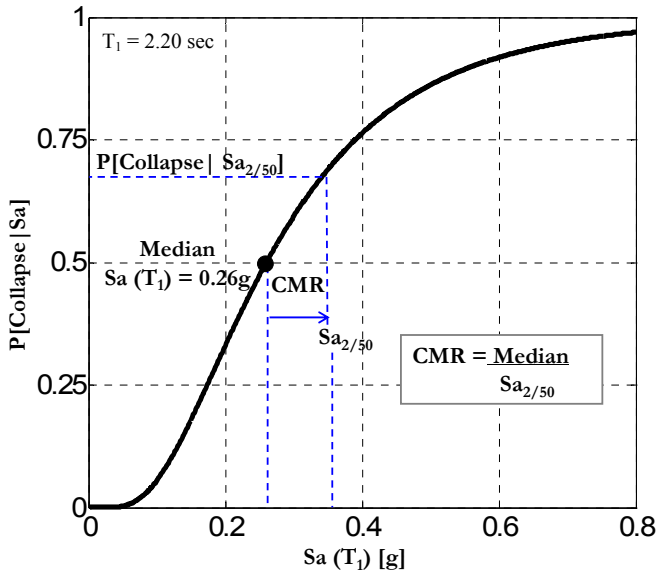

Figure 3.5 Collapse fragility curve for 8-story non-ductile RC space frame structure, illustrating key metrics for collapse performance.

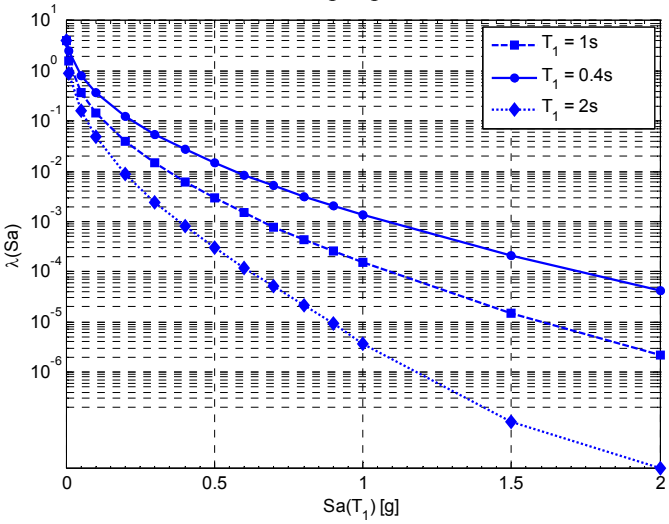

Figure 3.6 Hazard curve for the selected Los Angeles site, obtained from probabilistic seismic hazard analysis by Goulet et al. (2007).

3.2 Modeling of Non-Ductile Reinforced Concrete Frames

3.2.1 Analysis Model for Capturing Key Collapse Modes in Reinforced Concrete Frames

Analytical simulation of collapse requires accurate modeling of deterioration associated with seismic loading for each of the constituent elements in the structural system, such that all possible local and global collapse modes can be captured. Potential element deterioration and failure modes are dictated by the design and detailing requirements that are used in the structural design and the properties of the material and structural system. Once all collapse scenarios have been identified for a given structural system, the list can be narrowed down to a subset of likely collapse mechanisms using experimental test data, engineering judgment, analytical models, and observations from past earthquakes. The identified collapse modes then serve as the basis for selecting appropriate simulation and damage models that can be used to predict structural collapse.

Element Deterioration Modes

Potential deterioration modes for components of RC moment frame systems subjected to earthquake motions are summarized in Table 3.1. Failure modes are identified for each component based on a review of available literature and observations from experimental tests and past earthquakes. The deterioration modes are classified into five groups (A to F) depending on the type of structural element and the physical behavior associated with deterioration.[5] These deterioration modes are illustrated in Figure 3.7 and Figure 3.8. To simulate the nonlinear cyclic response of RC frame components, existing element models were evaluated to determine their appropriateness for collapse assessment of RC frame structures. Evaluations of the adequacy of available modeling techniques are included in Table 3.1. Choice of element models for deterioration related to beam-column flexural hinging, beam-column shear failure and beam-column joint shear failure are discussed in more detail below.

Yielding of reinforcement bars and concrete core crushing associated with flexural hinging in beams and columns of RC frames (A) can be simulated fairly accurately (e.g. Elwood (2004)). Models are less robust for simulating buckling and fracture of longitudinal reinforcement or stirrup fracture that also may occur as hinges develop. Even so, these

[5] Foundation failure modes have not been included because they are not thought to be critical for this system.

behaviors are important contributors to the deterioration of strength and stiffness at large deformations near collapse in RC frame elements. Either fiber-type or lumped plasticity (plastic hinge-type) models could be used to model behavior associated with flexural deterioration. For this study, a lumped plasticity model, calibrated to mimic the effects of yielding, spalling and bar buckling is used in the analysis model for RC frames. While lumped plasticity models lack the detail and spread-plasticity capabilities of fiber models, they can be calibrated to capture the deterioration associated with rebar buckling and stirrup fracture leading to loss of confinement (Ibarra 2003; Haselton 2006). Fiber-type models were judged unsuitable for simulating structural collapse because available steel material models are not able to replicate the behavior of rebar as it buckles and or fractures (Haselton 2006). The lumped plasticity models for beam-columns are calibrated to data from experimental tests, as described in Section 3.2.2. These models also account for bond-slip (E) that occurs in regions of high bond stresses in beam-column joints and other anchorage points. However, the models do not account for the possibility of rebar pull-out and the resulting loss in strength.

Table 3.1 Deterioration modes of reinforced concrete elements.

Deterioration Mode	Element	Behavior	Simulation Model Availability[1]	Fragility Model Availability[1]	Physical Behavior
A	Beam-column	Flexural	4	NR	Concrete cracking
					Concrete spalling
					Reinforcing bar yielding
					Concrete core crushing
					Reinforcing bar buckling (incl. stirrup fracture)
					Reinforcing bar fracture
B	Beam-column	Axial compression	2	4	Concrete crushing, longitudinal bar yielding
					Stirrup rupture, longitudinal bar buckling
C	Beam-column	Shear Shear + Axial	1	4	Concrete shear cracking
					Transverse tie pull-out or rupture
					Concrete crushing
					Loss of aggregate interlock
					Possible loss of axial looad carrying capacity in columns
D	Beam-column joint	Shear	3	2	Panel shear failure
E	Reinforcing bar connection	Pull-out or Bond-slip	2	2	Reinforcing bar bond-slip or anchorage failure at joint
					Reinforcing bar lap-splice failure
					Reinforcing bar pull-out (in beams or footings)
F	Slab connection	Shear	2	3	Punching shear or failure at slab-column connection
					Possible vertical collapse of slab

[1]Model Maturity-- 0:Non existent, 1-5: 1- low confidence to 5 - high confidence; NR - Not required; behavior can be simulated

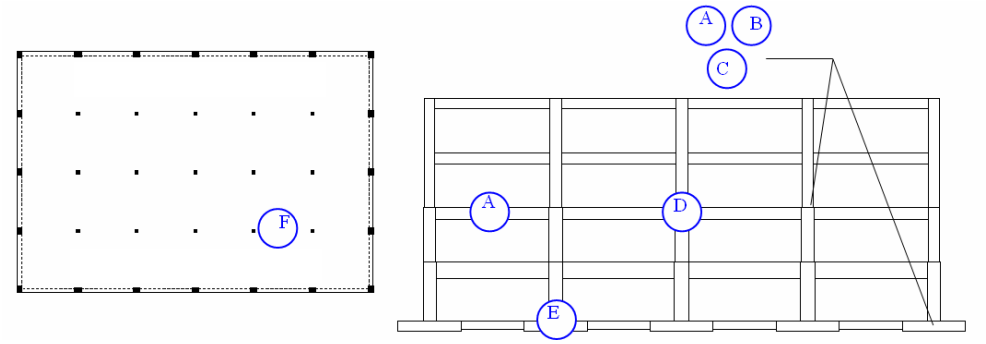

(a) (b)

Figure 3.7 RC frame building (a) plan and (b) elevation views, showing location of possible deterioration modes.

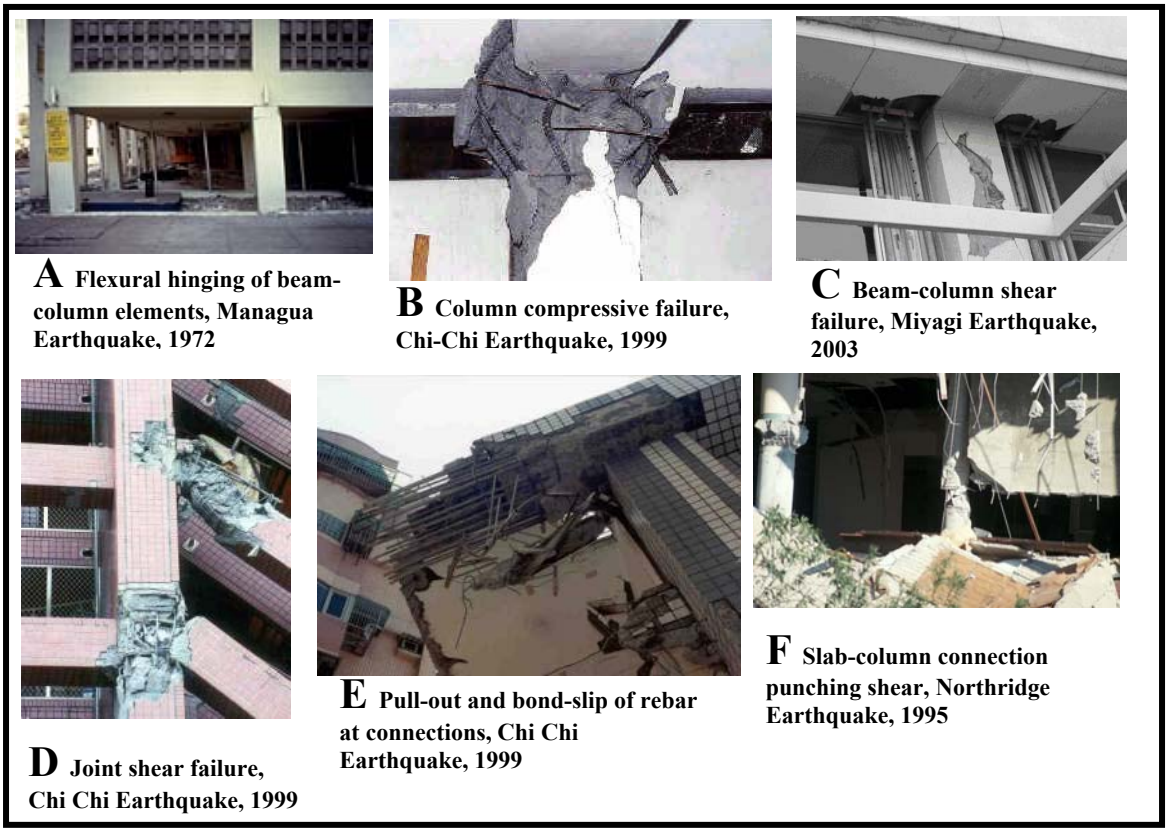

Figure 3.8 Illustration of possible deterioration modes for RC frame structures.[6]

Shear failure of beams and columns (C) is characterized by shear cracking in concrete and yielding, pull-out or fracture of transverse reinforcement. This mode of deterioration is particularly dangerous for columns with significant axial load, as shear failure can lead to subsequent vertical collapse of the column (Elwood and Moehle 2005). Modeling the cyclic

[6] Photo sources: NISEE, UCSD Structural Engineering and Earthquake Disaster-Research Laboratory (Tohoku Univ.)

response of a RC element experiencing shear deterioration is complex due to the interactions of shear, moment, and axial forces, as well as the overall brittle nature of the deterioration mode. Elwood (2004) and others have simulated the deterioration in the lateral strength and stiffness of a column by adding a shear spring. In the models developed here, this behavior is lumped in the flexural hinges described above. To date, the models for vertical collapse of columns following shear failure have been challenged by a lack of experimental data for columns experiencing vertical collapse. Where this failure mode is not prevented through capacity design provisions, fragility functions can be used to post-process dynamic analysis data to account for possible column collapse associated with shear failure.

To capture deterioration associated with degradation of shear strength and stiffness in the beam-column joint region (D), the shear panel is modeled with an inelastic rotational spring inserted at the joint (Altoontash 2004; Lowes et al. 2004). The modified compression field theory can be used to determine model parameters in seismically detailed joints that have high levels of confinement and transverse reinforcement (Vecchio and Collins 1986; Stevens et al. 2001), however, this method is not as reliable for non-conforming joints with less confinement (Lowes 2005). The properties of the joint model in this study are based on selected experimental data obtained from Lowes (2007).

Local and Global Collapse Scenarios

Structural collapse occurs when ground shaking causes element deterioration modes to combine to form a collapse mechanism. For RC frame structures, the possible collapse scenarios and contributing element deterioration modes are identified and organized as shown in Table 3.2. These scenarios were established through engineering judgment based on examination of collapses in previous earthquakes, experimental test data, and analytical studies.

For RC frame structures, design and detailing requirements govern which of the collapse modes may occur. The building code requirements for modern special moment frames are designed to promote ductile and more desirable collapse modes, and to prevent the formation of the brittle collapse modes (ACI 2002; ASCE 2002; ICC 2003). The strong column – weak beam requirement promotes flexural hinging in beams before columns, though it does not completely eliminate plastic deformations in columns (Ibarra 2003). Likewise, shear strength capacity design provisions for beams and columns are meant to ensure that shear failure is highly unlikely in beam-column elements. With minimal detailing requirements used in their

design, older RC moment frames are vulnerable to a wider range of possible collapse modes (Aycardi et al. 1994; Kurama et al. 1994; Kunnath et al. 1995; Kunnath et al. 1995; El-Attar et al. 1997; Filiatrault et al. 1998; Filiatrault et al. 1998). These structures have a demonstrated tendency to fail in soft story or column-hinging mechanisms. Column shear failure may occur, depending on the column's design and gravity loading. Less stringent detailing requirements may allow lap-splice failure, pull-out of the bottom beam reinforcing bars or shear failure in beam-column joints. Table 3.3 reports which collapse scenarios are expected in existing non-ductile and modern ductile RC frame structures, and through cross-reference to Table 3.2, the corresponding element deterioration modes, whose inclusion in the analytical model is essential.

Table 3.2 Possible collapse scenarios for RC frame structures.

Scenario		Element Deterioration Mode						Description
		A	B	C	D	E	F	
Sidesway Collapse Scenarios	FS1	■						Beam and column flexural hinging, forming sidesway mechanisms
	FS2	■						Column hinging, forming soft-story mechanism or a multi-story mechanism
	FS3	■		■				Beam or column flexure-shear failure, forming sidesway mechanism
	FS4	■			■			Joint shear failure, possibly with beam and/or column hinging
	FS5	■				■		Reinforcing bar pull-out or splice failure in columns or beams, leading to sidesway mechanism
Vertical Collapse Scenarios	FV1			■				Column shear failure, leading to column axial collapse
	FV2	■		■				Column flexure-shear failure, leading to column axial collapse
	FV3						■	Punching shear failure, leading to slab collapse
	FV4							Failure of floor diaphragm, leading to column instability
	FV5		■					Crushing of column, leading to column axial collapse; possibly from overturning effects

Table 3.3 Likelihood of observing various collapse scenarios, by frame type.

Systems	Sidesway Collapse					Vertical Collapse					
	FS1	FS2	FS3	FS4	FS5	FV1	FV2	FV3	FV4	FV5	FV6
Modern, Ductile RC Special Moment Frames	H	M	L	L	L	L	L	L	L	L-M	L-M
Existing, Non-Ductile RC Moment Frames	H	H	H	H	H	M	H	M	M	M-H	M-H

H: High, M: Medium, L: Low

Collapse Simulation Model

Analytical models for assessing collapse performance should account for all collapse scenarios that have been identified as likely to occur. These critical limit states are ideally

simulated directly in the nonlinear analysis, but can also be evaluated through separate checks based on fragility functions that predict failure in structural components as a function of structural response. The discussion above illustrates how element deterioration modes and collapse scenarios were used in identifying element models to use in modeling collapse of RC frame structures. For simulation of RC frame systems, these element models are used in the context of a two-dimensional three-bay variable-height archetype frame model, as shown in Figure 3.2. As described above, nonlinear model features include concentrated inelastic rotational hinges to capture flexure and bond-slip deformations in beams and columns, and finite size beam-column joints with joint shear spring. Destabilizing P-Δ effects are modeled using a leaning column.

3.2.2 Calibration of Lumped Plasticity Model for Beam-Column Elements

Beam-Column Element Model

Accurate modeling of inelastic behavior in beam and column elements is an essential component of collapse modeling of RC frame structures. The lumped plasticity element models used to simulate plastic hinges in beam-column elements utilize a nonlinear spring model developed by Ibarra, Medina, and Krawinkler (2005), and implemented in OpenSees by Altoontash (2004). This model is chosen because it is capable of capturing the important modes of deterioration that precipitate sidesway collapse of RC frames. Figure 3.9 shows the tri-linear monotonic backbone curve, which together with associated hysteretic rules of the model, permit versatile modeling of cyclic behavior. For simulating structural collapse, the most important aspect of this model is the post-peak response, which enables modeling the strain softening behavior associated with concrete crushing, rebar buckling and fracture, and/or bond failure. The model also captures four modes of cyclic deterioration: strength deterioration of the inelastic strain hardening branch, strength deterioration of the post-peak strain softening branch, accelerated reloading stiffness deterioration, and unloading stiffness deterioration. Cyclic deterioration is based on an energy index that has two parameters: normalized energy dissipation capacity, λ, and an exponent term to describe how the rate of cyclic deterioration changes with accumulation of damage, c.[7] In total, the model requires

[7] As implemented, distinct values of λ and c can be assigned for each cyclic deterioration mode. Simplifying assumptions in this study reduce these 8 parameters to 2 (see Table 3.4).

the specification of seven parameters to control the monotonic and cyclic behavior: M_y, K_e, M_c/M_y, $\theta_{cap,pl}$, θ_{pc}, λ, and c (defined in Figure 3.9). M_c/M_y is a measure of post-yield stiffness (such that $K_s = K_e\left(\theta_y/\theta_{cap,pl}\right)\left(\left(M_c - M_y\right)/M_y\right)$). Likewise, θ_{pc} is related to the post-capping stiffness, where $K_c = -K_e\left(\theta_y/\theta_{pc}\right)\left(M_c/M_y\right)$. The model can also be assigned a residual strength, as a function of the ultimate strength, which is not shown on Figure 3.9. In this research, 1% residual strength is used for all beams and columns to avoid problems with numerical convergence. It is likely that RC beams and columns actually have higher residual strength such that the model is quite conservative, but it is difficult to quantify on the basis of available experimental data. Notation is defined in the notation list.

In order to determine the appropriate values of each of these parameters, the Ibarra model parameters are calibrated to 255 experimental tests of RC columns. These calibrations are then used to develop empirical equations relating the design parameters of a beam or column to the modeling parameters needed for input in the lumped plasticity model. All calibrations are based on mean values, unlike the conservative values given in the FEMA 356/ASCE 41 documents. A full report on the calibration study is available in (Haselton et al. 2007).

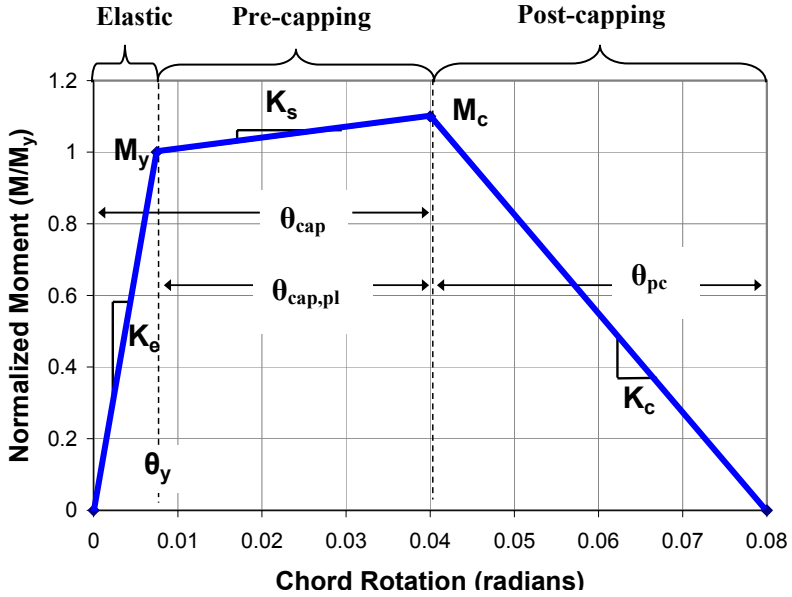

Figure 3.9 Monotonic behavior of Ibarra component model used to model beam-column elements.

Calibration Procedure

The parameters of the Ibarra material model are calibrated to data from rectangular columns included in the PEER Structural Performance Database (Berry et al. 2004). The database includes RC columns with both ductile and non-ductile detailing, and varying levels

of axial load and geometries and, for each, reports force-displacement history and other relevant data. Approximately 35 of the 255 column tests have non-ductile detailing and failed in flexure-shear, as expected for the older RC columns of interest in this study. In order to calibrate the element model parameters, each column test is modeled as a cantilever column in OpenSees, idealized using an elastic element and a zero-length Ibarra model plastic hinge at the column base. The properties of the plastic hinge are the subject of this calibration effort.

The calibration of the beam-column element model to the data from each experimental test follows a standardized procedure, as shown in Figure 3.10 and detailed in Table 3.4. Particular emphasis is placed on correct calibration of the capping point and post-capping strength deterioration, which can have a significant impact on structural response prediction. The calibration procedure carefully distinguishes between in-cycle and cyclic strength deterioration. In in-cycle strength deterioration, strength is lost in a single cycle, which means that the element exhibits negative stiffness. In cyclic strength deterioration, strength is lost between two subsequent cycles of deformation, but the stiffness remains positive. In-cycle strength deterioration is calibrated with a capping point only where a negative stiffness is observed in the data. Otherwise, a lower-bound capping point is determined. Because insufficient data is available to calibrate the monotonic and cyclic behavior separately, this calibration effort relies primarily on cyclic tests to calibrate both the monotonic backbone parameters and the cyclic deterioration rules. As a result, the monotonic backbone and the cyclic deterioration rules are interdependent, and the approximation of the monotonic backbone depends on cyclic deterioration rules assumed. A full table of calibrated model parameters for each of the 255 experimental tests used can be found in the extended report on this study (Haselton et al. 2007).

The calibrated model parameters from the 255 column tests are used to create empirical equations that predict model parameters on the basis of column design parameters. The functional form used in regression analysis was determined based on trends in the data and isolated effects of individual variables, previous research (e.g. Fardis et al. (Panagiotakos and Fardis 2001; Fardis and Biskinis 2003), Elwood and Eberhard (2006), Berry and Eberhard (2005), and others (Comité Euro-International du Béton 1996)) and judgment based on mechanics and expected behavior. Regression analysis was performed using the natural logarithm of the model parameter and the logarithmic standard deviation quantifies the uncertainty. The parent report on this study provides more details on how the data was

dissected to create empirical regression equations to predict each model parameter and the treatment of lower bound data in the analysis(Haselton et al. 2007).

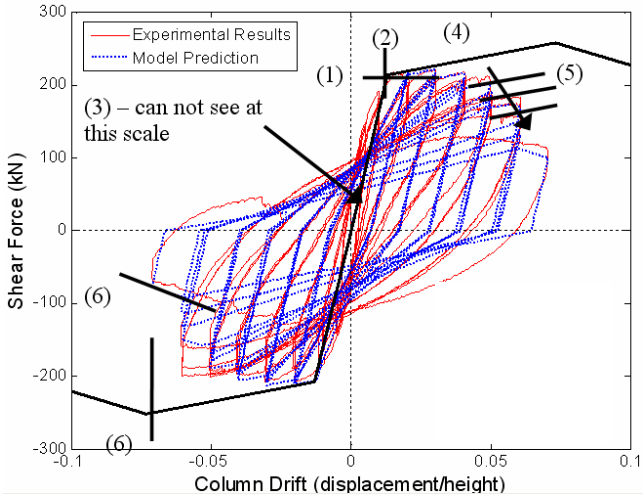

Figure 3.10 Calibration of Ibarra element model to a selected experimental test of a RC column, from (Haselton et al. 2007).

Table 3.4 Calibration procedure used to match element model to RC column tests.

Calibration Step	Parameter Calibrated	Notes
1	Shear force at yielding	Estimated visually from experimental results.
2	Displacement at yielding	Identified as the point of significant observed change in lateral stiffness, ie. where rebar yielding or significant concrete crushing occurs. Since RC elements may exhibit highly nonlinear behavior before rebar yielding occurs, judgment was required here.
3	Displacement at 40% of yield force	Measure of initial stiffness.
4	Post-yield hardening stiffness	Visually calibrated.
5	Normalized cyclic energy dissipation capacity (λ)	The element model allows cyclic deterioration coefficients λ and c to be calibrated independently for each of the four cyclic deterioration modes. The deterioration rates, λ, were set to be equal for the basic strength and post-capping strength deterioration modes. Based on observations of the hysteretic response of the RC columns, no accelerated stiffness deterioration was used.[1] c = 1.0 was found to be acceptable in a pilot study. These simplifications reduce the calibration of cyclic energy dissipation capacity to one parameter, λ. When calibrating λ, the aim was to match the average deterioration for the full displacement history, but with a slightly higher emphasis on matching the deterioration rate of the later, more damaging, cycles.
6	Post-capping point and post-capping deformation capacity	The capping point and post-capping stiffness were only calibrated when a negative post-peak stiffness was clearly observed in the data, ie. where strength loss occurs within a single cycle. Where no capping point was observed, a lower bound value of the capping point was calibrated.

[1]Unloading stiffness deterioration was neglected to avoid a bug in the OpenSees implementation of the element model.

Equations for Predicting Parameters of Beam-Column Element Model

The calibration process results in a comprehensive set of equations capable of predicting the parameters of a lumped plasticity element model for a RC beam-column. These

equations are proposed for use with the element model developed by Ibarra et al. (2005), but could in concept be used with any comparable model. Presented below, the predictive empirical equations provide a critical link between column design parameters, such as axial load or provision of transverse reinforcement, and element modeling parameters, facilitating the creation of nonlinear structural models of RC frame elements. Model parameters are predicted in terms of their mean value, as well as the uncertainty in that prediction. Estimates of uncertainty in the prediction of model parameters can be used in sensitivity analyses and propagation of structural modeling uncertainties.

Effective Stiffness (EI_y/EI_g and EI_{stf}/EI_g)

Since RC elements decrease in stiffness as cracking occurs, the definition of the stiffness of a RC element depends on the load and deformation level. Two measures of effective stiffness are defined here: (a) the secant stiffness to the yield point of the component (EI_y), and (b) the secant stiffness to 40% of the yield force of the component (EI_{stf}). Stiffness is quantified as a fraction of the stiffness of the gross (uncracked) section (EI_g). The component stiffness accounts for all modes of deformation, including flexure, shear, and bond-slip.

The equation for secant stiffness to yield depends on both axial load ratio ($\nu = P/A_g f'_c$) and shear-span ratio (L_s/H) of the column, and is given as

$$\frac{EI_y}{EI_g} = -0.07 + 0.59\left[\frac{P}{A_g f_c'}\right] + 0.07\left[\frac{L_s}{H}\right] \quad (3.2),$$

where $0.2 \le \frac{EI_y}{EI_g} \le 0.6$. The prediction uncertainty, assuming the residuals are lognormally distributed, is given by the logarithmic standard deviation: $\sigma_{LN} = 0.28$. The coefficient of determination, R^2, a measure of the extent to which the proposed equation explains the data, is 0.80. For Equation (3.2) and all equations to follow, these values are reported below in Table 3.5. The upper and lower limits on the stiffness were imposed because there is limited data for columns with very low axial loads and, at high levels of axial load, the positive trend diminishes and the scatter in the data is large. The limits were chosen based on a visual inspection of the data.

The effective initial stiffness, defined as the secant stiffness to 40% of the yield force of a RC column, is predicted by Equation (3.3):

$$\frac{EI_{stf}}{EI_g} = -0.02 + 0.98\left[\frac{P}{A_g f_c'}\right] + 0.09\left[\frac{L_s}{H}\right] \quad (3.3),$$

where $0.35 \le \frac{EI_{stf}}{EI_g} \le 0.8$. For a typical column, Equation (3.3) predicts an initial stiffness approximately 1.7 times stiffer than the secant stiffness to yield (Equation 3.2). The stiffer effective stiffness (EI_{stf}/EI_g) is used in creation of nonlinear analysis models. Typical model parameters for columns like those found in older, non-ductile RC frame structures are reported in Table 3.6. The same stiffness equation is used for modeling RC beams.

The effective stiffness of RC beam-columns has been the subject of much research and for comparison, selected studies are presented here. FEMA 356 guidelines permit the use of standard simplified values based on the level of axial load in columns: $0.5EI_g$ when $\nu < 0.3$ and $0.7EI_g$ when $\nu > 0.3$ (ASCE 2000). The stiffness predictions in FEMA 356 are higher than the values predicted in this study. Most of this difference can be explained if the FEMA 356 values only include flexural deformation and not bond-slip deformations, which can account for a significant proportion of an element's flexibility. More recently, Elwood and Eberhard (2006) proposed an equation for effective stiffness that includes all components of deformation (flexure, shear, and bond-slip), where the effective stiffness is defined as the secant stiffness to the yield point of the component (see also (Elwood et al. 2007)). The equations developed here for EI_y are similar to those recently proposed by Elwood and Eberhard, except that the models used here include an L_s/H term to reduce prediction uncertainty.

Flexural Strength (M_y)

The flexural strength, M_y, is calculated using equations previously developed and published by Panagiotakos and Fardis (2001). As illustrated by Haselton et al. (2007), their equations show good agreement with the test data from the PEER Structural Performance Database.

Plastic rotation capacity ($\theta_{cap,pl}$)

The plastic rotation capacity ($\theta_{cap,pl}$) of a RC element can be predicted by Equation (3.4). The plastic rotation capacity depends primarily on the axial load ratio ($\nu = P/A_g f'_c$) and the area ratio of transverse reinforcement (ρ_{sh}), though the concrete compressive strength (f'_c), the longitudinal reinforcement ratio (ρ), and the rebar buckling coefficient (s_n) were also

statistically significant.[8] a_{sl} is a flag to indicate whether or not reinforcing bar slip is included in the rotation capacity. As slip is usually always present, $a_{sl} = 1$ for almost all columns. It is included in Equation (3.4) because some of the experimental test configurations prevented bond-slip.

$$\theta_{cap,pl} = 0.12(1+0.55a_{sl})(0.16)^{v}(0.02+40\rho_{sh})^{0.43}(0.54)^{0.01f'c}(0.66)^{0.1s_n}(2.27)^{10.0\rho} \quad (3.4)$$

All input to Equation (3.4) is unit-less except f'_c, which should be given in MPa. For beams or columns with asymmetric arrangements of reinforcement, it is proposed to multiply the rotation capacity obtained from Equation (3.4) by a term proposed by Fardis and Biskinis (2003), which accounts for the ratio between the areas of compressive and tensile steel: $\left(\frac{\max(0.01, \frac{\rho' f_y}{f'_c})}{\max(0.01, \frac{\rho f_y}{f'_c})} \right)^{0.225}$, where ρ' is the is the area ratio of longitudinal reinforcement in compression and ρ is the area ratio of longitudinal reinforcement in tension. Equation (3.4) does not directly distinguish between seismic (e.g. 135º) and non-seismic hooks (e.g. 90º) on transverse reinforcement. Since structures with widely spaced shear stirrups often have non-seismic hooks, this effect is indirectly lumped with the ρ_{sh} term. Non-ductile columns and beams of the type considered in this study are expected to have non-seismic hooks.

It is useful as verification to compare the predicted rotation capacity to the ultimate rotation capacity predicted by Fardis et al., based on their study of 700+ RC elements, including beams, columns and walls (Panagiotakos and Fardis 2001; Fardis and Biskinis 2003). Since Equation (3.4) predicts the capping point and the Fardis equation is based on the ultimate (20% strength loss) point, the Fardis equation is used to back-calculate a prediction of $\theta_{cap,pl}$ for purposes of comparison. The proposed Equation (3.4) predicts slightly lower deformation capacities than Fardis et al., with a mean ratio of 0.94. Based on this comparison, Equation 3.4 may still include some conservatism. The predicted deformation capacities are already much higher than what is typically used. For example, values in FEMA 356 and ASCE/SEI 41 are typically less than one-half of those shown in Table 3.6.

[8] The rebar buckling coefficient (s_n) is defined by Dhakal and Maekawa (2002): $s_n = (s/d_b)(f_y/100)^{0.5}$, where f_y is the yield strength of the longitudinal rebar in MPa, s is the spacing of transverse reinforcement, and d_b is the diameter of the longitudinal bars.

Post-capping Rotation Capacity (θ_{pc})

The proposed equation for post-capping rotation capacity is

$$\theta_{pc} = (0.76)(0.031)^{\nu}(0.02 + 40\rho_{sh})^{1.02} \leq 0.10 \quad (3.5),$$

where it is predicted that post-capping rotation capacity (θ_{pc}), like plastic rotation capacity, is sensitive to axial load levels (ν) and provision of transverse reinforcement (ρ_{sh}). The upper bound imposed on Equation (3.5) is due to lack of reliable data for elements with shallow post-capping slopes, but the limit is expected to be conservative for well-confined columns. Since the experimental tests that exhibited post-capping behavior were the less ductile columns, Equation (3.5) is expected to provide better predictions for non-ductile RC columns.

Post-Yield Hardening Strength Ratio (M_c/M_y)

Regression analysis shows that axial load ratio and concrete strength are statistically significant in prediction of hardening stiffness. Even so, inclusion of these parameters scarcely improved the regression analysis, so a constant value of M_c/M_y is recommended.

$$M_c/M_y = 1.13 \quad (3.6)$$

Cyclic Energy Dissipation Capacity (λ)

Based on the observed trends in the data, the following equation is proposed for the mean energy dissipation capacity:

$$\lambda = (170.7)(0.27)^{\nu}(0.10)^{s/d} \quad (3.7)$$

The energy dissipation (λ) depends on many of the same parameters as the measures of deformation capacity: axial load ratio (ν) and spacing of transverse reinforcement (s/d). d is the column depth. The same value of λ is to be used for both basic strength deterioration and post-capping strength deterioration.

The proposed equations (Equations 3.2 – 3.7) can be evaluated to determine how well they reflect the mean tendencies in the data from model calibrations and to quantify prediction uncertainty. Table 3.5 reports the median ratio of predicted (from Equations 3.2 to 3.7) to observed values (from model calibrations) for each proposed equation. The ratio varies between 1.00 and 1.06 for the proposed equations, showing that the predictive equations have little bias. Due to its particularly large effect on collapse assessment, it is useful also to examine the prediction bias for selected subsets of the data for the equation for

$\theta_{cap,pl}$ (Equation 3.4). For non-ductile RC elements that are the focus of this thesis (i.e. those with $\rho_{sh} < 0.003$) the prediction is unbiased, with a median ratio of predicted to observed values of 1.02. Table 3.5 also shows that the prediction uncertainty is large for many of the important parameters. Previous research has shown that these large uncertainties in element deformation capacity cause similarly large variability in predictions of collapse capacity (Ibarra 2003; Haselton et al. 2008). These uncertainties are associated with the inherent randomness in the underlying physical phenomena and limitations in the available test data.

Table 3.5 Prediction uncertainties and bias in proposed equations for modeling parameters of RC columns.

Equation	Median (predicted/observed)	σ_{ln}	R^2
Effective Stiffness to Yield (3.2)	1.03	0.28	0.80
Effective Stiffness to 40% Yield (3.3)	1.02	0.33	0.59
Plastic Rotation Capacity (3.4)	1.02	0.54	0.60
Post-Capping Rotation Capacity (3.5)	1.00	0.72	0.51
Post-Yield Hardening Strength Ratio (3.6)	1.01	0.10	n/a
Cyclic Energy Dissipation Capacity (3.7)	1.06	0.47	0.51

Table 3.6 Predicted material model parameters for selected non-ductile RC columns.

	Column Design Parameters						Material Model Parameters				
Design Description	v	L_s/h	f'c	ρ	ρ_{sh}	s/d	EI_{st}/EI_g	M_c/M_y	$\theta_{cap,pl}$	θ_{pc}	λ
8-story Space Frame, 1st Story Interior Column	0.31	2.8	4 (27.6)	0.014	0.0023	0.55	0.53	1.17	0.013	0.028	32
8-story Space Frame, 5th Story Interior Column	0.21	2.8	4 (27.6)	0.014	0.0017	0.56	0.44	1.19	0.016	0.030	36
8-story Perimeter Frame, 1st Story Interior Column	0.11	2.8	4 (27.6)	0.033	0.0050	0.45	0.35	1.20	0.025	0.100	51

Column Design Parameters -- v: axial load ratio, L_s/h: shear span ratio, f'c: concrete strength ksi (MPa), ρ: reinforcement ratio, ρ_{sh}: transverse reinforcement ratio, s: spacing of transverse reinforcement, d: column depth

Material Model Parameters -- EI_{st}/EI_g:initial stiffness, M_c/M_y:ratio of nominal and yield moment, $\theta_{cap,pl}$:plastic rotation capacity, θ_{pc}: post-capping rotation capacity, λ: cyclic deterioration parameter

To illustrate the impact of column design variables on the model parameters predicted by Equations (3.2) – (3.7), the modeling parameters obtained for typical columns in older RC frame structures are shown in Table 3.6. Compared to columns in ductile RC frame structures, non-ductile columns have smaller plastic rotation capacities, post-capping rotation capacities, and faster cyclic deterioration. A typical column at the base of an 8-story space frame with ductile detailing is modeled with $\theta_{cap,pl} = 0.051$ radians, $\theta_{pc} = 0.10$ radians and $\lambda = 80$, such that the deformation capacities are more than triple those in reported in the first line of Table 3.6 for a comparable non-ductile column (Haselton 2006). (The upper bound on the equation for θ_{pc} seems to be conservative for ductile RC columns, but is used here until better

estimates become available). Table 3.6 also serves to illustrate how changes in each design parameter impact the predicted model parameters. For example, the design parameters are highly dependent on the level of axial load (ν) in the column; decreasing the axial load ratio from 0.31 to 0.11 leads to a decrease in stiffness, an increase in plastic rotation capacity and post-capping rotation capacity, and an increase in energy dissipated as the column is cycled. Axial load ratio (ν), the lateral confinement ratio (ρ_{sh}), and stirrup spacing (s/d; s_n) have the largest effect on parameters important for modeling collapse, while concrete strength (f'_c), and longitudinal reinforcement ratio (ρ) have less dominant effects. s_n is not shown in Table 3.6.

3.2.3 Modeling of Joint Shear Panel

In existing non-ductile RC frames, joints often have insufficient confinement and transverse reinforcement, and joint shear damage can be an important component of strength and stiffness deterioration in the structure. Nonlinear models of RC frame structures in this study employ a two-dimensional joint model developed and implemented by Lowes and Altoontash (Altoontash 2004; Lowes et al. 2004). This model accounts for the finite joint size, and includes rotational springs and a system of constraints for direct modeling of the shear panel and bond-slip behavior, as illustrated in Figure 3.11. These RC frame models use a relatively simple approach for determining joint model parameters, which are based on available experimental data for joints with similar design and detailing characteristics as expected in existing RC frames. Due to limitations in available data, this process is not as rigorous as that described above for beam-columns. The shear panel spring is implemented in OpenSees, again using the same Ibarra material model (Ibarra et al. 2005).

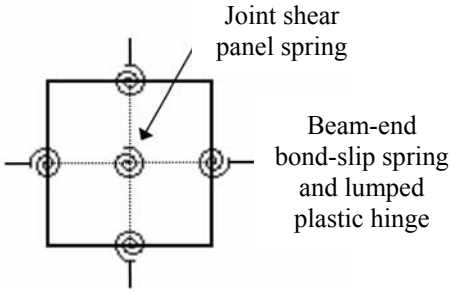

Figure 3.11 Schematic diagram of joint model, after Altoontash (2004).

Model Parameters for Beam-Column Joints

Joint shear strength (V) is determined based on the codified equation for shear strength of RC beam column joints,

$$V = \gamma \sqrt{f'_c} b_j h \quad (3.8),$$

where b_j is the width of the joint, h is the depth of the joint (in the plane of transverse reinforcement) and the factor γ accounts for the amount of confinement in the joint. Confinement is provided by geometry, e.g. the presence of transverse beams and transverse reinforcement. ACI 318 values of γ depend on the geometry of the system, as shown in Table 3.7, but assume that seismically detailed transverse reinforcement is provided and are not directly applicable for the non-conforming joints in this study (ACI 2002). RC joints in older frames typically had few, if any, transverse stirrups. Instead, empirical data is used determine an appropriate value of γ for use in joints with non-ductile detailing of the type that are of interest in this study.

Table 3.7 Parameters for joint confinement in ACI 318, Chapter 21 (ACI 2002).

Joint Description	γ_{ACI}
Joints confined on all 4 faces	20
Joints confined on 3 faces, or 2 opposite faces	15
Others	12

Joint strength is examined using a database of experimental tests assembled by Mitra and Lowes (2007), which is sorted by the amount of transverse reinforcement present in the joints. Those joints in the Mitra and Lowes database with a transverse reinforcement ratio less than 0.003 have on average $\gamma = 0.70\ \gamma_{ACI.}$ This result is consistent with a study by Beres et al. (1996), which found a 30 to 40% decrease in joint shear strength in RC beam-column joints with little or no transverse reinforcement. For joints of the type in modern, special moment frames that are designed to meet capacity design requirements and have significant transverse reinforcement, it is found that $\gamma = 1.4\ \gamma_{ACI}$, implying the ACI values are conservative for conforming joints. These factors are applied in computing expected values of joint strength for simulation models. The results are written in terms of γ_{ACI} such that the relative difference in strength between interior and exterior joints, effectively the role of the transverse beams, is still accounted for. ACI predictions for the effects of geometry and transverse beams are relatively consistent with that from previous research (Meinheit and

Jirsa 1981; Bonacci and Pantazopoulou 1993; Biddah and Ghobarah 1999; Shiohara 2001). Other researchers have observed significant differences in joint strength depending on the axial load level and anchorage (Park 1997; Hegger et al. 2003); this variation is not captured in the models in this study.

For simplicity and consistency with the modeling of beam-column elements, the joint stiffness used in models is based on the secant stiffness (through curve at 40% of the yield force). After yield, a hardening slope of 4% of effective stiffness is assumed.

There is limited experimental data available for determining appropriate values for model parameters related to joint deformation capacity and energy dissipation. The joint shear deformation capacity is determined based on empirical evidence and past research, though there is limited data that shows post-capping behavior. FEMA 356 recommends a plastic rotation capacity of 0.005 for non-conforming joints, but this value is likely highly conservative (ASCE 2000). Based on an experimental study of RC joints, Moehle et al. (2006) suggests shear deformation capacities of 0.015 and 0.010 radians, respectively, for interior and exterior joints. Exterior joints typically have smaller deformation capacity due to insufficient anchorage. Additional data is available from Pantelides et al. (2002), who conducted an experimental study of exterior joints, focusing in particular on the effects of axial load, which has an important impact on deformation capacity. As with beams and columns, increased axial load significantly reduces deformation capacity. For the purposes of this study, the values recommended by Moehle et al. (2006) are used to model non-conforming joints. For joints with low axial load ($< 0.1A_g f'_c$), the deformation capacity is increased on the basis of the Pantelides et al. study.

Tests conducted by Shiohara (2001), Altoontash (2004) and Biddah and Gibborah (1999) were used to identify a small number of specimens in which a post-capping negative slope was observed in the experiment. Test results show that this negative slope varied between 0.08 and 0.30 of the initial stiffness of the joint component, with several tests having a negative slope of approximately 0.1 times the initial stiffness. This data suggests that a negative slope of approximately 10% of the effective stiffness is appropriate. More experimental data would be useful for improving this estimate.

The cyclic behavior of the joint shear panel is based on recommendations by Altoontash (2004). Joints are modeled with pinched hysteretic behavior, with the pinch point at 25% of the maximum historic stress and 25% of the maximum historic rotation. A sensitivity study revealed the value of these pinching parameters to have a very small effect on the overall

collapse capacity so the Altoontash recommendations were applied without modification. There is very little data available to indicate reasonable values for strength and stiffness degradation. Therefore the same deterioration parameters (λ and c) are used as for the beam-column elements. As a result, non-conforming non-ductile joints deteriorate faster than those with ductile detailing. The residual strength used in the hysteretic model will also have some impact on the collapse capacity, especially for those models in which damage is concentrated in the joints. Though tests indicate minimum lateral strength values between 9 and 33% of the ultimate strength, it is unclear that these tests were continued to large enough deformations to reach the residual strength limit (Biddah and Ghobarah 1999; Pantelides et al. 2002; Altoontash 2004; Moehle et al. 2006). 5% residual capacity is assumed in the hysteretic models of all the joints.

3.2.4 Post-Processing to Account for Vertical Collapse due to Column Shear Failure

The sidesway collapse models for RC frames described above simulate the important sources of strength and stiffness degradation associated with flexure and flexure-shear deterioration in RC beams, columns and joints. However, the analysis model does not directly simulate the loss of axial-load carrying capacity that may occur after a RC column fails in shear, if it is subjected to increasing lateral deformations. The loss of axial- load carrying capacity in one column may lead to progressive collapse of the structure if gravity loads cannot be redistributed. Due to lack of capacity provisions for shear design, columns in older non-ductile RC frames may be susceptible to this failure mode, as described in Table 3.3. On the basis of their design the columns in this study are assumed to fail in flexure-shear, i.e. yielding first and then failing in shear (Zhu et al. 2007). Ideally, all important failure modes would be directly simulated in the analysis model. The decision to forego modeling of the column vertical collapse mode was made due to limitations in currently available simulation models (reported in Table 3.1). Research is ongoing to develop these modeling capabilities, e.g. (Elwood and Moehle 2005; Zhu et al. 2006; Charlet et al. 2008), but is hampered by limited test data, and models require further validation.

To remedy this deficiency in the analysis model, dynamic analysis results are post-processed, using fragility functions for component limit states to detect if the vertical collapse mode occurred in the simulation. This post-processing, described mathematically in Equation (3.9), increases the probability of collapse to account for the possible occurrence of the non-simulated collapse mode (Aslani 2005; Krawinkler 2005).

$$P[C \mid Sa] = P[SC \mid Sa] + P[VC \mid No\ SC, Sa] \times P[No\ SC \mid Sa] \quad (3.9)$$

The cumulative probability of sidesway collapse, $P[SC \mid Sa]$, conditioned on the ground motion intensity (Sa), is computed directly from incremental dynamic analysis as described in Section 3.1. The probability of the vertical collapse mode ($P[VC \mid No\ SC,Sa]$), which is not simulated, is computed by conducting a limit-state check of column component behavior, using results of deformation demands on RC columns from dynamic analysis. Double-counting is avoided by conditioning the computation of non-simulated vertical collapse on no sidesway collapse, $P[No\ SC \mid Sa]$. (Note: here and elsewhere in this thesis, P[x] refers to the cumulative distribution function of x, whereas p[x] is the probability density function.)

To detect column shear failure and subsequent loss of gravity load carrying capacity in post-processing, this study uses fragility functions developed by Aslani (2005) on the basis of 92 cyclic tests of RC columns (see also Elwood et al. (2004; 2005)). These columns yielded first in flexure, and then failed in shear, the so-called "flexure-shear" failure mode. (Shear-critical columns that fail in shear before yielding are modeled differently are not discussed here.) After failing in shear, the column may lose its ability to carry its gravity loads. Aslani (2005) defines four damage states for flexure-shear critical RC columns: (1) light cracking, (2) severe cracking, (3) shear failure and (4) loss of axial carrying capacity. Lognormal fragility functions predict the probability of being in each damage state as a function of the column drift ratio, column axial load ratio and amount of transverse reinforcement. Column drift ratio (CDR) is analogous to the more commonly used interstory drift ratio, except that it excludes the drift that occurs due to rotation of the beams and deformations in joints, because the fragility functions are largely based on data from column component tests. Column drift ratio can be obtained directly from dynamic analysis results by subtracting beam rotation and joint shear deformation from interstory drift.

The third damage state is used to identify when column shear failure occurs, manifested by the characteristic X-cracking and yielding of transverse reinforcement. In the columns in the database, shear failure occurred at column drift ratios between 0.01 and 0.05 (Aslani 2005; Elwood and Moehle 2005). The fourth damage state signifies that the column has lost its capacity to carry gravity loads (LVCC). Only a limited number of experimental tests have been continued after column shear failure occurs, but existing data suggests that this may occur at drift ratios between 0.01 and 0.09, depending on the properties of the column (Aslani 2005). Since the loss of load-carrying capacity of a column may precipitate progressive

structure collapse, this fourth damage state is defined as collapse. The median column drift ratio ($\hat{CDR}$) at which shear failure and loss of vertical carrying capacity (LVCC) may occur in a column are given by Equations (3.10) and (3.11) from Aslani (2005),

$$\hat{CDR}_{shear} = \frac{1}{0.26\left(\frac{P}{A_g f'_c \rho_{sh}}\right) + 25.4} \geq \frac{1}{100} \tag{3.10}$$

$$\hat{CDR}_{LVCC} = \frac{1}{9.6 + 2.1\left(\frac{P}{A_{st} f_{yt} \frac{d_c}{s}}\right) + 25.4} \leq 0.10 \tag{3.11},$$

where P is the axial load on the column, A_g is the column's gross cross-sectional area, ρ_{sh} is the transverse reinforcement ratio, A_{st} is the area of transverse steel provided in the column, f_{yt} is the yield strength of transverse steel, and d_c is the centerline-to-centerline distance between ties. Aslani (2005) also provides predictions of the dispersion (σ_{ln}) in the fragility function. Columns with higher axial load levels or less shear reinforcement will experience these failure modes at lower levels of drift. Mean and standard deviation defining the fragility functions for shear and vertical failure in typical 1967-era non-ductile RC frame structures are calculated based on Equations (3.10) and (3.11) and Aslani (2005) and reported in Table 3.8 and illustrated in Figure 3.12.

Note, however, that Aslani's (2005) fragility functions do not depend on the amount of longitudinal reinforcement in the column, which is likely important for retaining load-bearing capacity and redistributing loads (Elwood and Moehle 2005). These fragility functions are based on a very limited set of experimental tests, most of which have very widely spaced transverse reinforcement (on the order of 18 inches) (Elwood and Moehle 2005). The predictions may therefore be conservative and should be revised as more data becomes available. The very high estimate of column drift capacity in the perimeter frame column is based on very limited data for columns with this type of characteristics and perhaps should be decreased.

The vertical collapse limit state is reached if the column drift ratio in any column exceeds the median value of the column loss of vertical carrying capacity fragility ($\hat{CDR}_{LVCC}$, calculated from Equation 3.11) during the analysis. Incorporating this vertical collapse limit state has the effect of reducing the predicted collapse capacity of the structure and increasing

the probability of collapse. Figure 3.13a illustrates how the predicted collapse capacity decreases when the vertical collapse mode is incorporated for a selected earthquake record in incremental dynamic analysis results for an 8-story non-ductile RC frame. Some earthquake records, like the one shown, are governed by the non-simulated failure modes. Others will collapse in sidesway before the non-simulated vertical collapse mode occurs. When this process is repeated for all earthquake records, the effect is to decrease the median collapse capacity reported and shift the collapse fragility to the left, as shown in Figure 3.13b. The amount by which the median shifts depends on the design of the structure, but varies between 2% to 30% for the non-ductile RC frame structures considered in this study. The third curve illustrates the predicted collapse fragility if a component check on the shear failure limit state in Figure 3.13b is treated as collapse. This curve illustrates the conservatism in component-based methods that analyze for shear failure in individual elements, where the mean value is reduced by 7% to 89%. A simple parametric study was devised to predict the dispersion (σ_{ln}) in the final collapse fragility depending on the importance of the non-simulated failure mode, based on the uncertainty in the sidesway collapse fragility ($\sigma_{ln,RTR + modeling} \approx 0.60$), the uncertainty in the prediction of the column drifts ($\sigma_{ln(CDR \mid Sa)} \approx 0.30$, on the basis of stripe data from dynamic analysis) and the uncertainty in the limit state prediction, represented by the fragility function ($0.20 \leq \sigma_{ln(Failure \mid CDR)} \leq 0.55$, on the basis of fragility functions defined by Aslani).[9]

The assumption that collapse occurs with failure in any one column is conservative as many frame structures will be able to redistribute loads from the collapsed column. However, the columns on a given floor of the structure are likely to undergo similar levels of column drift, and it is possible that this loss of vertical carrying capacity in one column may lead to collapse of an entire story or region of the building. This progression may be driven

[9] Use of the median value of the fragility function is a first-order approximation. A more complete approach is to convolve the component fragility function with the probability distribution of engineering demand parameters from incremental dynamic analysis as follows,

$$P[VC \mid NoSC, Sa] = \int_{EDP} P[VC \mid EDP]\, p[EDP \mid NoSc, Sa]\, dEDP$$

Here, P[VC | No Sc, Sa] is the cumulative probability of vertical collapse, given that no sidesway collapse occurred. P[VC | EDP] is the probability of vertical collapse as a function of the engineering demand parameter (EDP), in this case the column drift ratio (CDR). p(EDP | No Sc, Sa] is the probability distribution describing how the engineering demands vary at each level of ground motion intensity. Only the non-collapsed records are used to describe this distribution. A comparison of the two approaches confirmed that a check on the median of the fragility function provided very similar results.

by correlations between the failures of different columns, which are difficult to quantify with available data.

Table 3.8 Parameters defining lognormal fragility functions for shear failure limit states for typical non-ductile RC column designs.

Column Description	Shear Failure		Loss of Vertical Carrying Capacity	
	$\hat{CDR}$	σ_{ln}	$\hat{CDR}$	σ_{ln}
4-story Space Frame, 1st Story Interior Column	0.019	0.55	0.038	0.52
8-story Space Frame, 1st Story Interior Column	0.017	0.55	0.032	0.55
8-story Perimeter Frame, 1st Story Interior Column	0.032	0.55	0.10	0.20

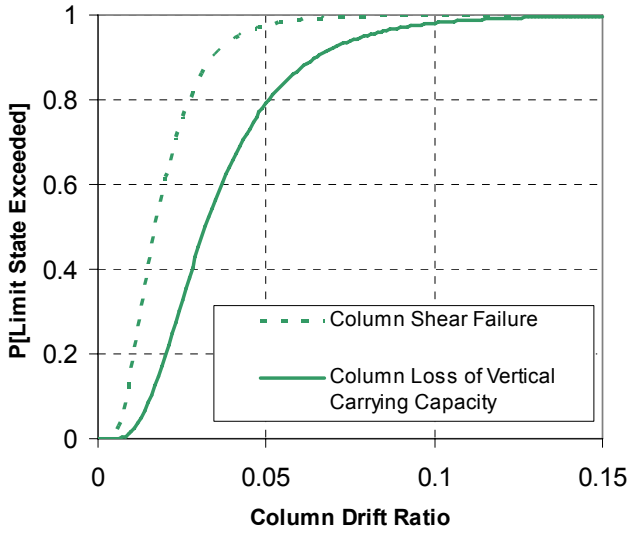

Figure 3.12 Component fragility functions for an interior first story column in the 8-story non-ductile RC space frame structure.

The procedure for post-processing, described here in reference to shear failure of RC columns, is generally applicable to collapse analysis of structural systems for which not all the failure modes can be accurately simulated. This method is an important component of the collapse assessment methodology because it permits analysis of systems for which simulation technologies are not sufficiently developed, provided that (1) the dynamic analysis results are accurate until the non-simulated limit state is reached, (2) the fragility functions for the non-simulated limit state are based on sufficient test data and (3) the component limit state is a reasonable measure of system collapse. Other example applications include prediction of punching shear failure in flat-plate gravity systems (Aslani 2005). Collapse assessment of steel special moment frames in the ATC-63 (ATC 2007) project incorporated ductile fracture

of reduced beam connections, which is difficult to model accurately, using fragility function data developed by Lignos and Krawinkler (2007).

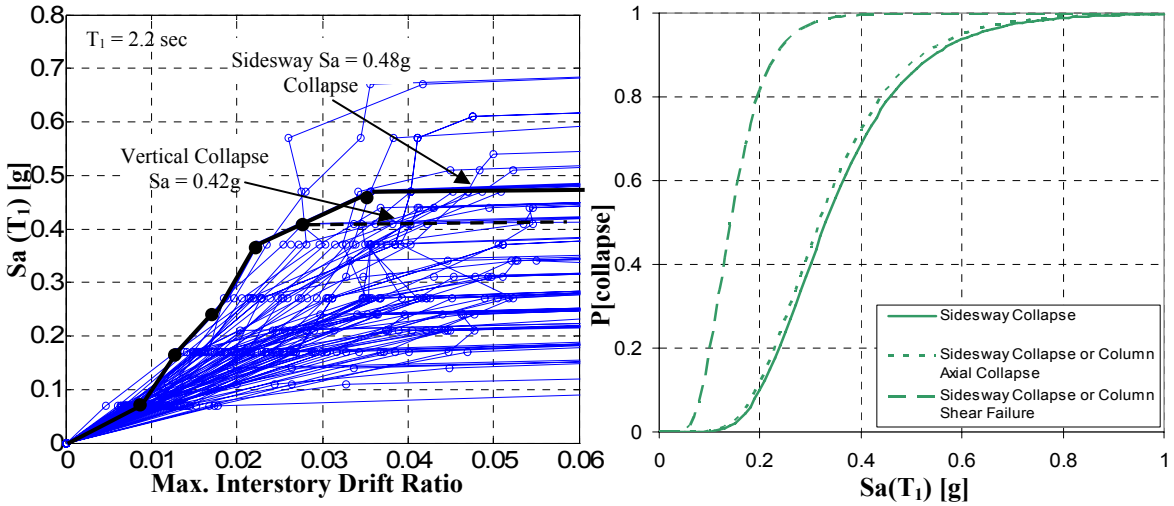

Figure 3.13 (a) Incremental dynamic analysis results for an 8-story space frame structure, illustrating the effect of vertical collapse mode on collapse capacity for a selected earthquake record. (b) Comparison of collapse fragilities for 8-story non-ductile RC space frame for sidesway collapse only and combined sidesway and vertical collapse.

3.2.5 Modeling Deficiencies

The nonlinear simulation model developed for non-ductile RC frame structures is an idealization of the structural geometry, loading and dynamic behavior. Although the analysis model is representative of the real structure, as with any idealization, the model has deficiencies that may limit the application of the model or the results.

The simulation model for RC frames reduces a complex three-dimensional structure to a two-dimensional planar analysis of the lateral resisting system. The two-dimensional model cannot capture the effects of bidirectional loading, torsion, or floor diaphragm flexibility in the analysis. Columns are likely to be much more highly stressed under biaxial loading. We partially compensate for the lack of 3-dimensional loading on the columns by designing the columns only for loading in one direction – thus, both the capacity of the column and the demand on the column are underestimated from the real, three-dimensional situation. However, the model is inappropriate for structures with significant torsional irregularities that tend to worsen collapse performance, e.g. (Marusic and Fajfar 2005). Additionally, the model does not incorporate structural and non-structural components that are not part of the lateral resisting system. Haselton et al. (2008) has shown that neglecting gravity-designed columns in the analysis may lead to an under-prediction of the collapse capacity of a structure by 10% to 30%. The under-prediction is more significant for weaker, more flexible

buildings like those presently being considered and may be quite pessimistic for the perimeter frame structures in this study. Non-structural partitions may also contribute significantly to strength and stiffness in some cases, altering the dynamic properties of this system. For example, older RC structures with infill masonry-type partitions likely warrant a detailed study of the effect of these walls on structural response. The analysis model also neglects soil-structure interaction. Previous studies have shown that the inertial effects of foundation flexibility and damping and kinematic effects of ground motions at the foundation level have a limited impact on structural response for relatively flexible frame structures (e.g. Goulet et al. (2007)). For very short period structures unlike the RC frames in this study, however, soil-structure effects may need to be re-examined.

Additional limitations are present in modeling of element deterioration and collapse modes of RC frame structures. Behavior related to flexural hinging, which is modeled using a lumped plasticity material model that has been calibrated to experimental data for RC columns, lacks flexural-axial interaction, and thus cannot simulate changes in axial load due to overturning. Although overturning is most important in taller structures, columns in mid-height structures may experience significant variation in axial load levels in columns during an earthquake. To capture these effects, more complex models involving axial-flexure interaction are needed (e.g. Kaul (2004)). The calibration of models described in Section 3.2.2 for flexure and flexure-shear behavior in RC columns could be further improved if more data were available. Specifically, there is a need for columns tested at large deformations so as to permit more accurate calculation of post-peak response and there is a need for pairs of identical columns tested under monotonic and various types of cyclic loading protocols (Haselton et al. 2007). The contribution of the reinforced concrete slab to the frame's strength and stiffness is based on simplifying assumptions regarding effective width that may have a significant impact on frame behavior and the failure mechanism (Robertson 2002). Models for inelastic joint shear failure could benefit from additional data for calibrating joint shear behavior and incorporation of axial-shear interactions.

A few other failure modes are not incorporated in the analysis model. Older RC frame structures frequently had short lap-splices located just above the floor level (Lynn et al. 1996; Pincheira et al. 1999; Melek and Wallace 2004). The model does not simulate the effects of short lap-splices that may pull out when subjected to tensile loading. Various models for bar pull-out do exist, but are not incorporated in the models in this study (Reyes 1999; Melek et al. 2003; Pincheira 2005). Older RC frames also sometimes had discontinuous bottom beam

bars in the joint. Under load reversals in earthquakes, these discontinuities could reduce the bending moment capacity of beams, which is not accounted for in the nonlinear simulation models. Foundation failure modes are also not simulated and assumed not to govern the response. Punching shear failure could occur in slab-column connections of the gravity frame structure (Hueste and Wight 1999; Aslani 2005). Since older RC frames do not necessarily have slab bottom reinforcement running continuously through the column, the slab could fall soon after punching shear failure occurs, leading to a local collapse. This collapse mode is not incorporated into the analysis model since the gravity system is not modeled.

3.3 Collapse Assessment of 8-Story Non-Ductile Reinforced Concrete Frame Structure

3.3.1 Structural Design

The case study is an 8-story office building with a RC space frame lateral resisting system (Design ID 3016). It has a floor plan measuring 125 ft by 125 ft. and columns spaced at 25 feet. The total height of the structure is 106 feet, with typical story heights of 13 feet and a basement.

The structure is designed according to the provisions of the 1967 Uniform Building Code (ICBO 1967). Structural design considered all relevant load combinations, including dead loads, live loads and seismic loading. The building is assumed to be located in Los Angeles, and lateral loading calculations are based on Seismic Zone 3. The resulting design base shear coefficient is 0.054g. The structure is designed as a space frame, such that all columns and beams are part of the lateral resisting system. The structure is designed with concrete strength f'_c = 4 ksi and reinforcing bars with f_y = 60 ksi in both beams and columns. All beam and column elements have the same amount of overstrength, such that each element is 15% stronger than the code-minimum design level. Data summarizing the design is reported in Table 3.9, including typical member sizes, reinforcement ratios and provision of transverse reinforcement. The design is governed by strength and stiffness requirements, as the 1967 UBC had few requirements for special seismic design or ductile detailing. As designed, the 8-story structure is a typical regular structure, meeting all code requirements and without any specific characteristics that are likely to make perform particularly better or worse than average in an earthquake.

3.3.2 Nonlinear Analysis Models

Based on the structural design characteristics, this 8-story RC frame structure is then modeled according to the discussion in Sections 3.1.2 and 3.2. The two-dimensional model represents a three-bay portion of one of the lateral resisting frames in the structure. Key parameters defining the material models for lumped plasticity beams and columns are calculated according to empirical equations developed in Equations (3.2) through (3.7), based on the geometry and reinforcement in each element. The resulting range of modeling parameters is reported in Table 3.10. Those columns with the lowest plastic rotation capacity typically have high axial loads and little transverse reinforcement. The RC beams tend to have larger deformation capacities ($\theta_{cap,pl}$; θ_{pc}) and smaller (slower) cyclic deterioration (λ) than columns because the beams have no axial load. Monotonic backbones for beams are asymmetric, since there are usually more top bars than bottom bars in beams. Joint shear panels are modeled as described in Section 3.2.3. For these structures the joint shear deformation capacity is estimated between 0.014 and 0.022 radians, depending on the axial load level in the joint. As modeled, the fundamental period of this 8-story frame structure is T_1 = 2.2 seconds.[10]

Table 3.9 Design details for 8-story RC space frame structure designed according to the 1967 UBC.

Design Parameter	Minimum	Maximum	Units
Frame Geometry			
Bay Width	25		ft.
Story Height	13	15 (1st Story)	ft.
Column Design			
Size	24 x 24	28 x 28	in. x in.
Longitudinal Reinforcement Ratio (ρ_{total})	0.010	0.032	--
Transverse Reinforcement Ratio (ρ_{sh})	0.0015	0.0036	--
Stirrup Spacing	12	14	in.
Beam Design			
Size	20 x 24	24 x 26	in. x in.
Longitudinal Reinforcement Ratio (ρ_{bot})	0.006	0.009	--
Longitudinal Reinforcement Ratio (ρ_{top})	0.012	0.018	--
Transverse Reinforcement Ratio (ρ_{sh})	0.0018	0.0037	--
Stirrup Spacing	8.8	11.8	in.
Other			
Column Axial Load Ratio (Expected) $P/A_g f'_c$	0.03	0.40	--
Strong Column-Weak Beam Ratio $\Sigma M_{uc}/\Sigma M_{ub}$	0.6	1.4	--

[10] This value is significantly larger than the code-calculated period of T = 0.1N = 0.8 sec. Code period formulas typically underestimate a structure's fundamental period as a source of conservatism in establishing earthquake design forces. In addition, this model period represents a secant stiffness rather than initial stiffness, and accounts for both flexural and bond-slip deformations in reinforced concrete elements. See further discussion in Section 5.3.1.

Table 3.10 Modeling parameters for typical columns and beams in 8-story non-ductile RC building.

Modeling Parameter	Minimum	Maximum	Units
Columns			
EI/EI_g	0.35	0.53	--
$\theta_{cap,pl}$	0.013	0.024	rad
θ_{pc}	0.028	0.058	rad
λ	32	46	--
Beams			
EI/EI_g	0.35	0.35	--
$\theta_{cap,pl}$	0.039	0.080	rad
θ_{pc}	0.068	0.10	rad
λ	105	123	--

3.3.3 Collapse Performance Assessment

The simulation model of the 8-story building is first subjected to static pushover analysis, to determine levels of static overstrength in the design and to anticipate possible structural collapse modes. Lateral overstrength, the ratio of ultimate to design strength, results from differences between design and expected material properties and from additional resistance provided by gravity load design. As shown in Figure 3.14a, the 8-story case study structure has an ultimate lateral resistance 60% larger than the design base shear. Figure 3.14b illustrates the concentration of deformations in the bottom two stories of the structure, with limited inelastic deformations above the fourth story.

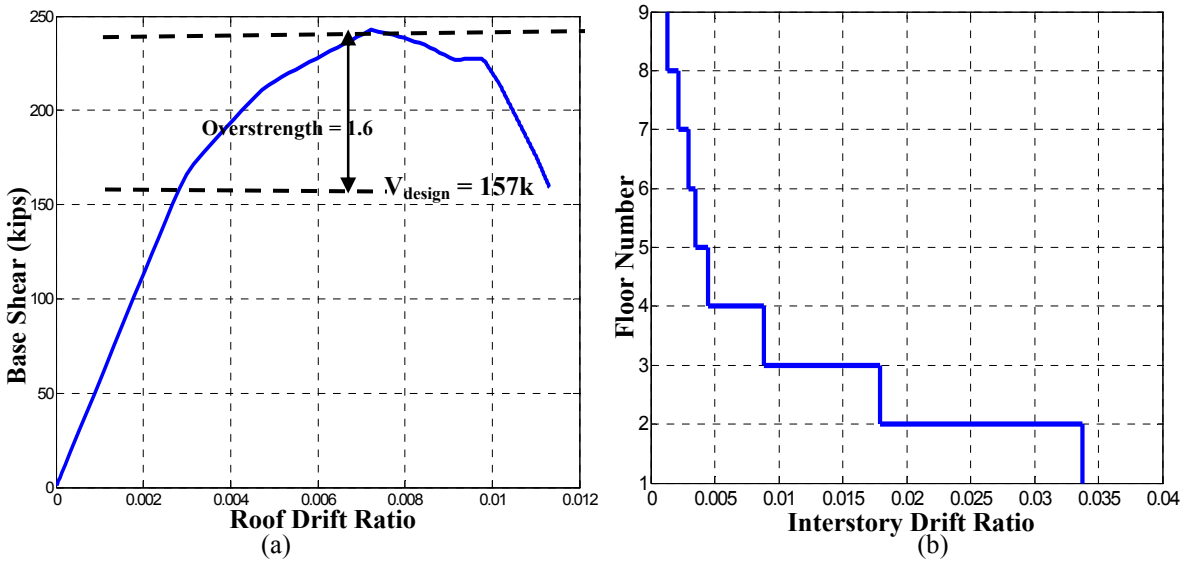

Figure 3.14 Static pushover analysis for 8-story non-ductiel RC frame structure: (a) base shear versus roof drift ratio and (b) distribution of interstory drift ratios at the end of the analysis.

The collapse performance assessment of the 8-story non-ductile RC frame structure follows the procedure described previously in this chapter. Incremental dynamic analysis

results are illustrated in Figure 3.15. On average the structure has a collapse capacity of 0.26g, and collapse occurs at a maximum interstory drift ratio between 3% and 5%. Figure 3.15 also illustrates the most common failure modes of the 8-story structure. It typically fails in either a two-story mechanism (64% of ground motion records) or a three-story mechanism (36% of ground motion records) at the base of the structure. The collapse fragility obtained from incremental dynamic analysis is illustrated in Figure 3.16a, which accounts for record-to-record variability. A revised collapse fragility with increased dispersion ($\sigma_{ln,modeling} = 0.50$) to account for uncertainties in structural modeling, is shown in Figure 3.16b. Key data from the collapse assessment is summarized in Table 3.12.

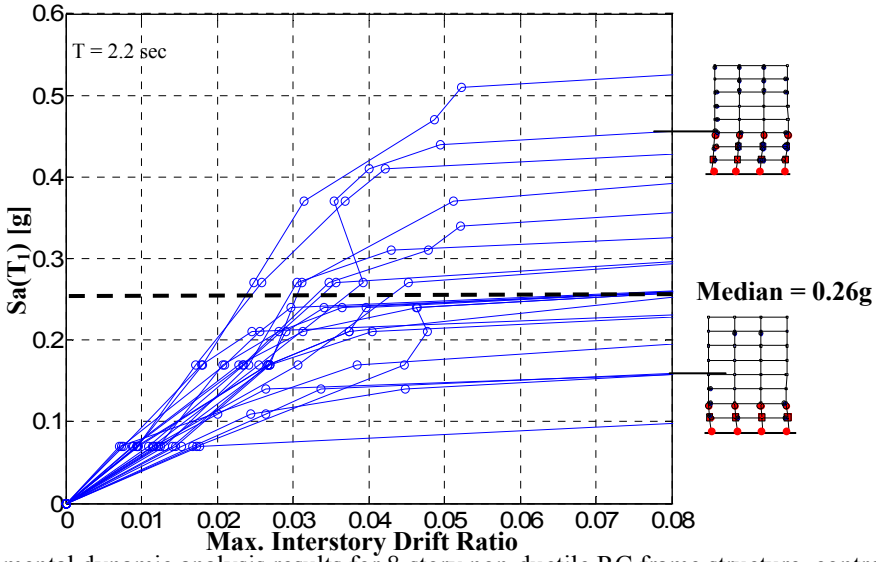

Figure 3.15 Incremental dynamic analysis results for 8-story non-ductile RC frame structure, controlling components only. Collapse mechanisms are shown for selected earthquake records.

Post-processing is conducted to account for possibility of column shear failure followed by column vertical collapse, which is not simulated, but could lead to progressive collapse of the structure. The most vulnerable columns in this 8-story space frame structure are predicted to experience column vertical failure at a column drift ratio of 0.032, which corresponds to an interstory drift ratio of approximately 0.04. For some ground motion records, the vertical collapse mode may occur before the sidesway collapse mode, leading to a decrease in the collapse capacity of the structure (as illustrated in Figure 3.13). However, the structure is already prone to collapse in sidesway at interstory drift ratios of 4%, so the non-simulated failure mode does not have a significant effect on the collapse capacity. As reported in Table 3.12, the effect of considering non-simulated failure modes is to slightly reduce the median collapse capacity from 0.26g to 0.25g.

Finally, the collapse fragility is also modified to account for the spectral shape of rare ground motions in California, following the procedure described in Section 3.1.4. For this structure, the median collapse capacity is increased by a factor of 1.28 for a median collapse capacity of 0.32g, as reported in Table 3.12.

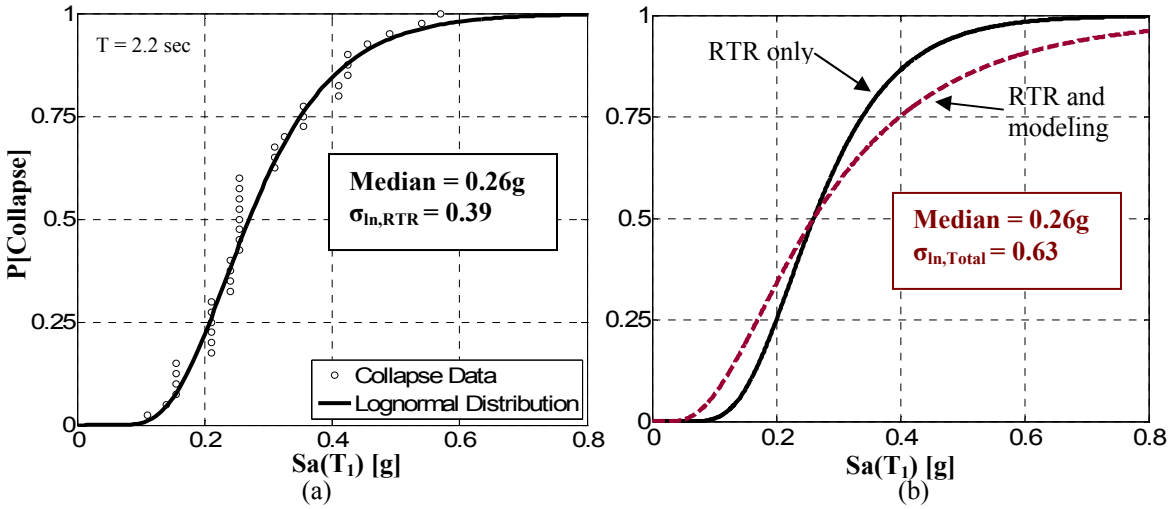

Figure 3.16 Sidesway collapse fragility for 8-story non-ductile RC frame structure, including (a) record-to record variability only and (b) record-to-record and modeling variability.

Table 3.11 Metrics for collapse safety obtained for the 8-story non-ductile RC space frame structure.

Collapse Metrics	
Median Collapse Capacity, Sa(T_1) [g]	0.32g
σ_{Total}	0.63
Collapse Margin Ratio	0.78
P[Collapse|$Sa_{2/50}$]	0.65
$\lambda_{collapse}$	65 x 10^{-4} [collapses / year]
Median Roof Drift Ratio at Collapse	0.011
Median Interstory Drift Ratio at Collapse	0.042

The result of the collapse assessment procedure for the 8-story existing non-ductile structure is a collapse fragility function that predicts the probability of collapse, as a function of ground motion intensity. Reported in Table 3.11 and Figure 3.5, the final collapse assessment accounts for both simulated and non-simulated failure modes, sources of uncertainty related to ground motion variability and uncertainty in structural modeling, and reflects the appropriate spectral shape of rare ground motions in California. The collapse performance is then compared to the predicted seismic hazard at the site of interest, which is obtained for a Los Angeles site by Goulet et al. (2007). As Table 3.11 shows, this structure collapses on average below the intensity of the 2% in 50 year ground motion ($Sa_{2/50}$). It also

has a relatively high collapse rate of 65 x 10^{-4} (collapses per year). These collapse metrics are put in context in later chapters.

Table 3.12 Effect of aspects of the collapse assessment procedure on performance assessment.

Effect of Collapse Assessment Procedure	
All vs. Controlling Ground Motion Components	
Median Collapse Capacity - All components	0.31g
Median Collapse Capacity - Controlling components	0.26g
Modeling Uncertainties	
σ_{RTR} - Record-to-record variability only	0.39
σ_{Total} - Modeling and Record-to-record variability	0.63
Non-Simulated Failure Modes	
Median Collapse Capacity - Sidesway only	0.26g
Median Collapse Capacity - Including non-simulated collapse mode	0.25g
Spectral Shape (ε)	
Median- ε Neutral	0.25g
Median - Appropriate spectral shape (ε = 1.2)	0.32g

3.3.4 Comparison to ASCE/SEI 41 Assessment

The collapse performance assessment described here can be compared to first-generation performance-based earthquake engineering guidelines that have been widely used by practicing engineers and incorporated into commercially available structural analysis platforms. In this section, the 8-story case study non-ductile RC frame assessed above is reevaluated following the guidelines provided in the ASCE/SEI 41 Standard for *Seismic Rehabilitation of Existing Buildings* (ASCE 2007). ASCE/SEI 41 is the latest publication in a family of guidelines for deterministic seismic performance evaluation that grew out of FEMA 273 and FEMA 356 (ASCE 2000). The provisions for reinforced concrete in this comparison are based on the ASCE/SEI 41 Supplement developed by an ad hoc committee following the Standard's publication (Elwood et al. 2007).

The procedure for seismic evaluation and rehabilitation described in the ASCE/SEI 41 Standard evaluates the existing structure on the basis of a selected performance objective. If the performance objective is not met, the structure is a candidate for seismic upgrading, and retrofit strategies can be designed and analyzed. Although in concept an owner could choose any performance objective, the 'basic safety objective', which aims to protect life safety, is considered here. The basic safety objective requires that the Life Safety limit state is not exceeded under the ground motion intensity that occurs with 10% likelihood every 50 years ($Sa_{10/50}$), and that the Collapse Prevention limit state is not exceeded under the ground motion intensity that occurs with 2% likelihood every 50 years ($Sa_{2/50}$). Evaluation of the

performance limit states is based on component acceptance criteria defined in the document for components of typical structural systems. Analysis of demands in structural components may utilize linear or nonlinear analysis. For this comparison, the nonlinear static procedure (pushover) is used.

To evaluate the 8-story non-ductile RC case-study structure according to the ASCE/SEI 41 guidelines, nonlinear static analysis is performed, and at a specified target displacement, the component demands are compared to the element performance criteria defined in the Standard. The target displacement (δ_t), defined in ASCE/SEI 41, represents the maximum displacement likely to be experienced during the earthquake of interest, and is calculated as shown in Equation (3.12).

$$\delta_t = C_o C_1 C_2 C_3 S_a \frac{T_e}{4\pi^2} g \tag{3.12}$$

$S_a \frac{T_e}{4\pi^2}$ is the elastic displacement (S_d) of a single degree of freedom oscillatory (SDOF) with period, T_e= 1.2 sec (based on code equations), subjected to a spectral intensity, Sa = $Sa_{10/50}$ = 0.48g for the design level earthquake (DBE). The factor C_o relates the spectral displacement of an equivalent SDOF to the roof displacement of the building MDOF system; factor C_1 relates expected maximum inelastic displacements to displacements calculated for linear elastic response; factor C_2 represents the effect of pinched hysteretic shape, stiffness degradation and strength deterioration on the response; factor C_3 modifies the target displacement to represent increased displacements due to dynamic P-Δ effects. These coefficients are taken as C_0 = 1.3, C_1 = 1.0, C_2 = 1.1 and C_3 = 1.0. For the design level earthquake, the target displacement computed for this structure corresponds to a roof drift ratio of 0.008 (δ_t = 9.67 in.; total height of structure = 106 ft.). For the MCE level earthquake ($Sa_{2/50}$), the target displacement computed for this structure corresponds to a roof drift ratio of 0.013 ($Sa_{2/50}$(T_1 = 1.2sec) = 0.73, C_0 = 1.3, C_1 = 1.0, C_2 = 1.2, C_3 = 1.0 for δ_t = 16.0 in).

The demands on structural components, obtained from pushover analysis results at the target displacement, are compared to the acceptance criteria defined for each component. The acceptance criteria defined in the ASCE/SEI 41 Supplement for reinforced concrete are illustrated in Figure 3.17. The Supplement was developed with improved data for RC components. The new criteria tend to be less conservative for more ductile columns and

slightly more conservative for columns with high axial load. Additionally, the revised backbones distinguish better between columns dominated by flexure, flexure-shear and shear failure modes (Elwood et al. 2007). Other differences in component backbones are in estimates of initial stiffness – the Supplement estimates of initial stiffness are lower than those provided in earlier documents (e.g. FEMA 356), which are more consistent with the values used in this study, e.g. Equations (3.2) and (3.3). Differences between the modeling assumptions in this study and the ASCE backbones are illustrated through comparison of Figure 3.18 with Figure 3.17. Though the ASCE-41 Supplement has become less conservative for reinforced concrete, the plastic rotation capacities of the generalized backbones (Figure 3.17) are still smaller (by approximately half) than those predicted by model calibration in Section 3.2.2 (illustrated in Figure 3.18). For columns expected to fail in shear or flexure-shear, like those in this study, the deformation capacities predicted in ASCE-41 are lower bounds, and chosen to be less than the true deformation capacity 85% of the time. This conservatism was incorporated in the Supplement to account for the scatter in available experimental data and potential consequences of a brittle failure mode (Elwood et al. 2007).

The static pushover analysis follows the ASCE/SEI 41 Nonlinear Static Procedure except that the element backbone uses the model defined in Figure 3.18, rather than the ASCE backbones (Figure 3.17). Acceptance criteria follow ASCE/SEI 41. To determine whether the life safety objective is met under the design basis earthquake, the hinge rotations in the critical columns at the target displacement (obtained from pushover analysis) are compared to the acceptance criteria. (In concept, this process would be repeated for other structural elements as well, but the columns are assumed to govern in this analysis.) The columns at the base of the structure have acceptance criteria as illustrated in Figure 3.17b, such that if the rotation demands in any column exceeds 0.01 radians, the life safety criteria is violated. For the purposes of this example, it is assumed that the rotation demands in the column are equal to the interstory drifts, such that the acceptance criteria for columns essentially limit the interstory drifts to 1%.

At the target displacement of 9.7 inches for the design level earthquake ($Sa_{10/50}$), the maximum interstory drift ratio at the base of the structure is approximately 0.025, and the acceptance criteria is clearly violated in the first-story columns. Therefore, the ASCE/SEI 41 procedure concludes that the life safety objective is not met. Based on the acceptance criteria in Figure 3.17b, for which the life safety and the collapse prevention limit states are the same,

the structure fails to meet the collapse prevention limit state requirements at $Sa_{2/50}$ either. In fact, 1% interstory drift is exceeded at a roof displacement of approximately 4.5 inches, or $Sa(T_1 = 1.2sec) = 0.22g$. In comparison, the performance-based collapse assessment procedure described in this thesis predicts a 39% probability of collapse under a design level earthquake ($Sa_{10/50}$), a 68% probability of collapse under the MCE earthquake ($Sa_{2/50}$) and a median collapse capacity of $Sa(T_1 = 2.2sec) = 0.31g$. This median collapse capacity $Sa(T_1 = 2.2sec) = 0.31g$ from dynamic analysis is approximately equal to $Sa(T_1 = 1.2 sec) = 0.57g$ when corrected for differences between the code period (1.2 seconds) and the period from eigenvalue analysis (2.2 seconds). This value of 0.57g from the collapse assessment procedure describe here is comparable to the Sa = 0.22g obtained for the collapse prevention limit state from the ASCE/SEI 41 Standard.

The ASCE/SEI 41 standard provides a procedure through which structural performance of potentially vulnerable structures, such as non-ductile RC frame structures, can be systematically evaluated. For the 8-story older non-ductile RC structure considered, these guidelines predict that the structure does not meet the basic safety objectives. These judgments can provide useful information to building owners and designers making decisions about seismic retrofit or replacement and in identifying the most vulnerable elements in the building. However, the performance-based collapse assessment procedure described in this study, which relies on incremental dynamic analysis, provides substantially more data about seismic performance. Instead of a deterministic binary limit state evaluation, structural response (collapse) is represented probabilistically, e.g. $P[Collapse|Sa_{10/50}] = 0.39$, accounting for uncertainties in the predictions. The quantification of system-level performance metrics, rather than the component-based criteria developed in ASCE/SEI 41 (and illustrated in Figure 3.17), provides a more systematic method of comparing performance among different buildings. Component-based criteria can be overly pessimistic because the structure fails the evaluation if any of the elements in the structure do not meet the acceptance criteria and do not allow for redistribution of loads. In addition, the approach taken here uses modeling backbones based on expected parameter values rather than lower bounds, eliminating some of the conservatisms present in the ASCE/SEI 41 force-deformation relationships and acceptance criteria. A comparison of the spectral accelerations at which the collapse prevention limit state is reached from ASCE/SEI 41, $Sa(T_1 = 1.2sec) = 0.22g$, and from the performance-based dynamic collapse assessment, $Sa(T_1 = 1.2sec) = 0.57g$, reveals the conservatisms in the ASCE/SEI 41 guidelines.

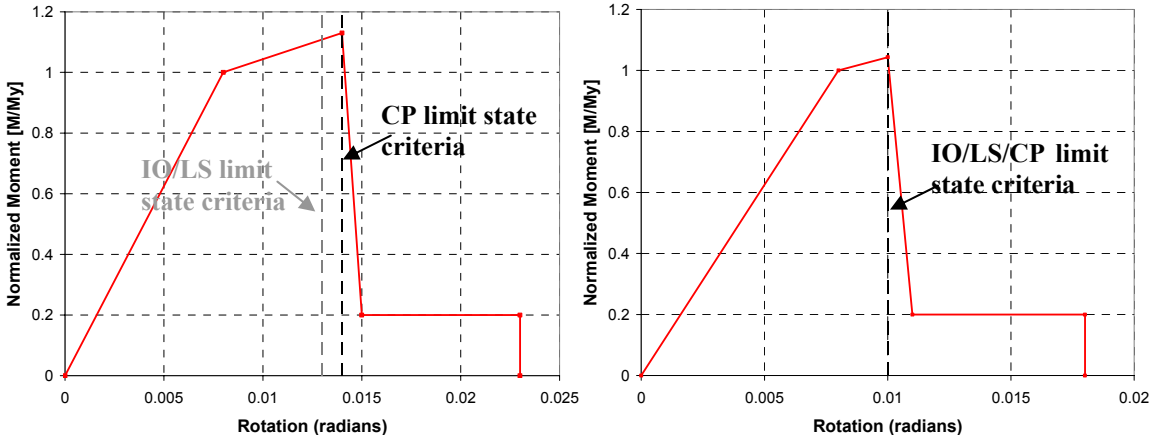

Figure 3.17 Component backbones defined by the ASCE 41 Standard for Seismic Rehabilitation of Existing Buildings (Supplement), showing (a) column with low axial load and high shear strength and (b) column with high axial load. Acceptance criteria for immediate occupancy (IO), life safety (LS) and collapse prevention (CP) limit states are superimposed.

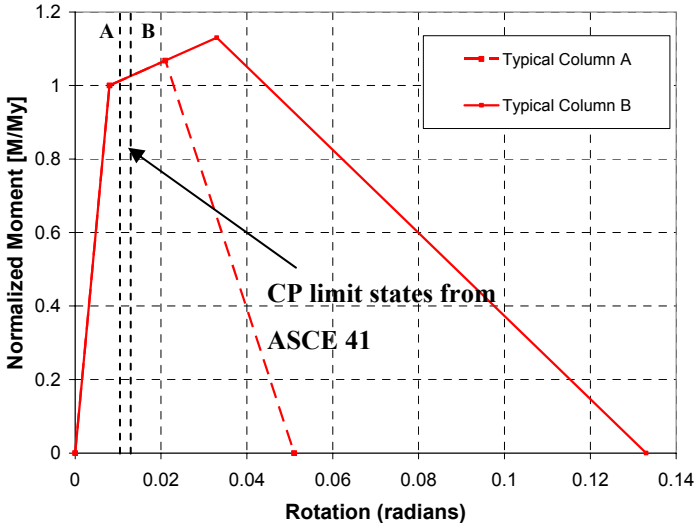

Figure 3.18 Model backbones defined by calibration effort in this study, for two typical columns found in non-ductile RC frame structures. Column A has relatively high axial load and less transverse reinforcement than Column B. Collapse prevention limit states from ASCE 41 for columns A and B are superimposed.

3.4 Conclusions

The methodology for performance-based collapse assessments described here can be used to systematically evaluate the risk of earthquake-induced collapse in California's existing non-ductile RC frame structures. The details of the procedure are illustrated in this chapter for an 8-story space frame structure, and will be repeated for each of the archetypical older RC frame structures in later chapters to evaluate the safety of this class of structures.

The collapse assessment methodology relies on creation of nonlinear analysis models of archetypical non-ductile RC frame structures, which are envisioned to be frames designed according to the 1967 Uniform Building Code. These models have been calibrated to available experimental data for RC components. The calibration study for modeling of RC beam-columns results in a set of predictive equations, which relate RC design parameters to model parameters for lumped plasticity elements. Material model validation for modeling of the RC joints is more qualitative, due to limitations in available data. Once the structure is modeled, incremental dynamic analysis methods are used to evaluate model response to the point of structural collapse using a suite of recorded ground motions. Where well-developed simulation models are not available, failure modes are incorporated by post-processing dynamic analysis results using component fragility functions.

Chapter 4

Incorporating Modeling Uncertainties in the Assessment of Seismic Collapse Risk of Buildings

Liel, A.B., C.B. Haselton, G.G. Deierlein and J.W. Baker, "Incorporating Modeling Uncertainties in the Assessment of Seismic Collapse Risk of Buildings," *Structural Safety* (accepted).

4.1 Abstract

The primary goal of seismic provisions in building codes is to protect life safety through the prevention of structural collapse. To evaluate the extent to which current and past building code provisions meet this objective, the authors have conducted detailed assessments of collapse risk of reinforced-concrete moment frame buildings, including both 'ductile' frames that conform to current building code requirements, and 'non-ductile' frames that are designed according to out-dated (pre-1975) building codes. Many aspects of the assessment process can have a significant impact on the evaluated collapse performance; this study focuses on methods of representing modeling parameter uncertainties in the collapse assessment process. Uncertainties in structural component strength, stiffness, deformation capacity, and cyclic deterioration are considered for non-ductile and ductile frame structures of varying heights. To practically incorporate these uncertainties in the face of the computationally intensive nonlinear response analyses needed to simulate collapse, the effect of modeling uncertainties is assessed through a response surface, which describes the median collapse capacity as a function of the model random variables. The response surface is then used in conjunction with Monte Carlo methods to quantify the effect of these modeling uncertainties on the calculated collapse fragilities. Comparisons of the response surface based approach and a simpler approach, namely the first-order second-moment (FOSM) method, indicate that FOSM can lead to inaccurate results in some cases, particularly when the modeling uncertainties cause a shift in the prediction of the median collapse point. An alternate simplified procedure is proposed that combines aspects of the response surface and FOSM methods, providing an efficient yet accurate technique to characterize model

uncertainties, accounting for the shift in median response. The methodology for incorporating uncertainties is presented here with emphasis on the collapse limit state, but is also appropriate for examining the effects of modeling uncertainties on other structural response limit states.

4.2 Introduction

Comprehensive assessment of the risk of earthquake-induced structural collapse requires a robust analytical model that captures nonlinear behavior and, also, explicit consideration of the many important sources of uncertainty. The largest uncertainty lies in characterizing the earthquake ground motion. Uncertainties in ground motion intensity are commonly represented by a site-specific hazard curve, which relates spectral intensity to the frequency of exceedance; the additional uncertainties associated with frequency content and other attributes of the ground motion records are termed 'record-to-record' variabilities. Apart from ground motions, there are uncertainties in simulating the structural response, which relate to the analysis method and the extent to which the idealized model accurately represents real behavior. Where detailed nonlinear response history analysis is used to simulate structural response, a primary source of modeling uncertainty lies in definition of the analysis model parameters – specifically the strength, stiffness, deformation capacity, and energy dissipation characteristics of the building components – as compared to the components' actual behavior. Other sources of modeling uncertainty relate to how the structural system is modeled, such as whether the model is two- or three-dimensional, characterization of brittle failure modes or methods and level of damping defined.

This study involves probabilistic assessment of structural collapse risk through nonlinear response history simulation, which incorporates the uncertainties associated with ground motions and structural modeling. However, the primary focus of this study is on modeling parameter uncertainties and how to realistically and expediently quantify their effects in nonlinear response history analysis. Past research, e.g. (Porter et al. 2002), (Lee and Mosalam 2005), has indicated that modeling uncertainties associated with damping, mass, and material strengths have a relatively small effect on the overall uncertainty in seismic performance predictions, but these studies have focused primarily on pre-collapse performance of structures. In contrast, Ibarra and Krawinkler (2003) have shown that the uncertainty associated with modeling deformation capacity and post-peak softening response of

component element models can have a significant influence on the predicted collapse performance. This study builds on the work by Ibarra and Krawinkler to quantify the significance of modeling uncertainties associated with component deformation capacity and other parameters critical to collapse prediction of reinforced concrete (RC) moment frame buildings. Only modeling parameter uncertainties are considered here, leaving other aspects of modeling uncertainty for future study. Though we use RC frame structures for illustration purposes, the procedure developed for incorporating modeling uncertainties is systematic and applicable to other structural systems.

To begin, we provide an overview of the collapse assessment procedure and results for reinforced concrete moment frames in highly seismic regions. We then review methods for quantifying the effects of uncertainty in element and system level modeling, and propose a procedure that combines response surface analysis and Monte Carlo methods. This procedure is applied to six case study frame structures of varying heights and ductility capacity. The results of these case studies indicate that modeling uncertainties tend both to increase the dispersion (σ_{ln}) and also to shift the median ($\hat{m}$) of the probability distribution for structural response. We compare the response surface results with first-order second-moment reliability methods, which are easier to implement but rely on simplifying assumptions that do not necessarily apply. Finally, we propose a new simplified method ("ASOSM"), which captures the critical effects of modeling uncertainties, but requires less computational time than the response surface based method. Throughout this study, we focus primarily on the effects of modeling uncertainties on the assessment of collapse risk, but also demonstrate the applicability of the response surface based method to structural response limit states other than collapse.

4.3 Overview of Collapse Assessment Procedure and Results

The procedure for collapse assessment utilizes the performance-based earthquake engineering methodology developed by the Pacific Earthquake Engineering Research Center, which provides a probabilistic framework for relating ground motion intensity to the structural response and building performance through nonlinear time-history simulation (Deierlein 2004). Assessment of global sidesway collapse capacity is based on the Incremental Dynamic Analysis (IDA) technique (Vamvatsikos and Cornell 2002). In IDA, the structural model, which captures both material and geometric nonlinearities, is analyzed

for a specific ground motion record. This time-history analysis is repeated, each time increasing the scale factor on the input ground motion, until that record causes structural collapse, as identified by runaway interstory drift displacements. This process is repeated for an entire suite of ground motion records.[1] In our study, the ground motion intensity measure is the spectral acceleration at the first mode period of the building [$Sa(T_1)$]. The outcome of the IDA procedure is a collapse fragility function, a cumulative probability distribution that defines the probability of structural collapse as a function of the ground motion intensity. The median value of the fragility (or median "collapse capacity") corresponds to the ground motion intensity that causes collapse in half of the records of the ground motion suite. For a given structural model, the uncertainty in the collapse fragility from IDA represents the so-called record-to-record variability.

Several different metrics can be used to quantify collapse performance, either in absolute terms or relative to the earthquake intensity used for design. In the United States, design levels for seismic effects in building codes are based on the definition of a "maximum considered earthquake" or MCE. Accordingly, the collapse capacity can be described through the following metrics: (a) the collapse capacity margin, equal to the ratio of median collapse capacity obtained from IDA to the MCE intensity, (b) the probability of collapse conditioned on the MCE (or other hazard level of interest), and (c) the mean annual frequency of collapse, obtained by integrating the collapse probability distribution with the hazard curve for a particular site.

This procedure has been applied to assess the performance of both ductile and non-ductile RC frame buildings. The ductile frames represent designs that conform to current building code requirements, whereas the non-ductile frames represent older buildings that do not meet current building code design and detailing requirements, and typically exhibit worse seismic performance. The nonlinear analysis models consist of the two-dimensional three-bay frame, as shown in Figure 4.1a. Modeled in OpenSees, the simulation model captures material nonlinearities in beams, columns, and beam-to-column joints and large deformation (P-Δ) effects. Inelasticity in the beams, columns, and joints are modeled with concentrated springs idealized by the backbone response curve shown in Figure 4.1b and the associated

[1] For this study, the ground motions were selected to represent large earthquakes with moderate fault-rupture distances (i.e., non near-field conditions). This is the basic Far-Field ground motion set assembled by Haselton and Kircher as part of an Applied Technology Council project, ATC-63 (ATC 2007). These records were selected without consideration of epsilon, a measure of spectral shape which has been shown to have a significant impact on collapse capacity (Haselton 2006).

hysteretic rules developed by Ibarra et al. (Ibarra et al. 2005). An important attribute of the inelastic model is that it captures both in-cycle and between-cycle strength degradation, the former being particularly important for realistic simulation of collapse behavior (Ibarra 2003; Haselton 2006). Properties of these inelastic springs are obtained from calibration to experimental tests of RC beam-columns and joints, as described by Haselton (2006). These spring properties are calibrated to mean or expected values of the structural components. When used in combination with nonlinear geometric transformations and robust convergence algorithms, these structural models are capable of simulating structural response into the collapse limit state. These collapse models have been used in several applications, including the validation of seismic performance factors for building codes in the ATC-63 project (Applied Technology Council 2007; Deierlein et al. 2007).

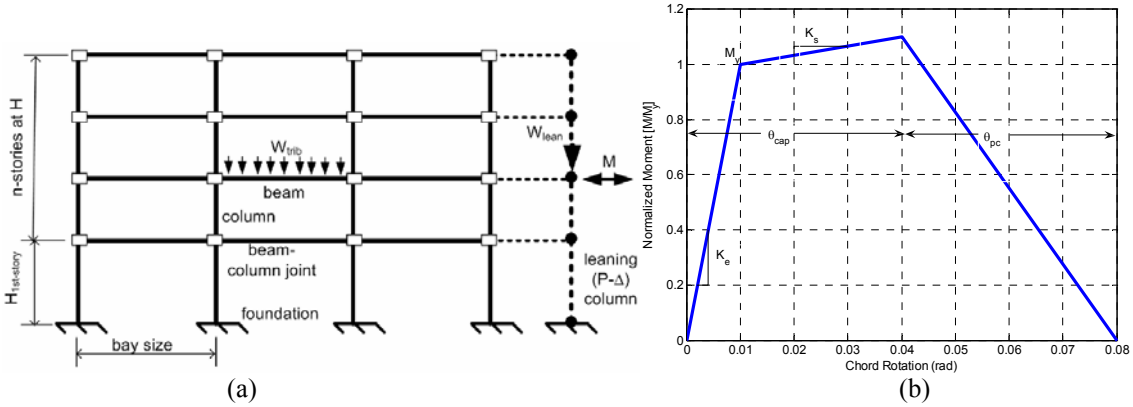

(a) (b)

Figure 4.1 Schematic diagram of analytical model for frame structures, showing (a) generalized two-dimensional model configuration and (b) nonlinear material features of beam-column hinges.

Haselton (2006) evaluated the collapse capacity of 30 ductile RC moment frames of varying height (1 to 20 stories) which were designed according to current building code provisions (ASCE 7-02, ACI 318-02 and IBC 2003 requirements for 'special' moment frames). The buildings are assumed to be located at a site in Los Angeles, for which the hazard curve has been defined through probabilistic seismic hazard analysis (Goulet et al. 2007). The calculated collapse margins (relative to the MCE) range from 1.1 to 2.1 and the conditional probabilities of collapse at the MCE vary from 0.12 to 0.47. When the collapse fragility is combined with the site hazard curve, the mean annual frequency of collapse ($\lambda_{collapse}$) varies between 2.2 x 10^{-4} and 25.5 x 10^{-4} collapses/year, corresponding to collapse return periods from 400 to 4500 years. These collapse assessments are conservative (ie. overstating the collapse risk), because they do not include an adjustment for spectral shape (Haselton 2006). The authors have also conducted a similar study of non-ductile RC frame

structures (Chapter 5). The collapse assessment results for the six case-study structures are reported in Table 4.1. (Note that the collapse rates are obtained by assuming all random variables to be ergodic. The approximation is not strictly true, as uncertain model parameters take a single value fixed over a structure's lifetime, while ground motion intensities will take a unique value for each earthquake. The error introduced by this approximation is trivial, however, for the small rates of interest here (DerKiureghian 2005).)

Table 4.1 Collapse metrics for case study reinforced concrete frame structures.

Num. of Stories	Frame Ductility	Framing System	T_1(s)[1]	Mean Sa_{gm}, collapse (g)	Margin compared to MCE	λ_{col} (x 10^{-4})
1	ductile	space	0.42	2.95	2.11	1.2
4	ductile	perimeter	1.12	1.30	1.71	1.7
12	ductile	perimeter	2.01	0.61	1.32	6.7
2	non-ductile	perimeter	1.04	0.71	0.89	15
4	non-ductile	space	1.98	0.30	0.65	62
12	non-ductile	space	2.26	0.35	0.83	22

[1]All metrics refer to model with mean parameters and are obtained form subset of 20 earthquake records

The collapse metrics reported here include the effects of both record-to-record and modeling uncertainties. The record-to-record uncertainties are calculated from the IDA results, where the logarithmic standard deviation ($\sigma_{ln,RTR}$) ranges between 0.35 to 0.45 depending on the structure of interest. Haselton (Haselton 2006) determined the modeling uncertainty through detailed study of a 4-story RC frame using the FOSM procedure and the mean estimates approach (discussed later). The logarithmic standard deviation associated with modeling uncertainties ($\sigma_{ln,modeling}$) is 0.45. When combined with the record-to-record uncertainties using SRSS, the modeling uncertainty increased the aggregate uncertainty by about 40% to 60%, depending on the structure. Although Haselton does not predict a shift in the median or margin associated with collapse, this increase of dispersion (σ_{ln}) has a significant impact on both the computed conditional collapse probabilities and mean annual frequencies of collapse, indicating the importance of accurately incorporating modeling uncertainties in the assessment. When structural modeling uncertainties are excluded from the analyses, the computed $\lambda_{collapse}$ is only $0.3x10^{-4}$ to 8.3×10^{-4} collapses/year.

4.4 Treatment of Modeling Uncertainties

4.4.1 Techniques for Incorporating Modeling Uncertainties

A variety of approaches have been used to study the effects of these modeling uncertainties on the fragilities for structural response. These approaches range from methods

that simplify the calculations by discretely interrogating the effects of one or more model random variables to specialized structural reliability methods and more general Monte Carlo-type methods.

Sensitivity analyses provide a straightforward method for interrogating the effects of modeling uncertainties on response quantities of interest. The effect of each random variable on structural response is determined by varying a single modeling parameter and re-evaluating the structure's performance. These studies, such as those conducted by Esteva and Ruiz (1989), Porter et al. (2002), Ibarra and Krawinkler (2003), and Aslani (2005), are used to select those modeling parameters that have the most significant impact on the response. While useful for identifying trends in the behavior, sensitivity analyses alone are not sufficient to quantify the effect of modeling uncertainties in the collapse risk assessment.

First-order-second-moment (FOSM) reliability methods can be used to propagate modeling uncertainties to quantify their effect on the collapse fragility (Baker and Cornell 2007). Here, we use FOSM to predict the parameters of the response distribution directly rather than a probability of failure or reliability index (β). Where X represents the set of model random variables with mean values M, in FOSM, the limit state g(x) is linearized using a Taylor series expansion about the mean (x = M), such that the mean of the fragility is unchanged (μ_g = g(M)) and the variance of the response due to sources of modeling uncertainty is computed from the gradients of g(x). Where the limit state function does not have a defined functional form, the needed gradients of the linearized limit state function can be obtained through perturbation of individual random variables in a series of sensitivity analyses. However, the linear approximation may be problematic when the limit state functions are highly nonlinear. FOSM will not predict a shift in the mean value of the fragility resulting from the effects of modeling uncertainties.

Several researchers have explored the effects of modeling uncertainties with FOSM, including Ibarra and Krawinkler (2003), and Lee and Mosalam (2005). In the study described previously, Haselton (2006) investigated the effects of modeling uncertainties on the collapse capacity of a code-conforming 4-story RC frame. Haselton used sensitivity analysis results to compute the relationship between model random variables and structural response for the gradients needed in FOSM calculations.[2] For the most realistic modeling case, the

[2] Haselton (2006) uses a one-sided gradient for the FOSM computations, calculating the slope separately in the two directions away from the mean and using the higher value (higher rate of change).

logarithmic standard deviation contribution from modeling and design uncertainties on collapse capacity is 0.45, which is roughly equivalent in magnitude to the record-to-record variability. This work by Haselton et al. provides the basis for comparison with the present study.

Another class of reliability-based methods that might be considered for this problem is the First-Order Reliability Method (FORM) and related Second-Order Reliability Method (SORM). These methods use linear or quadratic approximations, respectively, of the failure surface, and the approximations are centered around a design point (the point on the failure surface associated with the highest probability of failure). These methods are very effective at handling large numbers of random variables, and the approximation is very good at low failure probabilities. Further, probabilities are computed directly, unlike FOSM where only means and variances are computed. The challenge with using FORM/SORM is that the fragility function is a complete probability distribution for collapse capacity, so its specification requires calculations of the body of the distribution, where the FORM/SORM approximations are not as good as in the tails of the distribution. Further, specification of the complete fragility function requires repeated FORM/SORM calculations at many limit-state thresholds (ie. each ground motion intensity level), resulting in much greater computational expense than the FOSM approach. For these reasons, the older FOSM approach is generally preferred to FORM/SORM for incorporating modeling uncertainties into fragility functions.

An alternative approach uses Monte Carlo methods to determine the effect of modeling uncertainties on the structural response predictions (Rubinstein 1981; Helton and Davis 2001). Using Monte Carlo, one can generate realizations of each modeling random variable, which are inputted into a simulation model, and the model is then analyzed to determine the collapse capacity. When the process is repeated for hundreds or thousands of sets of realizations, a distribution of collapse capacity results associated with the input random variables is obtained. The simplest sampling technique to generate the realizations of model random variables is based on random sampling using the distributions defined for the input modeling random variables, though other techniques, known as variance reduction, can decrease the number of simulations needed. Porter et al. (2005) used Monte Carlo methods to predict structural damage in an existing 6-story non-ductile RC frame building located in Van Nuys, California based on a set of uncertain model random variables. Their study employed a two-dimensional non-deteriorating structural model. In another study, Zhang and Ellingwood (Zhang and Ellingwood 1995) investigated the effects of uncertain material

properties on structural stability problems using a Monte Carlo approach. While conceptually straightforward, these Monte Carlo procedures can become computationally very intensive if the time required to evaluate the limit state for each set of realizations of model random variables is non-negligible. For this reason, past seismic reliability studies using Monte Carlo analysis have tended to use less computationally intensive structural models, eg. (Porter et al. 2005), than the degrading, highly nonlinear models in this study.

The computational effort associated with Monte Carlo methods can be reduced when combined with response surface analysis (Helton and Davis 2001; Pinto et al. 2005). A response surface is a simplified functional relationship or mapping between the input random variables and the limit state criterion, such as collapse capacity of a structure. The price of this efficiency is a loss of accuracy in the estimate of the limit state, which depends on the degree to which the highly nonlinear predictions of structural response can be accurately represented by the simplified response surface. Ibarra and Krawinkler (2003) analyzed the collapse capacity of a single degree-of-freedom oscillator and used a response surface to represent the collapse capacity as a function of one of the model random variables, post-capping stiffness. In that particular case, Ibarra and Krawinkler's study found that the simplified FOSM procedure, the full Monte Carlo procedure, and the combined response surface/Monte Carlo approach all produced comparable results. However, this observation is based on a single degree-of-freedom model and only one random variable, and may not be easily generalized to multiple random variables and degrees of freedom.

Whichever procedure is utilized, correlations between the input random variables may significantly affect the extent to which modeling uncertainties impact the performance assessment (Val et al. 1997; Haselton 2006). For the nonlinear structural analyses considered here, questions about correlation involve both correlations between the multiple model parameters associated with a single structural component, and correlations between parameters for multiple components in a building. There is insufficient data to quantify these correlations, so values are typically based on expert judgment. In general, increased correlation tends to increase the dispersion (σ_{ln}) in the response quantity of interest and, hence, the fully correlated case is often considered to be conservative (Aslani 2005; Haselton 2006).

4.4.2 Combination of Sources of Uncertainty

Once the effects of modeling uncertainties have been predicted there remains significant debate related to interpretation of these results, centering on how the effects of modeling uncertainties should be combined with the effects of other sources of uncertainty, such as record-to-record uncertainties. For this purpose, different sources of uncertainty are sometimes characterized as either 'aleatory' (randomness) or 'epistemic' (lack of knowledge) (DerKiureghian and Ditlevsen 2007).

One approach for combining the effects of different sources of uncertainty is the confidence interval approach, e.g. (Cornell et al. 2002; Ellingwood 2007). The confidence interval method is illustrated by the collapse fragilities shown in Figure 4.2a. Record-to-record variability (treated as aleatory) is shown by the cumulative distribution function obtained directly from IDA analyses, and the epistemic uncertainty (related to modeling variability) creates the distribution on the median of that cumulative distribution. The distribution associated with epistemic uncertainty in this case may be obtained from FOSM, Monte Carlo methods, or expert judgment. In order to make predictions at a specified confidence level, the aleatory distribution is shifted to the appropriate percentile on the epistemic distribution (see e.g. Zariean and Krawinkler (2007)). For example, if the median of the aleatory distribution is shifted to the 10% probability of exceedance of the epistemic distribution, then the probabilities associated with the shifted aleatory distribution in Figure 4.2a are consistent with a 90% prediction of confidence. In other words, the 90% confidence measure implies a 90% probability that the true collapse capacity is higher than the collapse capacity predicted by the shifted fragility function. Although this approach is conceptually appealing, the resulting structural performance predictions become highly dependent on the level of confidence chosen, as shown in Haselton (2006). For example, at a spectral demand of $Sa(T_1) = 1$ g, the probability of collapse is close to zero for the median (50% confidence) estimate and over 0.4 for the 90% confidence estimate. In addition to the high sensitivity in results, this method requires distinguishing between aleatory and epistemic uncertainties, a subjective and debatable distinction.

A second approach, referred to as the mean estimates approach, can be used to combine the contributions of record-to-record and modeling uncertainties in structural response fragilities, provided that certain assumptions are made. When aleatory (record-to-record) uncertainties only are considered, the structural response is well-described by a lognormal distribution (Cornell et al. 2002), with logarithmic mean (λ) and standard deviation (σ_{ln}). In

the mean estimates approach, it is assumed that the epistemic (modeling) uncertainty describes uncertainty in the logarithmic mean (λ), and that this random variable is also lognormally distributed with log mean μ_λ and log standard deviation σ_λ. The random variables associated with epistemic and aleatory uncertainty are assumed to be independent. It can be shown that when these two distributions are combined the resulting distribution is also lognormal with the logarithmic mean of μ_λ (and median = $\exp[\mu_\lambda]$), and a logarithmic variance that is the sum of the two logarithmic variances (Benjamin and Cornell 1970). Thus, when the mean estimates approach is used, the median is unchanged when modeling uncertainties are incorporated, but the variance increases, as shown in Figure 4.2b. The results derived from this approach are not sensitive to whether individual uncertainties are classified as aleatory or epistemic, which is helpful when the classification of a particular uncertainty is not obvious.

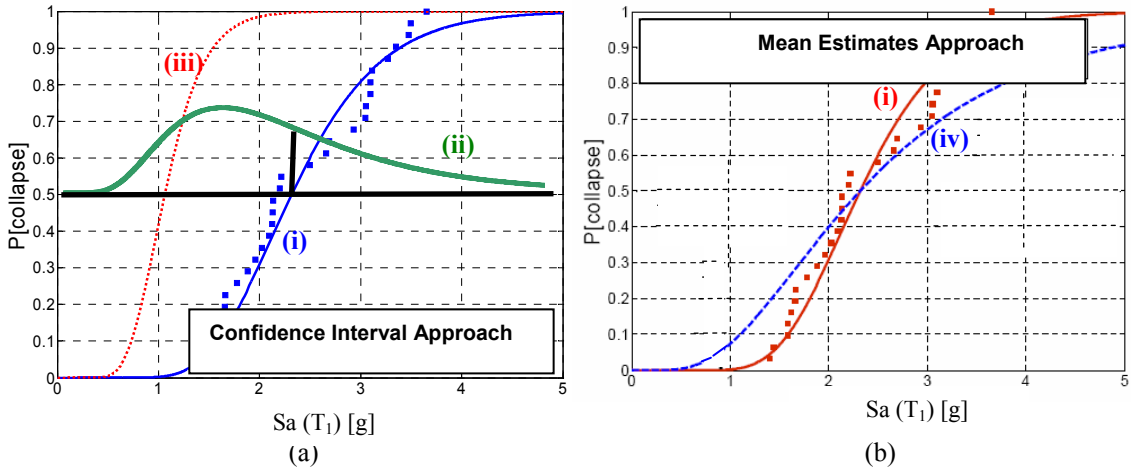

Figure 4.2 Collapse fragilities for a 4-story RC ductile frame structure, illustrating (a) the Confidence Interval Approach and (b) the Mean Estimates Approach. Legend: (i) distribution of collapse capacity due to aleatory (record-to-record) uncertainties only; (ii) distribution of the median of the collapse capacity distribution due to epistemic (modeling) uncertainties; (iii) aleatory distribution shifted to the 10th percentile of the epistemic distribution, ie. "90% confidence level"; (iv) distribution with expanded variance (SRSS) to account for epistemic and aleatory uncertainties.

The third approach, adopted here, uses Monte Carlo simulation of the uncertain model parameters to generate a set of alternate potential descriptors of the real structural response fragility. The record-to-record uncertainty is captured in the individual fragility curve variances. A combined fragility, incorporating both aleatory and epistemic uncertainties, is then computed as the expected value of the probability over the Monte Carlo realizations at

each spectral acceleration level.[3] This approach is explained in more detail below. Unlike the mean estimates approach, the more general formulation here allows for modeling uncertainty to both shift the median and the variance of the fragility function. It also does not assume independence between the aleatory and epistemic random variables, as was required above.

4.4.3 Proposed Procedure for Evaluating the Effects of Modeling Uncertainties

Owing to the relative advantages and disadvantages of the various methods and the significance of various sources of uncertainty in the assessment process, the response surface methodology in combination with a Monte Carlo approach is proposed as the preferred method to quantify the effects of modeling uncertainties on structural response. The most complete method, the full Monte Carlo procedure, is infeasible because of the computationally intensive nature of the time history analysis in this study (it takes approximately 300 minutes to compute the median collapse capacity for one set of realizations of the input random variables, and hundreds of realizations would be needed for each structure considered). FORM/SORM methods would also require many evaluations in order to obtain a continuous prediction of the probability of collapse as a function of spectral acceleration. The simplest method, FOSM with mean estimates approach, is unable to capture the potential shift in the median of the distribution associated with the effects of modeling uncertainties, and, as a result, it provides an insufficient representation of the effects of model uncertainties.

In the response surface based method, sensitivity analyses are first used to probe the effects of modeling variables on the median collapse capacity of the system. The results of the sensitivity analysis provide the inputs to regression analysis used to create the response surface, which represents the median collapse capacity as a function of model random variables. The response surface is idealized by a second-order polynomial functional form, which is capable of representing nonlinear limit states and interactive effects between the model random variables. Engineering judgment is used to confirm that the functional form is a realistic representation of the limit state, particularly where it is extrapolated beyond the region where sensitivity analysis data is available. Following creation of the response surface, a Monte Carlo procedure is used to obtain a suite of sample realizations for the set of random

[3] This approach does not preclude computation of confidence intervals, if needed. For a 90% confidence level, for example, compute the 90th percentile of the probabilities at each spectral acceleration level, rather than the expected (mean) value.

variables under consideration. For each set of realizations, the median collapse capacity of the structure is computed from the response surface. The outcome is a set of simulated collapse fragilities for the structure. At a given spectral acceleration level, each individual fragility curve will provide a probability representing record-to-record uncertainties, and the variation of these probabilities among the simulations represents the effect of model uncertainty. We compute the expected value of these probabilities at each spectral acceleration level to obtain the structural collapse fragility. These studies focus largely on the collapse limit state, but the same methodology is equally applicable to other limit states for which a response surface can be defined.

4.5 Evaluation of the Effects of Modeling Uncertainties on Case Study Structures

4.5.1 Overview and Discussion of 4-Story Ductile Frame Structure

The proposed method to assess modeling uncertainties is illustrated by applying it to the set of case study RC buildings that include both ductile and non-ductile design features. All frames have 6.1 m (20 ft) or 7.6 m (25 ft) bay spacings and 4.0 m (13 ft) story heights, except for the first story which has a 4.6 m (15 ft) height. Three different building heights are considered (1, 4, and 12-story ductile structures; 2, 4, and 12-story non-ductile structures). The frames are modeled as shown in Figure 4.1. The details of the design and the collapse assessment for these structures are available in Haselton (2006) and Chapter 5.

The assessment of modeling uncertainties focuses on uncertainties in the modeling parameters that define the lumped plasticity plastic hinges for beams, columns and joints. The beam-column hinges are modeled using an inelastic spring model developed by Ibarra and Krawinkler (2005). The element backbone (Figure 4.1b) and hysteretic rules are defined by six parameters: flexural strength (M_y), initial stiffness (K_e), post-yield (hardening) stiffness (K_s), capping point (θ_{cap}), post-capping deformation capacity (θ_{pc}) and cyclic deterioration (λ).[4] These parameters are assumed to be lognormally distributed, where the mean and standard deviation are obtained from previous research; Table 4.2 summarizes the logarithmic standard deviation for the parameters of each type of component. The joint modeling parameters, also shown in Table 4.2, are based on representative data from Mitra and Lowes (2007) and on engineering judgment where insufficient data is available. Modeling uncertainties associated with the beam-column joints are neglected for the ductile

[4] In this study, hardening stiffness is neglected because of its very small influence on collapse capacity.

moment frame structures, because capacity design provisions and transverse reinforcement requirements for joints have been shown to be sufficient to ensure that failure occurs outside the joints. For simplicity, other parameters related to element level modeling (e.g. pinching and residual strength) and system level behavior (e.g. damping, mass, live and dead loading) are not considered; earlier sensitivity studies found that modeling variables related to component strength and deformation capacity are the dominant model parameters affecting collapse assessment (Haselton 2006).

Table 4.2 Uncertainties in modeling parameters for RC beams, columns and joints.

Random Variable[1]	σ_{ln}	Source
Beam or Column Strength	0.19	Panagiatakos and Fardis (2001)
Beam or Column Stiffness	0.33	Haselton et al. (2008)
Beam or Column Plastic Rotation Capacity ($\theta_{cap,pl}$)	0.59	Haselton et al. (2008)
Beam or Column Post-Capping Rotation Capacity (θ_{pc})	0.72	Haselton et al. (2008)
Beam or Column Cyclic Deterioration (λ)	0.50	Haselton et al. (2008)
Joint Strength	0.39	Mitra and Lowes (2007)
Joint Stiffness	0.39	same as joint strength
Joint Rotation Capacity	0.59	limited data; same as beam-columns
Joint Post-Capping Rotation Capacity	0.72	limited data; same as beam-columns
Joint Cyclic Deterioration	0.50	limited data; same as beam-columns

[1]Normalized variables, with $\mu_{ln} = 0$.

Independent assessment of each of the random variables described in the preceding discussion is computationally prohibitive, given the analysis time that would be required to assess combinations of the five random variables for each plastic hinge location and beam-column joint in the frame. To further reduce the number of variables under consideration, correlations are assumed between parameters within each component and between components in the building. At the element level, two meta random variables are created. The *strength* meta variable represents the strength and stiffness model parameters (M_y, K_e) in an element, implying that the strength and stiffness are perfectly correlated within each element. The *ductility* meta variable does the same for ductility parameters (θ_{cap}, θ_{pc}, and λ), such that plastic rotation capacity, cyclic deterioration, and post-capping rotation capacity are assumed to be perfectly correlated. At the structural level, the *strength* and *ductility* meta variables are assumed to be perfectly correlated with like variables among all like components in the entire structure. These correlation assumptions leave six meta variables: beam strength, beam ductility, column strength, column ductility, joint strength and joint ductility. Each meta variable is a standard lognormal random variable (with $\mu_{ln} = 0$ and $\sigma_{ln} = 1$), which can be mapped to the model parameters of interest. While these assumptions are loosely supported by observations from the model calibration study of RC columns (Haselton 2006), there is

insufficient empirical evidence to quantify correlations and the assumed correlations are made primarily for tractability.

Based on the definition of these meta random variables, sensitivity analyses are conducted to quantify the effects of each meta modeling variable on the structural response. The realizations of random variables used in the sensitivity analysis are based on central composite design, including star points (in which only one random variable is changed at a time) and factorial points (capturing interactions between the random variables) (Pinto et al. 2005). In total, 33 sensitivity analyses were conducted for each ductile structure based on the four meta random variables of interest. For the non-ductile frames, 93 sensitivity analyses were necessary to account for the joint strength and ductility meta variables in addition to the column and beam strength and ductility variables. Each random variable was perturbed +/- 1.7 standard deviations[5] away from the mean individually, and in combinations with other random variables at +/-1σ. For each sensitivity analysis, a nonlinear model is created with modified element material properties, and the incremental dynamic analysis is run with a subset of 20 earthquake records.[6] The nonlinear IDA collapse assessment procedure is conducted as described in Section 2 and in more detail in Chapter 3.

To examine the effects of modeling uncertainty on structural behavior, two distinct limit states are considered for the 4-story ductile moment frame building, corresponding to (a) exceedance of 1% interstory drift and (b) collapse. The fragility functions are defined in terms of the spectral acceleration at the structure's fundamental period.

A summary of sensitivity analysis results for the two limit states of interest for the 4-story ductile frame are shown in Figure 4.3, where Figure 4.3a and Figure 4.3c provide a histogram of the 33 analyses for each limit state and Figure 4.3b and Figure 4.3d provide a tornado diagram of sensitivity results. As shown in Figure 4.3b, of the four random variables, column strength has the largest effect on the median collapse capacity, followed by column ductility, beam strength and beam ductility. Beam strength has an inverse effect on collapse since the weaker beams tend to delay the formation of unfavorable story mechanisms. Comparing the two different limit states (Figure 4.3a and Figure 4.3c), it is apparent that modeling

[5] 1.7 ≈√3; chosen for practicality (and with reference to values typically used in the experimental design literature).

[6] This subset of earthquake records was chosen to reduce the computational time needed to conduct the study. The response spectra of this subset were verified to be characteristic of the response spectra of the whole suite of records, but the collapse capacities reported may be somewhat different than those reported elsewhere because of the smaller number of records used.

uncertainties are more significant for the collapse limit state than the 1% interstory drift limit state. In particular, the beam and column ductility meta variables have virtually no effect on the 1% drift fragility, as these uncertainties are related to highly nonlinear structural behavior that does typically not occur before 1% interstory drift.

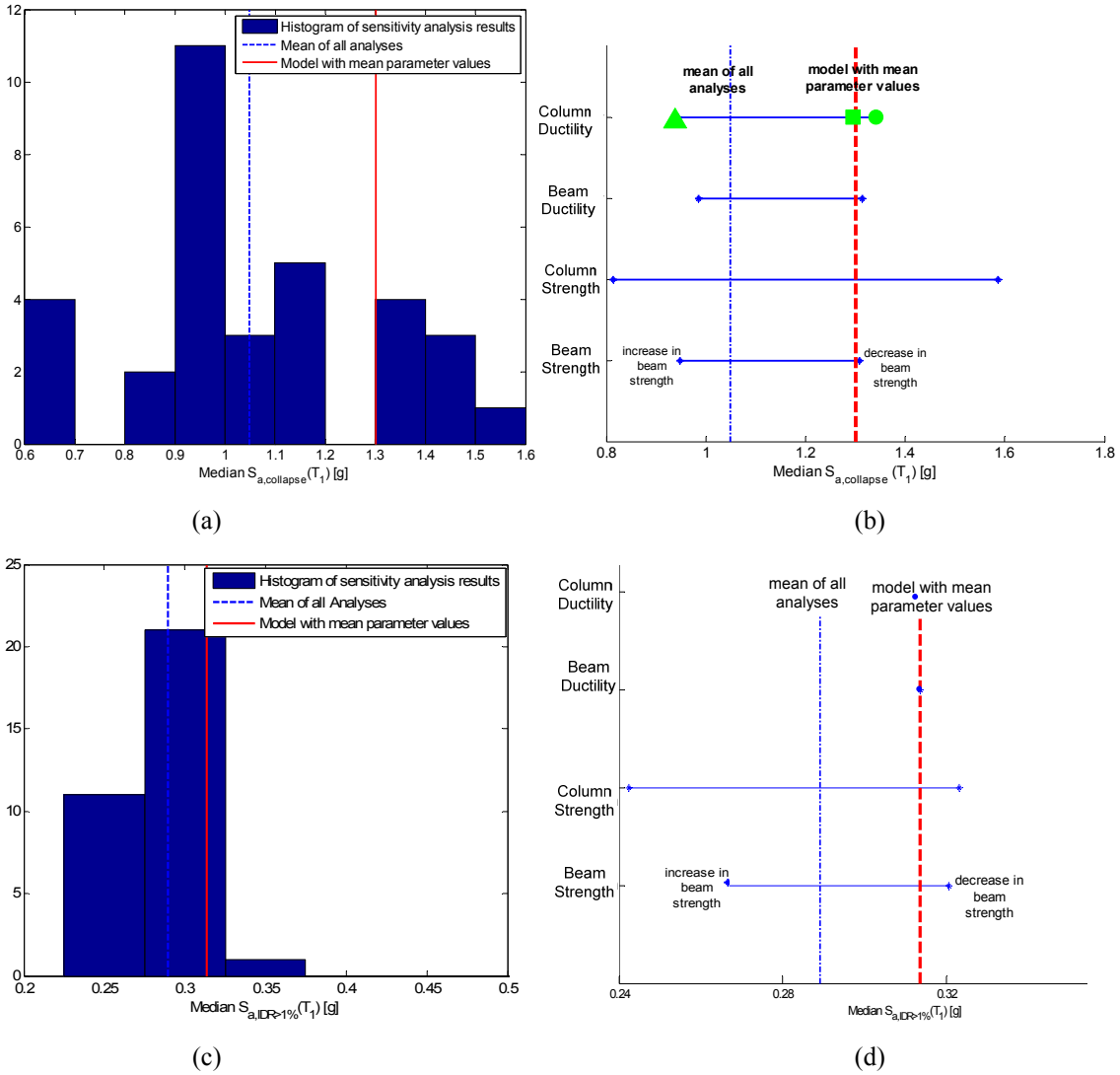

Figure 4.3 Histogram showing the results of 33 sensitivity analyses for the median spectral acceleration corresponding to (a) the collapse capacity and (c) the 1% interstory drift limit state. Tornado diagram from sensitivity analysis results, demonstrating the effect of varying each meta variable individually (+/- 1.7σ) for: (b) median collapse capacity and (d) 1% interstory drift limit state. The markers on column ductility in Figure 4.3b are shown for easy comparison to Figure 4.4.

The sensitivity analyses also demonstrate that the random variables have an asymmetric effect on the response, e.g., decreases in ductility tend to have proportionally more significant effects on collapse capacity than increases. This behavior is further illustrated in Figure 4.4, where we observe the effects of saturation in collapse capacity. These nonlinearities are particularly acute in the collapse limit state, but are also apparent at the 1% drift limit state.

This characteristic cannot be captured by the linearized limit state functions in FOSM analysis.

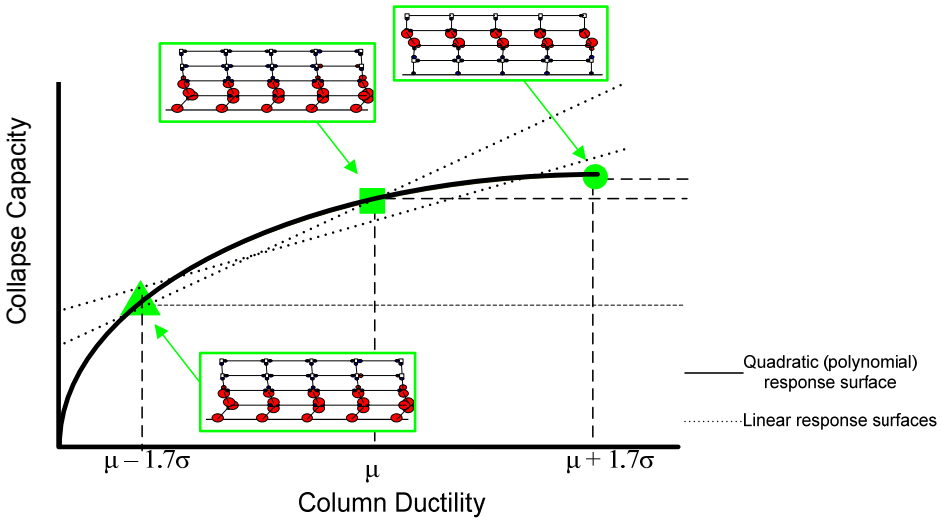

Figure 4.4 Illustration of nonlinear relationship between model random variables (eg. column ductility) and structural response (eg. collapse capacity). The quadratic response surface provides a good fit to the data, while the linear response surface(s) are only able to capture average trends. The nonlinearities are largely due to the structure's many possible collapse modes, illustrated by the superimposed 4-story frame structures.

The sensitivity analysis results are used to create a response surface that describes each limit state as a function of the input random variables. The response surface is idealized by a second-order polynomial that is fitted to the data through standard regression analysis (eg., the 'regress' function in Matlab). As opposed to linearized limit state for standard FOSM methods, the quadratic response surface enables representation of the nonlinearities and asymmetries in the relationship between the model random variables and the structural response.

For the 4-story ductile moment frame example, the quadratic response surfaces for the two limit states, median collapse capacity [$\hat{m}_{\text{collapse}} = \exp(\mu_{\ln,Sa,col})$] and 1% interstory drift [$\hat{m}_{IDR>1\%} = \exp(\mu_{\ln,Sa,IDR>1\%})$] are given by the following equations,

$$\mu_{\ln,Sa,col} = 0.26 - 0.077(BS) + 0.20(CS) + 0.073(BD) + 0.098(CD) - 0.052(BS^2) + 0.064(BS)(CS) - 0.019(BS)(BD) + 0.078(BS)(CD) - 0.045(CS^2) + 0.052(CS)(BD) - 0.043(CS)(CD) - 0.044(BD^2) + 0.019(BD)(CD) - 0.047(CD^2) \quad (4.1)$$

$$\mu_{\ln,Sa,IDR>1\%} = -1.15 - 0.063(BS) + 0.085(CS) - 0.025(BS^2) + 0.067(BS)(CS) - 0.038(CS^2) \quad (4.2)$$

where *BS* refers to beam strength, *BD* to beam ductility, *CS* to column strength and *CD* to

column ductility meta variables. The response surface of Eqn. (4.1) is evaluated according to statistical measures of goodness of fit with R^2 equal to 0.99 and a p-value of 1.11×10^{-16}. In addition, the variance inflation factors are computed to be << 10, indicating that collinearity is not a problem. The fit of Eqn. (4.2) yields similarly robust values. A graphical representation of the response surface for median collapse capacity (Eqn. 4.1) is shown in Figure 4.5. As expected, column strength, column ductility and beam ductility all have a positive effect on the median collapse capacity, while beam strength has an inverse effect.

The response surface provides a good representation of the sensitivity analysis results in the region +/- 1.7σ for each of the normalized random variables. However, when extrapolated outside this region, it is possible that the fitted second-order response surface may not increase monotonically as we would expect. In these cases, we modified the fitted response surface to have monotonic behavior. These changes were implemented for completeness, but they do not have a large influence on the final results because these discrepancies only exist in the region rarely sampled in the Monte Carlo procedure.

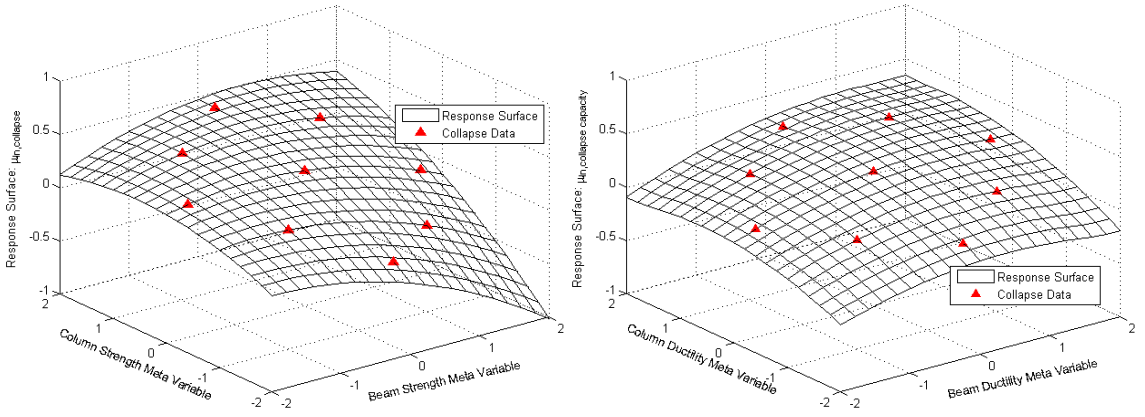

Figure 4.5 Graphical representation of the polynomial response surface for collapse capacity of the 4-story ductile moment frame. Each of these represents a slice of a multi-dimensional surface. In (a) the effects of column strength and beam strength are shown, while beam ductility and column ductility meta variables are held constant (at 0, their mean values); likewise, (b) illustrates the effects of varying beam and column ductility.

Using the calculated response surfaces as a surrogate for time-history analyses, the Monte Carlo method is used to incorporate the effects of the uncertain model random variables on the predicted limit state fragilities. The model random variables are sampled 10,000 times, each time generating a set of realizations that are consistent with the assumed lognormal distributions of the meta model random variables. For each set of realizations, the response surface is used to calculate the median capacity of the structure. Therefore, from each of the

ten thousand sets of realizations, predictions of the median collapse capacity and 1% interstory drift limit state are obtained. As noted previously, since a reduced set of ground motion records is used to assess the response surface, only the median collapse point is extracted from the surface. The logarithmic standard deviation due to record-to-record uncertainties is assumed to be constant over the response surface and set equal to the value obtained for the collapse analyses of the median structural model using the full record set (44 records). This assumption is made for practical convenience, since conceptually it is possible to re-estimate σ_{ln} for each realization, provided that the analyses used to generate the response surface are based on a sufficiently large number of ground motion records.

The final step is to recreate the limit state fragility function, based on the Monte Carlo results, to include both the effects of record-to-record and modeling uncertainties. Each Monte Carlo realization is associated with a different fragility describing the probability of failure as a function of spectral acceleration. As an example, shown in Figure 4.6a are results for the probability of collapse at $Sa(T_1) = 1.91g$ for all the 10,000 Monte Carlo realizations. The final fragility probability is the expected value of the collapse probability at each spectral acceleration level. Figure 4.6b illustrates the effects of modeling uncertainties showing both the collapse fragility curve for the mean structural model considering only record-to-record uncertainties (the lower curve), and the collapse fragility including both record-to-record and modeling uncertainties (the upper curve). The superposition of histograms of the probabilities at selected spectral acceleration levels in Fig. 6b are included to demonstrate the method through which the upper curve is obtained.

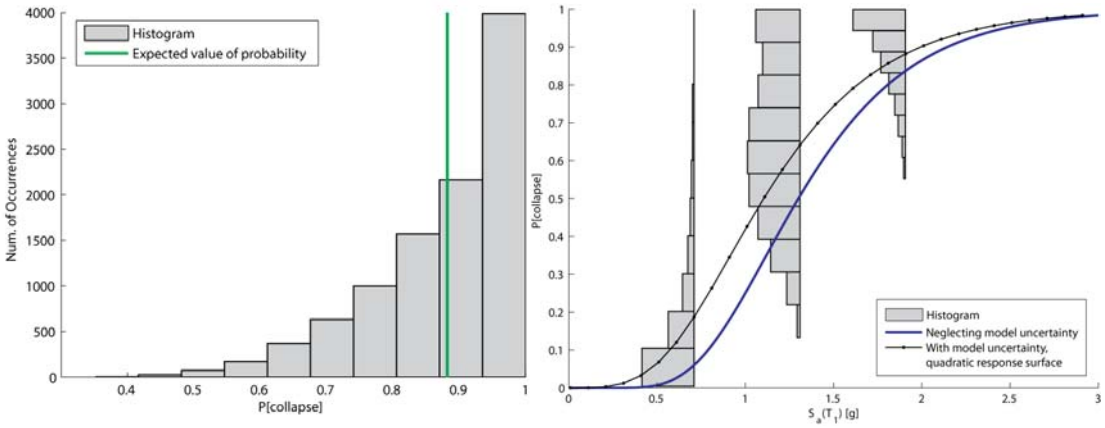

(a) (b)

Figure 4.6 (a) Histogram of collapse probabilities obtained from Monte Carlo realizations at $Sa(T_1) = 1.91g$ and (b) Computed collapse fragilities with histograms superimposed at selected Sa levels.

Using the response surface procedure we observe that modeling uncertainties tend to both increase the dispersion (σ_{ln}) in the structural response fragility and shift the prediction of the median. Figure 4.7 illustrates the fragility curves for the two limit states (collapse and 1% drift), where the proposed response surface based method for including modeling uncertainties (Figure 4.7a and Figure 4.7c) is contrasted with a FOSM approach (Figure 4.7b and Figure 4.7d). Several observations can be drawn from these figures. First, comparing the plots in Figure 4.7a versus Figure 4.7b and Figure 4.7c versus Figure 4.7d, the response surface based method captures the shift in the median point, which is not predicted by the FOSM-type approaches. This inability to predict the shift in the median is a significant limitation of FOSM, especially at the collapse limit state, for which we observe a 19% decrease in the median collapse capacity of the 4-story ductile moment frame. Overall, the comparison of Figure 4.7a and Figure 4.7c demonstrates that the model random variables have a less significant impact on pre-collapse limit states, and we observe both a smaller shift in the median (~3%) and a smaller increase in the logarithmic standard deviation. The lesser effect of modeling uncertainties on the one-percent drift limit state is unsurprising, because much of the model uncertainty relates to element deformation capacity and cyclic degradation properties that do not have a significant effect when nonlinear deformations in the structure are much smaller.

The results illustrated in Figure 4.7a and Figure 4.7c are somewhat contrary to the conventional expectation that the effect of modeling uncertainties is to flatten the response fragility, but not to shift the median. For example, suppose we use the FOSM with mean estimates approach to quantify the impacts of model uncertainties on the fragility representing exceedance of one-percent interstory drift, obtaining the results shown in Figure 4.7d; we observe the characteristic flattening from incorporating additional sources of uncertainty. The same results are obtained if we use the response surface based method, provided that the response surface is linear, as illustrated in Figure 4.7b. Therefore, it is apparent that it is the nonlinear shape of the relationship between the structural response limit state and model random variables, as shown in Figure 4.4 and Figure 4.5, that predicts the shift in the median, and which cannot accurately be captured by the linearization in FOSM or a linear response surface.

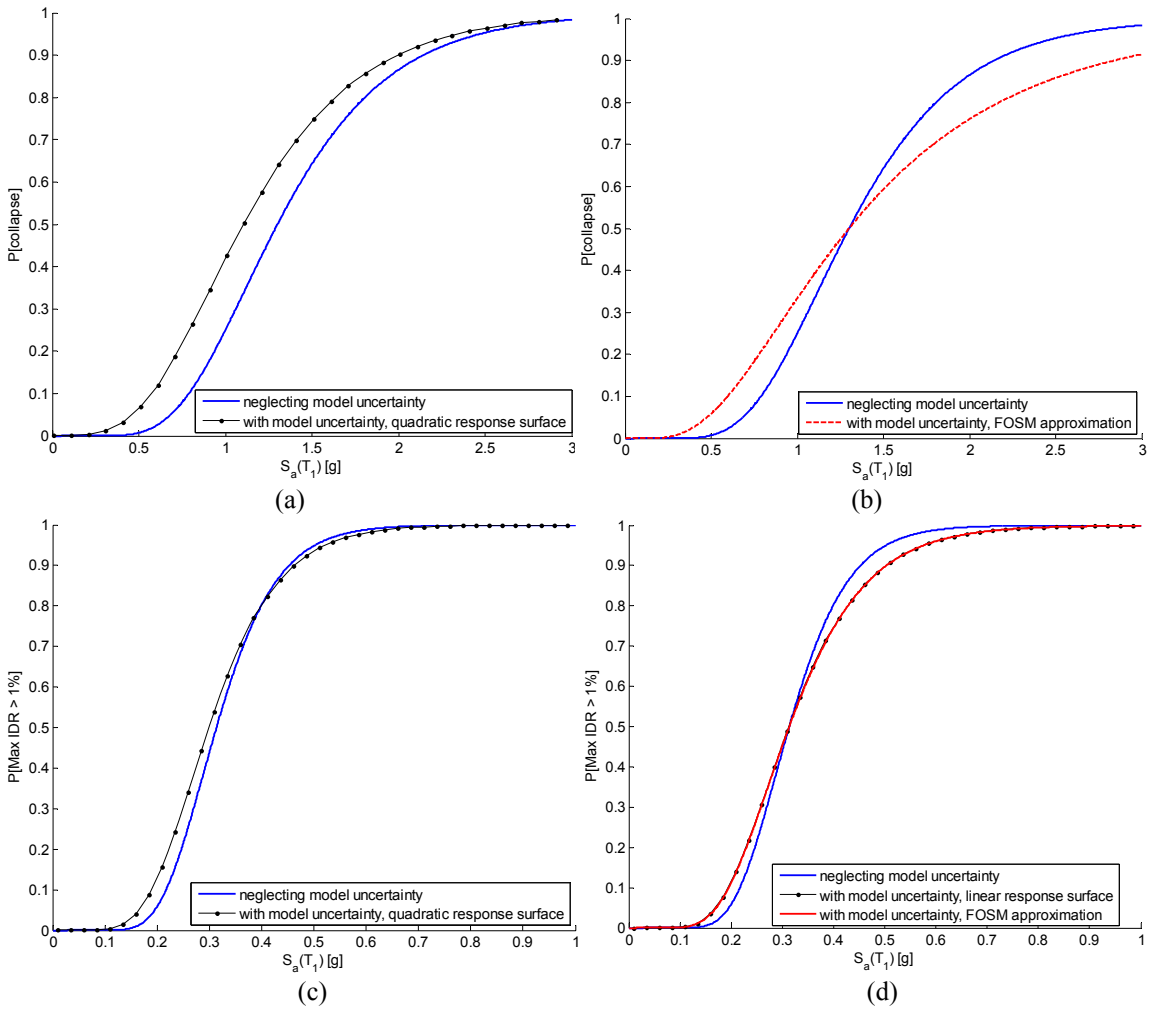

Figure 4.7 Structural response fragilities representing the collapse limit state, obtained using (a) quadratic (polynomial) response surface and (b) FOSM approximation, and the 1% interstory drift (IDR) limit state, obtained using (c) quadratic response surface and (d) FOSM approximation/linear response surface.

This nonlinear relationship depends on both the limit state of interest and the properties of the structure. For the 4-story example structure, the saturation of collapse capacity as a function of model random variables occurs because the structure has many possible failure modes, and an increase in a given model random variables tends to switch the failure mode. Hence, we do not see a large improvement in the collapse capacity as model random variables increase (see Figure 4.4). Additional unpublished parametric studies by the authors indicate that "balanced designs," where the structure is not dominated by a single failure mode, tend to see a more significant shift of the median collapse capacity caused by the effects of modeling uncertainties. We observe below, for example, a smaller shift in the median for the one-story building, which has only one failure mode. For more discussion of the collapse failure modes for the case study structures see Haselton (2006) and Chapter 5.

4.5.2 All Case Study Structures

This same Monte Carlo and response surface method was used to investigate the effects of modeling uncertainties on the collapse fragility for five other RC frame buildings. These effects are summarized for the case study structures in Table 4.3 and Table 4.4, and the collapse probability distributions are illustrated in Figure 4.8. As described earlier, the effect of incorporating modeling uncertainties is to shift the median collapse capacity and to increase the dispersion (σ_{ln}) of the collapse fragility. However, the extent of the change depends on the structure under consideration. Consideration of model uncertainties actually increases the median collapse capacity of the 12-story non-ductile RC frame, which is atypical and contrary to the decrease observed for the 4-story ductile frame and all the other frame structures. The increase for the 12-story non-ductile frame occurs because the nonlinearities in the relationship between joint strength and collapse capacity are reversed from those shown in Figure 4.4. For the 12-story frame, there is a very strong benefit from increasing the joint strength and moving the collapse mechanism out of the joints and into the beams, but there is a much smaller decrease in collapse capacity if the joint strength meta variable is decreased. The 1-story ductile structure has only a small shift in the median; this structure has essentially one possible collapse mode, a story mechanism in the first story.

Table 4.3 and Table 4.4 illustrate the importance of accurately incorporating modeling uncertainties in the analysis. The base case, no consideration of modeling uncertainty, may be highly unconservative, and under-predicts the rate of collapse by a factor of 2.3 on average. The simplified FOSM approach may underestimate or overestimate the rate of collapse depending on the structure. Referring to Figure 4.8, we observe that in many cases the left tail of the collapse fragility obtained by the FOSM (using the mean estimates approach) and proposed response surface based method are fairly close. However, when integrated with the hazard curve to obtain the mean annual frequency of collapse there are more significant differences between the FOSM/mean estimate approach and the response surface based approach in some cases. FOSM will also significantly underestimate the conditional probabilities of collapse for high probabilities of collapse. These differences are most significant when the relationship between the model random variables and the structural response is highly nonlinear and a shift in the median collapse capacity is likely. They are also more critical for structures, like the non-ductile RC frames, that have low collapse capacity relative to the MCE.

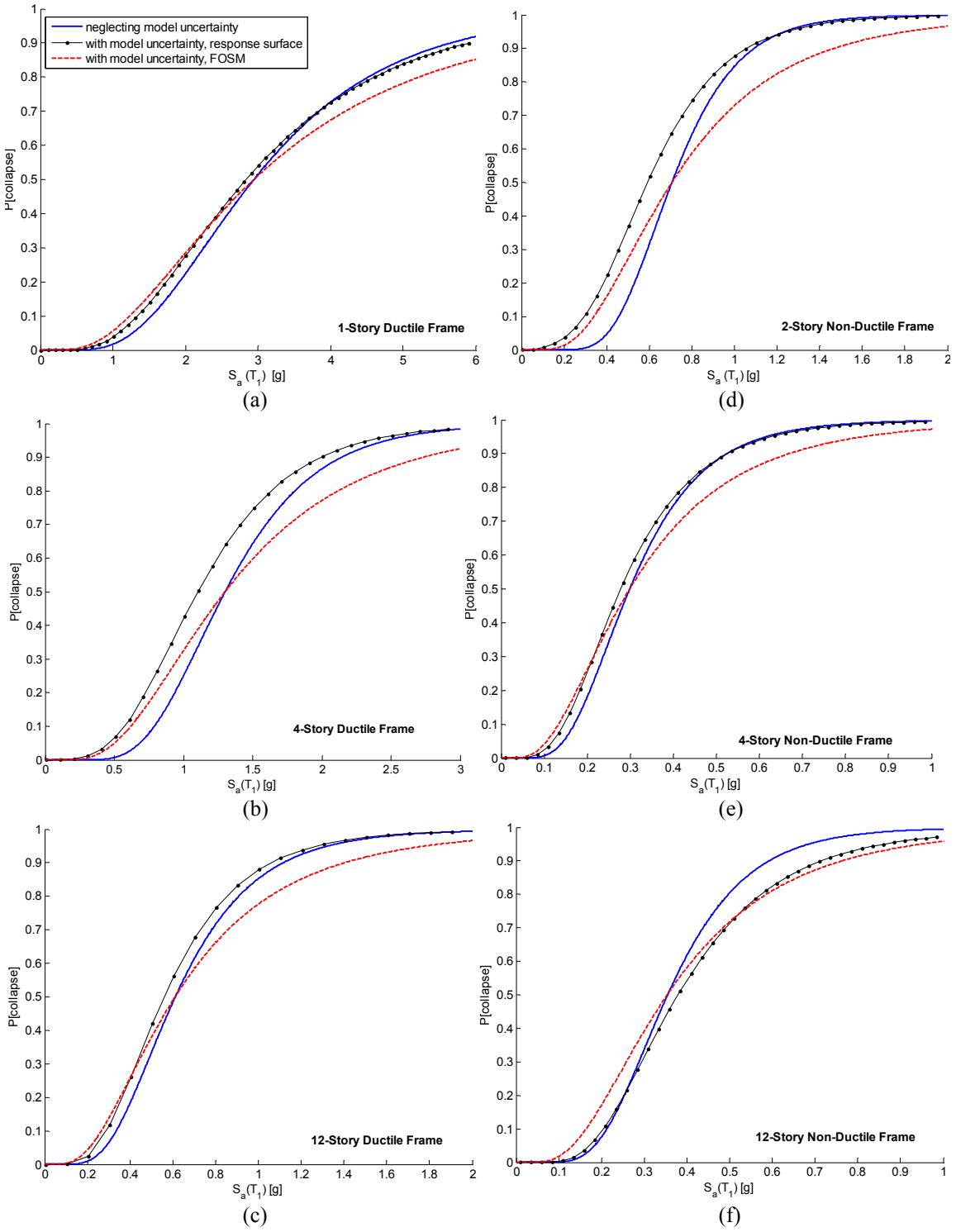

Figure 4.8 Collapse fragilities obtained for case study RC frames.

Table 4.3 Predicted effect of modeling uncertainties on median and dispersion (σ_{ln}) of collapse fragility, comparing response surface based approach and FOSM with mean estimates.

		Response Surface		FOSM	
Num. of Stories	Frame Ductility	% change in median	% change in dispersion	% change in median	% change in dispersion
1	ductile	-4%	12%	0%	25%
4	ductile	-19%	19%	0%	35%
12	ductile	-9%	10%	0%	28%
2	non-ductile	-18%	28%	0%	39%
4	non-ductile	-7%	12%	0%	30%
12	non-ductile	8%	18%	0%	23%

Table 4.4 Effect of modeling uncertainties on conditional probabilities and mean annual frequency of collapse ($\lambda_{collapse}$), comparing the response surface and FOSM methods.

Num. of Stories	Frame Ductility	No consideration of modeling uncertainty	FOSM with mean estimates, where $\sigma_{inmodeling}$ = 0.45	Response surface method
			P[Collapse|MCE]	
1	ductile	0.09	0.16	0.14
4	ductile	0.11	0.21	0.26
12	ductile	0.26	0.32	0.33
2	non-ductile	0.73	0.64	0.80
4	non-ductile	0.82	0.74	0.83
12	non-ductile	0.62	0.58	0.54
			$\lambda_{collapse}$ x10^{-4}	
1	ductile	1.2	4.1	1.6
4	ductile	1.7	6.1	5.9
12	ductile	6.7	17	12
2	non-ductile	15	36	44
4	non-ductile	62	111	89
12	non-ductile	22	46	24

4.5.3 Effects of Correlations between Model Random Variables

In the results presented thus far the meta random variables are assumed to be uncorrelated. Since correlations are very difficult to quantify, it is important to evaluate the impact of the correlation assumptions on the effects of modeling uncertainties. In order to examine the implications of these assumptions, two other sets of correlation assumptions are considered for the 4-story ductile frame. In the first case (Case I), the strength meta variables and the ductility meta variables are assumed to be correlated between beams and columns, but there is no correlation assumed between the strength and ductility parameters. In the second case (Case II), the beam meta variables (strength and ductility) are assumed to be correlated, as are the column meta variables, but the beam and column variables remain uncorrelated. The correlations only affect the Monte Carlo stage of the procedure, and they do not affect running of the nonlinear response analyses to conduct the sensitivity analyses and build the response surface. Therefore, it is relatively easy to vary the correlation model assumptions and obtain new results. The ease with which correlations can be studied is another benefit of the response surface based approach. To vary correlation assumptions in a

full Monte Carlo approach, these dependencies would need to be included at the structural analysis stage, a painstaking process for each of the hundreds of Monte Carlo realizations needed. Thus the response surface approach is particularly well-suited to research applications, such as those presented here, where correlation assumptions are still being investigated.

For Case I, full correlation between the meta variables leads to a 6.4% increase in the median collapse capacity from the baseline uncorrelated case [from 1.10 to 1.17g], thus reducing the overall effect of modeling uncertainties on the outcome. These results, summarized in Table 4.5, suggests that the relative difference in beam and column strength and beam and column ductility is a larger factor in determining collapse capacity than the absolute values. In Case II, as the assumed correlation between the meta random variables decreases the median collapse capacity decreases and the dispersion (σ_{ln}) increases. At higher levels of correlation it becomes more likely that beam behavior is either very good (in terms of both strength and ductility) or very bad in relation to column behavior. Since poor behavior tends to decrease the collapse capacity more than good behavior increases it, the median reduces with increasing Case II correlation. It is difficult to quantify correlations of this sort, but the Case II correlations (relating beam strength for example, to beam ductility) are not supported by the currently available data, eg. Haselton (2006). Thus, the Case II correlation study is more for illustration than practical application. On the other hand, the Case I correlations (similar properties among similar members in a frame) are more likely, but the Case I correlation effects are relatively small and assuming zero correlation tends to be conservative. Negative correlations were also examined, but these are unsubstantiated by experimental data.

Table 4.5 Parametric study of element level correlation assumptions on collapse fragility for 4-story ductile frame.

(a) Case I

Correlation Assumptions	Collapse Fragility	
ρ	median Sa(T_1) (g)	σ_{ln}
0[a]	1.10	0.48
0.5	1.12	0.47
1	1.17	0.47

(b) Case II

Correlation Assumptions	Collapse Fragility	
ρ	median Sa(T_1) (g)	σ_{ln}
0[a]	1.10	0.48
0.5	1.05	0.51
1	1.01	0.55

[a]Uncorrelated meta random variables; these are the results presented previously

To probe the effects of structural level correlation assumptions on modeling uncertainties, we considered another case where the meta variable definitions were revised to examine a situation in which correlations between certain beams and columns were imposed to

intentionally accentuate a critical collapse state. As initially defined, the meta variables are assumed to be perfectly correlated over every element in the building, e.g. beam strength of the 1st-floor beams is correlated to the beams in all the other floors. To further examine building level correlation assumptions in the study of the 4-story ductile frame structure, additional meta variables were created for the 3rd-floor beam strength (BS3) and the 2nd-story column strength (CS2). These meta variables are assumed to be uncorrelated from the other strength meta variables in the structure. Since the 4-story ductile frame structure often fails in a story mechanism in the second story (see Haselton (2006) for more details), these additional meta variables were chosen to represent an upper bound on the effects of spatial correlation assumptions in the frame. To incorporate the two new meta variables, additional sensitivity analyses were run, a new response surface was created, and the Monte Carlo procedure was repeated. Based on these analyses, relaxation of the full correlation assumption by the addition of two meta random variables lead to a 10% decrease in the median collapse capacity of the structure, as compared to the default case where the beam and column properties were assumed to be perfectly correlated in the building. Given the fact that the situation considered (3rd-floor beams and 2nd-story columns uncorrelated from the other random variables) is intentionally pessimistic for this frame, the change in median is relatively modest. If each story, or each column, were treated separately, or with partial correlation assumptions, the effects of relaxing the correlation assumptions would likely be much smaller.

4.6 Simplified Method

This study demonstrates the importance of appropriately treating structural modeling uncertainties in collapse performance assessments. However, the response surface based procedure requires significant computational and analysis time, necessitating running between 30 and 95 sensitivity analyses (depending on the number of meta random variables), as well as the creation of the response surface, and generation of Monte Carlo realizations. Of these, the sensitivity analyses are the most time consuming. Depending on the level of complexity of the structural model, the number of earthquakes used in incremental dynamic analysis, and the available computing power, each sensitivity analysis could take 5 to 20 hours of computing time. This level of effort may not be warranted for all problems, and it is

therefore desirable to develop a simplified method that can be used to approximate the effects of modeling uncertainties.

The proposed simplified method is capable of estimating both the shift in the median and the increase in the dispersion (σ_{ln}) due to modeling uncertainties. We call this method ASOSM, for approximate second order second moment. The method requires running sensitivity analyses, though fewer than required for the response surface based method. Beyond the mean model, the sensitivity studies involve running nonlinear response analyses for each of the key random variables scaled to +/-1.7σ. For the ductile RC frames with four meta variables, this requires the mean model analysis, plus eight additional analyses in which each meta variable is increased or decreased independently (ie. $X_i^+ = \mu_{Xi} + 1.7\sigma_{Xi}$ and $X_i^- = \mu_{Xi} - 1.7\sigma_{Xi}$). In this sense, the method is similar to the analyses required for the FOSM assessment.

The logarithmic standard deviation of the response fragility, including the effects of modeling uncertainties, can be computed following the standard first order (FOSM) approach. The gradients used in FOSM computations should represent the average slope about the mean i.e.,

$$\frac{\partial g(X)}{\partial X_i} = \frac{\Delta \mu_{\ln Sa,col}}{\Delta X_i} = \frac{\mu_{\ln Sa,col}(X_i^+) - \mu_{\ln Sa,col}(X_i^-)}{X_i^+ - X_i^-}, \tag{4.3}$$

where g(X) is the collapse capacity. Note that Eqn. (4.3) differs from some of the FOSM calculations reported earlier, which used a maximum or one-sided gradient. After the gradients are calculated, the dispersion associated with modeling uncertainties is computed from the following equation for n random variables,

$$\sigma^2_{\ln,\mathrm{mod}} = \left[\sum_{i=1}^{n} \sum_{j=1}^{n} \left[\frac{\partial g(X)}{\partial X_i} \frac{\partial g(X)}{\partial X_j} \right] \rho_{ij} \sigma_i \sigma_j \right] \tag{4.4}$$

and combined with the record-to-record uncertainties using SRSS,

$$\sigma^2_{\ln,total} = \sigma^2_{\ln,\mathrm{mod}} + \sigma^2_{\ln,RTR}. \tag{4.5}$$

As shown in Table 4.6, the resulting σ_{ln} shows very good agreement with those obtained from the response surface based procedure for the six RC frame buildings.

Table 4.6 Comparison of predicted dispersion (σ_{ln}) of the collapse fragility when record-to-record and modeling uncertainties are included, using the response surface based approach and ASOSM.

Num. of Stories	Frame Ductility	σ_{ln} (response surface)	σ_{ln} (ASOSM)	% Error[1]
1	ductile	0.58	0.58	0%
4	ductile	0.48	0.46	-4%
12	ductile	0.52	0.52	0%
2	non-ductile	0.47	0.39	-16%
4	non-ductile	0.50	0.49	-2%
12	non-ductile	0.49	0.47	-3%

[1] ASOSM compared to response surface approach

The shift in the median is predicted based on the nonlinearities in the relationship between structural response and the model random variables (again, refer to Figure 4.4). The response asymmetry is given by the parameter Δ^+/Δ^- ,

$$\Delta^+ \Big/ \Delta^- = \frac{\hat{m}^+ \Big/ \hat{m}}{\hat{m} \Big/ \hat{m}^-}, \tag{4.6}[7]$$

where $\hat{m}$ is the median capacity of the model with mean model parameters, and

$$\hat{m}^+ = \frac{1}{n}\sum_{i=1}^{n} m_{X_i + x\sigma_i} \text{ and } \hat{m}^- = \frac{1}{n}\sum_{i=1}^{n} m_{X_i - x\sigma_i}, \tag{4.7}$$

represent the average of the median collapse capacities when the model random variables are perturbed individually to +1.7σ, and –1.7σ respectively, and n is the number of perturbed analyses performed (equal to the number of model random variables). Using data from the six RC frame example structures, the resulting shift in the median collapse capacity can be calculated by the following,

$$\frac{\hat{m}_{\text{mod}}}{\hat{m}} = 0.64\left(\Delta^+ \Big/ \Delta^-\right) + 0.36 \tag{4.8}$$

This equation was obtained from linear regression of the results for the collapse capacity of the six case study RC frame structures ($R^2 = 0.97$), as shown in Figure 4.9.[8] The median

[7] Eqn. (4.6) is equivalent to: $\dfrac{\exp(\mu_{\ln}^{+} - \mu_{\ln})}{\exp(\mu_{\ln} - \mu_{\ln}^{-})}$.

[8] It is also possible to run sensitivity analyses at +/- 1σ (instead of +/- 1.7σ), as is more typical. However, this tends to slightly under-predict the dispersion in some cases (due to nonlinearities, particularly in the negative direction) if used in Eqns. (4.3), (4.4) and (4.5). If used to predict the median, it is suggested that Eqn. (4.8) be replaced with $\dfrac{\hat{m}_{\text{mod}}}{\hat{m}} = 0.83\left(\Delta^+ \Big/ \Delta^-\right) + 0.17$ ($R^2 = 0.92$). However, this is based on fewer data points than Eqn. (4.8), and the statistical fit is not as good.

value of the fragility, including the effects of model uncertainties as predicted by ASOSM, is computed by multiplying the ratio, $\frac{\hat{m}_{\text{mod}}}{\hat{m}}$, from Eqn. (4.8), by the median obtained in the original fragility, where only record-to-record uncertainties are considered. Note that if the relationship between a random variable and collapse capacity is linear, then $\Delta^+/\Delta^- = 1$, and thus median capacity is unchanged as would be expected, and as predicted by FOSM. Comparisons of ASOSM and the response surface based approach are tabulated in Table 4.7 for the six RC frames. Since Eqn. (4.8) has been derived from the results of this study it has not been validated for other structural systems (eg. steel frames, RC walls, etc.), but it should provide a reasonable approximation for other systems. The coefficients in Eqn. (4.8) may need to be re-examined for prediction of other limit states.

This method is capable of capturing the significant decrease in the median collapse capacity observed for the 4-story ductile structure, and 2-story non-ductile structure, as well as the increase observed for the 12-story non-ductile structure. Note that once the sensitivity analyses for the FOSM assessment have been completed, no additional analyses are needed to compute Δ^+/Δ^-. Thus, this simplified approach provides a significant savings in computational time as compared to the response surface based method. For the case with four random variables, the response surface method requires 33 sets of IDA analyses, while the simplified method requires only 9 (twice the number of random variables, plus the mean model). The advantage of the simplified analysis is even larger when more model random variables are investigated.

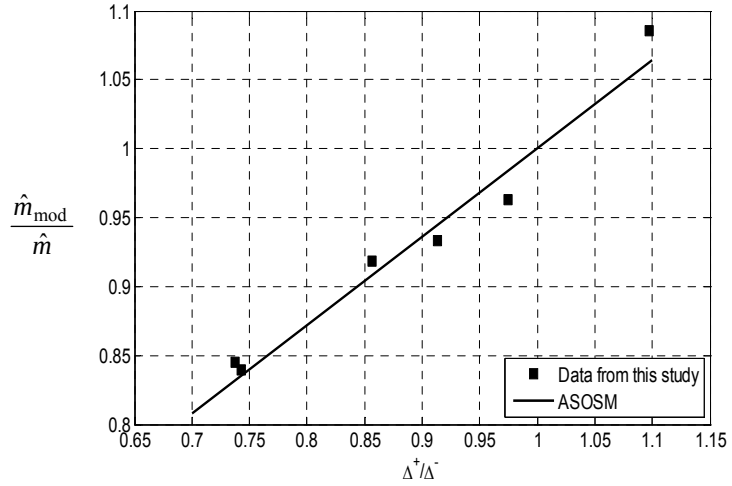

Figure 4.9 Prediction of the shift in median associated with model uncertainties, as a function of Δ^+/Δ^-, a measure of the degree of nonlinearity in the relationship between model random variables and the limit state function. ASOSM provides good agreement with the data from the response surface method.

Since the measure of nonlinearity, Δ^+/Δ^-, is obtained by varying each modeling random variable individually, the simplified method may miss some of the complex interactions between the random variables that are captured by the response surface. If Eqns. (4.8) and (4.5) predict that modeling uncertainties have a significant effect on the collapse fragility, the more complete response surface based method may be warranted.

Table 4.7 Comparison of predicted median collapse capacity using different approaches for incorporating model uncertainties.

Num. of Stories	Frame Ductility	$\frac{\hat{m}_{mod}}{\hat{m}}$ (Eqn 4.8)	Median (without model uncertainty) [g]	Median Predicted (ASOSM) [g]	Median Predicted (reponse surface) [g]	% Error[1]
1	ductile	0.98	2.95	2.90	2.84	2%
4	ductile	0.84	1.31	1.09	1.10	-1%
12	ductile	0.91	0.61	0.55	0.56	-1%
2	non-ductile	0.83	0.71	0.59	0.60	-2%
4	non-ductile	0.94	0.30	0.28	0.28	1%
12	non-ductile	1.06	0.35	0.37	0.38	-2%

[1] ASOSM compared to response surface approach

4.7 Conclusions

In this study, we propose a procedure for incorporating structural modeling parameter uncertainties into probabilistic collapse risk assessments and other predictions of structural response. To accomplish this expediently and accurately, we advocate using Monte Carlo sampling with a response surface. The response surface is a multivariate function representing the relationship between the model random variables and a structural response parameter of interest (e.g. interstory drift, collapse capacity, etc.). Once the response surface is created from the results of sensitivity analyses, Monte Carlo methods are used to sample the model random variables and the structural response is predicted using the response surface, avoiding time consuming nonlinear simulations. The outcome of this process is a structural response fragility that incorporates both the uncertainty in the structural modeling parameters and in the ground motion.

We illustrate this method by applying it to RC frame buildings, though the approach developed here is widely applicable. From the case study of RC frames we observe the following:

- Neglecting the effects of modeling uncertainties is *unconservative* in almost all cases.
- Incorporating modeling uncertainties increases the dispersion (σ_{ln}) in the response fragility, and also *shifts the prediction of the median*. The median of the response fragility

typically decreases, and may decrease by as much as 20% for nonlinear limit states such as collapse.

- Modeling uncertainties have greater impact when the key modeling parameters are more uncertain.
- Modeling uncertainties have greater impact when the relationship between model parameters and structural response is highly nonlinear.

The importance of incorporating modeling uncertainties in the analysis is dependent upon both the structure and limit state of interest. The final two bulleted observations serve to explain why this study finds that modeling uncertainties have a more significant effect on performance predictions compared to previous studies. For one, the model variables important for predicting collapse include parameters related to component deformation capacity and post-capping (softening) behavior, which are highly uncertain. In addition, the relationship between the model random variables and collapse capacity is typically nonlinear, due in part to the many possible collapse modes in frame structures (and that these collapse modes may alternate depending on the values of the model random variables). These case studies demonstrate that comprehensive assessment of collapse risk requires careful propagation of modeling uncertainties.

The response surface method proposed here improves upon the often used FOSM approach because it is able to capture the effects of nonlinearities in the relationship between model random variables and the limit state function. This improvement is crucial for nonlinear limit states like collapse. We also show that this improvement is important when predicting mean annual rates of exceeding a limit state, or predicting conditional probabilities of exceedance when the probabilities are large. FOSM, however, may be an adequate approximation for predicting conditional probabilities of exceedance when the probabilities are small, and, correspondingly, for predicting mean rates of exceedance that are dominated by the lower tail of the collapse fragility.

To remedy FOSM's potential deficiencies, but to avoid the extra effort needed for the response surface approach, we also propose a simplified method, termed ASOSM (approximate second order second moment). ASOSM uses FOSM to predict the increase in fragility's logarithmic standard deviation, but also provides a method for predicting the potential shift in the median of the limit state fragility. As a result, it will provide more accurate predictions of the mean rate of limit state exceedance and conditional probabilities in the upper tail of the distribution, and can serve as a diagnostic tool to investigate the

importance of modeling uncertainties in the assessment process. Once sufficient analyses have been run for FOSM, ASOSM does not require any additional time history simulations.

These results point more generally to the importance of appropriately characterizing and propagating uncertainties in performance-based earthquake engineering. Since simplified approaches may have a large effect on calculated risks, the accuracy of simplifying assumptions should be considered with care when the results will impact important decisions.

Chapter 5

Assessments of the Risk of Earthquake-Induced Collapse of Non-Ductile Reinforced Concrete Frame Structures

5.1 Introduction

It is well-known that California's existing non-ductile reinforced concrete frame structures may present a threat to life safety, due to the possibility of earthquake-induced collapse. In this chapter, performance-based earthquake engineering methods are applied to systematically assess the seismic collapse risk of a set of typical non-ductile RC frame office building structures. These structures are designed according to the 1967 Uniform Building Code and, as such, are representative of California construction in the 1950s and 1960s. By evaluating a suite of archetypical non-ductile RC frame structures of different heights and framing systems, the safety of this class of structures is quantified in terms of a variety of collapse performance metrics and accounting for variability among non-ductile RC structures. These metrics are compared to the collapse safety of modern code-conforming RC frame buildings to evaluate differences in seismic safety between non-ductile and ductile construction in California.

5.2 Structural Design, Modeling and Collapse Assessment Procedure

5.2.1 Design of Archetypical Non-Ductile Reinforced Concrete Frame Structures

To systematically assess the collapse risk of older RC frame structures, a set of typical structures, or archetypes, is identified. These archetypes are a group of building designs selected to be representative of older RC frame structures in California, whose assessment will constitute the basis for the evaluation of the collapse risk of the class of non-ductile RC frame structures. For the purposes of this study, a set of 26 archetypical non-ductile RC frame structures is identified, listed in Table 5.1 and Table 5.2. The structural configurations (beam spans and story heights) are representative of typical office buildings. The archetype

structures vary in terms of structural height (number of stories), lateral resisting system (space or perimeter frame systems), as well as detailing decisions, design overstrength, and strength and stiffness irregularities in elevation.

The archetype non-ductile RC frame structures range in height from 2 to 12 stories. All frames have 25 foot column spacing. This value is typical of mid-rise RC office buildings of that era (refer back to Table 2.2), and variations in beam span length have not been shown to have a significant impact on the collapse assessment (Haselton 2006). Story heights are typically 15 ft. in the first story and 13 ft. in all other stories. Both space and perimeter frame structures are included as illustrated in Figure 5.1. Space frame structures are more typical of older RC frame structures, especially office buildings, but some examples of perimeter frame structures with flat-slab gravity systems can be found, particularly in industrial facilities. The selected archetype buildings also include those with irregularities in elevation, such as the presence of a weak story at the base (relative to stronger upper stories). Variability in quality of detailing is investigated, due to the observation that some designers provided more transverse stirrups than required for code-minimum design in beam-columns or joints, what engineer Henry Degenkolb referred to as "California practice" (Degenkolb 1994). Other variations, such as those associated with construction quality, are not considered. The "baseline" archetype structures (design variant A) include a space and perimeter frame structure of each height, for a total of eight structures. Details of the archetype design variants are defined in Table 5.2.

Each of the archetype non-ductile RC structures is designed according to the requirements of the 1967 Uniform Building Code (UBC), such that the structures are representative of California seismic design between approximately 1950 and 1975 (ICBO 1967). The 1967 UBC used an equivalent static force procedure for seismic design and computes the required design base shear for a structure as a function of the weight of the structure, the structural period, the system's ductility and redundancy (K), and the seismic zone. The archetypical structures are designed for seismic zone 3, the highest seismic zone at the time, which included most of California. All structures are designed with the standard level of detailing ($K = 1$). The designs meet all other requirements present in the 1967 UBC, including maximum and minimum reinforcement ratios, maximum stirrup spacing, and requirements on hooks, bar spacing and anchorage, etc. Reflecting conventional practice, the interstory drifts are limited to 2% under design lateral forces.

Table 5.1 Archetype non-ductile RC frame structures.

Design ID	Num. of Stories	Bay Width (ft)	Framing System[1]	Design Variant
3001	2	25	Space (1.0)	A
3002		25	Perimeter (0.2)	A
3003	4	25	Perimeter (0.2)	A
3004		25	Space (1.0)	A
3009		25		F1
3010		25		F2
3012		25		H
3032		25		I
3015	8	25	Perimeter (0.2)	A
3034		25		J
3016		25	Space (1.0)	A
3017		25		B
3018		25		D (65%)
3019		25		D (80%)
3020		25		F1
3021		25		F2
3022	12	25	Perimeter (0.2)	A
3035		25		J
3023		25	Space (1.0)	A
3024		25		B
3026		25		D (65%)
3027		25		D (80%)
3028		25		F1
3029		25		F2
3031		25		H
3033		25		I

[1](Ratio of gravity to lateral tributary areas)

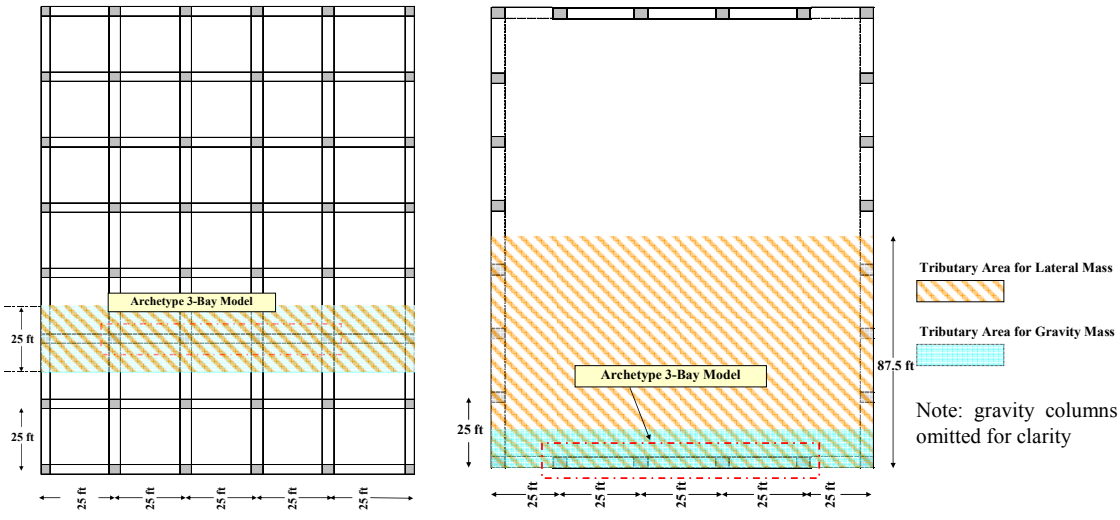

(a) (b)

Figure 5.1 Plan view of (a) space frame and (b) perimeter frame systems. The 2- and 4-story buildings measure 125 ft x 175 ft. in plan. The 8 and 12-story buildings are 125 ft. x 125 ft.

Table 5.2 Description of design variations in archetype non-ductile RC frame structures.

Design Variant	Description
A	Baseline design. Strength stepped down at every story. Size of elements decreased where a 6 in. decreases is possible.
B	Strength and stiffness of beams and columns constant over the height of the structure.
D	Weak story. The % refers to the difference in strength between the weak story and the story above.
F1	Beams systematically over-designed [use beam overstrength factor of 1.45 instead of 1.15].
F2	Columns systematically over-designed [use column overstrength factor of 1.45 instead of 1.15].
H	Improved Detailing: A larger number of ties provided in columns and beams [decrease spacing by factor of 1.5 from code minimum].
I	Improved Detailing: Continue column ties through the beam-column joints.
J	Reduced (10 ft.) story heights

To systematize the design of the 26 structures in this study, a generalized procedure was followed. For the purpose of this study, the archetype structures are designed as three-bay, two-dimensional frames. Code-defined loading combinations for seismic and gravity (dead and live) loads were considered, but wind loads are not expected to govern. The structures meet the 1967 UBC code minimum requirements in terms of strength and reinforcement provided. All beam and column elements have the same amount of flexural overstrength, such that each element is 15% stronger than the code-minimum design level. This element overstrength results from finite choices for rebar sizes, concrete cover and other design decisions. All structures were designed using ultimate strength design.[1] In addition, the same material strengths were used in designing all the buildings: 4 ksi concrete and 60 ksi steel for both longitudinal and transverse reinforcement. All designs use deformed rather than smooth reinforcing bars. Furthermore, a 6 inch step size was used in reducing the sizes of beams and columns over the height of the building, i.e. element sizes were kept constant until it was possible to reduce a dimension by 6 inches. Foundation rotational restraints were assumed to be provided by either a grade beam (for interior columns) or a basement wall (for columns on the exterior of the structure). Columns are designed for uniaxial rather than biaxial bending in order to be consistent with the analysis, which is conducted in two dimensions.[2]

[1] Allowable strength design was more commonly used in 1967, but the resulting designs should be similar.
[2] The demands on columns are underestimated in a two-dimensional model. We compensate for this effect by also designing the columns for uniaxial bending (smaller capacity).

The archetype buildings are designed to represent typical pre-1975 structures, slightly exceeding code-minimum requirements. It is assumed that the structures have been faithfully constructed according to design documents. Since the archetype structures are regular in plan and elevation, they are not representative of irregular structures with unusual configurations.

The computed design base shear for the archetype frames range from 5% to 9% and are reported in Table 5.3. Complete documentation of the designs is available in a separate appendix (Appendix A). Only one design is discussed in detail here: the 4-story space frame structure (Design ID 3004). The structure has 20 inch by 20 inch square columns and beam heights ranging between 20 and 26 inches, with reinforcement ratios in columns between 1 and 3%. Transverse reinforcement ratios are between 0.0022 (typical for columns) and 0.0055 (in beams where more significant shear reinforcement was required). Strength requirements controlled the design of beams and columns. The primary features of the design are summarized in Figure 5.2.

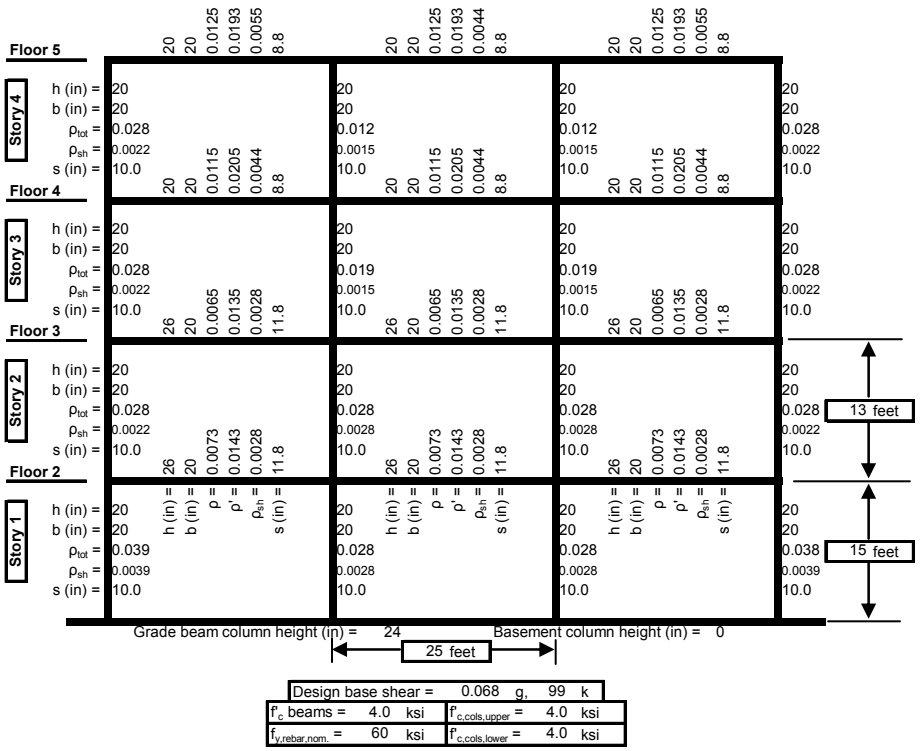

Figure 5.2 Design documentation for 4-story non-ductile space frame structure (Design ID 3004).

5.2.2 Nonlinear Analysis Models

Each archetype design is represented by a structural analysis model, which is used to simulate the dynamic response of the building for the purpose of collapse performance

assessment. A two-dimensional, three-bay frame model is employed, consisting of lumped plasticity beam-column elements and inelastic joint shear springs, as illustrated in Figure 5.3. Inelastic material models are used to simulate hysteretic behavior at the component level and geometric nonlinearities (P-Δ) are incorporated with a leaning column. The models in this study represent only the lateral resisting system, neglecting combination of the gravity system and non-structural components (see Chapter 3). Key features of the nonlinear analysis model have been discussed in more detail in Chapter 3.

The beam-column hinges are modeled using an inelastic spring model developed by Ibarra et al. (2005), consisting of a monotonic backbone (Figure 5.3a) and associated hysteretic rules. The parameters defining the moment-rotation relationships in the beam-column hinges are based on previous work (described in Chapter 3), which developed empirical relationships that predict modeling parameters for RC beam-column elements as a function of their design characteristics. For example, the modeled plastic rotation capacity of a column depends on the axial load ratio, the amount of transverse reinforcement, the concrete strength, the rebar buckling coefficient, and the longitudinal reinforcement ratio. Similar predictive equations are used to predict element stiffness and strength, post-capping rotation capacity and cyclic deterioration parameters. The parameters of the joint shear panel model are based on data assembled by Mitra and Lowes (2005) for RC joints with non-ductile detailing. All parameters are modeled by their mean values, such that the models represent expected behavior.

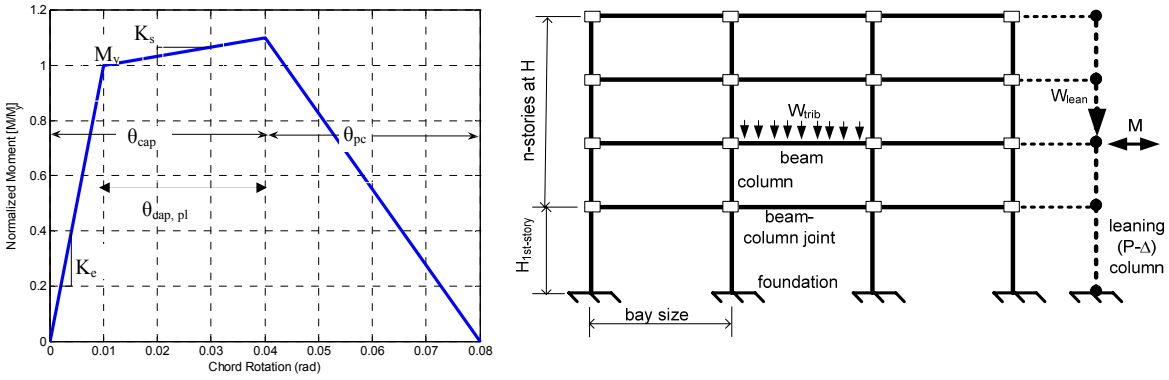

(a) (b)

Figure 5.3 Archetype analysis model for RC moment frame buildings: (a) monotonic backbone for Ibarra et al. (2005) element model and (b) two-dimensional, three-bay frame model.

Figure 5.4 shows the modeling parameters used for the 4-story non-ductile space frame structure. Initial stiffness of beams and columns ranges between 0.35 to 0.57EI_g, depending on the level of axial load in the element. The plastic rotation capacity ($\theta_{cap,pl}$) varies between

0.021 and 0.035 in the columns, and it is somewhat higher for beams. These plastic rotation capacities are significantly smaller than the 0.056 to 0.067 predicted for columns in a 4-story seismically detailed modern RC frame (Haselton et al. 2007). The cyclic deterioration parameter (λ) is calculated to be between 31 and 48. λ values of approximately 110, indicating higher energy dissipation capacity, are more representative of modern, code-conforming designs (Ibarra et al. 2005; Haselton et al. 2007). Modeling details for the other archetype structures are reported in a separate appendix (Appendix B).

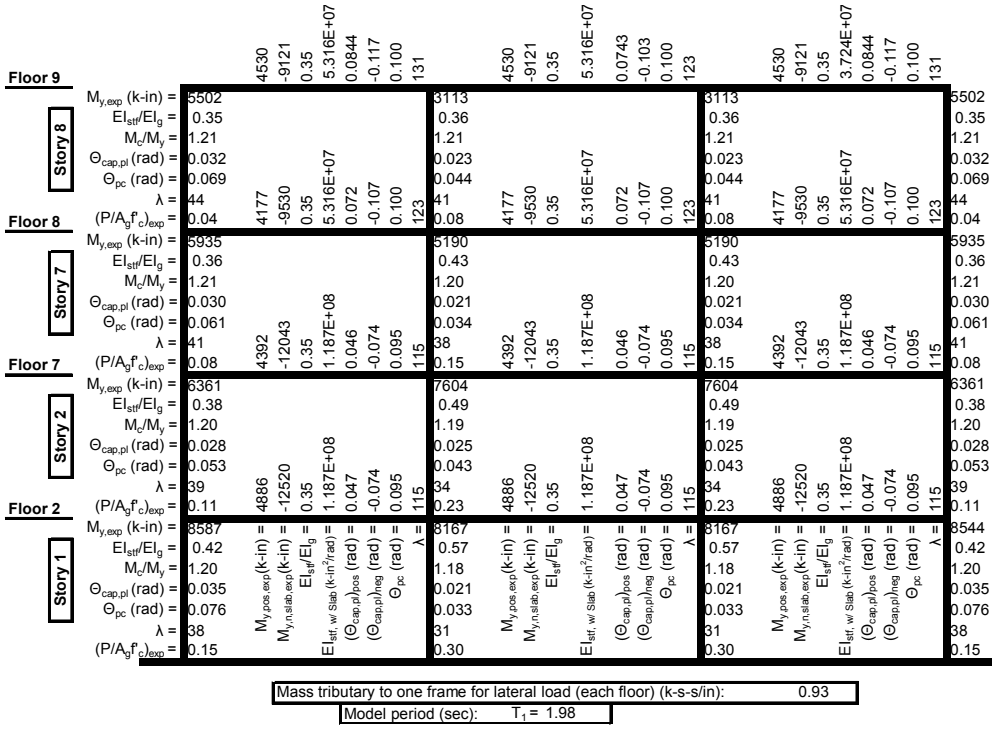

Figure 5.4 Modeling parameters used in the analysis model for the 4-story non-ductile space frame. Similar models are made for each of the 26 archetypical designs.

These lumped plastic hinge models are capable of capturing the key sources of deformation and deterioration leading to sidesway collapse of non-ductile RC frames, including flexural degradation in beams and columns and joint shear panel deterioration. However, the model is unable to simulate the behavior associated with shear failure in the RC columns, which could trigger collapse due to loss of vertical carrying capacity in a column. This type of shear failure has been observed numerous times in past earthquakes, particularly in frame structures that have short "captive" columns. Since the archetype non-ductile RC frame structures have taller story heights, they are not likely to be shear critical and, rather, they are expected to fail in a flexure-shear mode, yielding first and then failing in shear (Zhu et al. 2007). The calibration of the element model parameters reflects this expected flexure-

shear degradation, but does not have shear or axial spring to explicitly capture the shear failure and post-failure change in response and loss of column gravity bearing capacity (Elwood 2004; Elwood and Moehle 2005). These failure modes are instead included by post-processing the analysis results with fragility data associated with column shear failure and the subsequent loss of vertical carrying capacity (Aslani 2005; Elwood and Moehle 2005).

5.2.3 Collapse Assessment Procedure

Once an archetype analysis model has been created to represent each of the 26 archetypical non-ductile RC frame structures, the collapse performance assessment uses the incremental dynamic analysis technique (Vamvatsikos and Cornell 2002). In incremental dynamic analysis, a structural model is subjected to a set of ground motion records. For this study, the set includes 22 pairs of recorded ground motions, where each pair consists of two orthogonal components from the same record (ATC 2007). Each ground motion is scaled to increasing intensity and applied to the archetype analysis model until that ground motion causes collapse of the structure. Collapse happens when dynamic instability occurs in the model, indicated by runaway interstory displacements. The ground motion intensity measure of interest is the spectral acceleration of the record at the first mode period of the structure, denoted $S_a(T_1)$.[3] Assuming that the structure is equally strong and ductile in its two orthogonal directions, the component of each pair of records that causes the structure to collapse first, the so-called "controlling component", is used as the collapse level to approximate three-dimensional loading response in the two-dimensional frame models.

The dynamic analysis results for the 4-story space frame structure are presented in Figure 5.5. The median collapse capacity, based on the controlling component of the ground motion pairs, is $S_a(T_1) = 0.28g$. From the incremental dynamic analysis results, a cumulative collapse distribution is obtained, describing the probability of collapse as a function of the ground motion intensity. This collapse probability is shown in Figure 5.6a. The dispersion in this collapse fragility reflects the ground motion variability associated with frequency content and other characteristics not captured by the ground motion intensity measure, termed "record-to-record" (RTR) variability. For this structure $\sigma_{ln,RTR} = 0.38$.

[3]Specifically, the spectral acceleration is defined as the geometric mean of the spectral acceleration of the *pair* of records at T_1. It is therefore slightly different than the spectral acceleration of each component.

Several aspects of the assessment procedure can have an important influence on the collapse performance predictions. Ground motion spectral shape has been shown to have a significant effect on the predicted collapse capacity of a structure (Baker and Cornell 2005). The ground motion set used in this study was selected without consideration of spectral shape, so the results are corrected to reflect the appropriate spectral shape for rare ground motions in California. This process is described in Chapter 3. For these non-ductile structures and assuming a target epsilon of ε = 1.2 for coastal California, this correction typically increases the median collapse capacity by approximately 25%. The adjusted collapse fragility for the 4-story space frame structure is illustrated in Figure 5.6b. Appendix 5.1 presents a more detailed discussion of the treatment of spectral shape.

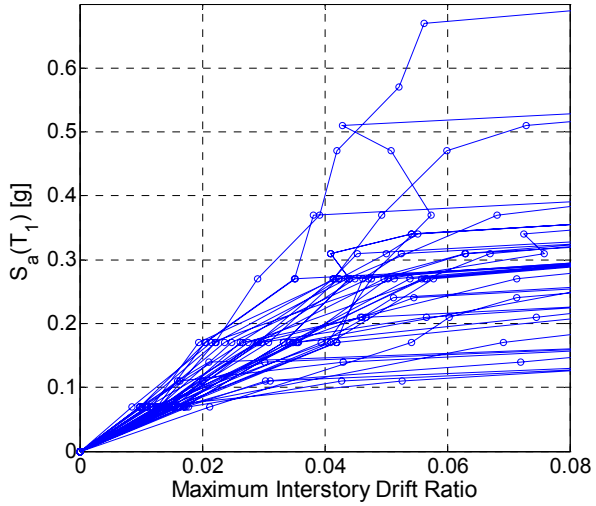

Figure 5.5 Incremental dynamic analysis results for 4-story RC space frame structure, controlling components only.

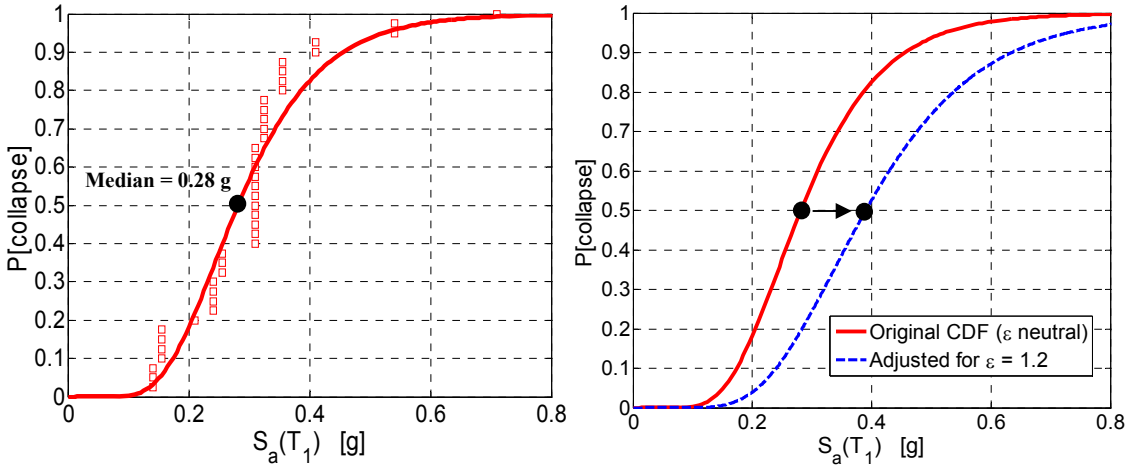

Figure 5.6 Cumulative collapse distribution for 4-story RC space frame structure (a) from incremental dynamic analysis and (b) adjusted for typical spectral shape of rare California ground motions (ε = 1.2). These collapse fragilities include the simulated sidesway failure modes only.

The effects of uncertainties in structural modeling parameters are incorporated using two methods. In the first method, a simplified procedure is used, increasing the dispersion in the collapse probability distribution to account for modeling uncertainties. The additional uncertainty due to modeling is assumed to be given by $\sigma_{ln,modeling} = 0.50$, based on a first-order-second-moment (FOSM) study of the effects of modeling uncertainty on a 4-story ductile RC frame structure (Haselton 2006). In this approach, logarithmic standard deviations associated with record-to-record and modeling uncertainty are combined using SRSS. A more accurate treatment of modeling uncertainties, following the recommendations of Chapter 4, uses Monte Carlo simulation and response surfaces to predict how both the mean of the distribution shifts and the dispersion increases when modeling uncertainties are considered. The collapse fragilities resulting from these two methods are shown in Figure 5.7 for the 4-story non-ductile RC frame structure, incorporating record-to-record and modeling variation. For expedience in conducting collapse assessments for a large number of buildings, the results here use the simplified FOSM approach to account for the effects of modeling uncertainties. A comparison of the two approaches is included in Chapter 4.

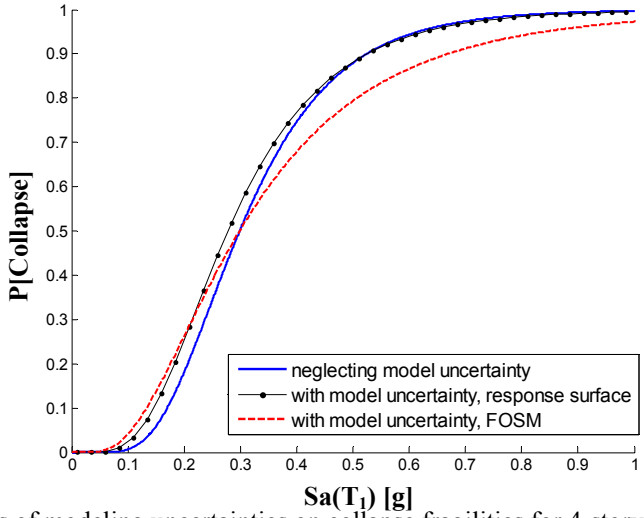

Figure 5.7 Effects of modeling uncertainties on collapse fragilities for 4-story non-ductile RC frame structure (without spectral shape adjustment).

The collapse fragility shown in Figure 5.6 includes only those sidesway collapse modes that are directly simulated in nonlinear analysis models. The sidesway-only collapse fragility may underestimate the probability of collapse, because it neglects the possibility of a gravity collapse induced by column shear failure. In order to account for the non-simulated column shear failure collapse mode, two additional collapse limit states are defined. In the first limit state, the structure has either collapsed in sidesway, or experienced shear failure in at least

one column. In the second limit state, the structure has collapsed in sidesway or experienced a loss of vertical carrying capacity (LVCC) in at least one column. A column can undergo significant lateral deformations after shear failure (first limit state) and before an axial failure occurs (second limit state). The shear failure limit state represents an upper bound on the risks of collapse. The second limit state is taken as the most appropriate collapse limit state in this study. The occurrence of non-simulated limit states is identified by post-processing incremental dynamic analysis results using component fragility data to determine if the shear or vertical collapse limit state has been reached. The fragility data relates shear and axial failure in RC columns to the drift in the column (Aslani 2005).

Figure 5.8 illustrates the three different collapse limit state fragilities for the 4-story non-ductile RC space frame structure. As expected, the inclusion of non-simulated failure modes increases the probability of collapse at each level of ground motion intensity, shifting the fragility to the left. For this structure, Figure 5.8 indicates that non-simulated failure modes have a significant effect on the predicted collapse fragility. As discussed later, these non-simulated failure modes have a much smaller effect on collapse performance results for other archetype structures.

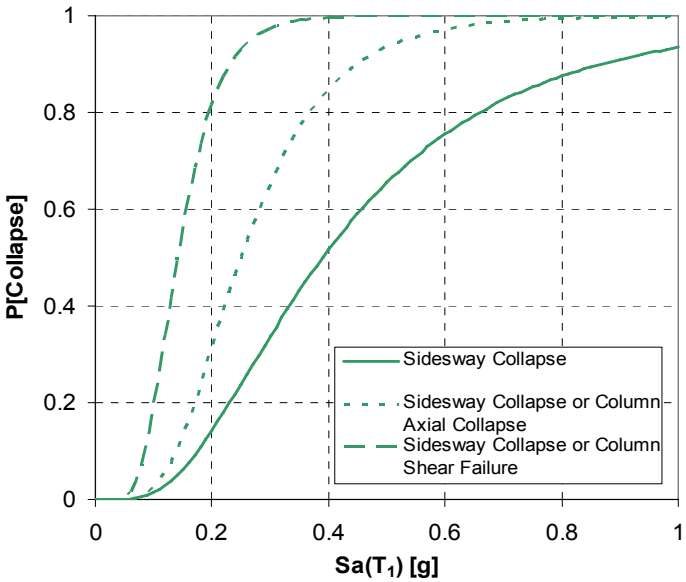

Figure 5.8 Collapse fragilities for 4-story non-ductile space frame structure, illustrating the effect of non-simulated failure modes.

The final collapse fragility for the 4-story space frame structure shown in Figure 5.9 incorporates both record-to-record and modeling uncertainties and has been adjusted for spectral shape effects. This collapse fragility includes both simulated (flexure, flexure-shear) and non-simulated (shear critical) failure modes. From this fragility, several metrics of

collapse performance can be obtained: the median collapse capacity, the collapse margin (the ratio of the median collapse capacity to the 2% in 50 year ground motion hazard level, $Sa_{2/50}$), and the conditional collapse probability (probability of collapse given an extreme ground motion, usually taken as the 2% in 50 year ground motion). The mean annual frequency of collapse is obtained by integrating the structure's collapse fragility with the site specific hazard curve. Assuming a Poisson distribution of earthquakes in time, the collapse return period can also be computed, or the probability that the structure will collapse within a 50 year period. The buildings are assumed to be at a typical high seismic non-near fault site in Los Angeles, for which the hazard curve has been defined through probabilistic seismic hazard analysis (Goulet et al. 2007). The hazard curve is given in Figure 3.6.

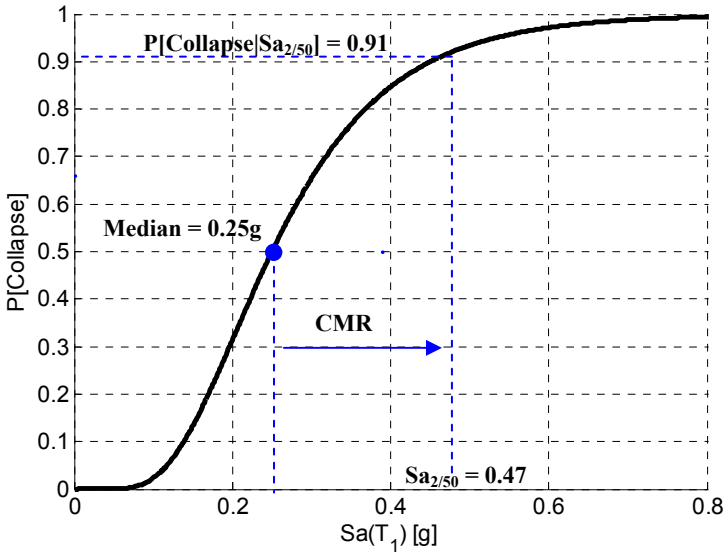

Figure 5.9 Final collapse fragility for 4-story non-ductile space frame, illustrating the definition of key measures of collapse performance.

The metrics obtained from these analyses represent our best estimate of the collapse performance of these structures, including uncertainties in both ground motion and modeling parameters, and without adding significant sources of conservatism. These models are limited by the exclusion of the gravity system from the analysis (likely conservative for perimeter frames), the use of fragility functions for non-simulated failure modes, and limitations in test data used to define the element material models and deterioration parameters. As improved simulation technologies develop, these can be easily incorporated into this collapse assessment procedure.

5.3 Assessments of Collapse Risk for Non-Ductile Reinforced Concrete Frame Structures

5.3.1 Static Pushover Analyses

The complete collapse assessment procedure was carried out for each of the 26 archetypical non-ductile RC frame structures. Table 5.3 and Figure 5.10 summarize the results from static pushover analyses. Overstrength (Ω) is a measure of the lateral strength of the structure relative to the design base shear. The ultimate roof drift ratio (RDR_{ult}) is a measure of the structure's ductility, defined as the roof drift ratio when the resistance is 20% less than the ultimate strength in the pushover analysis. The ultimate roof drift ratio decreases with structural height, making it an imperfect measure of ductility, but it can be used to make relative comparisons among different structures of the same height. While the static pushover analyses are not integral to the performance-based collapse assessment procedure, they provide a linkage between the results of the dynamic analyses reported below and codified non-linear static assessment procedures that are more frequently used in practice (ATC 2005; ASCE 2007).

The predicted lateral overstrength varies between 1.1 and 2.0, with the space frames typically having higher overstrength (1.7 on average) compared to the perimeter frame structures (1.2 on average).[4] The higher levels of overstrength in the space frame designs reflect the relative dominance of gravity loading compared to seismic loading in the design, due to their structural configuration that tends to provide some additional lateral strength. The analysis models for perimeter frame structures are also expected to be pessimistic, due to their exclusion of the flat-plate gravity system, which likely contributes significantly to lateral strength and stiffness. Haselton's (2006) study of RC special moment frames found that neglecting the gravity frame reduced the median computed collapse capacity of the structure by approximately 10%. The perimeter frame structures considered here are less stiff than those Haselton examined and relative differences in stiffness between the lateral and gravity systems are smaller, it is expected that the gravity frame would have a larger overall effect on the computed collapse capacity. Other building-specific studies have

[4] Like the dynamic analysis results reported later, these static pushover analyses use a model that includes both the lateral-resisting system (frame) and a leaning column, carrying the additional gravity loads on the structure. The leaning column reduces the computed overstrength.

computed lateral overstrengths on the order of 3 and 4 for non-ductile RC buildings. Part of the smaller overstrength observed in this study is the result of the absence of the gravity system. In addition, the archetype designs considered represent code minimum design, whereas other buildings may exceed these requirements in some cases (Miranda 1991).

Table 5.3 Results of static pushover analysis.

Design ID	Num. of Stories	Bay Width (ft)	Framing System	Design Variant	T_1 (s)	Design base shear coefficient	Overstrength (Ω)	RDR_{ult}
3001	2	25	Space	A	1.08	0.086	1.9	0.019
3002		25	Perimeter	A	1.04	0.086	1.6	0.035
3003	4	25	Perimeter	A	1.96	0.068	1.1	0.013
3004		25	Space	A	1.98	0.068	1.4	0.016
3009		25		F1	1.98	0.068	1.5	0.016
3010		25		F2	1.98	0.068	1.4	0.015
3012		25		H	1.98	0.068	1.4	0.016
3032		25		I	1.98	0.068	1.6	0.018
3015	8	25	Perimeter	A	2.36	0.054	1.1	0.007
3034		25		J	1.84	0.054	1.3	0.009
3016		25	Space	A	2.20	0.054	1.6	0.011
3017		25		B	2.17	0.054	1.6	0.011
3018		25		D (65%)	2.20	0.054	1.6	0.012
3019		25		D (80%)	2.20	0.054	1.6	0.011
3020		25		F1	2.20	0.054	1.6	0.011
3021		25		F2	2.20	0.054	1.6	0.011
3022	12	25	Perimeter	A	2.75	0.047	1.1	0.005
3035		25		J	2.23	0.047	1.3	0.006
3023		25	Space	A	2.26	0.047	1.9	0.010
3024		25		B	2.19	0.047	2.0	0.010
3026		25		D (65%)	2.26	0.047	2.0	0.010
3027		25		D (80%)	2.26	0.047	1.9	0.010
3028		25		F1	2.26	0.047	2.0	0.007
3029		25		F2	2.26	0.047	1.9	0.012
3031		25		H	2.26	0.047	1.9	0.012
3033		25		I	2.26	0.047	2.2	0.012
						Average	1.6	0.0125

The static pushover analyses also illustrate the smaller ductility of the perimeter frame systems, as measured in terms of the ultimate roof drift ratio. Perimeter frames are subject to higher P-Δ effects because they are less stiff, causing the damage to concentrate in a smaller number of stories. Interestingly, the perimeter frames are overall less ductile, despite having member level deformation capacities that are higher than space frame structures. This observation illustrates the importance of designs that enhance "system-level ductility" by distributing deformations over the height of the structure, in addition to deformation capacity at the member level. The larger ductility of the 2-story perimeter frame is the result of peculiarities in the design that cause a complete failure mechanism to occur in that structure, such that significant plastic deformations occur in both beams and columns.

The calculated structural periods of the non-ductile RC frame buildings, obtained from eigenvalue analyses of the nonlinear simulation models are reported in Table 5.3. The reported periods are longer than would be computed from traditional code formulas or the mean period estimate proposed by Chopra and Goel (2000), as illustrated in Figure 5.11. Code formulas in the 1967 UBC would predict T = 0.1N, where N is the number of stories. These explicitly underestimate structural periods for force-based design. Chopra and Goel's (2000) relationship is based on data from 27 instrumented RC moment resisting frame structures. The model stiffness in this study neglects the contribution from non-structural components and structural components that are not part of the lateral resisting system. Additional flexibility also results from the use of the secant stiffness to model RC elements, underpredicting initial stiffness.

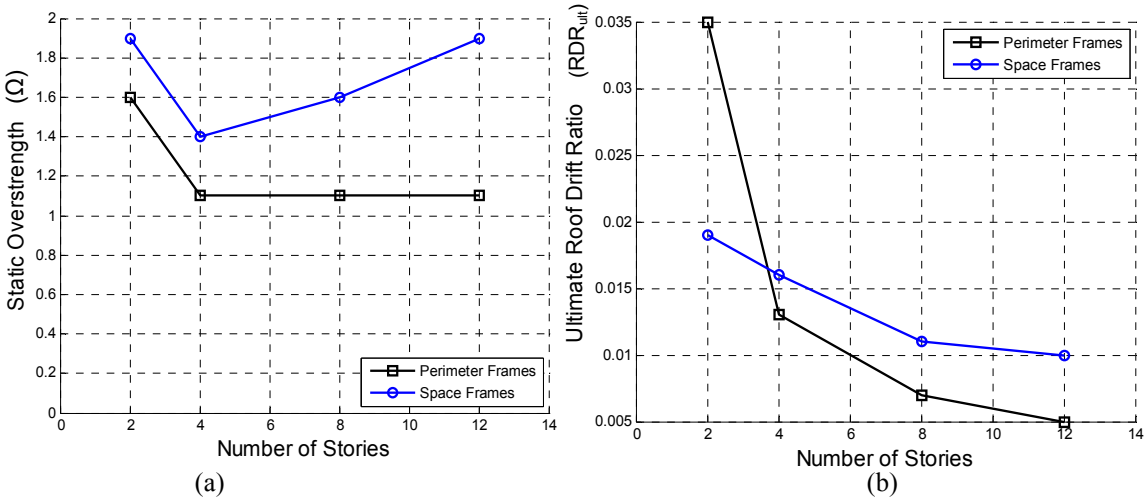

Figure 5.10 Results from static pushover analysis for baseline non-ductile RC frame structures, in terms of: (a) static overstrength (Ω) and (b) ultimate roof drift ratio (RDR_{ult}).

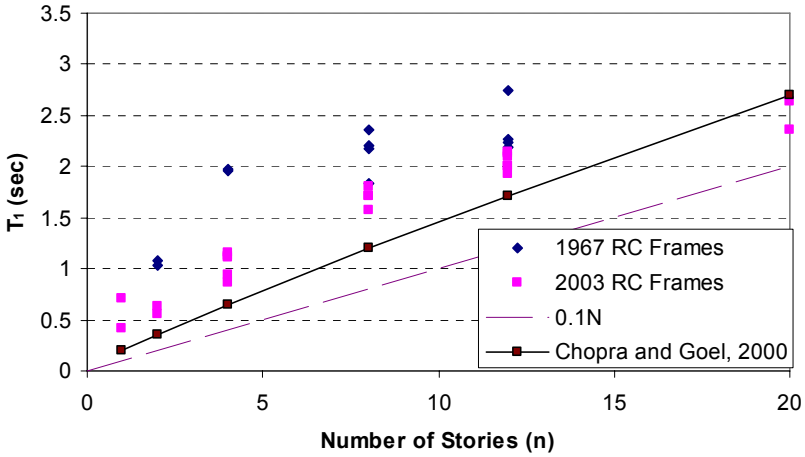

Figure 5.11 Comparison of structural periods with other standard formulas. Data for 2003 RC frames from Haselton and Deierlein (2007).

5.3.2 Collapse Assessment Results

The results of the collapse assessment procedure for the 26 archetypical non-ductile RC frame structures are reported in Table 5.4 and Figure 5.12. For each structure, Table 5.4 reports the median collapse capacity and record-to-record variability of the collapse fragility. The tables also include several collapse metrics defined previously: collapse margin ratio, conditional probability of collapse, and mean annual frequency of collapse. In addition, the roof drift ratio and interstory drift ratio preceding collapse are tabulated. These are the drifts recorded from the highest earthquake intensity that did not cause collapse of the structure. Note that these results are for sidesway simulated collapse modes only; non-simulated failure modes are incorporated later.

As shown in Table 5.4, this study finds that these structures have sidesway collapse margin ratios between 0.44 and 1.32, with an average value of 0.79. For the selected Los Angeles site, the probability of collapse, given the occurrence of a very rare ground motion ($Sa_{2/50}$), is predicted to be 0.66 on average. These results indicate that rare ground motions are likely to collapse a typical non-ductile RC frame structure. The probability of collapse under the design level earthquake, $Sa_{10/50}$, is predicted to vary between approximately 0.3 and 0.6. When integrated with the site hazard curve, the mean annual frequency of collapse computed ranges between 16 and 223 x 10^{-4} [collapses per year], corresponding to a predicted collapse return period of between 45 and 670 years, depending on the design characteristics of the structure of interest.

A wide range in predicted collapse performance is associated with the variability in height, lateral resisting system and other design variations represented in the set of archetypical non-ductile RC frame structures. Figure 5.13 shows that space frame structures typically perform better than perimeter frame structures, corroborating the results of the static pushover analyses. The average conditional probability of collapse given $Sa_{2/50}$ is 0.67 for the space frame structures compared to 0.77 for the perimeter frame structures, or approximately 15% better performance. The reasons for the superior performance of the space frame structures are largely the same as those outlined previously in the discussion of static pushover analysis – higher system level overstrength and larger ductility because of smaller P-Δ effects. The absence of the gravity frame in the analysis model also contributes to the lower measured collapse capacities of the perimeter frame structures. These trends between space and perimeter frames are consistent with Haselton's (2006) observations for modern, code-conforming RC frame structures.

Table 5.4 Collapse assessment results for archetype structures (including ε-adjustment, FOSM approximation for modeling uncertainties, sidesway collapse modes only).

Design ID	Num. of Stories	Framing System	Median Collapse Sa [g]	$\sigma_{ln,RTR}$	Margin: Median Collapse Capacity/ $Sa_{2/50}$	P[Collapse| $Sa_{2/50}$]	$\lambda_{collapse}$ x 10^{-4}	RDR preceding collapse	IDR preceding collapse
3001	2	Space	0.48	0.32	0.60	0.80	106	0.017	0.031
3002		Perimeter	0.68	0.35	0.84	0.61	49	0.028	0.04
3003	4	Perimeter	0.32	0.39	0.66	0.75	100	0.017	0.037
3004		Space	0.39	0.38	0.83	0.62	57	0.023	0.054
3009			0.30	0.36	0.63	0.77	108	0.023	0.052
3010			0.38	0.38	0.81	0.63	60	0.023	0.052
3012			0.38	0.37	0.81	0.64	59	0.024	0.056
3032			0.43	0.35	0.92	0.56	41	0.026	0.061
3015	8	Perimeter	0.23	0.36	0.58	0.82	135	0.009	0.034
3034			0.30	0.41	0.58	0.80	141	0.008	0.030
3016		Space	0.33	0.39	0.78	0.65	65	0.011	0.042
3017			0.33	0.40	0.76	0.67	70	0.013	0.046
3018			0.32	0.42	0.75	0.67	78	0.014	0.046
3019			0.32	0.39	0.77	0.66	71	0.012	0.044
3020			0.31	0.39	0.72	0.70	82	0.011	0.042
3021			0.33	0.39	0.77	0.66	69	0.014	0.046
3022	12	Perimeter	0.20	0.31	0.58	0.82	116	0.006	0.031
3035			0.20	0.41	0.46	0.88	223	0.006	0.034
3023		Space	0.35	0.33	0.84	0.62	48	0.009	0.039
3024			0.40	0.41	0.94	0.54	43	0.01	0.049
3026			0.40	0.36	0.96	0.52	35	0.009	0.042
3027			0.39	0.36	0.93	0.55	38	0.009	0.043
3028			0.29	0.31	0.71	0.72	70	0.008	0.035
3029			0.40	0.36	0.96	0.53	35	0.01	0.045
3031			0.39	0.32	0.93	0.55	35	0.0088	0.039
3033			0.55	0.40	1.32	0.33	16	0.012	0.056
			Average	0.37	0.79	0.66	75	0.014	0.043

The performance of perimeter frame structures worsens with height (Figure 5.13). This trend is related to P-Δ effects. These geometric nonlinearities have the biggest effect on flexible structures, and particularly perimeter frame systems where the tributary seismic mass is much larger than the gravity loads acting directly on the frame. The effect of P-Δ is illustrated in Figure 5.14, which displays normalized pushover curves for the baseline non-ductile RC frame structures. For perimeter frames, the post-peak performance in Figure 5.14a becomes increasingly steep as the height of the structure and the gravity loads (P) on the leaning column increase. The same trend is not observed in Figure 5.14b for space frame

structures, which are stiffer and less sensitive to P-Δ because the gravity loads are tributary directly to the lateral resisting system. The collapse performance of space frame structures is relatively constant over the height of the structure, with the exception of the 2-story space frame, whose notably worse performance is discussed in more detail below.

The height of the structure also affects the collapse capacity and degree of damage concentration. As shown in Figure 5.15, both the roof drift ratio preceding collapse and the interstory drift ratio preceding collapse tend to decrease with height. The interstory drift ratio preceding collapse is a measure of element level deformation capacity and tends to decrease as gravity load levels in columns increase. As the height of the structure increases, the collapse mechanisms become concentrated in a smaller percentage of the building due as column strength is insufficient to distribute demands over the height of the structure. The extent of damage concentration in the baseline archetype structures is reported in Table 5.5, showing that the fraction of stories involved in the collapse mechanism tends to decrease with height. As shown in Table 5.5, these structures frequently fail in 1 or 2 stories, even the taller structures.

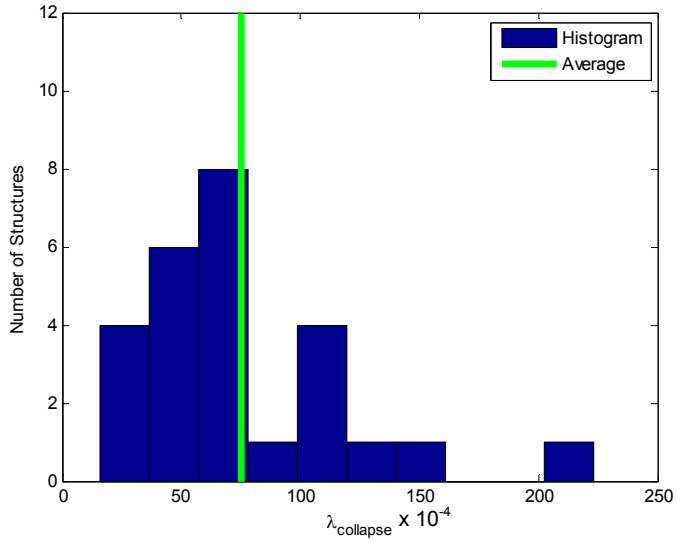

Figure 5.12 Histogram of $\lambda_{collapse}$ data for all 26 archetypical non-ductile RC frame structures.

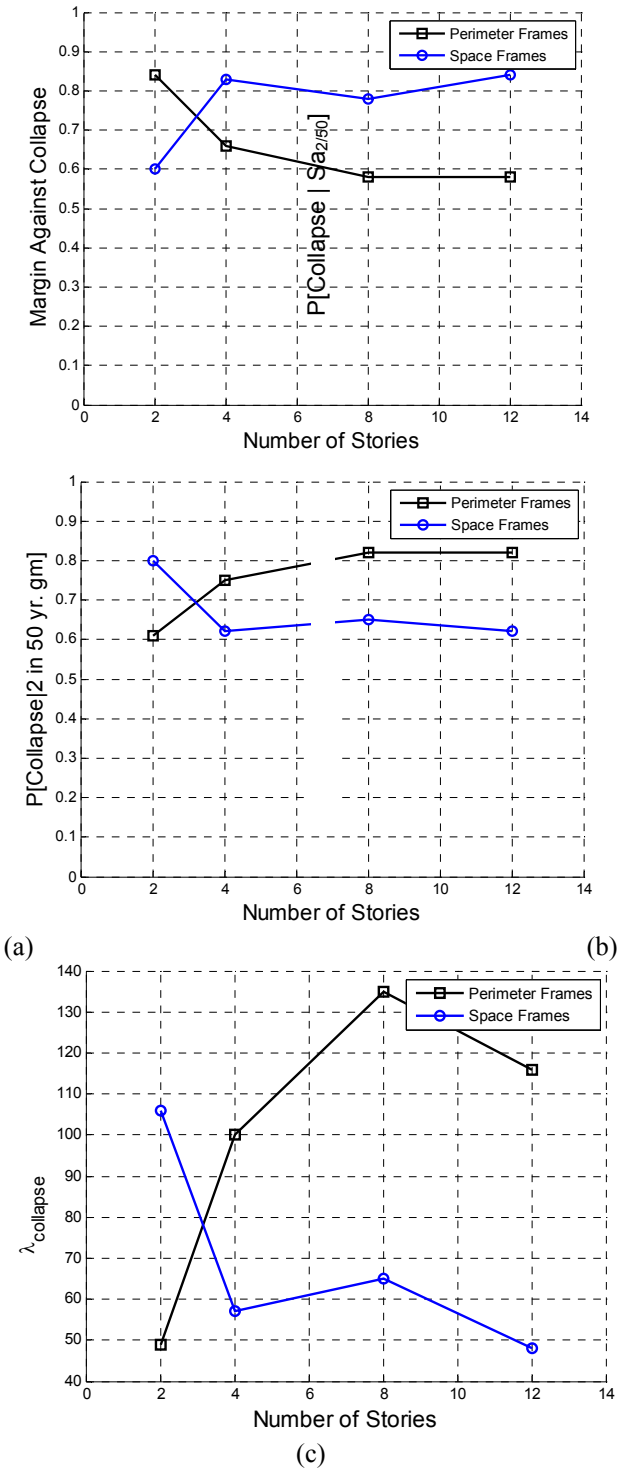

Figure 5.13 Effect of height and lateral resisting system (space vs. perimeter frames) on the collapse performance of baseline non-ductile RC frame structures.

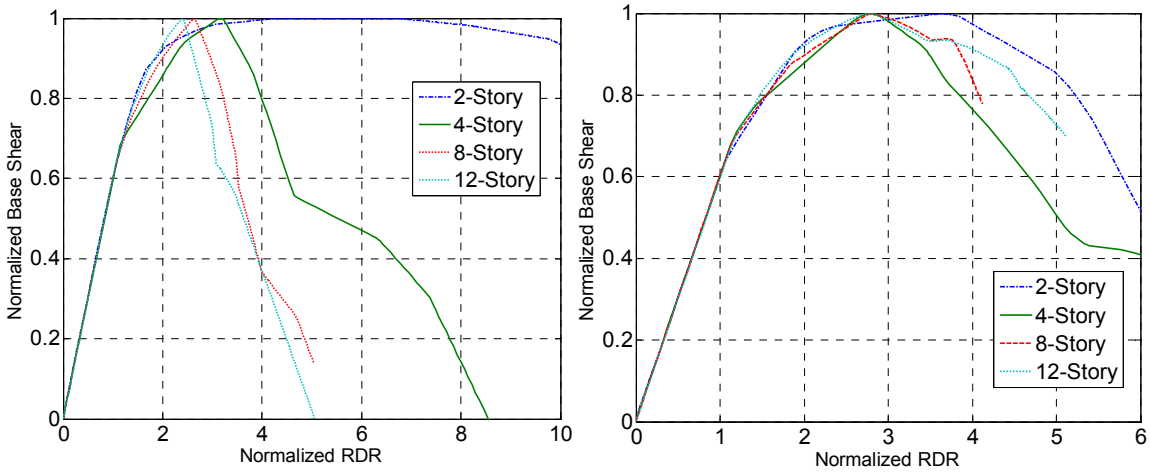

Figure 5.14 Pushover curves normalized for (a) baseline perimeter frame and (b) baseline space frame structures. In each case, base shear is normalized by the ultimate base shear and roof drift ratio is normalized by the roof drift ratio at 60% of the ultimate base shear.

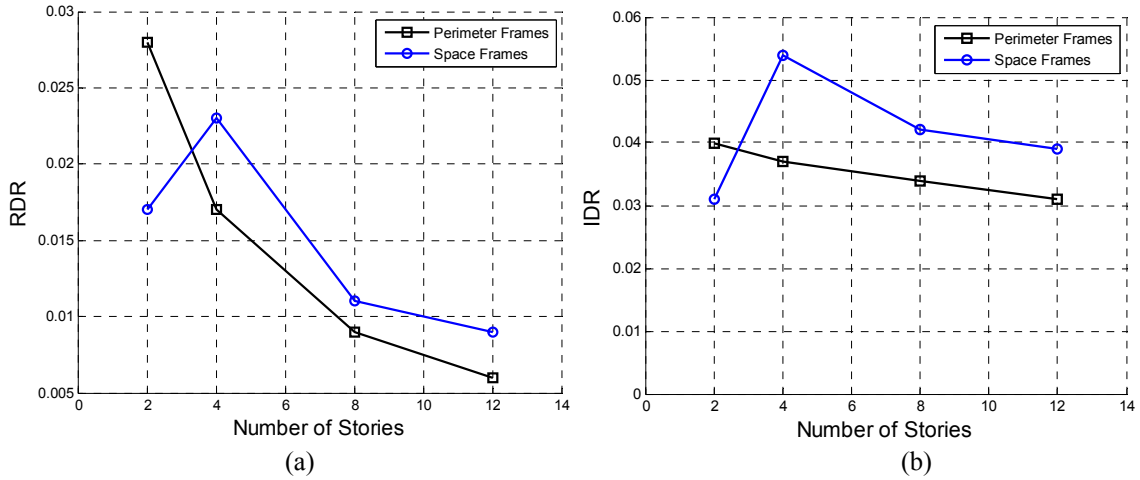

Figure 5.15 Effect of height and lateral framing system on (a) roof drift ratio and (b) interstory drift ratio preceding collapse.

Table 5.5 Extent of damage concentration in baseline non-ductile RC frame structures.

Design ID	Num. of Stories	Framing System	Number of Stories Engaged in Principal Collapse Mechanism[1]	Fraction of Stories Involved in Collapse Mechanism
3001	2	Space	1.0	0.50
3004	4	Space	2.0	0.50
3016	8	Space	2.4	0.30
3023	12	Space	3.0	0.25
3002	2	Perimeter	1.6	0.82
3003	4	Perimeter	2.0	0.50
3015	8	Perimeter	2.0	0.25
3022	12	Perimeter	2.1	0.17

[1]Where there are multiple collapse mechanisms a weighted average is used

Although the trends described above are generally observed, the 2-story space and perimeter frame structures appear to be outliers, as shown in Figure 5.13 and Figure 5.15.

The 2-story perimeter frame structure performs relatively better than expected, consistently failing in a complete collapse mechanism over both stories. In contrast, the 2-story space frame has relatively less strength and ductility than we might expect. These differences appear to be related to the dominance of lateral loading in the 2-story perimeter frame design, as well as other minor design decisions, which give this structure a very balanced design. There are no obvious deficiencies in the 2-story space frame design.

5.3.3 Effect of Column Vertical Failure on Collapse Assessments

The collapse metrics presented above include only the simulated, sidesway limit states. When the non-simulated failures associated with column shear failure are included in the collapse fragility for the archetype non-ductile RC frame structures, the collapse performance metrics in Table 5.6 and Figure 5.16 are obtained.

The sidesway/column shear failure limit state has a much higher probability of occurring than the sidesway-only limit state for the baseline archetype structures. This result implies that column shear failures are expected to occur before sidesway collapse in many of these structures. These are so-called flexure-shear failures, because the columns yield first and, subsequently, experience shear failure. Inclusion of the column shear failure mode, increases the average probability of failure given $Sa_{2/50}$ from 0.72 to 0.93 and the mean annual frequency of failure from 99 x 10^{-4} to 284 x 10^{-4} on average for the baseline structures. The results are corroborated by observations from past moderate to severe earthquake events, in which many RC columns exhibited the characteristic x-cracking resulting from shear failure. Of course, the metrics shown for the column shear failure limit state in Table 5.6 significantly overestimate the risk of collapse as column shear failure, by itself, does not typically threaten life safety.

The sidesway/column axial collapse limit state leads to an increase in the predicted risk of collapse as compared to the sidesway-only case, with the mean annual frequency of failure increasing from 99 to 108 x 10^{-4} on average. This limit state is more representative of collapse than the shear failure limit state, as it implies that either the structure has collapsed in sidesway or that at least one column has been sufficiently damaged such that it cannot carry its tributary gravity loads. Progressive collapse may result from the gravity bearing failure of one column if the structure is unable to redistribute loads. The difference in collapse performance metrics between the sidesway limit state and the sidesway/column

gravity load limit state is relatively small as these structures typically fail in sidesway before the structure has undergone sufficient lateral deformations to lead to axial failure in the column.

Also apparent from Table 5.6 and Figure 5.16 is that the effects of column shear failure and loss of gravity load carrying capacity are not uniform across the baseline archetype structures. These failure modes have a much more significant effect on the predicted collapse performance of the space frame structures than the perimeter frame structures. On average, the margins decrease by 67% from the sidesway limit state to shear failure limit state for the space frame, while decreasing by only 14% for the perimeter frame systems. The larger axial load levels in columns of the space frame structures imply that the shear and axial limit states occur at smaller column drift ratios than the perimeter frame structures. The median column drift ratio at which shear failure is predicted to occur in the interior base column in the 4-story perimeter frame structure is 0.033, compared to 0.019 for the same column in the 4-story space frame structure. Due to the dominance of lateral loads in perimeter frame design, there is also higher transverse reinforcement in the perimeter frame columns in some cases, which increases the shear strength, provides more confinement, and decreases the likelihood of column shear failure. (Perimeter and space frame designs are documented in Appendix A.) As a result, the collapse capacity of the space frames is much more adversely affected by the incorporation of the non-simulated failure modes. When column shear failure modes are included in the assessment the difference in collapse performance between space and perimeter frame structures becomes much less significant than in the sidesway-only case.

Table 5.6 Effects of non-simulated failure modes on collapse metrics for archetype non-ductile RC frame structures.[5]

	Sidesway Collapse Only			Sidesway Collapse /Column Shear Failure Limit State			Sidesway Collapse /Column Axial Failure Limit State		
Design ID	Margin	P[Limit State Reached| $Sa_{2/50}$]	$\lambda_{limit\ state} \times 10^{-4}$	Margin	P[Limit State Reached| $Sa_{2/50}$]	$\lambda_{limit\ state} \times 10^{-4}$	Margin	P[Limit State Reached| $Sa_{2/50}$]	$\lambda_{limit\ state} \times 10^{-4}$
3001	0.60	0.80	106	0.25	0.99	595	0.59	0.81	109
3002	0.84	0.61	49	0.56	0.90	89	0.85	0.61	47
3003	0.66	0.75	100	0.59	0.83	113	0.66	0.75	100
3004	0.83	0.62	57	0.26	1.00	572	0.54	0.91	107
3015	0.58	0.82	135	0.49	0.87	209	0.58	0.81	135
3016	0.78	0.65	65	0.32	0.99	380	0.75	0.68	64
3022	0.58	0.82	116	0.54	0.86	127	0.56	0.83	119
3023	0.84	0.62	48	0.48	0.95	128	0.83	0.62	50
Average	0.71	0.71	85	0.44	0.92	277	0.67	0.75	91

[5] Modeling uncertainties incorporated using FOSM approximation; adjusted for spectral shape

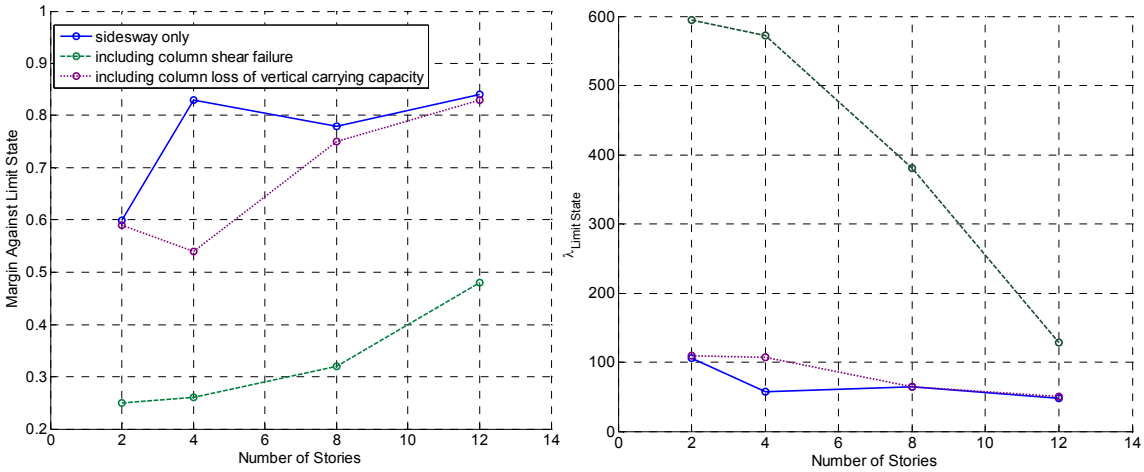

Figure 5.16 Effect of column shear failure and subsequent vertical collapse on collapse metrics for baseline non-ductile RC space frames: (a) collapse margin ratio, and (b) mean annual frequency of collapse.

Two other factors appear to be important in characterizing the effects of the non-simulated limit states on the collapse performance predictions. Firstly, shear failures and local column collapses are more likely in low to mid-rise structures, where gravity loads are more dominant in the design. In addition, the relative importance of the non-simulated failure mode depends on the sidesway failure mode observed. For example, the 2-story perimeter frame structure fails in a complete mechanism with significant hinging in the beams such that a smaller portion of the deformations are in the columns, reducing the effect of these non-simulated failure modes that are a caused by large column deformations. As a result of gravity dominated design and stronger beams than columns, the 4-story space frame structure is particularly susceptible to column shear failure modes.

5.3.4 Assessment of Archetype Design Variants

The baseline set of archetype designs consists of eight non-ductile RC frame structures: a space frame and perimeter frame each with 2, 4, 8 and 12 stories. The other archetype structures are variations of these designs, as described in Table 5.2. These design variations are included in the set of archetype structures to evaluate the extent to which specific decisions made by the structural engineer may affect the predicted collapse capacity of the structure. The design decisions investigated include the level of overstrength in beams and columns, the presence of additional transverse reinforcement in beam-columns or joints that exceeds the code-minimum requirements, and the uniformity of strength and stiffness over

the height of the building. These design variations are not intended to represent the worst-case designs, but rather to probe the variability in collapse capacity associated with the RC frame structures of the type constructed in California between 1950 and 1975.

Modifications to the distribution of strength and stiffness over the height of the building are reflected by design variants B and D. Design variant B represents a case where, for ease in design and construction, the same column design and beam design is used over the height of the building. These are conservative designs, because the upper stories are over-designed in comparison to the design lateral loads. Design variants D have two weak stories at the base, relative to the upper stories, creating an irregularity in elevation. Note that because the structure must still meet code design requirements, this corresponds to overstrength in the upper stories, rather than under-design in the bottom story. As shown in Table 5.7, these design variations have only a small effect on the predicted structural collapse performance. The 8-story space frame design variant B (Design ID 3017), shows very little difference from the baseline 8-story space frame (Design ID 3016), despite the overstrength in the upper stories. Since these structures always fail in the bottom two or three stories, overstrength in upper stories does not help collapse performance. The two designs are very similar at the bottom stories, having the same stiffness, only a small difference in strength, and nearly identical parameters relating to ductility and deformation capacity. There is little effect due to design variant D for the same reason. Since neither B nor D alters the characteristic collapse mechanism. More significant differences in the collapse capacity are likely if other more drastic irregularities in elevation exist, such as a much taller first story.

Table 5.7 Collapse metrics for non-ductile RC frame structures, comparing the effects of designs that vary the distribution of strength and stiffness over the height of the structure.

Design ID	Num. of Stories	Framing System	Design Variant	Margin[1]	P[collapse| $Sa_{2/50}$]	$\lambda_{collapse}$ x 10^{-4}
3016	8	Space	A	0.78	0.65	65
3017		Space	B	0.76	0.67	70
3018		Space	D (65%)	0.75	0.67	78
3019		Space	D (80%)	0.77	0.66	71
3023	12	Space	A	0.84	0.62	48
3024		Space	B	0.94	0.54	43
3026		Space	D (65%)	0.96	0.52	35
3027		Space	D (80%)	0.93	0.55	38

[1]All metrics include sidesway failure modes only.

One might also expect that different structures might have different levels of detailing, depending on decisions made by the individual engineer. By the 1960s, some engineers had

begun to recognize the importance of seismic detailing and, in some cases, chose to space stirrups more closely and provide better anchorage of reinforcement (Blume et al. 1961; Degenkolb 1994). Better-than-average detailing is represented by two design variants: in I, column stirrups are continued in the joint, H reduces the spacing of stirrups in beams and columns by 33%.[6] These results are summarized in Table 5.8. I leads to a substantial increase in strength of the 12-story space frame structure, because the increase in joint strength is sufficient to move the deformations out of the joints and into the somewhat more ductile beams and columns. This results in allowing the damage being spread more over the height of the structure, as shown in Figure 5.17. The improvement in collapse capacity occurs even though the final failure mechanism, a multi-story mechanism in the bottom three stories is similar in both cases. A smaller improvement in collapse capacity for the 4-story structure is observed in design variant I.

The 50% increase in the amount of transverse reinforcement in beams and columns from design variants A to H, leads to an increase (10% to 25%) in the collapse margin, as shown in Table 5.8. The improved detailing represented by design variant H both increases the sidesway collapse capacity and decreases the likelihood of experiencing column collapse due to shear failure. The increase in ductility associated with better confinement produces a modest increase in the sidesway collapse margin ratio, by increasing the plastic rotation capacity and post-capping rotation capacity of RC elements, and decreasing the amount of cyclic strength and stiffness deterioration in beams and columns.

Table 5.8 Collapse metrics for non-ductile RC frame structures, comparing design detailing decisions. Metrics shown here include both sidesway and non-simulated failure modes.

Design ID	Num. of Stories	Framing System	Design Variant	Margin	P[collapse| $Sa_{2/50}$]	$\lambda_{collapse}$ x 10^{-4}
3004	4	Space	A	0.54	0.91	107
3012		Space	H	0.72	0.79	38
3032		Space	I	0.60	0.90	89
3023	12	Space	A	0.83	0.62	50
3031		Space	H	0.93	0.55	35
3033		Space	I	1.32	0.33	16

[6] In the structural models, I is associated with a 20% increase in the joint strength inputted for the joint shear panel. This value is based on the limited data assembled by Mitra and Lowes (2005) for joints where transverse steel confinement is provided.

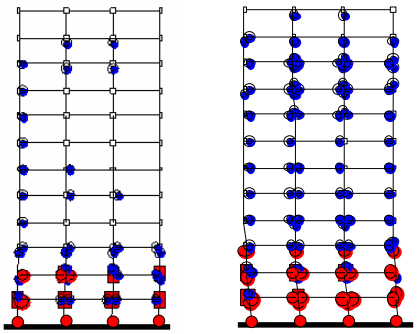

(a) (b)

Figure 5.17 Most frequent collapse mechanisms observed for (a) 12-story baseline space frame structure (Design ID 3023, variant A), and (b) 12-story space frame structure with increased strength in joints (Design ID 3033, variant I).

The final set of design variants considers design decisions that affect the relative strength of beams and columns in non-ductile RC frame structures. For example, some designers include the slab (T-beam effects) in design of beams, while others neglect both the contribution of the compression concrete and the slab steel. If the slab contribution is neglected in design, the actual strength may greatly exceed the design value. Unlike modern seismic building codes, the 1967 Uniform Building Code lacks provisions that mitigate the potentially negative effects of element overstrength through capacity design and the strong column-weak beam ratio. These decisions are represented in the set of archetypical non-ductile RC structures by design variants F1 and F2, which have higher flexural overstrength in the beams and columns, respectively. As reported in Table 5.9, increasing the overstrength of beams (F1) and not the columns leads to a reduction in capacity. Due to the adverse effects of concentrating damage in columns and joints, the collapse margin decreases by 15% on average. The effect of increasing the column strength (F2) is mixed. A small improvement is observed in the collapse capacity of the 12-story space frames, because the increased column strength delays the formation of the collapse mechanism in these structures, dissipating more energy through yielding in upper stories. There is essentially no change in the collapse capacity of the 4- and 8-story space frames when columns have higher overstrength because the strong columns push the non-linear deformations into the non-ductile joints.

Table 5.9 Collapse metrics for non-ductile RC frame structures, comparing element level overstrength decisions.

Design ID	Num. of Stories	Framing System	Design Variant	Margin[1]	P[collapse| $Sa_{2/50}$]	$\lambda_{collapse}$ x 10^{-4}
3004	4	Space	A	0.83	0.62	57
3009		Space	F1	0.63	0.77	108
3010		Space	F2	0.81	0.63	60
3016	8	Space	A	0.78	0.65	65
3020		Space	F1	0.72	0.70	82
3021		Space	F2	0.77	0.66	69
3023	12	Space	A	0.84	0.62	48
3028		Space	F1	0.71	0.72	70
3029		Space	F2	0.96	0.53	35

[1]All metrics include sidesway failure modes only.

The effects of story height on the predicted collapse capacity are also examined. Two perimeter frame structures (of 8 and 12 stories) were designed and analyzed with 10 ft. story heights, instead of the 13 ft. story heights used in the baseline designs. These short-story height designs are representative of hotel or multi-family residential type construction, which often have perimeter framing systems and short clear story heights on the exterior of the structure.. As shown in Table 5.4 for design variants A and J, the story height has a small effect on the predicted collapse capacity, even when non-simulated failure modes are included. Because we do not model nonstructural components or direct column shear failure, the study cannot completely capture the negative "captive column" effect that has been observed in some of these older buildings. Captive columns often occur when nonstructural walls effectively shorten the column, making the column much more likely to fail in shear than in flexure. When these captive columns are present, a more brittle failure mode is likely and, consequently, it is expected that these structures will have a higher collapse risk. These shear critical frames are an item left for future study.

The analysis of different design variations among the archetypical structures confirm that design decisions relating to relative strengths of beams, columns and joints, which impact the extent to which damage concentrates in the structure, have the greatest influence on the structure's collapse capacity. Neglecting T-beam contributions to beam strength in design, for example, could lead to an overdesign of beams that adversely affects collapse performance. Significant improvements in detailing are needed to obtain an appreciable increase in collapse capacity. Quantifying how these design decisions influence collapse performance assessments may prove useful in identifying especially vulnerable non-ductile RC frame structures.

5.3.5 Collapse Risks at Different California Sites

In the 1967 Uniform Building Code, the highest seismic hazard zone (Zone 3) covered almost all of California, and structures designed anywhere in Zone 3 were required to have the same design base shear. The 26 archetype designs, then, could hypothetically be located anywhere in the state. With improved knowledge of the seismic hazard, it is apparent that there are differences between sites, such that the assessed collapse risk, for the same structure, may vary widely across the state.

To compare the collapse risk of non-ductile RC frame structures at different locations around California, five different sites in the Los Angeles region are selected, as shown in Table 5.10. The probabilistic seismic hazard analysis for site 1 is based on a site specific analysis by Goulet et al. (2007), and was used to obtain the results presented in Table 5.4 and all those presented previously (Haselton et al. 2008). Site 2 is at the same location as site 1, but the hazard curve is obtained from the closest possible USGS data source. All the other sites (sites 3 – 5) are based on USGS hazard curve for the different sites, and are included to demonstrate the possible variation in collapse risk within southern California. Site 5 has virtually the same code-defined maximum considered earthquake (MCE) as site 1, but lies in the deterministic region of the USGS hazard maps, such that $Sa_{2/50}(1sec) = 1.41g$, much higher than at sites 1 or 2. All sites correspond to soil sites (NEHRP soil category D). The USGS spectra for rock (B) are modified to D using standard code multipliers.

Since they are at the same location, differences in assessed collapse risk between sites 1 and 2 are related to epistemic uncertainty in formulation of the hazard curve. These hazard curves are plotted in Figure 5.18, illustrating the significant differences between sites 1 and 2, with the Goulet et al. (2007) hazard curve predicting a larger number of smaller, more frequent events. Both Goulet et al. (2007) and the USGS (Frankel et al. 2002) use Boore, et al. (1997), Abrahamson and Silva (1997), Sadigh et al. (1997) and Campbell and Bozorgnia (2003) ground motion prediction equations, but attach different weighting functions to each.[7] The effect of soil-site factors also contributed to the difference, as the Goulet et al. curves use site-specific soil data and the USGS curves are modified from rock to soil using code factors. Recent research has improved the understanding of the relationship between hazard on rock and soil (Bazzurro and Cornell 2004; Stewart et al. 2005), as it is acknowledged that NEHRP

[7] The USGS hazard maps weight each of these attenuation relationships evenly. Goulet et al.(2007) puts a smaller weight on the Boore et al. (1997) relationship.

code multipliers give poor predictions of hazard under different soil conditions. In addition, the USGS predictions incorporate results from changes in the fault models for the Los Angeles region as of 2002, while Goulet et al. uses the 1996 fault models with some modifications.

Table 5.10 Ground motion hazard for 5 sites in the Los Angeles area.

Site ID	Location: Latitude, Longitude	MCE (T_{1sec}) [g]	$Sa_{2/50}$ ($T_{1\ sec}$) [g]	Notes
1	34.0, -118.2	0.91	0.81	hazard curve from Goulet et al. (2007)
2	34.0, -118.2	0.91	0.93	USGS hazard curve (Frankel et al. 2002)
3	34.8, -118.0	0.80	0.83	USGS hazard curve, Slightly lower hazard than site 1
4	34.1, -118.2	1.18	1.34	USGS hazard curve, Near field, Higher hazard than site 1
5	34.5, -117.7	0.92	1.41	USGS hazard curve, Same MCE as site 1, but higher hazard

The computed collapse metrics for the baseline 8 typical non-ductile RC frame structures structures, for the hazard curves defining sites 1 and 2, are reported in Table 5.11 and shown graphically in Figure 5.19. The computed margins against collapse (Figure 5.19a), are similar for the two different hazard analyses because of the similarities between the response spectra, especially at longer periods. However, there are significant differences in the mean annual frequency of collapse computed for the two cases (Figure 5.19b). The assessed mean annual frequency of collapse is significantly higher in all cases when the Goulet et al. hazard curve is used instead of the USGS hazard curve. This increase in the predicted collapse risk is associated with the high number of small events predicted by the Goulet et al. hazard curve (Figure 5.18). These small frequent earthquakes become important because these non-ductile RC frame structures have a non-negligible collapse probability at small spectral acceleration levels. The differences between sites 1 and 2 point more generally to the importance of continuing to improve the collapse assessment process as more data and simulation technologies become available, including careful investigation of the ground motion hazard. The hazard curve is yet another characteristic of the assessment process that must be consistent in order to obtain comparable performance predictions among buildings.

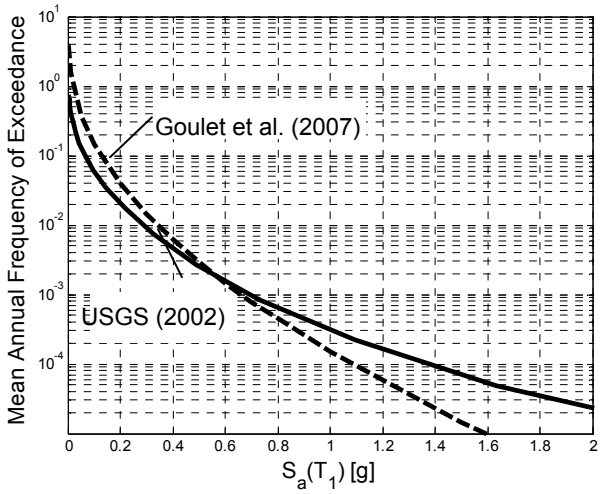

Figure 5.18 Two ground motion hazard curves (T_1 = 1 sec) for the same Los Angeles location (denoted sites 1 and 2).

Using the USGS hazard data for sites 2 – 5, the collapse risk at different sites in the Los Angeles region are compared as shown in Table 5.12. There may be significant differences in assessed performance depending on where a non-ductile RC frame structure is located. For the sites chosen, the average collapse margin ratio for the baseline structures ranges between 0.73 and 1.02 depending on the level of hazard at a particular site, and the mean annual frequency of collapse varies between 33 and 64 x 10^{-4} (a factor of 2). Site 5, which has a significantly larger $Sa_{2/50}$ because it lies in the deterministic region of the seismic hazard maps, leads to a 70% higher collapse risk, in terms of mean annual frequency, than site 2. Unsurprisingly, site 3, which has the lowest 2% in 50 year ground motion of the USGS sites, has the lowest collapse risk. Since all of these Los Angeles sites have high levels of seismicity relative to the collapse capacities of the buildings, the collapse rates predicted are within the same range. A much bigger difference is expected if collapse metrics were predicted from a hazard curve in a lower seismic area (Sacramento, for example).

Table 5.11 Effect of epistemic uncertainty in hazard curves on assessed collapse risk of non-ductile RC frame structures.

Design ID	Num. of Stories	Framing System	Margin [site 1]	Margin [site 2]	$\lambda_{collapse}$ x 10^{-4} [site 1]	$\lambda_{collapse}$ x 10^{-4} [site 2]
3001	2	Space	0.60	0.46	106	60
3002		Perimeter	0.84	0.74	49	31
3003	4	Perimeter	0.66	0.65	100	44
3004		Space	0.83	0.85	57	26
3015	8	Perimeter	0.58	0.60	135	56
3016		Space	0.78	0.82	65	30
3022	12	Perimeter	0.58	0.62	116	52
3023		Space	0.84	0.88	48	23
		Average	0.71	0.70	85	40

Table 5.12 Collapse predictions for non-ductile RC frame structures 4 different sites in the Los Angeles region.

Design ID	Num. of Stories	Framing System	Margin [site 2]	Margin [site 3]	Margin [site 4]	Margin [site 5]	$\lambda_{collapse}$ x 10^{-4} [site 2]	$\lambda_{collapse}$ x 10^{-4} [site 3]	$\lambda_{collapse}$ x 10^{-4} [site 4]	$\lambda_{collapse}$ x 10^{-4} [site 5]
3001	2	Space	0.46	0.89	0.55	0.54	60	38	82	78
3002		Perimeter	0.74	0.83	0.52	0.49	31	20	46	46
3003	4	Perimeter	0.65	1.01	0.77	0.76	44	33	58	63
3004		Space	0.85	1.29	1.00	0.94	26	20	37	43
3015	8	Perimeter	0.60	0.88	0.69	0.68	56	42	72	77
3016		Space	0.82	1.19	0.97	0.91	30	23	41	47
3022	12	Perimeter	0.62	0.95	0.74	0.68	52	39	67	72
3023		Space	0.88	1.31	1.05	0.98	23	18	32	40
		Average	0.70	1.05	0.78	0.75	40	29	54	58

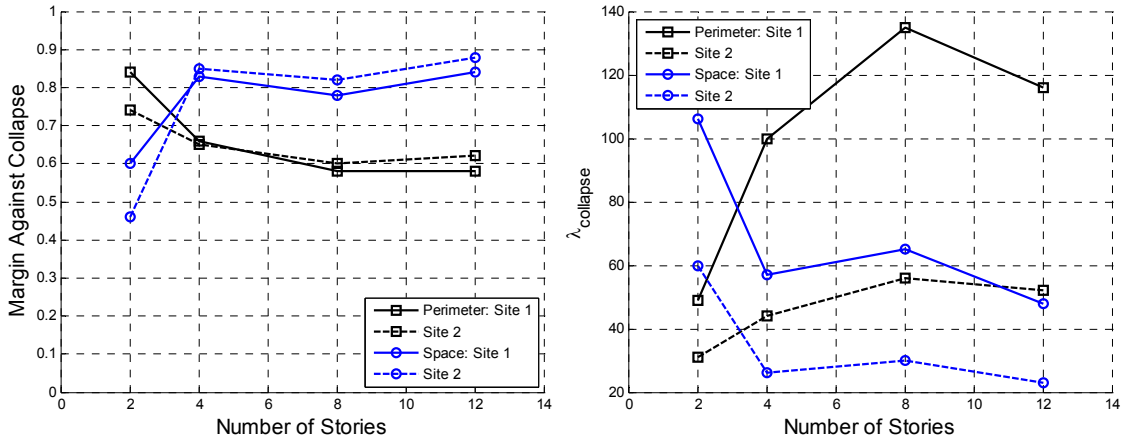

(a) (b)

Figure 5.19 Effect of epistemic uncertainty in hazard curves on (a) margin against collapse and (b) mean annual frequency of collapse for baseline archetype structures. Recall that sites 1 and 2 are at the same location, but defined by ground motion hazard curves generated by different researchers.

5.4 Comparing Collapse Performance of Modern and Older Reinforced Concrete Frame Structures

Structural engineers, public officials and others frequently remark on the seismic risk posed by the older, non-ductile RC frame structures that are the focus of this research.

While it is agreed that, as a group, these structures are more dangerous than other types of structures, including modern, seismically detailed RC frame structures, these comparisons have tended to be qualitative in nature. The collapse assessment procedure described here provides a mechanism through which the relative safety of older and modern RC frame structures can be systematically examined. By comparing the collapse metrics obtained in the previous section for the 1967-era archetypical non-ductile RC frame structures, with the same metrics for a set of archetypical code-conforming modern concrete frame structures, the difference in safety between these two types of structures is explicitly quantified.

5.4.1 Designs for Modern RC Frame Structures

The improved seismic performance of modern RC frame structures results from the additional building code provisions governing design and detailing of these structures incorporated into seismic design codes beginning in the 1970s. The requirements for special moment frame (SMF) structures in high seismic areas now include an assortment of capacity design provisions (eg. strong column-weak beam ratios, shear capacity design), detailing improvements (eg. increased lap splice requirements, 135° hooks on transverse stirrups) and other seismic provisions (eg. joint shear strength requirements). These requirements are in addition to those for minimum required strength and drift, which are very similar to the basic provisions of the 1967 Uniform Building Code. The design requirements for RC special moment frames are found in the relevant ASCE (ASCE 2002), ACI (ACI 2002) and IBC (ICC 2003) code documents. These seismic provisions increase the cost of construction by approximately 4%.

The collapse performance of 16 RC frame structures, designed as shown in Table 5.13, is compared. The collapse assessment of the modern RC frames is conducted by Haselton (2006), but is completely consistent with the procedure and assumptions used in this study for the non-ductile RC frame structures. The results are therefore comparable. The eight non-ductile RC frame structures are the baseline archetypical set discussed previously (Table 5.1 and Table 5.4). The eight modern code-conforming structures were designed and analyzed by Haselton (2006), following the same collapse assessment procedure as described here. The structures are designed for a Los Angeles site with S_1 = 0.90g. As indicated in Table 5.13, there have been changes in the code period-based equation for design base shear. The older structures are also typically more flexible because of differences in the design bay

width, as well as the indirect effect of strong column-weak beam and joint shear strength provisions in the 2003 code that tend to increase stiffness where drift does not govern.

Table 5.13 Design data for older (1967) era and modern (2003) RC frames.

Num. of Stories	Design ID	Governing Design Code	Bay Width (ft)	Framing System	T_1 (s)	Design Base Shear (V/W)
2	3002	1967 UBC	25	Perimeter	1.04	0.086
	2064	2003 IBC	20	Perimeter	0.66	0.125
	3001	1967 UBC	25	Space	1.08	0.086
	1001	2003 IBC	20	Space	0.63	0.125
4	3003	1967 UBC	25	Perimeter	1.96	0.068
	1003	2003 IBC	20	Perimeter	1.12	0.092
	3004	1967 UBC	25	Space	1.98	0.068
	1008	2003 IBC	20	Space	0.94	0.092
8	3015	1967 UBC	25	Perimeter	2.36	0.054
	1011	2003 IBC	20	Perimeter	1.71	0.050
	3016	1967 UBC	25	Space	2.20	0.054
	1012	2003 IBC	20	Space	1.80	0.050
12	3022	1967 UBC	25	Perimeter	2.75	0.047
	1013	2003 IBC	20	Perimeter	2.01	0.044
	3023	1967 UBC	25	Space	2.26	0.047
	1014	2003 IBC	20	Space	2.14	0.044

5.4.2 Comparative Collapse Assessment

The results of static pushover analysis provide the first evidence of the superior seismic performance associated with the improvement in seismic design and detailing rules between the 1967 Uniform Building Code and the 2003 International Building Code. These results are reported in Table 5.14. On average, the static overstrength is 30% higher in the 2003 designs than the 1967 designs. The higher overstrength in modern RC frames is due to the strong column-weak beam requirements, required ratios of positive and negative bending strength, as well as specifications for joint detailing and strength present in the 2003 IBC that tend to increase the lateral strength of the structure. The much higher ductility of the 2003 designs is also apparent from the pushover analyses. When ductility is measured in terms of ultimate roof drift ratio, a metric that aggregates member and system level ductility effects, the non-ductile RC frame structures exhibit approximately one-third the ductility of the modern, code-conforming designs. The larger ductility of the modern RC frames comes from improved member level deformation capacity in terms of plastic rotation capacity and post-capping rotation capacity associated with improved detailing requirements in the modern structures. Stronger columns in modern RC frames spread damage over more stories.

Table 5.14 Comparison of static pushover results for 1967 and 2003 archetype RC frame structures.

Data for '67 RC Archetype Frames and '03 RC Archetype Frames						Comparisons ['67/'03']	
Num. of Stories	Design ID	Bay Width (ft)	Framing System	Static Overstrength (Ω)	RDR_{ult}	Ratio of Overstrength	Ratio of RDR_{ult}
2	3002	25	Perimeter	1.6	0.035	0.89	0.52
	2064	20	Perimeter	1.8	0.067		
	3001	25	Space	1.9	0.019	0.54	0.22
	1001	20	Space	3.5	0.085		
4	3003	25	Perimeter	1.1	0.013	0.69	0.34
	1003	20	Perimeter	1.6	0.038		
	3004	25	Space	1.4	0.016	0.52	0.34
	1008	20	Space	2.7	0.047		
8	3015	25	Perimeter	1.1	0.007	0.69	0.30
	1011	20	Perimeter	1.6	0.023		
	3016	25	Space	1.6	0.011	0.70	0.39
	1012	20	Space	2.3	0.028		
12	3022	25	Perimeter	1.1	0.005	0.65	0.19
	1013	20	Perimeter	1.7	0.026		
	3023	25	Space	1.9	0.010	0.90	0.45
	1014	20	Space	2.1	0.022		
					Average	0.70	0.35

Table 5.15 and Figure 5.20 report the predicted seismic collapse performance for the modern (2003) RC frame structures and the older (1967) RC frame structures. These collapse performance metrics are appropriately adjusted for spectral shape, and use FOSM with mean estimates to incorporate modeling uncertainty. The 1967 structures' metrics include non-simulated failure modes, i.e. the collapse fragility includes both simulated (sidesway) collapse and collapse due to loss of vertical carrying capacity from column shear failure. Due to the capacity design requirements governing provision of shear reinforcement, it is highly unlikely that the modern RC frame structures will experience column shear failure and post-processing for non-simulated failure modes is unneeded. More details about the collapse assessment of modern RC frame structures is available in Haselton (2006)

On average, the collapse margin of the new structures is approximately three times higher than the collapse margin of the older RC structures, and this trend is consistent for both perimeter and space frame structures. The modern RC frames have collapse margins ranging from about 2 to 3, signifying that the structures are expected to withstand a ground motion with at least twice the intensity of the 2% in 50 year ground motion ($Sa_{2/50}$), on average. In contrast, the 1967 frames, with collapse margins between 0.5 and 0.9, are expected to collapse before the intensity of $Sa_{2/50}$ is reached, on average. Likewise, the computed probabilities of collapse conditioned on the occurrence of a rare ground motion ($Sa_{2/50}$) are approximately eight times higher for the older RC frame structures. In California, the 2% in 50 year ground motion is typically a *rare ground motion* (2475 year return period) that

results from a more *frequent event* (perhaps a 150 to 500 year return period), so these data do not imply that most of 1967-era structures would collapse in a big earthquake. Rather,we would expect significant damage in areas of low-moderate shaking and collapses in those areas with the highest level of ground shaking. An even greater difference in performance is observed when the collapse fragility is integrated with the site hazard curve to obtain the mean annual frequency of collapse ($\lambda_{collapse}$). The mean annual frequency of collapse can be interpreted as a collapse rate, or the number of collapses per year. For the Los Angeles site of interest, in terms of collapse rate, the 1967 perimeter frames are 20 times more likely to collapse than the 2003 perimeter frames, and the 1967 space frames are 60 times more likely to collapse.

Modern code provisions for RC frame structures also seem to provide more consistent levels of collapse safety. The conditional probabilities of collapse, P[Collapse|$Sa_{2/50}$], vary between 0.05 and 0.20 for ductile RC frame structures and 0.60 to 0.90 for non-ductile RC frame structures. The wide variation in predictions of collapse performance for the non-ductile RC frame structures is even more apparent when comparing mean annual frequencies of collapse.

Table 5.15 Comparison of collapse metrics for 1967 and 2003 RC frame structures.

Data for '67 RC Archetype Frames and '03 RC Archetype Frames							Comparisons ['67/'03]		
Num. of Stories	Design ID	Bay Width (ft)	Framing System	Margin	P[Collapse|$Sa_{2/50}$]	$\lambda_{collapse}$ x 10^{-4}	Ratio of Margins	Ratio of P[Collapse]	Ratio of $\lambda_{collapse}$
2	3002	25	Perimeter	0.85	0.61	47	0.39	5.0	13.8
	2064	20	Perimeter	2.19	0.12	3.4			
	3001	25	Space	0.59	0.81	109	0.19	20.3	109.0
	1001	20	Space	3.07	0.04	1.0			
4	3003	25	Perimeter	0.66	0.75	100	0.32	5.7	27.8
	1003	20	Perimeter	2.04	0.13	3.6			
	3004	25	Space	0.54	0.91	107	0.21	13.0	62.9
	1008	20	Space	2.56	0.07	1.7			
8	3015	25	Perimeter	0.49	0.81	135	0.28	4.3	21.4
	1011	20	Perimeter	1.77	0.19	6.3			
	3016	25	Space	0.75	0.68	64	0.33	7.6	26.7
	1012	20	Space	2.29	0.09	2.4			
12	3022	25	Perimeter	0.56	0.83	119	0.31	5.2	22.9
	1013	20	Perimeter	1.84	0.16	5.2			
	3023	25	Space	0.83	0.62	50	0.44	4.1	10.6
	1014	20	Space	1.91	0.15	4.7			
						Average	0.31	8.2	36.9

As expected, the ductility of the code-conforming RC frame structures is much higher than the older structures, with roof drift ratios just before collapse 2.5 times larger, and interstory drift ratios 1.8 times larger, as reported in Table 5.16. These differences result in part from increases in member-level deformation capacity associated with improved detailing requirements. For example, the plastic rotation capacities of code-conforming beams and

columns are typically three times larger than the beams and columns with non-ductile detailing, and there are similar improvements in post-capping rotation capacity. The code-conforming structures also have larger system level ductility, as indicated by the larger increase in roof drift ratios at collapse than interstory drift ratios at collapse. Strong columns in modern special moment frames tend to spread deformations and damage over a larger portion of the structure. While the modern structures still fail in single-story mechanisms in the shorter buildings and multi-story (2 to 3 stories) mechanisms in the taller buildings, the 2003 frames tend to have greater yielding in beams not directly involved in the collapse mechanism (see Table 5.17).

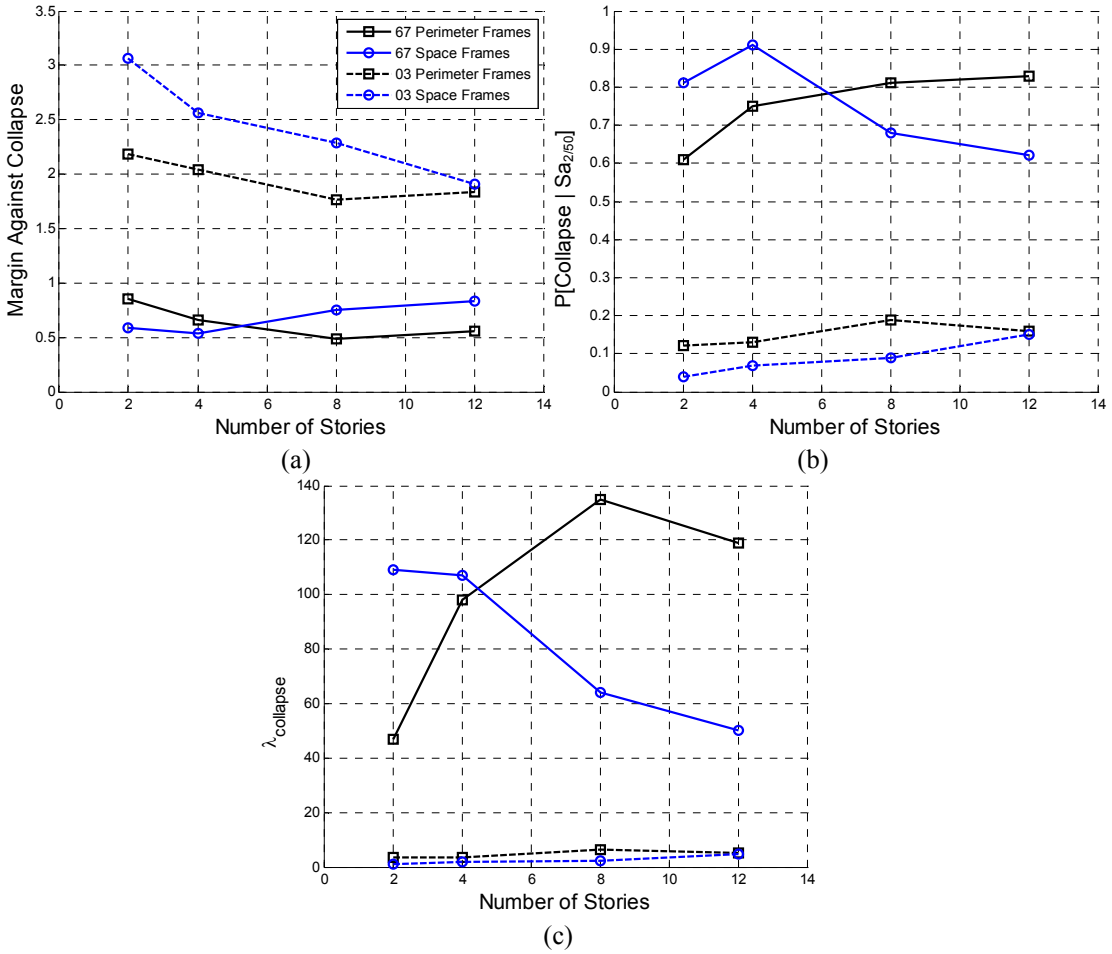

Figure 5.20 Comparison of collapse metrics for non-ductile and ductile RC frame structures, measured in terms of (a) margin against collapse, (b) probability of collapse conditioned on the 2% in 50 year ground motion, and (c) mean annual frequency of collapse.

Table 5.16 Comparison of collapse drifts for 1967 and 2003 RC frame structures.

Data for '67 RC Archetype Frames and '03 RC Archetype Frames						Comparisons ['67/'03]	
Num. of Stories	Design ID	Bay Width (ft)	Framing System	RDR preceding collapse	IDR preceding collapse	Ratio of RDRs	Ratio of IDRs
2	3002	25	Perimeter	0.028	0.040	0.46	0.53
	2064	20	Perimeter	0.061	0.075		
	3001	25	Space	0.017	0.031	0.23	0.34
	1001	20	Space	0.075	0.091		
4	3003	25	Perimeter	0.017	0.037	0.38	0.48
	1003	20	Perimeter	0.039	0.076		
	1009	30	Perimeter	0.050	0.078		
	3004	25	Space	0.023	0.054	0.47	0.66
	1008	20	Space	0.045	0.080		
	1010	30	Space	0.053	0.083		
8	3015	25	Perimeter	0.009	0.034	0.41	0.63
	1011	20	Perimeter	0.021	0.054		
	3016	25	Space	0.011	0.042	0.41	0.62
	1012	20	Space	0.027	0.068		
12	3022	25	Perimeter	0.006	0.031	0.38	0.58
	1013	20	Perimeter	0.016	0.053		
	3023	25	Space	0.009	0.039	0.50	0.71
	1014	20	Space	0.018	0.055		
					Average	0.40	0.57

Table 5.17 Comparison of collapse mechanisms in 1967 and 2003 RC frame structures

		1967 Frame Structures	2003 Frame Structures
Num. of Stories	Framing System	Fraction of Stories Involved in Collapse Mechanism[1]	Fraction of Stories Involved in Collapse Mechanism[1]
2	Space	0.50	0.64
4	Space	0.50	0.60
8	Space	0.30	0.28
12	Space	0.25	0.17
2	Perimeter	0.82	0.62
4	Perimeter	0.50	0.44
8	Perimeter	0.25	0.28
12	Perimeter	0.17	0.18

[1]Where there are multiple collapse mechanisms a weighted average is used

This improvement in predicted collapse capacity and ductility between the 1967 designs and the 2003 designs reflects the aggregate effect of the design and detailing changes made in seismic design codes for RC in the intervening years. The differences in amount of transverse reinforcement provided in the archetype designs are striking: the 12-story 2003 RC space frame (Design ID 1014) has shear stirrups spaced every 5 inches with cross-ties, while the 12-story 1967 space frame (Design ID 3023) has stirrups spaced every 10 – 15 inches with a single hoop. This increase in confinement leads to an increase in the modeled deformation capacity at the member level by a factor of three. Strong column-weak beam ratios in the 2003 code significantly increase the strength of columns, thereby delaying yielding of these members. At the 2nd floor of the 4-story space frame structures (Design IDs

3004 and 1008) the actual strong-column-weak-beam ratio is approximately 0.7 for the older structures, and 1.3 for the modern structure.

The 2003 structures also benefit more from the unique characteristics of spectral shape associated with rare ground motions in California (Baker and Cornell 2005). Structures that have higher ductility and can undergo larger inelastic deformations will have a significant elongation of the first mode period that moves the structure into less energetic regions of the response spectra. Since the 2003 RC frame structures have higher collapse capacities, they also collapse under more rare ground motions. The effects of spectral shape, as measured in terms of epsilon, are summarized for the sixties-era structures in Table A5.1. On average, proper treatment of epsilon is associated with a 20% improvement in the collapse capacity results for the non-ductile RC frame structures. Haselton et al. (2008) found that the ductile RC structures saw a 50% improvement in collapse capacity associated with appropriate consideration of spectral shape. Thus, the relationship between ductility and expected spectral shape for rare ground motions in California accounts for approximately 40% of the difference in the collapse predictions for the two groups of structures.

5.5 Conclusions

The modern (2003) RC frame structures demonstrate markedly superior seismic collapse performance for all heights and framing systems when compared to the non-ductile (1967) RC frame structures. The modern structures are able to withstand higher levels ground motion intensity before collapsing, and they are capable of undergoing more significant deformations before collapse. Both better detailing in individual members – closer tie spacing, use of closed hooks, transverse ties in joints – and system-level design requirements – strong column-weak beam and other capacity design provisions – have contributed to these improvements. These modern building code provisions for RC have the effect both of improving seismic performance, and providing more consistent collapse safety than previous code requirements. The assessed collapse performance of modern RC frames is an indicator of the level seismic safety provided by today's building codes, and provides a yardstick to which other structural systems, new and older, can be compared. The collapse performance assessment of older structures confirms the expectation that non-ductile RC structures are potentially vulnerable and, for the first time, systematically quantifies differences in safety for ductile and non-ductile reinforced frame concrete structures.

The collapse performance assessments also serve to illustrate the variability in seismic performance expected for non-ductile RC frame structures. Tall, perimeter non-ductile RC frame structures are most susceptible to sidesway collapse. Space frame structures, which tend to have much higher axial load levels in columns, are more at risk of a local collapse due to loss of gravity load carrying capacity in a column induced by column shear failure. Other highly irregular structures or those with design or construction flaws, not considered here, are likely to have even worse seismic performance. Some older structures, especially those with better than average detailing in beams, columns and joints, are at a smaller risk of earthquake-induced collapse. Modest detailing improvements, such as those that might have been provided by a particularly conscientious engineer, improve seismic performance of non-ductile RC frames, but do not bring them to modern code levels. These observations are useful for developing strategies for mitigating the most collapse-prone non-ductile RC frame structures first.

These metrics can be used to help quantify the debate about acceptable collapse risk and public safety in California and to identify the most vulnerable structures. It is clear that structures should be safe enough in future earthquakes to protect public welfare, but this goal is poorly defined. Since absolute seismic safety is an unrealistic objective, we must ask ourselves, "how safe is safe enough?" for our building structures. Seismic provisions in building codes represent the accumulated judgment of the structural engineering community and, when the collapse safety provided by these provisions is explicitly examined, as in this study, provide one measure of acceptable collapse safety. Due to the shorter remaining life span of existing buildings and the high cost of retrofit or replacement, some reduced collapse safety is probably acceptable for non-ductile RC frame structures.

A variety of approximations are made in generating these results, in characterizing future ground motions, in identifying a representative set of typical non-ductile RC frame structures and in developing simplified analysis models for RC frame structures. For example, despite the detailed analysis performed here, there are other contributions to collapse capacity of the structure that are not accounted for. For one, all perimeter frame systems have flat-plate gravity systems that will contribute strength and stiffness to the structure's lateral resistance. For another, many engineers of older buildings probably did more to improve on code-minimum design than presumed in the definition of archetypical structures. Conversely, there are other failure modes – anchorage failure in lap-splices, overturning effects on

columns, punching shear failure in slab-column joints – that are neglected from the analysis. The accuracy of the collapse performance evaluations generated is a function of the simplifying approximations (Krawinkler and Zareian 2007). Even for those who doubt the absolute values, however, relative values and comparisons of patterns in collapse capacity provide important metrics for seismic safety.

Continued validation of performance-based evaluation methods for seismic safety is a subject of ongoing research. The collapse assessment procedure can still benefit improvements in ground motion selection and scaling (e.g. Goulet et al. (2008)), calibration of component models (e.g. Lignos and Krawinkler (2007)), modeling propagation of collapse from local failure modes (e.g. Charlet et al. (2008)), among others. Comparison of observed experience in California earthquakes will serve to identify discrepancies between actual and predicted behavior, leading to improvement in the underlying models and more accurate metrics of seismic safety.

Appendix 5.1 Effect of Spectral Shape on Collapse Assessment

The effect of spectral shape on the collapse assessment is shown in Table A5.1. For these non-ductile RC frame structures, adjusting collapse results for a target epsilon consistent with a rare ($Sa_{2/50}$) earthquake increases the collapse capacity by a factor of between 1.1 and 1.3, depending upon the structure under consideration. This adjustment is performed using the regression analysis approach, described in Chapter 3. Not surprisingly, the average increase of 24% is smaller than the 30 – 80% increase of collapse capacity reported elsewhere for more ductile systems (such as seismically detailed special RC moment frames). However, these results demonstrate that neglecting to account for proper spectral shape can lead to collapse predictions that are conservative, even for relatively brittle structures. The effects of spectral shape are relatively constant as a function of building height. System level ductility tends to decrease with height due to P-Δ effects increasing the concentration of damage in a smaller percentage of the structure, but this is counterbalanced by the increased importance of higher modes for taller structures that are beneficially impacted by higher ε records. Table A5.1 also shows results obtained from the simplified relationship proposed by Haselton et al. (2008), which predicts the effect of epsilon as a function of building ductility. This simplified relationship provides good agreement with the regression analysis results for these structures on average, though some of the values for individual structures differ by as much as 10%.

Table A5.1 Effect of incorporation of ε on collapse assessment results for non-ductile RC frame structures.

			Neglecting Spectral Shape Effects	Effect of ε - Regression Approach		Effect of ε - Simplified Approach	
Design ID	Num. of Stories	Framing System	Median Collapse Capacity [g]	Median Collapse Capacity [g]	Ratio[1]	Median Collapse Capacity [g]	Ratio[1]
3001	2	Space	0.43	0.48	1.10	0.56	1.21
3002		Perimeter	0.58	0.68	1.17	0.86	1.35
3003	4	Perimeter	0.24	0.32	1.33	0.31	1.22
3004		Space	0.31	0.39	1.26	0.40	1.24
3015	8	Perimeter	0.18	0.23	1.26	0.23	1.21
3016		Space	0.26	0.33	1.28	0.34	1.25
3022	12	Perimeter	0.16	0.20	1.27	0.20	1.19
3023		Space	0.28	0.35	1.24	0.38	1.28
				Mean	1.24	--	1.24

[1]Ratio of *Median adjusted for epsilon* to *Median neglecting spectral shape*

Appendix 5.2 Collapse Risk in Near-Field Regions of California

The collapse metrics reported here are representative of sites in highly seismic areas in California, except that they exclude near-fault sites. Significant areas of the San Francisco and Los Angeles metropolitan areas lie in near-source regions. The seismic hazard at near-field sites is substantively different those at far-field sites, due to directivity and pulse effects in the velocity spectrum (Tothong et al. 2007). To determine whether these older frame structures are at higher risk at near-field sites, near-field ground motion records and applied in incremental dynamic analysis for two of the archetype non-ductile RC frame structures, the 4-story and 12-story space frames. Since the 1967 Uniform Building Code seismic design requirements do not distinguish between near and far-field sites, no changes are made to the structural designs.

The near-field ground motion set consists of 28 pairs of records, selected from recording stations within 10 km of a fault by Haselton and Kircher (ATC 2007). The set is further divided into two subsets, depending on whether or not the record has a pulse in the velocity spectrum. The records with pulses have a variety of pulse periods. Depending on the period of interest, the average response spectrum ordinate of the near-field records is 1.2 to 2 times the average response spectrum ordinate of the far-field records, with the most significant differences occurring at long periods (> 2 seconds) .

Table A5.2 shows that there is essentially no difference between the collapse assessment for the near-field and far-field sets, when the entire near-field set is used. When only the pulse (fault normal) subset of the near-field records is used, the median collapse capacity of the 4-story non-ductile RC space frame decreases by 11%. The median collapse capacity of the 12-story space frame decreases by 18%. Haselton and Kircher observed a 30% decrease in the median when the pulse subset of records was used in their study of special RC moment frames (ATC 2007). Special RC moment frames may be more sensitive to near-field effects because they are more ductile and subject to significant period elongation before collapse, such that they respond more to the higher energy of near-fault spectra at periods away from T_1.

These results are contrary to the conventional wisdom that structures near a fault represent a significantly higher collapse hazard than those far from a fault. This study suggests there is not universally higher risk of collapse at near-field sites. However, the near-field ground motion set is too general to capture the true source of the higher hazard in the

near-field. By not accounting for site specific or building specific studies that consider the likelihood of pulses at a particular site or the likely values of the pulse period, relative to the structure's fundamental period, the near fault effects are likely underestimated. The effect of building ductility on near-fault effects should also be considered. More detailed study of near-field effects is a topic of future research.

Table A5.2 Collapse assessments for non-ductile RC frame structures, using near-field record set.

Design ID	Num. of Stories	Far Field Record Set: Median Sa(T1) [g]	Near Field Record Set: Median Sa(T1) [g]	Near Field Record Set, Fault Normal Pulse Subset: Median Sa(T1) [g]
3004	4	0.35	0.33	0.31
3023	12	0.33	0.33	0.27

* These results do not include the ε adjustment. Both the near field and far field record sets are epsilon neutral.

** The results presented here are for all components, rather than controlling components, in order to make a comparison with the pulse subset of the near field ground motions.

Chapter 6

Predictions of Earthquake-Induced Economic Losses and Fatalities in Non-Ductile Reinforced Concrete Frame Structures

6.1 Overview

The previous chapter evaluated the collapse performance of non-ductile reinforced concrete office buildings, typical of those constructed in California in the 1960s, and compared the seismic collapse risk to modern code-conforming RC frame buildings. In this chapter, these results are extended to include two additional metrics of building seismic performance: economic losses and fatalities. Economic losses are a measure of financial losses that may be incurred due to damage in the structure in future earthquakes. The fatalities estimations extend predictions of collapse to explicitly evaluate the extent to which design characteristics of RC frame buildings present a life safety hazard to their occupants in earthquakes. Methods for predicting economic losses and fatalities are described in detail here, as well as results for the set of archetypical non-ductile RC frames that are the subject of this thesis. In the next chapter, this data is used to evaluate the costs and benefits of retrofitting or replacing these structures.

6.2 Economic Losses

6.2.1 Motivation

Economic losses are an alternative measure of building performance. Predictions of earthquake-induced economic losses can be used by building owners and designers "for more rational decision making about risk management" (Krawinkler and Miranda 2004). The insurance industry uses estimates of future economic losses to set premiums for earthquake insurance. Understanding their vulnerability to losses in future earthquakes may help owners of new buildings decide whether to invest in improving seismic resistance beyond current code requirements. Reduction in future economic losses may also provide a financial

incentive for owners of existing, non-code-compliant structures to seismically upgrade their buildings and facilities.

This financial incentive to retrofit or replace vulnerable structures is the reason economic losses are analyzed here. Life safety remains the most important reason for seismic retrofit, especially at the policy level, but if the retrofit also decreases economic losses, this provides an additional inducement for building owners to mitigate deficient structures. In this section, economic losses due to seismic damage in non-ductile RC frames of different heights and framing systems are assessed and compared to economic losses of code-conforming RC frame structures. These evaluations use loss estimation methodologies developed by researchers at the Pacific Earthquake Engineering Research Center. The intent here is not to improve loss estimation methods, but to examine the significance of calculated losses to policy decisions regarding older RC frame structures.

6.2.2 Methodology for Predicting Economic Losses

The purpose of building-specific loss estimation is to probabilistically predict the economic losses that may be incurred in a particular structure during future earthquakes. These economic losses may be due to damage to building contents, repairs needed in structural or non-structural elements, or business interruption. In the past, studies of earthquake induced losses have largely focused on regional loss estimation scenarios, e.g. ATC-13 (ATC 1985) or HAZUS (FEMA 2003). More recently, researchers at PEER, including Porter (2002), Aslani (2005) and Mitrani-Reiser (2007), have used the PEER framework for performance-based earthquake engineering to develop methods and data for building-specific loss estimation. This study utilizes work by Aslani (2005) and Mitrani-Reiser (2007), and readers are referred to these references for a more detailed discussion.

The general approach to loss estimation relies on structural analysis to calculate deformations and accelerations in the structure in an earthquake, which are used to predict to damage in structural elements, non-structural components, and building contents. The cost of providing needed repairs is determined directly from the damage state of the building's components. Other sources of economic loss, such as business interruption, could also be computed on the basis of the extent of damage in the building. The focus here is on direct losses, or the cost of repairing earthquake-induced damage in the building (Mitrani-Reiser 2007). The total repair cost is calculated by summing the cost of repairing each damaged

component in the building. Where the repair costs exceed the replacement cost of the building, it is assumed that the structure would be demolished and constructed anew.

The expected value of the total cost or total economic loss predicted at each level of ground motion intensity, denoted E[TC | IM], is given by Equation (6.1):

$$E[TC \mid IM] = E[TC \mid NC, IM]\,(1-P[C \mid IM]) + E[TC \mid C, IM]\,P[C \mid IM] \quad (6.1),$$

where TC = total cost of repairing seismic damage, IM = intensity measure, C = collapse and NC = no collapse. P[C |IM] is the cumulative probability of collapse, as a function of the intensity measure. Losses are conditioned on whether or not collapse occurs since if the structure has collapsed, the losses are based on the total replacement costs of the building, whereas if collapse does not occur, the losses are computed based on the repairs needed. For the non-collapsed (NC) states, the total cost is computed as the sum of the repair costs needed for each component, and scaled appropriately to account for inflation, location, and contractor overhead and profit (Mitrani-Reiser 2007).

The repair costs for each component, denoted $E[RC_i \mid NC, IM]$ depend on the severity of damage, which is defined by the probability of being in each damage state, and the cost of repairing that damage. Thus, the expected repair costs associated with each component (i) in the building are:

$$E[RC_i \mid NC,IM] = \sum_{j=1}^{n} E[RC_i \mid DM_{ij}]\; P[DM_{ij} \mid NC,IM] \quad (6.2), \text{ where,}$$

$$P[DM_{ij} \mid NC,IM] = \int_{EDP_i} P[DM_{ij} \mid EDP_i]\; p[EDP_i \mid NC,IM]\; dEDP_i \quad (6.3)$$

And n is the number of damage states considered for the component of interest, EDP_i is the engineering demand parameter of interest for the component under consideration and DM_{ij} is the j^{th} damage state associated with component i. (As before, P[x] refers to the cumulative distribution function, whereas p[x] is the probability density function.)

The damage in each component is due to the movement in the structure, recorded as engineering demand parameters during structural analysis, as described in Equation (6.3). Some elements are sensitive to interstory drifts, such as drywall partitions and exterior glazing, whereas other elements are sensitive to floor accelerations, such as most building contents and acoustical ceiling tiles. The relationship between EDPs and the damage state are given by a fragility function, which defines the probability of reaching or exceeding the specified damage state (j) as a function of EDP, for a particular type of component (i). The definition of damage states and fragility functions depends on the structural component of

interest and is typically based on a combination of experimental data and judgment, e.g. Aslani (2005). Following Aslani (2005) and Mitrani-Reiser (2007), damage states are defined in terms of the repair action needed, such that there is a direct relationship between the damage state the cost of repairs needed in Equation (6.2). This level of detail, obtained by disaggregating building components and separately considering the damage and loss in each component, distinguishes Porter's, Mitrani-Reiser's and Aslani's work from previous loss estimation studies that used a single fragility function to describe the level of damage in the entire building. It is assumed that damage states and repair costs (given EDP, IM) are perfectly correlated among like components at each level of the building.

The outcome of these analyses is a variety of measures of seismically-induced economic losses (Krawinkler and Miranda 2004; Miranda et al. 2006). Equation (6.1) predicts the expected value of the loss as a function of the intensity of the earthquake. The expected annual loss, obtained by integrating the total-cost curve with the site-specific hazard curve, is the economic loss that occurs on average every year in the building. Other metrics include the probability of exceeding a specified dollar loss in an earthquake with known intensity, the probability of experiencing a dollar loss larger than a certain amount at any time during the lifetime of the building or the mean annual frequency of exceeding a given dollar loss. The probable maximum loss (PML) is an economic loss that has a small probability of being exceeded that is commonly used by insurers and lending institutions, but it is vaguely defined. It is noted that all these measures are estimates of mean repair costs; correlations and variability in mean response are topics for future work.

The loss estimation analysis performed here, and represented by Equations (6.1) – (6.3), includes only repair and replacement costs, and neglects indirect losses associated with seismic damage to the building. Building downtime, or the amount of time that elapses between the occurrence of an earthquake and the completion of building repair work, may contribute significantly to economic losses due to business interruption and loss of rent or revenue-producing activity (Krawinkler and Miranda 2004; Comerio 2006; Mitrani-Reiser 2007). Downtime is affected by a variety of factors that are difficult to predict, including building inspection and damage assessment, financial planning, architecture and engineering consultations, availability of materials, labor and capital, economic and regulatory uncertainty, as well as repair time. If included, building downtime and related indirect losses would increase the predictions of economic losses in this study. Building closure, related to

'red-tagging' of the structure may significantly increase an owner's losses. Also neglected are the ripple effects of building closure on the economy of the surrounding region. For example, damage to large corporations or universities in an earthquake can have pernicious economic effects throughout the earthquake affected area. There may also be economic losses due to fatalities, which are addressed separately in Section 6.4 and Chapter 7.

6.2.3 MDLA Loss Estimation Toolbox for Reinforced Concrete Frames

Direct economic losses in this study are evaluated using the Matlab Damage and Loss Analysis (MDLA) toolbox created by Judith Mitrani-Reiser for loss analysis of a 4-story reinforced concrete special moment frame structure (Mitrani-Reiser 2007). The toolbox has been extended to apply generally to RC structures of different heights and with different levels of ductility. As input, the MDLA toolbox requires structural analysis results at varied levels of ground motion intensity, a table of damageable assemblies or listing of the components in the building, as well as fragility and cost distribution functions describing the damage states and repair costs for each component. MDLA toolbox output is the total repair cost as a function of the ground motion hazard and expected annual losses. The use of the MDLA toolbox in this study is thanks to Judith Mitrani-Reiser, whose assistance is gratefully acknowledged.

The table of damageable assemblies and structural analysis results are specific to the design of each RC frame building of interest, and are described in further detail below. The library of fragility functions and unit repair cost distributions for RC frame structures are created using experimental data, analytical investigation and/or expert opinion (Goulet et al. 2007; Mitrani-Reiser 2007). Table 6.1 lists the damageable components that are considered, the engineering demand parameter of interest, the possible damage states, as well as the source reference for developing the fragility function and estimating repair costs. (All components not listed in this table are assumed to be rugged, i.e. not damageable.) This organization is taken directly from Mitrani-Reiser's work, except that an additional fragility function has been defined for damage to beam-column joints in the frame structure. Joints are much more likely to be damaged in non-ductile RC frame structures than the code-conforming special moment frames examined by Mitrani-Reiser (Goulet et al. 2007; Mitrani-Reiser 2007). Note that in practice, the EDPs and table of damageable assemblies are

tabulated at each story of building, to account for differing levels of demand and damage at each story.

Table 6.1 Fragility functions used for prediction of damage and losses in RC frame structures, modified from Mitrani-Reiser (2007).

Type of Damageable Component	Relevant EDP	Damage States	Fragility Function	Repair or Replacement Costs[1]
reinforced concrete beams and columns[2]	damage deformation index (DDI) of Park-Ang damage index	* light * moderate * severe * collapse	Beck et al. (2002)	Repair costs by professional cost estimator [Beck et al. (2002)]
column-slab connections (perimeter frames only)	interstory drift ratio (IDR)	* light cracking * severe cracking * punching shear failure	Aslani (2005)	Repair costs by professional cost estimator [Beck et al. (2002)]
beam-column joints	interstory drift ratio (IDR)	* cracking * spalling * crushing * failure (rebar damage)	Pagni and Lowes (2006)	Repair costs estimated by Pagni (2003)
drywall partition and finish	interstory drift ratio (IDR)	* visible damage * significant damage	Porter (2000)	Repair costs by professional cost estimator [Beck et al. (2002)]
exterior glazing	interstory drift ratio (IDR)	* cracking * fallout	Porter (2000)	Cannot be repaired and component must be replaced.
automatic sprinklers	peak floor acceleration (PFA)	* fracture	Porter (2000)	Cannot be repaired and component must be replaced.
hydraulic elevators	peak ground acceleration (PGA)	* failure	Porter (2007)	Cannot be repaired and component must be replaced.
acoustical ceiling tiles	peak floor acceleration (PFA)	* collapse	Porter (2000)	Cannot be repaired and component must be replaced.

[1]Adjusted such that they are given in terms of 2006 $.

[2]It is assumed that columns fail in flexure-shear. To avoid double counting of repair costs, all damage to columns is given in terms of the Park-Ang damage index.

6.2.4 Economic Losses in Non-Ductile Reinforced Concrete Frame Structures

Using the MDLA toolbox, economic losses are predicted for each of the archetypical non-ductile RC moment frames described in Chapter 5. These archetypical structures include RC moment frames of different heights (2, 4, 8 and 12 stories) and with different framing systems (space and perimeter frame systems) and with other variations in design and detailing. The design, modeling and structural analysis results for these structures, as presented in Chapter 5, are used as in input to the loss estimation process. Nonstructural architectural details and building replacement costs are described below. Together with the library of fragility functions in the loss estimation toolbox, these provide the needed input to evaluate earthquake-induced losses.

Structural Analysis Results

Structural analysis results for the 2, 4, 8 and 12-story archetypical existing non-ductile RC frame structures are taken from the incremental dynamic analysis results in Chapter 5. As before, sidesway collapse results are adjusted to account for appropriate spectral shape and modeling uncertainty. The non-collapse engineering demand parameters are also

obtained from the IDA results, as shown in Figure 6.1 for the 4-story non-ductile RC space frame (Design ID 3004).[1,2]

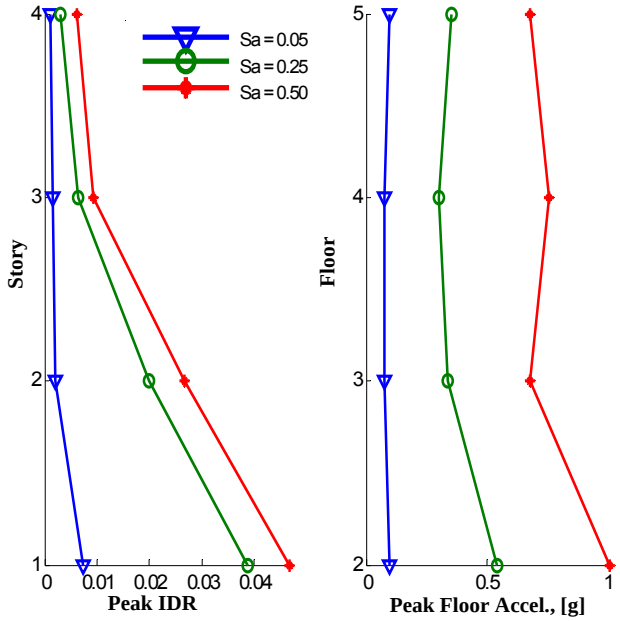

Figure 6.1 Selected engineering demand parameters from non-collapsed records for 4-story non-ductile space frame at specified intensity levels, Sa(T_1 = 1.98sec), obtained from incremental dynamic analysis for use in loss analysis.

Architectural Layouts

The structural designs for the archetypical 1967-era RC frame office buildings were described in Chapter 5. Architectural designs for the 8- and 12-story structures (125 ft. x 125 ft.) are illustrated in Figure 6.2. It is assumed that the ground level of office buildings is primarily composed of assembly areas, such as conference rooms and a cafeteria. The layout of the ground floor in Figure 6.2a is also based on egress and service requirements and observations of typical configurations and sizes of common spaces and conference rooms. The upper floors are designed with both fully-enclosed offices and open office space, where offices are separated by removable partitions. The architectural layout in Figure 6.2b has 36% open office space, which is assumed to be typical for office buildings in California. The 2- and 4-story buildings are larger in plan, 125 ft. x 175 ft., and are not shown here, but are

[1] Note that the interstory drift ratios and peak floor accelerations in the loss analysis are not adjusted for spectral shape or modeling uncertainties. Both spectral shape and modeling uncertainties have a much smaller effect on structural response at lower intensity levels, like those that are important for loss prediction, so this is not expected to have a significant effect on the final results. See Baker (2005), Porter et al. (2002) and Chapter 4.

[2] The collapse losses include those from sidesway collapse only. Possible localized collapse due to column shear failure, discussed in more detail in Chapter 5, is accounted for in the non-collapse losses.

assumed to be similar in terms of percentage of open office space to total floor area, the ratio of non-removable partition to the total floor area and the ratio of removable partition length to the total floor area.

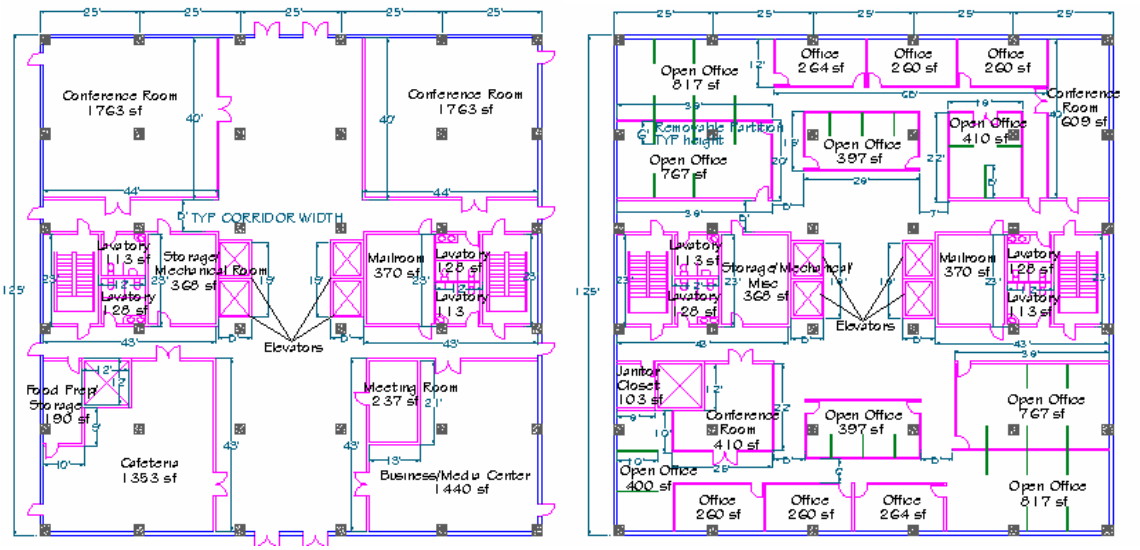

Figure 6.2 Architectural floor plans developed for typical highrise office building for (a) ground floor and (b) typical office floor.

The architectural designs are used to populate tables of damageable assemblies needed for loss analysis, identifying the square footage of drywall partitions and interior surfaces that may need to be painted after an earthquake. The number of exterior glazing units, square footage of acoustical ceiling, number of elevators and length of piping/sprinklers are also tallied. The number of columns, beams, joints and slab-column connections are available from the structural designs. These quantities are tabulated at each floor or story of the building.

Building Replacement Costs

When ground-shaking causes very significant damage or collapse, the structure will need to be replaced. For cost-estimation purposes it is assumed that if a non-ductile concrete frame structure needs to be replaced, it will be replaced with a comparable modern code-conforming RC office building. Replacement costs for 2, 4, 8 and 12-story concrete frame structures were estimated using RS Means Building Construction Costs (Waier 2005), as reported in Table 6.2. These estimates account for construction of all significant structural and nonstructural components, including HVAC systems, partitions and interior finishes, exterior enclosures, services, and basements (for the 8 and 12-story buildings). The new

structures are assumed to have typical level of finishes, including nylon carpet, ceramic tiles and hollow oak doors. The estimates also include a 25% contractor fee. For the 4-story RC perimeter frame structure, these costs breakdown as follows: 26% for the structure, including superstructure and substructure, 19% for exterior enclosures, 24% for interior and finishes, 14% for HVAC, 10% for electrical systems and 6% for other. All values are 2006 dollars, and are factored to account for the cost of construction in Los Angeles, California. Anecdotal evidence from project and property managers suggests that these RS Means-based replacements costs are at least 25% lower than the actual cost of construction, and may underestimate total project costs (e.g. including permits, financing and administrative costs) by as much as $200 per square foot (Reis 2008). It is therefore expected that the replacement costs obtained here provide a lower bound on the true cost of replacement. Since most of the loss results are normalized by the replacement cost, the underestimation of repair costs will not bias the results, provided that the RS Mean values are used to estimate both the cost of needed repairs and replacement values. The absolute value of the losses, however, will reflect the lower bound estimates on repair and replacement costs.

Table 6.2 Estimated replacement costs for 2, 4, 8 and 12-story RC frame office buildings.

Num. of Stories	Framing System	Total Cost ($, millions)	Cost per sq. foot ($)
2	space	6.1	140.4
	perimeter	6.5	150.7
4	space	12.5	144.4
	perimeter	12.0	138.3
8	space	19.9	172.7
	perimeter	19.4	168.4
12	space	29.1	168.4
	perimeter	28.1	162.6

Estimated Economic Losses

The predicted economic losses for the 4-story non-ductile RC space frame structure (Design ID 3004) are shown in Figure 6.3 and Figure 6.4. It is an office building with a floor plan measuring 125 ft. x 175 ft. and an estimated replacement cost of $12.5 million. Results of nonlinear time history analysis were discussed in detail in Chapter 5, where it was observed that the structure is likely to collapse in a multistory sidesway mechanism in the first and second stories, with significant damage to columns and joints and only limited hinging in the beams. Selected dynamic analysis results are repeated in Figure 6.1.

The damage in selected components of the structure, as predicted from the fragility functions in the loss analysis tool box, is illustrated in Figure 6.4. Note that because this structure has fairly weak columns, the beams are not damaged in the ground shaking, particularly at upper stories, but the columns and partitions sustain severe damage, even at relatively small shaking intensities. Although not shown in Figure 6.4, the 1st floor beam-column joints also experience significant damage. This damage assessment is used to estimate the repairs needed in the structure.

Figure 6.3 illustrates how the mean repair costs for this structure vary as a function of the ground motion intensity, calculated as shown in Equation (6.1). These repair costs are presented in both absolute terms ($ millions) and relative to the cost of the replacing the structure. The losses are disaggregated to account for the relative contribution of collapse and non-collapse losses. For small ground motion intensities, referring again to Figure 6.3, non-collapse losses dominate the losses. These non-collapse losses are due to damage in structural elements, partitions, paint and glazing that can be repaired or replaced at the component or story level. As the spectral intensity of the ground motion increases, collapse losses, or those associated with replacing the structure if it collapses in sidesway, dominate the predicted repair costs.

Non-collapse losses can be disaggregated to determine what structural and non-structural components contribute most to the losses. The partitions are damaged even at small spectral acceleration levels. As the ground motion intensity increases, the cost of repairing and painting partitions saturates at the ground motion intensity at which all partitions need to be repaired, and the damage to structural components becomes more important, especially in the columns and beam-to-column joints.

When the mean repair cost curve is integrated with the hazard curve for the site of interest, which accounts for the likelihood of experiencing an earthquake ground motion of the specified intensity, the expected annual losses (EAL) are computed. Again, it is assumed that the building is located at the selected location in Los Angeles, for which the hazard curve has been obtained through probabilistic seismic hazard analysis (Goulet et al. 2007). The EAL is the amount the owner would expect to lose yearly due to earthquake repairs on average. For this 4-story non-ductile RC frame structure the EAL is estimated at $290,000 or 2.29% of the replacement cost of the structure. Over 50 years, the present value of the total expected loss can be computed from the following equation,

$$\text{Present value (50 years)} = \sum_{t=1}^{50} \frac{EAL}{(1+r)^t}. \qquad (6.4)\,[3]$$

For the 4-story non-ductile RC space frame, assuming a discount rate (r) of 3%, the present value of losses over the next t = 50 years is equal to 59% of the value of the structure. An alternative measure of economic loss is the mean repair cost expected when an earthquake of specified intensity occurs. The intensity used here is the design spectral acceleration level, which has roughly a 10% chance of occurring over 50 years.[4] The loss caused by this event is roughly 65% of the value of the structure. These results would be different at other sites, where the hazard curve is dominated by different faults and levels of seismicity, but the metrics reported here are representative of a high seismic, far-field California site.

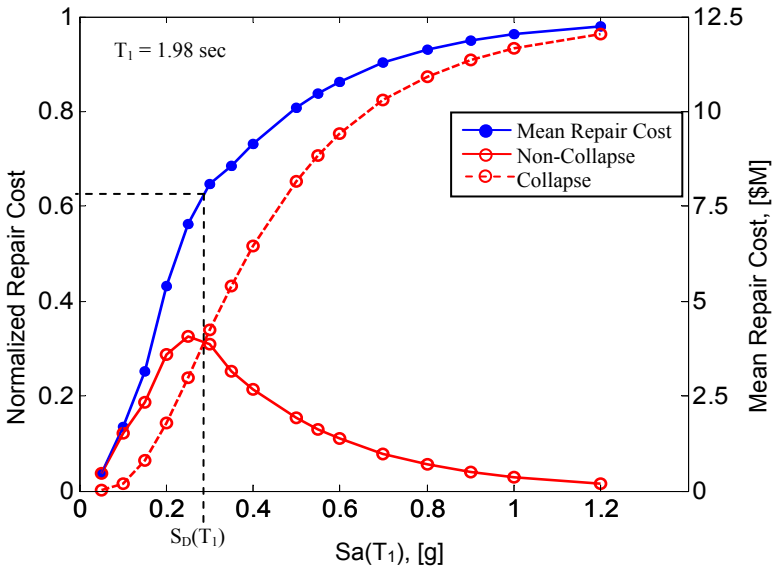

Figure 6.3 Mean repair costs for a 4-story non-ductile RC space frame structure as a function of the ground motion intensity.

The loss estimation process is repeated for each of the other archetypical non-ductile RC frame structures. As shown in Table 6.3 and Figure 6.5, the expected annual losses (EAL) predicted for these archetypical existing non-ductile RC frame buildings varies between 1.2% and 5.2%, with an average of approximately 2%. In economic terms, the best buildings are the 12-story space frame structures and the worst, discussed later, is the 2-story space frame.

[3] Calculations of losses over 50 years in terms of present value assume a discount rate of 3%, assuming real earned interest of 5% and rate of inflation of 2%.

[4] The design of new buildings is based on this spectral acceleration value; the 1967 UBC obtained the design base shear coefficient differently, but the design spectral acceleration, S_D, still provides a useful measure of the hazard at the site.

Looking again at Figure 6.5, the estimated EALs decrease with increasing structural height; reasons for this trend are discussed below. Since the EAL is the amount a building owner would lose annually, if the expected seismic losses were averaged over the lifetime of the structure, it can be interpreted as the amount it would make sense to invest yearly, either in retrofitting the structure to improve seismic performance or in earthquake insurance. These losses are dependent on the level of seismicity where the building is located, such that in near field regions the predicted losses would likely be higher and, elsewhere in California, where ground motions tend to have less energy, monetary losses would be significantly lower.

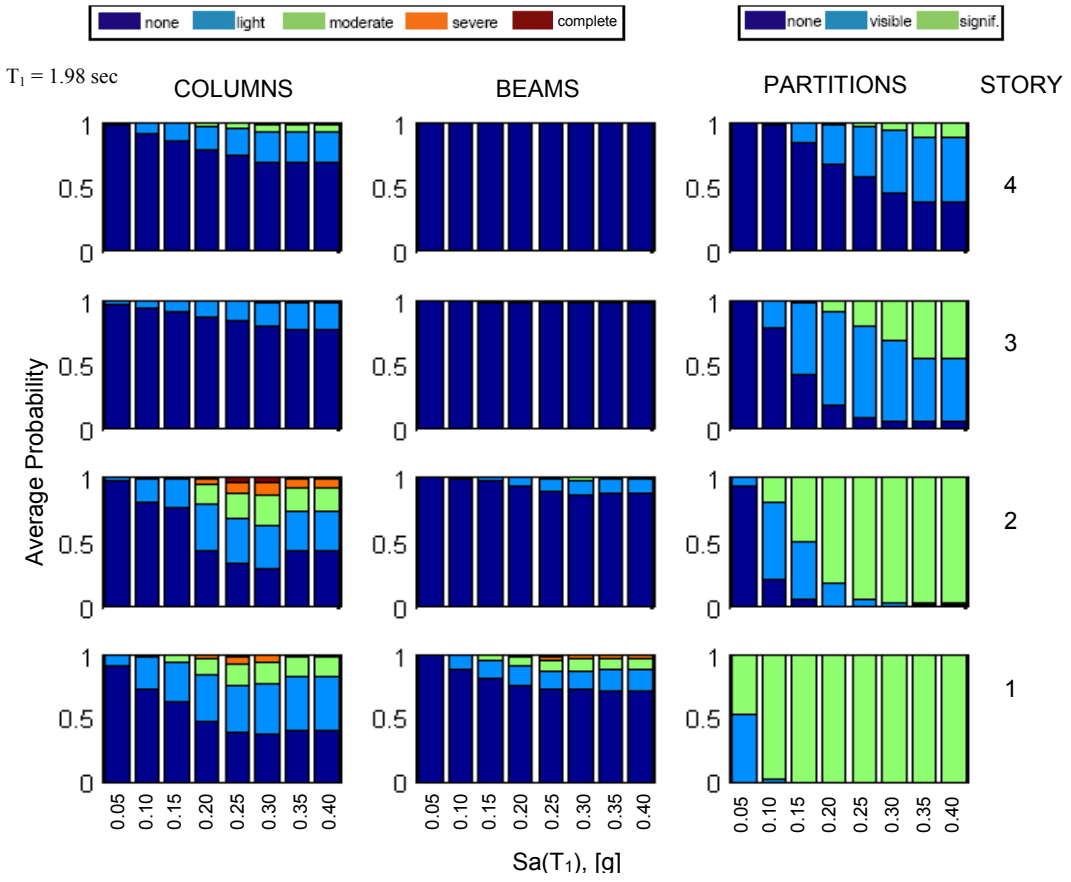

Figure 6.4 Damage to columns, beams and partitions in 4-story non-ductile RC frame structure as intensity measure increases (non-collapsed records only).

The predicted losses caused by the design level earthquake are reported in Table 6.3 and Figure 6.6. Again, the results are normalized by the replacement cost of the structure. For this scenario earthquake, the average expected loss is 59% of the building value, with the best performing building losing 44% of its value and the worst performing building losing 83% of its value.

The average EAL of 2.0% corresponds to a loss of approximately 50% of the value of the structure over 50 years (in present value). Reported in Table 6.3, this metric accounts for predicted earthquake losses to the structure over the next 50 years. As such, it can be interpreted as the amount a risk-neutral owner would be willing to invest in seismic improvements today, in order to mitigate economic losses over the next 50 years. If these structures cost approximately $160 per square foot to construct (Table 6.2), given the predicted economic losses at the location of interest, an owner would be willing to pay approximately $80 per square foot if earthquake-induced losses in the next 50 years could be prevented. These computations are highly sensitive to the assumed 3% discount rate, which depends on real interest rates and inflation. Values between 2 and 7% are frequently used for public safety projects (Rackwitz 2004). If a lower discount rate were used, the present value of losses would increase, such that it would make sense for owners to invest more now in securing their property against future seismic damage.

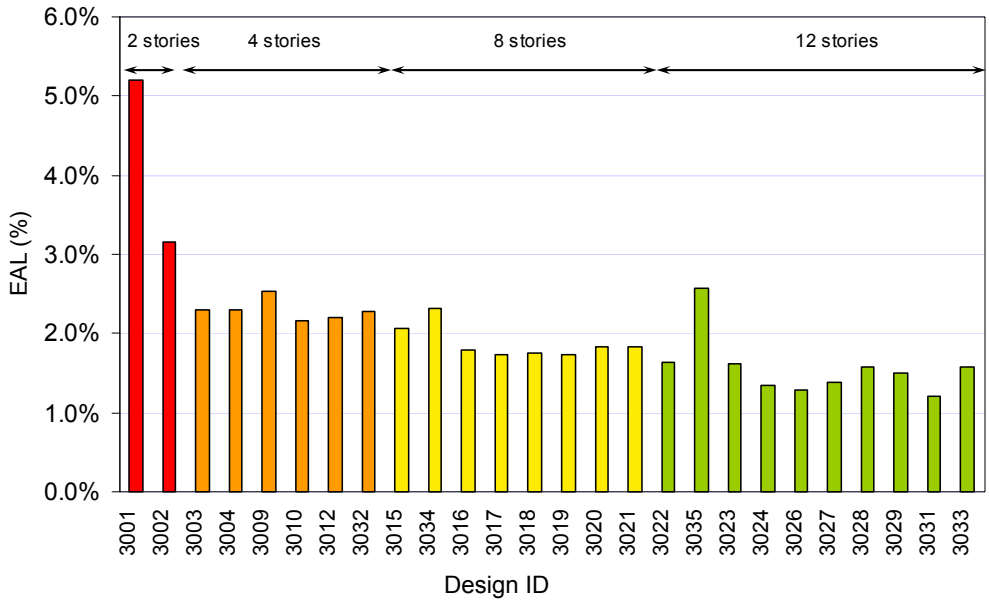

Figure 6.5 Expected annual losses in archetypical existing non-ductile RC frame structures.

Table 6.3 Predicted earthquake-induced economic losses in archetypical existing non-ductile RC frame structures.

Design ID	Num. of Stories	Design Variant	Framing System	EAL (%)	Loss, given S_D (%)	PV of Losses over 50 years (%)[1]
3001	2	A	Space	5.2	83	134
3002		A	Perimeter	3.2	75	81
3003	4	A	Perimeter	2.3	62	59
3004		A	Space	2.3	65	59
3009		F1		2.5	72	65
3010		F2		2.2	61	56
3012		H		2.2	63	57
3032		I		2.3	68	59
3015	8	A	Perimeter	2.1	63	53
3034		J		2.3	63	60
3016		A	Space	1.8	57	46
3017		B		1.7	56	45
3018		D (65%)		1.8	56	45
3019		D (80%)		1.7	56	45
3020		F1		1.8	59	47
3021		F2		1.8	58	47
3022	12	A	Perimeter	1.6	62	42
3035		J		2.6	71	66
3023		A	Space	1.6	54	42
3024		B		1.3	47	34
3026		D (65%)		1.3	44	33
3027		D (80%)		1.4	47	36
3028		F1		1.6	57	40
3029		F2		1.5	49	39
3031		H		1.2	45	31
3033		I		1.6	50	41
			Average	2.0	59	52

[1] Assuming an annual discount rate of 3%.

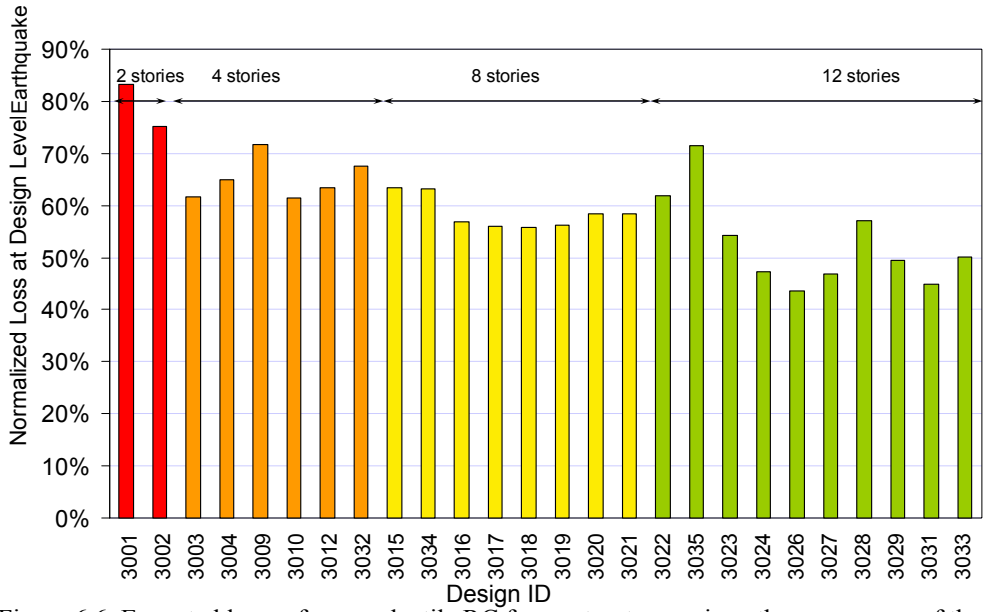

Figure 6.6 Expected losses for non-ductile RC frame structures, given the occurrence of the design level earthquake.

As illustrated in Figure 6.5 and Figure 6.6, the expected losses vary significantly among the archetypical buildings according the structure's height, framing system and other variations in the design. When losses are normalized as a percentage of the total repair cost of the structure, the predicted losses tend to decrease as the height of the structure increases, as shown in Figure 6.7, though, in absolute terms, the taller buildings have higher losses because they are costlier to replace. The reduction in losses as building height increases is largely a function of damage concentration observed in nonlinear analysis. Whereas a 4-story building may incur significant damage in 1 or 2 stories (25 to 50% of the building) the damage in a 12-story building concentrates in the bottom 2 or 3 stories (16 to 25% of the building). Reasons for this concentration of damage as discussed in more detail in Chapter 5. The lower stories subjected to large deformations incur significant economic losses, whereas upper stories tend to see much lower levels of damage and losses. Losses do not follow the same pattern as collapse results (illustrated in Figure 5.13, for example); collapse risk tended to increase with height for perimeter frame structures. This difference illustrates the importance of considering performance metrics related to collapse, losses and fatalities in making retrofit decisions. In addition, the trend with height exposes a potential deficiency of component-by-component loss estimation metrics as it neglects losses associated with system damage effects such as residual drift that could contribute significantly to losses, especially for taller buildings (Ramirez 2008).

In general, tall perimeter frame structures are predicted to incur slightly higher losses than tall space frame structures at the same level of ground motion intensity (see Figure 6.8). Due to their flexibility, the 8- and 12-story perimeter frames tend to undergo higher deformations and collapse earlier than the stiffer and more redundant space frame systems leading to an increase in the estimated losses. This effect dominates the estimated losses in perimeter frames at high levels of ground motion intensity. However, since the perimeter frames typically concentrate damage in a smaller number of stories, differences in losses at small shaking intensities are less significant. As a result, there is not a substantial difference in predicted EALs for space and perimeter frame structures. The differences in performance between space and perimeter frames are not as apparent for the 2- and 4- story structures. Shorter non-ductile perimeter and space frame structures have very similar fundamental periods, such that they are subjected to comparable levels of deformation. However, it is noted that differences between the space and perimeter frame system are overestimated

because of the absence of the gravity frame in the structural analysis model (see discussion in Chapters 3 and 5). If the gravity frames were included the predicted economic losses in perimeter frames are expected to decrease. Goulet et al. (2007) found that excluding the gravity frame from the analysis model increased expected annual losses in a modern RC special moment frame by 12%, and the difference may be even greater for the relatively flexible RC frames considered in this study.

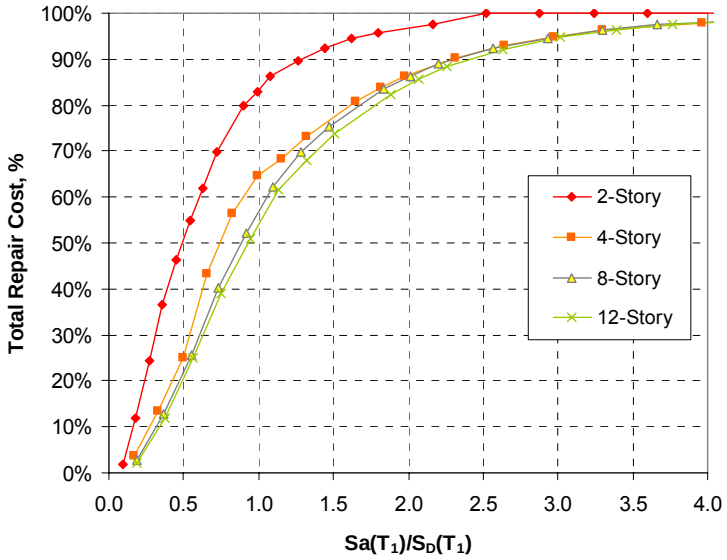

Figure 6.7 Predicted repair costs as a function of ground motion intensity (normalized) for non-ductile RC space frames of different heights. $S_D(T_1)$ is the design level earthquake. Needed repairs at very low levels of ground motion intensity are due to damage levels in partitions predicted by Porter (2000).

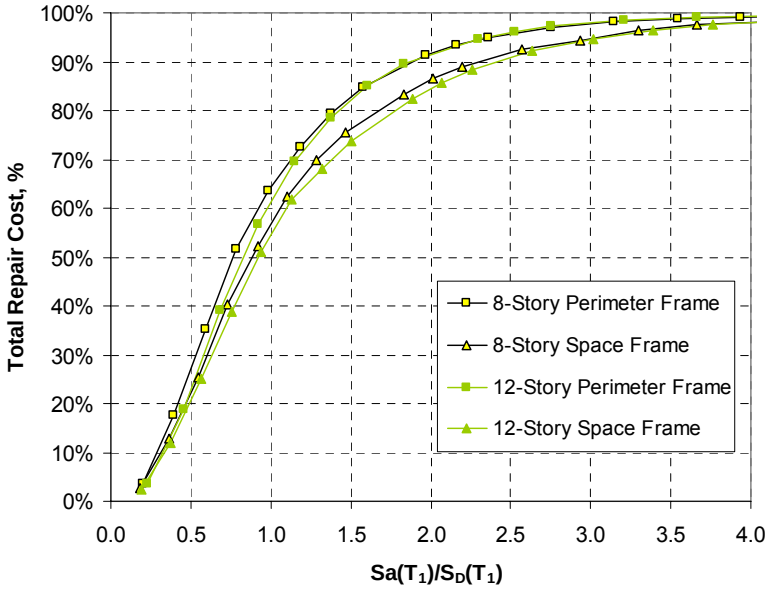

Figure 6.8 Predictions of economic losses in archetypical non-ductile RC frames, illustrating differences between space and perimeter frame systems.

The set of archetypical non-ductile RC frame structures included structures that differed in height and framing system, as discussed previously, and in other aspects of design and detailing. Figure 6.9a illustrates the effects of design decisions affecting the relative strength of beams and columns for 4-story space frame structures, where design variant A is the baseline design and design variants F1 and F2 have overdesigned beams and columns, respectively. At the design spectral intensity Sa = $S_D(T_1)$, the estimated repair costs for design variant A is 65% of the replacement cost of the structure. For design variant F1 the losses are higher, approximately 72% of the replacement cost, and F2 has smaller losses, approximately 60%. Increased strength in beams (variant F1) causes the predicted economic losses to increase as it forces damage into the columns and other non-structural components sensitive to interstory drift. Recall from Chapter 5 that F1 also exhibited a higher likelihood of collapse. Note that all the structures shown in Figure 6.9a have comparable EALs, since the biggest differences in estimated losses occur under large, infrequent ground motions. The effect of design variants B and D for 12-story space frames are illustrated in Figure 6.9b. Both B and D tend to decrease the predicted losses, as damage concentrates in a smaller number of stories. B has columns and beams of constant strength and stiffness over the height of the buildings such that the upper stories are overdesigned, limiting losses at the top of the building. Likewise, the weak stories in D cause damage and losses to concentrate in that portion of the structure. 8-story design variants B and D followed a similar pattern. B and D are likely to be more susceptible to building closure due to residual drifts, which is not currently included in the loss estimation methodology.

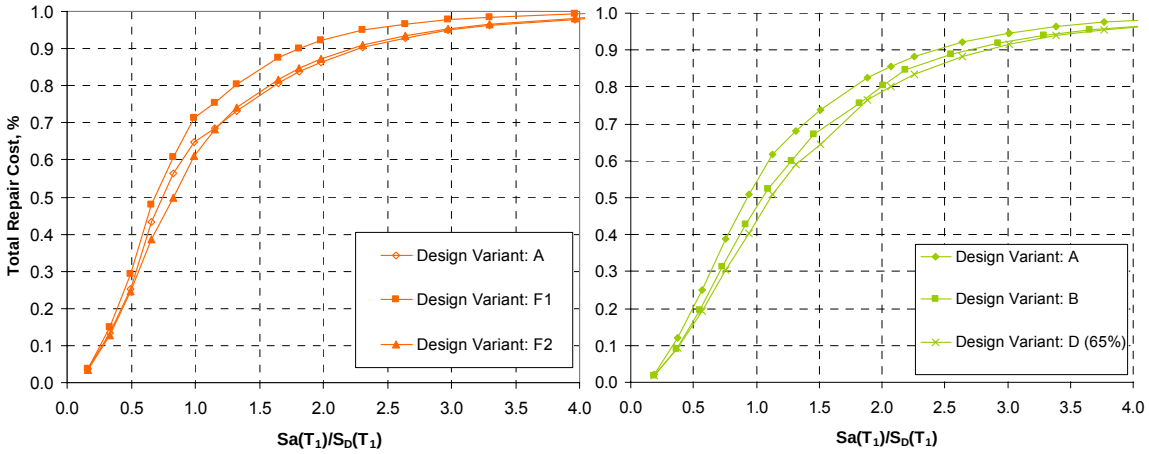

Figure 6.9 Predicted losses in different design variants of (a) 4-story and (b) 12-story non-ductile space frames. A is the baseline archetype design. F1 and F2 have overdesigned beams and columns, respectively. B has constant strength and stiffness over the height of the structure. D is weak in the bottom stories.

Design ID 3001 is a 2-story space frame with expected annual losses of 5.2%, by far the largest of the archetype structures under consideration (see Table 6.3). This structure has below average (but not the worst) collapse performance, with a collapse margin ratio of 0.6. The high estimated losses for this structure are the result of a couple of factors. First, as noted previously, percentage losses tend to be higher in shorter structures because deformations cause damage to a larger portion of the structure. The 2-story structure always fails in a 1st-story mechanism, causing severe damage and losses in at least 50% of the building. In addition, this 2-story space frame has the lowest ratio of column to beam strength of the set of archetype 1967-era structures, due to the dominance of gravity loading in beam design. Since the beams are significantly overdesigned with respect to lateral loads, especially when T-beam effects and slab steel are accounted for in determining their actual strength, this structure has particularly poor performance.

Data comparing collapse rates in non-ductile RC frames and expected annual losses are illustrated in Figure 6.10. Structures that are more likely to collapse also tend to have higher economic losses. However, the expected annual losses are highly dependent on damage and losses that occur in relatively small earthquakes, whereas the collapse rate depends only on what happens in large enough earthquakes to cause collapse of the structure. The variability in Figure 6.10 emphasizes the importance of considering a variety of different performance metrics in evaluating the seismic performance of a structure.

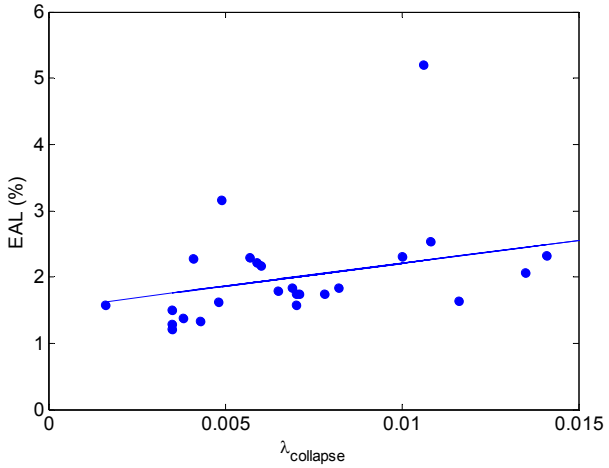

Figure 6.10 Relationship between expected annual losses (EAL) and mean annual frequency of collapse ($\lambda_{collapse}$) in non-ductile RC frames. $\lambda_{collapse}$ includes sidesway collapse modes only.

Comparison to Van Nuys Testbed

These predicted losses show reasonable agreement with loss studies of a non-ductile concrete hotel structure conducted in conjunction with the PEER's Van Nuys testbed study (Krawinkler 2005; Miranda et al. 2006). The Van Nuys hotel structure was originally constructed in 1966 and is located in the San Fernando Valley region of the Los Angeles metropolitan area. The hotel's structural system consists of 7-story RC frames on the perimeter, with an interior, gravity flat slab floor system. The design and detailing of the Van Nuys hotel are very similar to the archetypical non-ductile RC frame structures considered in this study (see Table 2.2). Compared to the generic Los Angeles site used in this study, the Van Nuys site has comparable, but slightly higher, levels of seismicity (Krawinkler 2005).

The Van Nuys hotel testbed study used a performance-based methodology for loss estimation like the one followed here, though the specific component damage states, fragility functions and repair costs were defined independently. Engineering demand parameters were predicted from a two-dimensional fiber element model, with additional inelastic hinges and shear springs in beams and columns, but neglecting P-Δ effects (Krawinkler 2005). The analysis model was validated through comparison with data from strong motion instrumentation and damage experienced during the 1994 Northridge Earthquake. To compute losses, the study considered damage and repair costs for both structural and non-structural components, including beams, columns, slab-column connections, beam-column connections, windows, and acoustical ceilings. To account for non-structural components for which fragility data was unavailable, the authors utilized generic fragility curves for drift and acceleration sensitive components. Only direct economic losses were considered.

In total, the expected annual losses predicted for the Van Nuys hotel building were $198,000 (in 2002 dollars) or 2.2% of the replacement cost of the structure (estimated in the report as $9 million). In this study, we predict expected annual losses of 2.1% of the replacement cost of the structure are predicted for an 8-story perimeter frame structure, and approximately 1.8% annually for the 8-story space frame structures. Despite differences in assumptions regarding damage and repair costs, the final results are notably consistent.

6.2.5 Comparison of Economic Losses in Non-Ductile and Ductile Reinforced Concrete Frame Structures

Economic losses in existing (non-ductile) and modern (ductile) RC frame structures are compared in Table 6.4 and Figure 6.11. The modern RC frame structures are designed according to the 2003 IBC with structural analyses conducted by Haselton (2006). The code-conforming RC frames have expected annual losses between 0.8% and 1.3% of the replacement cost of the structure. When only the baseline designs are considered, i.e. the 2, 4, 8 and 12-story space and perimeter frames of design variant A, the 1967 frames have more than twice the expected annual losses of the 2003 frames, with an average (median) EAL of 2.2% compared to 1.0% for the modern, code-conforming structures. Likewise, when the design level ground motion (S_D) occurs it is expected that the 63% of the value of the 1967 frame structures will be lost, compared to only 32% of the value of the 2003 frame structures on average – losses in the non-ductile structures are approximately double.

Reduced economic losses associated with improved seismic design and detailing, such as those shown in Table 6.4, can provide an important incentive to encourage building owners to retrofit or replace potentially dangerous structures, such as the 1967-era non-ductile RC frames. These financial savings are in addition to other benefits to retrofitting or replacing vulnerable structures, such as improved collapse performance (discussed in Chapter 5) and reduced life safety hazard (the topic of Section 6.3). The cost effectiveness of upgrade and rehabilitation measures, considering the impact on both earthquake fatalities and economic losses, and the cost of seismic retrofit are the focus of Chapter 7.

Table 6.4 Estimated seismic-induced losses in modern (2003) and existing (1967) RC frame structures. All values are reported as a percentage of building replacement costs.

Num. of Stories	Framing System	EAL (%)	Losses given S_D (%)	PV of Losses over 50 years (%)	EAL (%)	Losses given S_D (%)	PV of Losses over 50 years (%)
2	Perimeter	3.2%	75%	81%	1.0%	35%	25%
	Space	5.2%	83%	134%	1.0%	49%	27%
4	Perimeter	2.3%	62%	59%	1.2%	30%	30%
	Space	2.3%	65%	59%	1.1%	32%	34%
8	Perimeter	2.1%	63%	53%	1.0%	25%	26%
	Space	1.8%	57%	46%	1.3%	32%	32%
12	Perimeter	1.6%	62%	42%	0.8%	22%	20%
	Space	1.6%	54%	42%	1.1%	30%	27%

Key: 1967 RC Frames; 2003 RC Frames

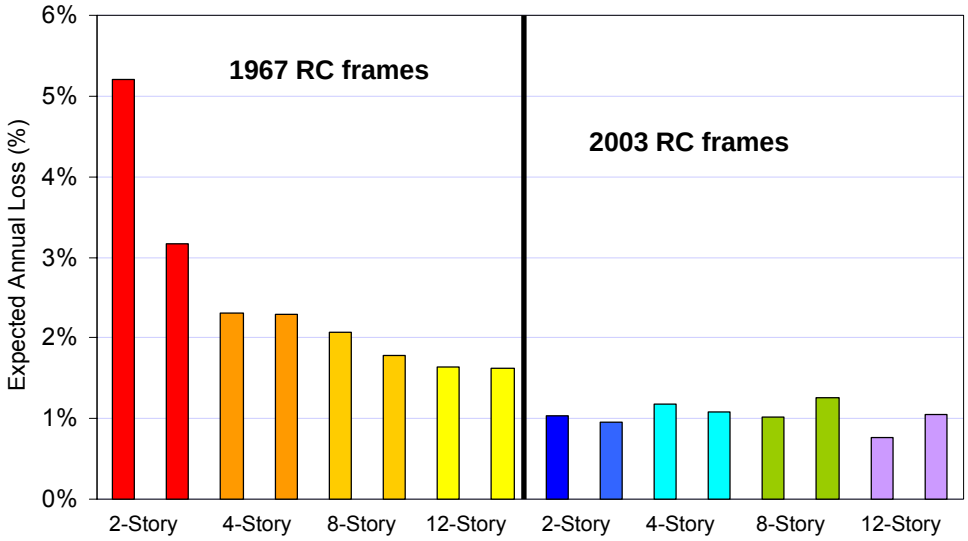

Figure 6.11 Comparison of expected annual losses as a percentage of building replacement cost for code-conforming and older RC frame structures in California.

6.2.6 Summary and Future Research Needs

Earthquake-induced losses in RC frame office buildings are predicted using the framework of performance-based earthquake engineering to quantify potential losses and identify design characteristics that may affect them. Expected annual losses in non-ductile RC frame structures are predicted to be on the order of 2.2% of the replacement cost of the structure. Over the lifetime of the structure, the owner of a modern ductile structure is likely to incur significantly smaller losses (expected annual losses are approximately halved) than the owner of a comparable older RC frame structure. The factor of two difference between seismic losses in older and modern RC frame structures is significant, but smaller than the factor of 40 times in the collapse rate predictions. Evaluation of economic losses in new structures is useful for owners and design engineers interested in comparing the seismic performance several possible design alternatives. In older structures, estimations of economic losses are useful for owners evaluating earthquake insurance options, wishing to self-insure against future earthquake losses or considering retrofit or seismic strengthening.

The results presented here are accurate, given the underlying assumptions about building components and repair costs. It has been noted that the predictions of economic losses obtained here are higher than might be expected, given scattered evidence about earthquake damage and losses in past California earthquakes (Kircher 2007). More work is needed to formally compare loss data to California experience to qualify and improve the methods and

data in this study. Even so, all the loss results generated are based on the same underlying data and relative predictions of different types of RC frame structures provides useful data for making design, retrofit or policy decisions.

Estimations of economic losses will require refinement as improved fragility functions and repair costs become available. In the future, estimates of repair and replacement costs may be improved through a survey of professional cost estimators. In addition, more research is needed so that indirect losses, such as downtime, can be more expediently incorporated in the loss predictions. Other researchers have shown that building downtime may be the dominant contributor earthquake losses; evidence from Mitrani-Reiser (2007), for example, suggests that downtime increases expected annual losses by 30% for code-conforming RC moment frame structures.

6.3 Fatalities

6.3.1 Overview

Seismic provisions in building codes exist primarily to protect the life safety of building occupants. In the previous chapter, collapse capacity was evaluated as a proxy for measuring life safety of RC frame structures, based on the simple observation that structures that are more likely to collapse are more likely to endanger their inhabitants. Collapse performance assessment alone, however, is incomplete to predict the threat these structures pose to life safety in future earthquakes. Even if a structure collapses, it is unlikely that all the occupants will be killed, and the number killed will depend on the type of construction, the time of day, the response time of emergency crews, the severity of the earthquake, and a variety of other factors. Wood-frame residential structures and RC office buildings may have comparable collapse rates, for example, but their fatality rates are likely to be very different. To identify the most dangerous buildings, then, it is useful to directly estimate fatalities. Fatality prediction can also provide public health officials with much needed data for planning for health care and emergency response following a major earthquake (Durkin and Thiel 1992; Aleskerov et al. 2005; Shoaf et al. 2006).

The objective of this study is to predict the number of fatalities that are likely to occur in a given building, based on the structural behavior predicted by dynamic collapse analyses. The methodology developed herein is used to predict the number of fatalities that may occur in the archetype non-ductile RC frame structures when subjected to severe ground-shaking.

Fatalities are estimated building-by-building, quantifying the threat to life safety posed by each structure, such that relative differences in fatalities among the archetype non-ductile structures can be identified, and the predicted fatalities of that group of structures can be compared to safer modern RC frame structures. In this sense, the approach is different from other studies that have attempted to predict the number of fatalities in an urban area in future earthquake scenarios. This study utilizes the detailed structural models and analysis results of individual buildings from Chapter 5.

6.3.2 Literature Review

Previous studies on casualties in earthquakes have been conducted by historians, epidemiologists, statisticians and engineers, and differ widely in methods and approach. When taken together, the existing literature on earthquake fatalities identifies many factors that affect the number of fatalities that may occur in future earthquakes, including building design and construction quality, cultural and behavior aspects, and the quality and availability of emergency response and medical care. Some of these studies are described briefly here.

Several researchers have conducted historical studies that use descriptive and predictive methods to identify those people, urban areas and/or countries that are most at risk in future earthquake events. Alexander (1996) collected data on all earthquake deaths that occurred globally in the 30-month period between September 1993 and February 1996, finding that most of the fatalities and injuries were associated with a small number of large earthquakes. The study also observed that casualties were often the result of a relatively small number of catastrophic structural collapses, and that behavioral factors, such as whether a person exits the building during the quake have a large effect on survivability. Based on data from historic deadly earthquakes, Nichols and Beavers (2003) created an earthquake fatality function to predict future earthquake fatalities in urban areas, as a function of the earthquake intensity and characteristics of the urban area. Gutierrez et al. (2005) related earthquake fatalities and injuries world-wide to demographic and physical data and found economic well-being (measured in terms of GDP) and population density to be important predictors of the number of earthquake casualties. The USGS has recently developed an analytical method for predicting casualties for use by USAID and other end-users involved in relief and aid deployment (Porter et al. 2007).

Other researchers have sought to identify those factors that may affect an individual's risk of dying as the result of ground-shaking during a given earthquake event. These studies are descriptive in that they explain trends in data from a single earthquake to identify vulnerable groups of people. The methods used to obtain data on earthquake casualties vary, and may include data from coroners and hospital admissions, questionnaires and photographic surveys. Several of these studies are summarized in Table 6.5. The intensity of the ground-shaking at the victim's location, and building structural characteristics, including type, age of construction and structural damage, significantly affect the victim's earthquake risk. Behavioral characteristics, such as what the victim did to respond to the earthquake, and socio-cultural factors, such as age, gender and income of victim, also matter. Most of the explanatory variables identified as having an important impact on fatality risk were reported by several researchers. A smaller number of these studies are also used to develop data for predictive purposes. The Turkey survey conducted by Shoaf et al. (2005) provides much-needed data on fatality rates in RC frames as tabulated in Table 6.6.

In addition to the descriptive studies in Table 6.5, there has also been research to directly predict fatalities in future earthquakes. Most of these studies try to anticipate the level of structural damage in future earthquakes, and use the expected level of structural damage to predict the number casualties that are likely to occur. These predictions may either be building-specific, i.e. the expected number of fatalities that are likely to occur in a single building, or for an earthquake scenario, i.e. the number of fatalities in the entire earthquake-affected area. The design of the building of interest or the typical design and construction characteristics of the geographic area of interest, which are indicators of the type and extent of structural damage that are likely to occur, are important inputs to the casualty prediction framework.

The first systematic effort to estimate casualties in future earthquakes focused on the San Francisco bay region (NOAA 1972). This study aimed to provide usable data to earthquake planning officials and state and local governments regarding expected earthquake losses and fatalities. Using data from a combination of relevant earthquakes, theoretical considerations and expert judgment, the study estimated the at-risk population in the San Francisco bay area, inventoried residential, commercial and industrial structures, and predicted the casualties based on simplistic fragility functions. During a magnitude 8.3 earthquake on the San Andreas fault, a predicted death rate of 50 out of 100,000 people was proposed. The number

of severely injured was expected to be four times higher. A 1985 study by the Applied Technology Council (ATC-13) refined the casualty prediction procedure used in the NOAA report (ATC 1985). ATC-13 explicitly predicts the fraction of building occupants that are dead and/injured as a function of a building damage state. For example, in a RC structure that has sustained major damage, 1% of the building occupants at the time of the earthquake are expected to die. 20% of the occupants are predicted to die in a building that has been destroyed. All buildings have the same death rate except wood frame and light steel construction, which are assumed to be less deadly. It is assumed that the number of serious injuries is four times the number of deaths, and that the number of minor injuries is 30 times the number of deaths. ATC-13 casualty prediction methods are summarized in Table 6.6.

Building on the approach developed in the NOAA and ATC reports, the Federal Emergency Management Agency's HAZUS software implemented earthquake fatality prediction capabilities (FEMA 2003). In HAZUS, structural damage in a particular geographically-delimited study area is predicted using building inventory data and generalized building and bridge fragility functions. Fatalities and injuries are then estimated according to the level of building damage and type of construction, as shown in Table 6.6. Like the preceding ATC and NOAA studies, the relationship between structural damage and expected fatalities in largely based on engineering judgment and the fatality rates are highly dependent on the building type and structural system. HAZUS identifies four levels of injury severity ranging from "instantly killed" to "injuries requiring basic medical aid." The HAZUS predictions also depend on the time of day the earthquake occurs, distinguishing between 2:00 AM, when most people are at home, 2:00 PM, when most people are at work, and 5:00 PM, when many people are in transit. With minor modifications to the HAZUS inventory data and damage fragility functions for non-ductile concrete and unreinforced masonry construction, Kircher et al. (2006) used HAZUS to estimate the number of fatalities that would occur in a modern repeat of the 1906 San Francisco earthquake. If this earthquake were to occur at 2 AM, Kircher et al. (2006) predicts more than 800 deaths and 3,900 serious injuries in the San Francisco Bay region. If the earthquake were to occur at 2 PM, the study predicts more than 1,500 deaths and 6,000 serious injuries.

Table 6.5 Literature review of casualty studies, reporting the many factors that affect earthquake fatalities.

Authors	Earthquake and Estimated Death Toll[1]	Factors Affecting Earthquake Fatalities[2]	Other
Durkin and Murakami (1988)	Mexico City Earthquake, 1985, 10,000 killed; San Salvador Earthquake, 1986, 1,000 killed	* location of victims within building * entrapment * behavior of victims * search and rescue operations	Case study of victims in two buildings: a 8-story reinforced concrete dormitory in Mexico City and a 5-story office building in San Salvador
Armenian et al. (1997)	Armenian Earthquake, 1988; 25,000 killed	* building geographical location * height of building * location of victims within building	
Wagner et al. (1994)	Loma Prieta Earthquake, CA 1989; 62 killed	* construction materials * age of building * height of building * location of victims within building * behavior of victims * entrapment	Note: Observations here are largely from Wagner et al.'s review of previous literature, due to the small number of fatalities in the Loma Prieta earthquake.
Peek-Asa et al. (2000)	Northridge, CA Earthquake, 1994; 33 killed	* ground motion intensity * building damage * injury mechanism	The authors also observe that while building damage is a good predictor of fatalities, it is not as highly correlated with injuries.
Peek-Asa et al. (2003)		* ground motion intensity * multi-family residential or commercial construction * age of victim * gender of victim	The age of buildings also has an effect on casualties; typically, occupants of newer buildings are less likely to die, but are more likely to be injured.
Hengian et al. (2003)	Kobe, Japan Earthquake, 1995; 5,500 killed	* building damage * collapse volume/survival space	
Tabata et al. (2004)		* ground motion intensity * age of dwelling * structural capacity * collapse volume/survival space	Note: Study based on wooden dwellings only.
Murakami et al. (2004)		* dwelling damage * entrapment * location of victim within building * furniture falling * age of victim	
Ikuta et al. (2004)		* building collapse * building type/construction material	Study finds that most injuries are due to compression/suffocation.
Shoaf et al. (2005)	Izmit, Turkey Earthquake, 1999; 17,000 killed	* building collapse * building height * location of victim within building * gender of victim * victim behavior	Note: Study based on reinforced concrete buildings only.
Liao et al. (2003)	Chi-Chi, Taiwan Earthquake, 1999; 2,500 killed	* ground motion intensity * structural collapse * age of victims	
Tien et al. (2002)		* ground motion intensity * structural collapse	Details: 45% of victims died in mudbrick residences; approx. 45% died in multi-story reinforced concrete residences
Tsai et al. (2001)		* ground motion intensity * structural collapse * age of victims * search and rescue operations	
Chou et al. (2004)		* victim's income (lower) * mental disorders, physical disability and recent hospitalization	

[1]Fatality estimates from past earthquakes are approximate and based on available data from USGS and elsewhere.
[2]These lists are not ordered according to importance identified by researchers.

While the data and methods of the NOAA, ATC and HAZUS are useful for broad estimates of casualties in a geographic area in a future earthquake scenario, a particularly detailed methodology for prediction of building-specific earthquake casualties has been developed by Coburn et al. (1992). According to Coburn et al.'s model, the fatalities incurred in a particular building and earthquake event are given by $K = M_1 \times M_2 \times M_3 \times (M_4 + M_5)$, where M_1 is the population of the building, M_2 is the occupancy rate at the time of the earthquake and M_3 is the percentage of occupants trapped by collapse. M_4 describes the rate of immediate death and injury among the entrapped

population and if the injured are not rescued and treated quickly, their death rate is given by M_5. Prediction of structural collapse could be obtained from nonlinear model predictions or other more generic fragility data. The Coburn et al. (1992) framework relies on prediction of not only structural collapse, but the collapsed volume of the structure, which is judged to be of critical importance for determining the number of victims that are trapped and killed in the earthquake. From observations in previous earthquakes, for example, they distinguish between 'bottom-up', 'top-down', 'pounding' and 'overturning' collapse of RC frames; since these collapse modes may leave different voids and escape routes they may have a significantly different number of fatalities. The death rate (M_4) is heavily dependent on the type of construction, with reinforced concrete and masonry construction identified as the deadliest. Other researchers, including Murakami (1992) and Stonjanski and Dong (1994), have also developed fatality prediction models. Though specific assumptions differ, all rely on linking predictions of earthquake intensity, structural damage and collapse, and death rates to estimate the number killed in a particular building.

More recently, Yeo and Cornell (2003) and Mitrani-Reiser (2007) have examined fatality prediction within the framework of performance-based earthquake engineering in order to evaluate life safety performance objectives for a specific building. Yeo and Cornell use nonlinear dynamic analysis to quantify building collapse performance in extreme earthquakes, and depending on the extent of structural collapse (local collapse, story collapse or global collapse), estimate the number of people killed. The Yeo and Cornell framework is illustrated by application to a 3-story post-Northridge steel moment frame, but the approach is applicable to any structure for which a detailed nonlinear analysis model is available. Similarly, Mitrani-Reiser (2007) predicted earthquake-induced losses and fatalities in modern, code-conforming RC frame office buildings. Mitrani-Reiser uses a "virtual inspector" to determine the likelihood of local or sidesway collapse from nonlinear analysis data, and predicts the number of fatalities that are likely to occur, based on assumptions of structural occupancy levels and death rates. Since her study focuses on RC moment frames, Mitrani-Reiser uses definition of damage state and fatality rates defined by Shoaf et al. (2005).

This study builds on the building specific fatality prediction framework developed by previous researchers. These fatality predictions require an understanding of the site-specific seismic hazard, methods of predicting structural collapse, an estimation of the number and

distribution of people in a building over the course of the day, and predictive relationships relating structural collapse and damage to fatalities. Though significant progress has been made in these areas, the casualty predictions described in this section are hampered by a lack of data linking structural collapse of different types of structures with the fatalities that are likely to occur. A great deal of judgment is inherent in the fatality prediction process.

Table 6.6 Literature review of engineering studies of earthquake fatalities in RC frame structures. The probability of fatality is the fraction of building occupants at the time of the earthquake who do not survive.

Author	Building Characteristics	Structural Damage States	Probability of Fatality, Given the Damage State	Source/Method
ATC (1985)	all construction, except light steel and wood frame	moderate	0.0001	expert judgment
		heavy	0.001	
		major	0.01	
		destroyed	0.2	
Coburn et al. (1992)	reinforced concrete frame structures	collapse, severity depending on volumetric reduction	0.31 to 0.49[1]	study of collapse volume in RC structures in Mexico City, Bucharest, Armenia and Greece, with additional assumptions
HAZUS (2003)	reinforced concrete moment frames	extensive damage	0.00001	expert judgment
		complete damage (no collapse)	0.0001	
		complete damage (collapse)	0.1	
Shoaf et al. (2005)	non-ductile reinforced concrete frame structures	partial collapse	0.0015	survey following 1999 Izmit earthquake
		total collapse	0.11	
			0.13 (midrise RC frames)	
			0.16 (upper floors of midrise RC frames)	

[1]Obtained by multiplying Coburn et al. 1992's collapse volume [M_3] and fatality rate [M_4] factors

6.3.3 Methodology for Fatality Prediction

The goal of the fatality prediction methodology developed here is to predict the number of fatalities that will occur in a given structure when subjected to a specified level of ground shaking. Though the method is generally applicable, this study focuses in particular on the RC moment frames that are the subject of this thesis. When a structure is analyzed for several levels of ground motion intensity, the expected number of fatalities as a function of the ground motion intensity can be predicted or – in combination with a ground motion hazard curve – the expected annualized number of fatalities. These metrics are used to quantify the life safety performance of modern and older RC moment frame structures, explicitly measuring the impact of modern building code provisions on seismic safety.

Figure 6.12 summarizes the fatality prediction methodology used in this study. The fatality prediction relies on several modules described in more detail below. The structural occupancy module estimates how many people will be in the building at the time the earthquake occurs. The structural damage module predicts the degree of damage that occurs in the structure on the basis of nonlinear simulation models described in previous chapters. Fatalities are then estimated based on the damaged state and collapsed volume of the

structure, and an assumed death rate for RC moment frame structures. The methods and assumptions for each of these modules are described below. It is noted that this methodology accounts only for deaths due to structural deterioration and collapse due to ground-shaking, neglecting the impacts of non-structural damage and other earthquake effects, such as landslides, fires or tsunamis.

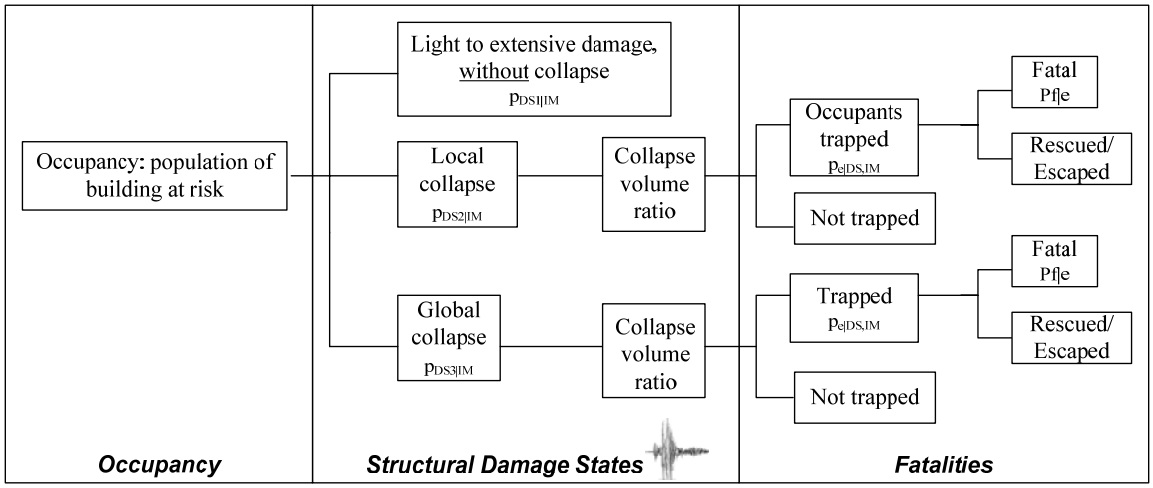

Figure 6.12 Methodology used for prediction of fatalities in this study.

Building Occupancy

The occupancy module predicts how many people will be in the building at the time that a future earthquake occurs. All of the case study structures are designed for office occupancy which are primarily occupied during weekday working hours. During working hours, the number of occupants is estimated based on data from ATC-13 for "professional, technical and business services," which specifies a typical occupancy of four people per 1000 square feet (ATC 1985). The RC archetype buildings are therefore estimated to have between 60 and 90 occupants per floor, depending on the plan dimensions of the structure. These occupancy estimations are consistent with the floor layouts shown in Figure 6.2. As illustrated in the architectural plans (Figure 6.2), the ground floor has a large meeting area and conference rooms that are used intermittently throughout the week so it is assumed that the ground floor has two-thirds the population of the typical floors. It is further assumed that the population of each floor is evenly distributed, neglecting the tendency of people to congregate in particular areas. Since people tend to exit buildings during earthquakes, we assume fifty percent of the ground floor occupants will leave during the ground-shaking, following Coburn et al. (1992).

Outside working hours and on weekends and holidays office buildings have far fewer occupants. Figure 6.13 shows the assumed number of people in an office building, as a function of the time of day and day of the week (modified from Coburn et al. (1992)). The y-axis of Figure 6.13 represents the fraction of building occupants that are in the building at a specified time. Overall, 114 out of 365 days are treated as weekends or holidays (Mitrani-Reiser 2007). Given the assumptions of Figure 6.13, approximately 15% of the occupants are assumed to be in the office on weekends. The average occupancy over the course of the year is therefore 33%. The assumptions are relatively consistent with other researchers; HAZUS (FEMA 2003) and Yeo and Cornell (2003) assume an average yearly occupancy for office buildings of 33% and 36%, respectively.

The outcome of the occupancy module is a prediction of the fraction of the building's occupants that will be present when an earthquake occurs, $p_o = 0.33$, accounting for the unknown time and day of the earthquake. In addition, the total number of building occupants is reported. The number of people at risk on average in an earthquake is the product of the total number of building occupants and p_o.

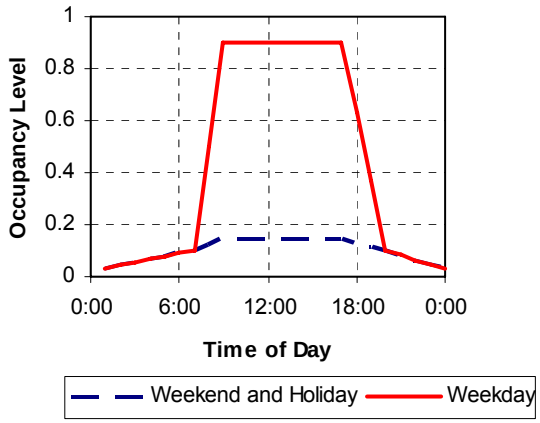

Figure 6.13 Temporal variability in building occupancy.

Structural Damage and Collapsed Volume

The structural damage module describes the degree of damage incurred in a structure (see Figure 6.12). For the purposes of fatality estimation, three structural damage states are defined: (1) light to extensive damage without collapse, (2) local collapse and (3) global collapse. These damage states are assumed to be mutually exclusive. Since fatalities are primarily associated with partial to complete structural collapse, it is not necessary to more completely distinguish between lesser damage states (as was necessary for the prediction of

economic losses, for example). For a given structure and level of ground motion intensity (IM), the probability of being in each damage state is predicted ($p_{DSi|IM}$) from nonlinear dynamic analysis. Since these analyses use structure-specific models, these damage states are more robustly defined than in other studies that use generic building level fragility functions, such as those available in HAZUS.

Global collapse occurs when sidesway collapse is predicted by nonlinear time history analysis. In the collapse performance assessment procedure presented here, the probability of global collapse is represented by the cumulative collapse distribution obtained from incremental dynamic analysis.[5] Local collapse implies a localized failure mode that has not led to sidesway collapse, but still represents a threat to life safety. In RC frame structures, local collapse is associated with either punching shear failure in flat-slab connections in gravity-designed interior columns (perimeter frame structures only) or loss of vertical carrying capacity induced by brittle shear failure in columns of the lateral resisting system. It is assumed that modern code-conforming special moment frames will not experience either of these local collapse modes prior to sidesway collapse. Capacity design and ductile detailing requirements prevent column shear failure from occurring and, likewise, the requirement of at least two continuous bottom bars in slab-column connections in code-conforming structures ensures that, while punching shear failure of the slab can occur, it will not fall and endanger the lives of those below. Local collapses are predicted with fragility functions as described in Section 3.2.4.[6] Local collapse due to punching shear failure occurs when the slab-column connection loses its gravity load carrying capacity, as defined by fragility functions based on Aslani (2005). The fragility function used to predict local column failure is also based on Aslani (2005), and corresponds to the damage state in which the column loses its gravity load carrying capacity following shear failure. In some cases shear failure of the column may occur significantly earlier, but it is assumed that life safety is not

[5] As described in Chapter 5, these probabilistic predictions of structural damage and collapse should account for both appropriate spectral shape (in this case, given by $\varepsilon = 1.2$) and effects of modeling uncertainties (in this case, FOSM assumptions are used).

[6] The probability of local collapse is defined as the probability of local collapse occurring, given that global collapse has not occurred. As such, the computation of the local collapse probability is highly sensitive to the number of non-collapsed records, and at spectral acceleration levels where many of the earthquake records have collapsed, the predicted probability may be somewhat unstable. To avoid discontinuities in the predicted probability of local collapse, it was assumed that the probability of local collapse is 0 until any local collapses are observed in the analysis and then varies linearly between 0 and 1. The slope of the linear assumption depends on the data from collapse analyses. The predictions of local collapse are adjusted for spectral shape in the same manner as used in adjusting the global collapse fragility (described in Chp. 3).

endangered until the column can no longer carry gravity loads. (See Chapter 3 for more detailed discussion of the fragility functions developed by Aslani(2005)).

The number of fatalities predicted depends on the structural damage state. It is assumed that no fatalities will occur in the first damage state and only the collapse limit states threaten life safety. This assumption is validated by numerous studies that have shown that the majority of fatalities due to ground shaking are associated with collapse of at least part of the structure (Tsai et al. 2001; Hengjian et al. 2003; Liao et al. 2003; Ikuta et al. 2004). Not accounted for are the small number of people are killed by damage to a building's nonstructural components (e.g. masonry walls) or interior contents such as furniture (Durkin and Thiel 1992; Stojanovski and Dong 1994; Tien et al. 2002; Hengjian et al. 2003; Ikuta et al. 2004). Damage to nonstructural elements and building contents may be a more significant source of injury than death (Porter et al. 2006).

In the local and global collapse damage states, the number of fatalities is predicted based on the collapsed volume of the structure. It has been repeatedly observed that even in a collapsed structure, some of the structure's occupants survive, because they occupy a part of the structure that did not collapse completely (Durkin and Murakami 1988; Tien et al. 2002). In their study of the 1995 Kobe earthquake, Tabata et al. (2004) found the internal space loss to be an important predictor of the number of casualties in the structure. Murakami et al. (2004) and others have also documented the importance of collapsed volume and collapse pattern on earthquake-induced fatalities. Accordingly, Coburn et al. (1992) and Yeo and Cornell (2003) used predictions of collapsed volume in the fatality prediction studies. In this study, the collapsed volume in local and global collapse states is estimated based on structural analysis results and judgment.

There is limited data quantifying the collapsed volume of structures, which is highly dependent on the type of structural system and quality of design and construction. Coburn et al. (1992) examined collapsed (mostly, non-ductile) RC frame buildings in Mexico City, Armenia and Greece and estimated that 3- to 5- story RC frame buildings typically lost 50 to 75% of their volume when they collapsed. To augment these observations, a database of 84 photos of collapsed or partially collapsed multi-story RC frames was assembled from field reconnaissance studies of 11 deadly earthquakes, included in Appendix 6.2. Since the focus of this study is on the consequences of collapsed RC frame buildings in California, the photos would ideally be representative of U.S. modern and existing non-ductile RC construction, but

there are very few cases of earthquake-induced collapses in modern California. Also, most of the photos are of collapsed non-ductile RC structures, as very few modern code-conforming buildings have collapsed. In addition it is noted that, while all of the photos are framed structures, some have infill walls and shear walls and, therefore, differ from the structures modeled here. Despite these limitations, the compiled database provides photographic evidence of the type of collapse modes that have been observed to occur in RC structures, to inform the assumptions about collapsed volume made in this study.

Methods for determining the collapsed volume ratio in this study are described in Figure 6.14. The most severe damage state, global collapse, may either (a) collapse only a few stories, leaving parts of the structure relatively undamaged, or (b) induce a pancake collapse of the entire structure. As described in Chapter 5, the nonlinear collapse analysis can be used to predict the number of stories in which damage concentrates for a given structure. The degree of damage concentration depends on the ductility and height of the structure, as well as design features, as reported in Table 6.7. The values in Table 6.7 are based on the number of stories that formed part of the collapse mechanism in dynamic analysis (e.g. 2 stories collapsed out of 8 total stories = 0.25). For buildings in which multiple collapse mechanisms occurred, a weighted average is used. The range indicates the variability in collapsed volume for different structures analyzed of the same height.

For the purposes of the fatality prediction, it is assumed that in some cases the collapsed volume is limited to those stories where the damage concentrates in the analysis (as described in Table 6.7). However, in a certain percentage of the collapses, the structure may pancake, collapsing the entire structure. In cases where the structure pancakes, the collapsed volume ratio is assumed to be 1, i.e. the entire structure collapses. The likelihood that global collapse of a structure leads to pancaking is assumed depending on the ductility of the RC frame and the number of stories, as reported in Table 6.8. The values reported in Table 6.8 are based on the photographic survey of collapsed and partially collapsed RC frames and judgment. Ductile frames are able to undergo larger deformations before collapse occurs, so it is judged that P-Δ effects make pancaking more likely for these frames. For this reason, the likelihood of pancaking, p[Pancake|Collapse], is higher in ductile structures. Taller buildings (8+ stories) with higher axial loads are also more sensitive to P-Δ effects and judged to be more

likely to collapse than shorter buildings (2 and 4 stories).[7] There is very limited data on the collapsed volume of structures to inform these judgments.

Table 6.7 Collapse volume ratios from nonlinear dynamic analysis of RC frame structures.

Num. of Stories	Ductility of RC Frame	Collapsed Volume Ratio, from Dynamic Analyses
1	ductile	1
2	ductile	0.55 to 0.81
	non-ductile	0.50 to 0.63
4	ductile	0.38 to 0.52
	non-ductile	0.50 to 0.61
8	ductile	0.15 to 0.28
	non-ductile	0.27 to 0.43
12	ductile	0.08 to 0.24
	non-ductile	0.20 to 0.29
20	ductile	0.18 to 0.22

Table 6.8 Assumptions regarding the likelihood that global collapse of a structure leads to complete collapse of the structure.

Num. of Stories	Ductility of RC Frame	Likelihood that collapse leads to pancaking p[Pancake|Collapse]
4 or fewer	ductile	0.3
	non-ductile	0.15
8+	ductile	0.6
	non-ductile	0.3

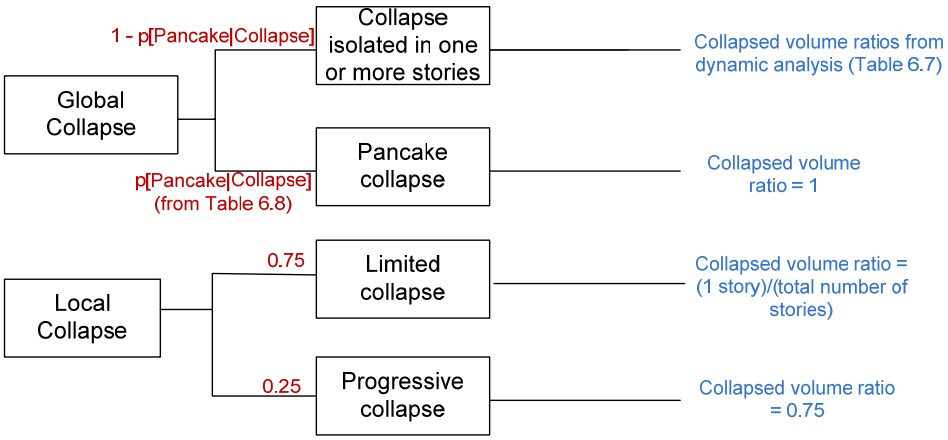

Figure 6.14 Event tree calculation of collapsed volume in RC frame structures for purposes of seismic fatality estimation.

[7] This discussion assumes that collapse volume is independent of the intensity level at which collapse occurs. It could be hypothesized, however, that ground motions that cause collapse at higher spectral acceleration levels may have larger collapsed volume ratios. The relationship between collapse capacity and collapse volume deserves future study.

When either of the local collapse modes occurs it is assumed to completely collapse that story of the structure. This assumption is consistent with observed earthquake failures, in which punching shear failures or column shear cracks are frequently observed across an entire floor. The collapse volume ratio of the local collapse is therefore typically 1/(total number of stories) (as shown in Figure 6.14). However, these local collapse modes could also trigger progressive collapse. Here, it is predicted that progressive collapse will occur 25% of the time. If progressive collapse due to local collapse modes occurs it is assumed that the collapsed volume ratio for purposes of fatality prediction is 0.75.

Earthquake Fatalities

Referring again to Figure 6.12, the final step in the methodology to predict the number of fatalities that are likely to occur in a given structure, based on the results of the occupancy and structural damage assessments. It is assumed that the probability of entrapment ($p_{e|DS,IM}$), the probability that an occupant of the building is trapped by the collapsed structure, is equal to the collapsed volume ratio following Coburn et al. (1992). The collapsed volume ratio is computed according to the guidelines described above (and shown in Table 6.7, Table 6.8 and Figure 6.14).

The final step is to estimate the probability that the earthquake will be fatal to the entrapped victims (p_{fatal} or p_f), which reflects the lethality of the structural system. This value is based largely on judgment. For RC frame structures, p_{fatal} is estimated through comparison with existing literature, especially data from HAZUS study (2003) and Shoaf et al. (2005) reported in Table 6.6. From these considerations, p_{fatal} is estimated to be 0.17, i.e. if a victim is trapped, the probability of death is 17%. For a typical 4-story ductile RC frame structure and the collapse volume and entrapment assumptions above, p_f = 0.17 implies that approximately 11% of the people in the building during the earthquake will be killed when the structure collapses. (The collapsed volume ratio from dynamic analysis for this structure is 0.50. There is a 30% chance that this collapse will lead to a pancake collapse, so the average collapse volume ratio is 0.50*(1 – p[Pancake|Collapse]) + 1* p[Pancake|Collapse] = 0.575. Therefore, $p_{entrapment}$ = 0.65. It is assumed that 0.17 of those entrapped die: 0.17*0.65 = 0.11. Calculations will differ depending on the collapsed volume ratio from dynamic analysis and the likelihood of pancaking (Table 6.8).) This value lies between the HAZUS assumption of 10% and Shoaf et al.'s estimate of 13% (FEMA 2003; Shoaf et al. 2005).

The outcome of the structural damage and fatalities module is the probability that a building occupant will die (p_d), given the ground motion intensity. Mathematically, the structural damage and fatalities modules can be written as

$$p_{d|IM} = \sum_{k=1}^{3} (p_{DS=k|IM})(p_{e|IM,DS})(p_f) \tag{6.5}$$

where the 3 possible damage states are defined in Figure 6.12, $p_{DS=k|IM}$ is the probability that a structure is in the k^{th} damage state (given the ground motion intensity), $p_{e|IM,DS}$ is the probability of entrapment (which depends on predicted collapsed volume ratio from analysis results and judgment in Table 6.8), and p_f is assumed to be constant for RC frames (and independent of the intensity level or damage state). Finally, the expected number of fatalities at level of ground motion intensity is obtained by taking the product of the number of people in the building, p_o, and p_d. Recall, p_o accounts for temporal variability in the number of people in the building. p_d is the percentage of people in the building who are killed due to building collapse.

Earthquake Injuries

A similar approach may be used to estimate the number of people in a building that will be injured when an earthquake occurs. A couple of simplifying assumptions are needed, due to the scarcity of available data regarding the type and prevalence of serious injuries in earthquakes. Following HAZUS, it is assumed that the number of people who experience life threatening injuries is half the number of fatalities. The number of people who endure serious injuries, defined as those requiring hospitalization, but not life-threatening in nature, is assumed to be twice the number of those killed. These assumptions predict the number of injured from the number killed. Where injuries and fatalities are not induced by the same mechanisms, e.g. if injuries are dominated by nonstructural damage and fatalities are governed by collapse of the structural system, this method will not provide a good estimate of injuries incurred. These assumptions are difficult to validate because injury data is largely anecdotal (Coburn et al. 1992; Durkin and Thiel 1992; Tsai et al. 2001), and should be updated when further information becomes available.

Limitations

The methodology described herein can be used to estimate the number of earthquake-induced fatalities that will occur in a given structure, based on structural collapse analysis results. Within the broader context of performance-based earthquake engineering, it allows us to extend predictions of collapse performance to directly emphasize the consequences of collapse, namely the threat to human life. The direct prediction of fatalities becomes particularly useful where structures with comparable collapse probabilities may represent a very different threat to the safety of their inhabitants.

The methodology for predicting earthquake-induced fatalities, however, is limited by (1) the insufficiency of data relating structural damage, collapse and fatalities for different types of structural systems and (2) its inability to account for non-engineering factors such as cultural, social and behavior effects, level of preparedness or the higher risk of dying for women, the elderly and the infirm. In addition, the methodology does not account for deaths due to non-structural damage and non-collapse limit states.

6.3.4 Predicted Fatalities in Non-Ductile Reinforced Concrete Frames

In this section, the methodology described above is used to make predictions about earthquake-induced fatalities in the non-ductile RC archetype buildings, which consist of 2, 4, 8 and 12-story non-ductile RC moment frames. Since retrofit provisions and building codes are primarily concerned with collapse prevention as a means of protecting life safety, these fatality predictions build on the collapse performance assessments to directly quantify the life safety threat imposed by these structures. The fatality predictions are reported primarily in terms of two metrics (a) the expected number of fatalities as a function of ground motion intensity, or, on average, how many people will be killed when the structure is subjected to ground motion of a specified intensity and (b) the expected annual number of fatalities (EANF), obtained by integrating the expected number of fatalities as a function of ground motion intensity with the site specific hazard curve. In order to compare the deadliness of structures with different numbers of occupants, the expected annual number of fatalities is normalized by the total number of building occupants.

Occupancy Estimates

The number of occupants in each structure is estimated according to the guidelines of ATC-13 (ATC 1985) and the other assumptions described above, as reported in Table 6.9.

Table 6.9 Predicted number of occupants in archetype office buildings.

Num. of Stories	Num. of Occupants per Floor (Ground)	Num. of Occupants per Floor (Upper)	Total
2	70	105	175
4	62	96	350
8	44	66	500
12	44	65	750

Fatality Predictions for 4-Story Non-Ductile Reinforced Concrete Frame Structure

In order to illustrate the methodology for fatality predictions, the results are first discussed for a 4-story non-ductile RC space frame structure with an estimated occupancy of 350 people. From the collapse performance assessment of Chapter 5, the structure has a median collapse capacity $Sa(T_1) = 0.39g$ and a collapse margin ratio of 0.54.

Fatality predictions for the 4-story non-ductile RC frame structure are shown in Table 6.10 and Figure 6.15. In Figure 6.15a, the estimated number of fatalities is plotted as a function of the ground motion intensity. As expected, at very small spectral acceleration values, few fatalities are expected. For ground motion intensities significantly above the median collapse point, the fatalities saturate, predicting that on average approximately 10 people or 3% of the building's population will be killed. At the 2% in 50 year shaking intensity ($Sa_{2/50}(T_1) = 0.47g$), 8.1 fatalities are predicted. The expected annual number of fatalities, obtained by integrating Figure 6.15a with the site specific hazard curve for the Los Angeles site, is 62.4×10^{-3} (people killed/year). It is emphasized that the fatalities predicted in Figure 6.15a are expected values, and represent an average of the number of fatalities that could occur. The effect of the day and time the future earthquake occurs is further illustrated in Figure 6.15c. If an earthquake with an intensity of $Sa(T_1) = 1g$ were to occur at 11 PM on a weekday, a very small number of people would be killed – maybe 1 person. If the same earthquake occurred at 11 AM on a weekday, it is predicted that approximately 30 people would be killed, an additional 60 with injuries requiring medical attention and 15 with life-threatening injuries. It is also interesting to note (Figure 6.15d), the contribution of local collapse modes to the overall death rate. Local collapses due to loss of column gravity capacity are predicted to kill a small, but not insignificant, number of people.

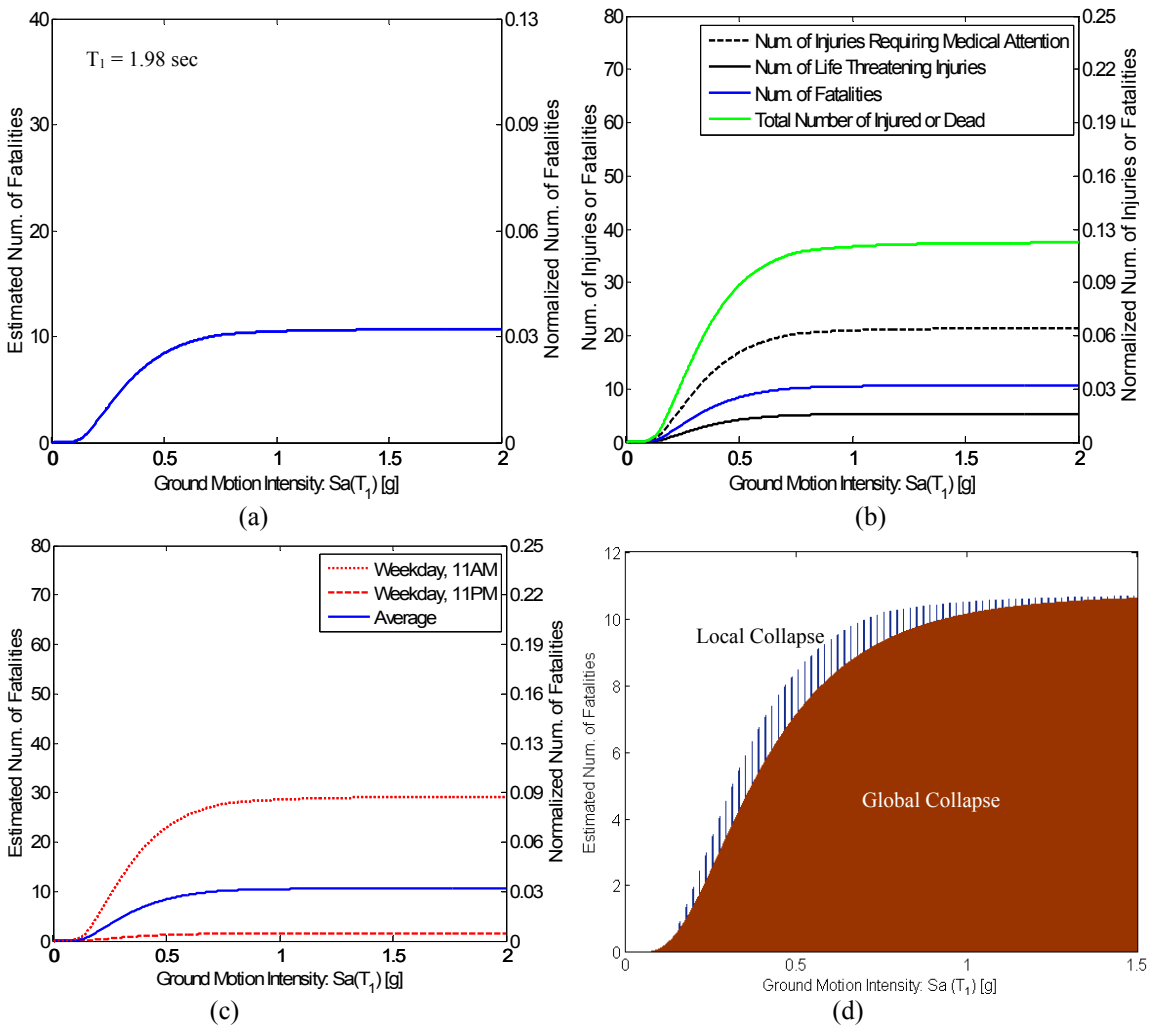

Figure 6.15 Estimated fatalities in 4-story non-ductile RC space frame structure as a function of the ground motion intensity, illustrating (a) expected fatalities, (b) expected fatalities and injuries, (c) effect of temporal variability in occupancy on fatality predictions, and (d) the expected number of fatalities disaggregated according to whether they occur due to local or global collapse modes.

Table 6.10 Fatality prediction metrics for the 4-story non-ductile RC space frame structure.

Collapse Margin	0.54
P[Collapse|$Sa_{2/50}$]	0.91
Expected Annual Number of Fatalities	62.4 x 10^{-3}
Normalized Annual Number of Fatalities	0.018%
Expected Number of Fatalities given $Sa_{2/50}$	8.05 (of 350 occupants)

Fatality Predictions for Archetypical Non-Ductile Reinforced Concrete Frame Structures

The fatality prediction methodology is applied to each of the archetypical non-ductile RC frame structures described in detail in Chapter 5, including structures that vary in terms of height (2 – 12 stories), framing system (perimeter or space frame systems), and other design and detailing characteristics. The collapse assessment results from Chapter 5, including

collapse capacity and collapse mechanisms, are directly utilized for input in the fatality prediction process. Results are for a high seismic far-field Los Angeles site.

Table 6.11 and Figure 6.16 report the predicted number of earthquake-induced fatalities for all of the archetypical 1967-era California RC frame structures. A useful metric for comparing different structures is the normalized annual number of fatalities, an annualized measure of the number of predicted fatalities over the lifetime of the structure. On average for the baseline structures (design variant A), the normalized expected annual number of fatalities is 0.020%, slightly larger than the 0.018% reported for the 4-story space frame structure described in detail above. Of the baseline space and perimeter frame structures, the safest structure is the 12 story space frame, with a normalized expected annual number of fatalities of 0.010%. The least safe structure is the 8-story perimeter frame, with a normalized expected annual number of fatalities of 0.028%. This difference in annualized fatalities results in an increase from 2 to 5.6 predicted deaths in 50 years (in a structure with an assumed 400 occupants).

Characteristics of the structural designs lead to variability in predictions of earthquake-induced fatalities in Figure 6.16. As shown in Figure 6.17, the space frames are typically safer than perimeter frames structures. Space frames have higher sidesway collapse capacities, and although they are more susceptible to non-simulated (local) failure modes, the local collapses have lower fatality rates.

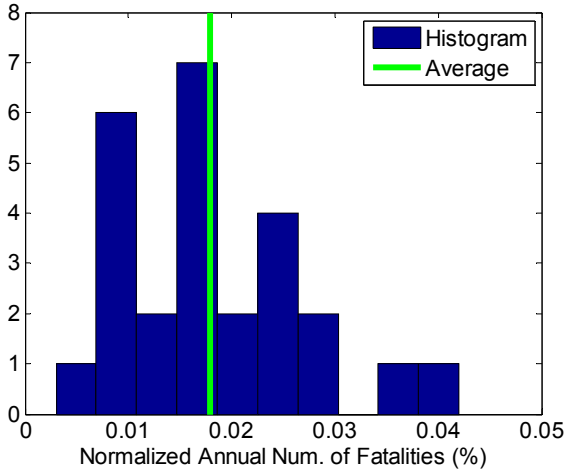

Figure 6.16 Predicted expected annual number of fatalities in existing non-ductile RC frame buildings.

Table 6.11 Predicted expected annual number of fatalities in archetype non-ductile RC frames.

Design ID	Num. of Stories	Framing System	Total Num. of Occupants[1]	EANF ($x10^{-3}$)	Normalized EANF (%)
3002	2	P	175	23.7	0.014
3001		S	175	40.7	0.023
3003	4	P	350	97.4	0.028
3004		S	350	62.4	0.018
3009			350	128.0	0.037
3010			350	83.8	0.024
3012			350	62.1	0.018
3032			350	42.8	0.012
3015	8	P	500	141.2	0.028
3034			500	128.7	0.026
3016		S	500	76.6	0.015
3017			500	85.3	0.017
3018			500	104.3	0.021
3019			500	93.3	0.019
3020			500	89.5	0.018
3021			500	85.1	0.017
3022	12	P	750	191.8	0.026
3035			750	318.2	0.042
3023		S	750	75.5	0.010
3024			750	71.2	0.009
3026			750	55.0	0.007
3027			750	58.1	0.008
3028			750	118.2	0.016
3029			750	54.2	0.007
3031			750	53.6	0.007
3033			750	24.2	0.003
			Average	91.0	0.018

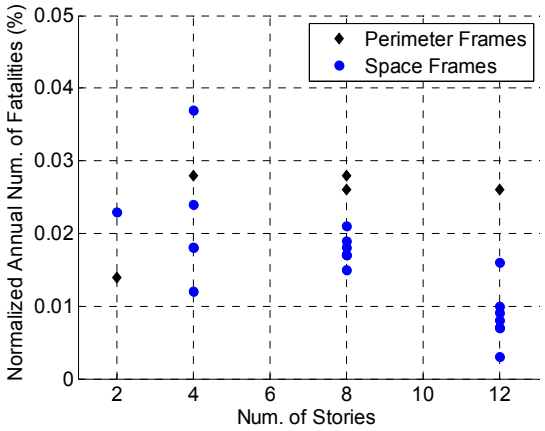

Figure 6.17 Variation in predicted number of fatalities for non-ductile RC frame structures, as a function of building height and framing system.

6.3.5 Life Safety of Non-Ductile and Ductile Reinforced Concrete Frame Structures

Chapter 5 compared the collapse capacities of older and modern RC frame structures and demonstrated that, when measured in terms of collapse rate, older, non-ductile RC frames are 40 times more likely to collapse. Since the primary motivation for preventing structural

collapse in seismic events is to mitigate threats to life safety from earthquake-induced collapse, it is also relevant to compare measures of the life safety consequences of collapse for these different types of structures.

Predicted fatalities for the archetypical modern code-conforming RC frame structures designed and analyzed by Haselton (2006), and subjected to the fatality prediction methodology discussed in this study, are presented in Table 6.12 and Table A6.1. On average, these structures are predicted to have a normalized annual number of fatalities of 0.0008%. The safest structures are the 2-story space frames, with 0.0002% fatalities per year. The most dangerous is the 8-story perimeter frame, for which a normalized EANF of 0.0018% is predicted.

The expected number of fatalities is much larger for the existing non-ductile RC frames than the modern RC frame structures. Whereas well-detailed, modern RC frames have a seismic fatality rate of 0.001% of their occupants per year, the fatality rate in non-ductile frames is 0.02% of occupants, an increase of twenty times. This data implies that over the next 50 years, on average 4 people would be killed in a older building (assuming 400 occupants) as compared to 0.2 people, on average, in a modern RC office building (also with 400 occupants). These results should not be interpreted as a prediction that 4 people will be killed in every existing non-ductile RC frame structure in a highly seismic region of California over the next 50 years, but rather that within the 50-year time frame perhaps 1 out of 100 structures will experience significant damage and collapse, killing many of its occupants. Life safety risks are much reduced in the code-conforming structures.

The importance of comparing a wide variety of performance metrics in assessing safety is illustrated in Figure 6.18, which shows the relationship between collapse capacity and the fatality predictions. The relationship between the mean annual frequency of collapse and the annualized number of fatalities are highly correlated, because the methodology assumes all building related fatalities in earthquakes are due either to partial or complete structural collapse. Variations occur because different structures collapse in different mechanisms, killing a different percentage of the occupants; this effect of collapsed volume is especially noticeable in the non-ductile data due to the occurrence of local collapse modes that are typically less deadly. As illustrated by this figure, collapse capacity is an important indicator of life safety, but it does not provide data on the relative magnitude of differences in life safety between different types of structure. Additional data, such as expected number of

fatalities, are useful for an informed discussion of acceptable safety in retrofit policy and for investigating costs and benefits of replacement as in Chapter 7.

Table 6.12 Predicted expected annual number of fatalities in archetype code-conforming RC frame structures.

Design ID	Num. of Stories	Framing System	Total Num. of Occupants[1]	EANF ($x10^{-3}$)	Normalized EANF (%)
2064	2	perimeter	173	1.73	0.001
1001	2	space	173	0.41	0.0002
1003	4	perimeter	346	2.7	0.0008
1008	4	space	346	1.28	0.0004
1011	8	perimeter	461	8.33	0.0018
1012	8	space	461	3.08	0.0007
1013	12	perimeter	692	9.9	0.0014
1014	12	space	692	9.38	0.0014

[1] Weekday, daytime occupancy. These values reflect a 120 ft. x 180 ft. footprint for the shorter buildings and a 120 ft. x 120 ft. footprint for the taller buildings ≥ 8 stories.

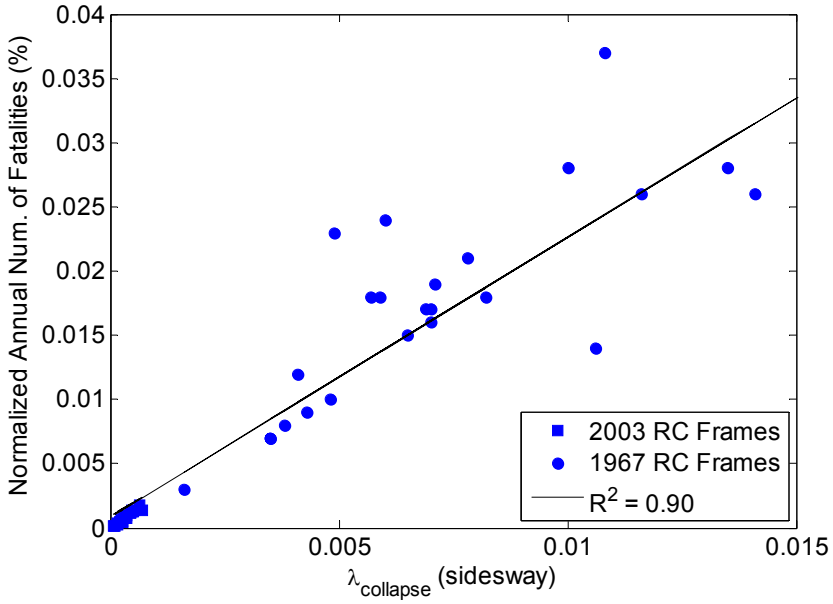

Figure 6.18 Relationship between mean annual frequency of collapse ($\lambda_{collapse}$) and predicted normalized annual number of fatalities [Includes fatality data from all buildings in Table 6.4 and Table A6.1].

6.3.6 Validation and Comparison with Previous Studies

There is limited previous research that provides building-specific fatality estimations. Many studies have documented deaths in past earthquakes, but without data on how many buildings collapsed, what types of buildings collapsed, and how much of the building collapsed, their findings cannot be directly compared to the results here. Other studies, such as Kircher et al. (2006)'s prediction of damage, losses and fatalities during a repeat of the 1906 earthquake in the San Francisco bay region, relied on similar assumptions to those used

here, but use simplified structural analysis data and predict results for a scenario of the entire bay area, rather than an individual building.

Therefore, the comparisons below are limited to work by Mitrani-Reiser (2007) and Yeo and Cornell (2003). When the methodology proposed in this study is used to predict fatalities in the code-conforming 4-story RC benchmark structure evaluated by Mitrani-Reiser (2007), slightly fewer fatalities are predicted (0.0003% expected annual fatalities, compared to 0.0004% expected annual fatalities predicted by Mitrani-Reiser).

Yeo and Cornell (2003) examined expected earthquake-induced fatalities in a 3-story post-Northridge steel moment resisting frame. Compared to the archetype RC frames in this study, Yeo and Cornell predict higher number of fatalities for large intensity earthquakes and lower numbers of fatalities for smaller earthquakes. Differences in the large spectral acceleration region are largely due to Yeo and Cornell's conservative (and somewhat unrealistic) assumption about what constitutes collapse for local and global collapse and the extent of the structure affected by these collapse. This study predicts higher fatalities for lower ground motion intensities because the collapse fragilities used properly accounts for the increase in collapse probability at the tail of the distribution associated with modeling uncertainties (see Chapter 4).

6.3.7 Effects of Sources of Uncertainty on Fatality Predictions

There are many sources of uncertainty in the prediction of earthquake-induced fatalities. These sources of uncertainty reflect the scarcity of data and lack of knowledge in the fatality prediction process, as well as the inherent randomness in ground motions, structural response and the number of people killed when a structure collapses. The predicted fatalities described above are expected values, hiding the variability in the possible number of fatalities that could occur. In this section, the effect of these uncertainties on the performance predictions is evaluated in order to identify those that have the biggest impact on the fatality predictions and to illustrate the range of possible casualties that may occur. In future, some of these uncertainties can be reduced when better data is available. These effects are investigated with reference to a 4-story modern, code-conforming RC perimeter frame structure with 30 ft. spans; the expected fatalities for this structure are illustrated in Figure 6.19. (This structure is Design ID 1009 from Table A6.1.)

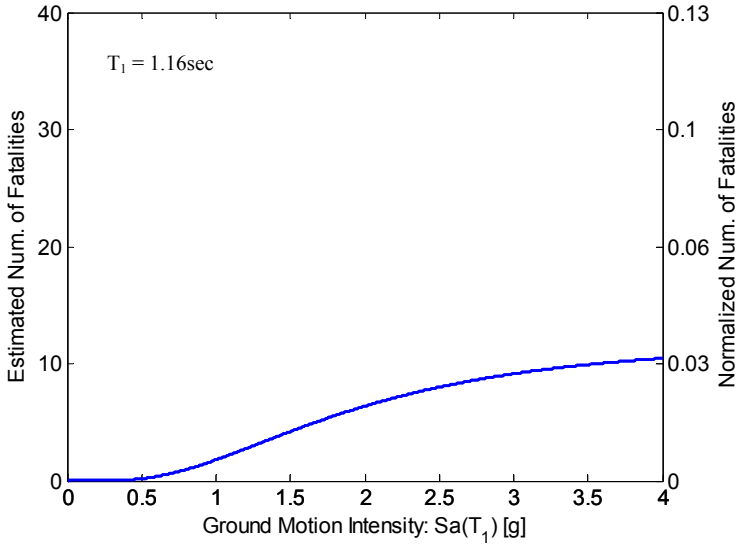

Figure 6.19 Expected number of fatalities for a 4-story modern RC perimeter frame office building.

Sources of Uncertainty

Selected random variables associated with fatality prediction are listed and described in Table 6.13. The mean value of each these random variables was used in obtaining the fatality predictions reported above. In this section, as reported in Table 6.13 and illustrated in Figure 6.22, the probability distribution associated with each random variable is explicitly defined, for the purpose of identifying the impact of each on the variability in predicted number of earthquake-induced fatalities. Some of the random variables, such as collapse, are defined with discrete probability distributions, such that they can take on only a finite set of values, i.e. the structure has either collapsed or not collapsed. Others are defined as continuous random variables. All random variables are assumed to be independent. There are many other possible sources of uncertainty that may affect the prediction of earthquake-related fatalities, such as building occupant behavior during the earthquake, but only those described in Table 6.13 are considered here.

Table 6.13 Description of key sources of uncertainty in fatality prediction.

Random Variable	In Brief	Description of Source of Uncertainty
Structural Collapse	Will the structure collapse under a ground motion of intensity Sa = x?	The outcome of the collapse assessment procedure described in Chapters 3,4 and 5 is a cumulative collapse distribution as a function of spectral acceleration, accounting for record-to-record and modeling uncertainties.[1] At each spectral acceleration level, this collapse CDF is used to define a discrete probability distribution for collapse where the structure has either collapsed or not collapsed. See Figure 6.20a.
Collapse Volume	How much of the structure will collapse?	Given that the structure has collapsed, a discrete probability distribution defines the volume of the structure that has collapsed. This distribution is based on the collapse volumes observed in dynamic analyses as well as the assumptions (Table 6.8) on the likelihood of story or multi-story collapses leading to progressive pancake collapse of the entire structure. See Figure 6.20d.
Number of Occupants	How many people work in the building?	The expected number of building occupants is based on data from ATC-13 (1985) and the floor plan of the structure. It is assumed that the actual number of occupants is normally distributed, with a mean value of 314 (from ATC-13) and a coefficient of variation of 0.15. Not all the occupants will be in the building at any given time, but this is accounted for separately. See Figure 6.20b.
Day of the week	Will the future earthquake occur on a working day or weekend/holiday?	Following Mitrani-Reiser (2007), it is assumed that 69% of days are work days, accounting for both weekends and federal holidays. See Figure 6.20e.
Estimation of $p_{fatal\|entrapment}$	How likely are trapped victims to die?	On average, it is assumed that 17% of trapped victims will die. This value is uncertain, due to lack of data. To quantify this source of epistemic uncertainty, it is assumed that p_f is lognormally distributed with mean value of 0.17 (median $\exp(\mu_{ln}) = 0.15$) and $\sigma_{ln} = 0.50$. See Figure 6.20c.

[1]Only global collapse modes are considered because ductile detailing in this structure prevents local collapse modes.

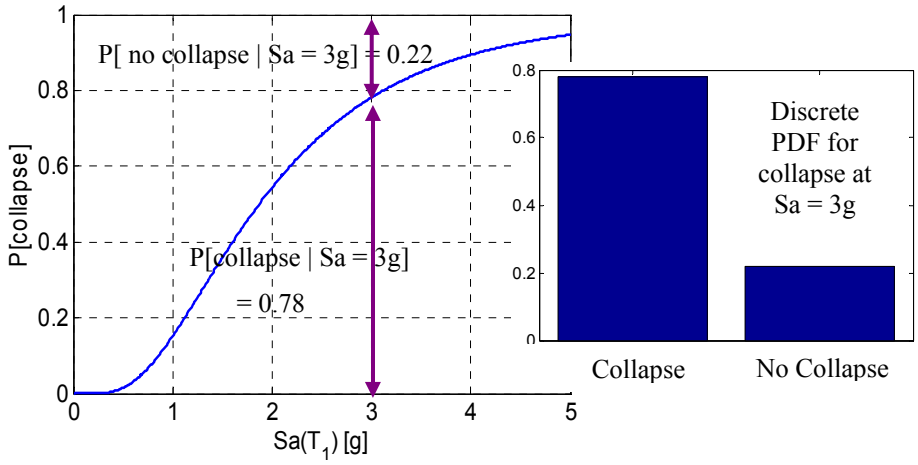

(a) Collapse probability distribution for 4-story modern RC frame obtained from incremental dynamic analysis, used to define a discrete probability distribution associated with collapse at each spectral acceleration level. (T_1 = 1.16 sec)

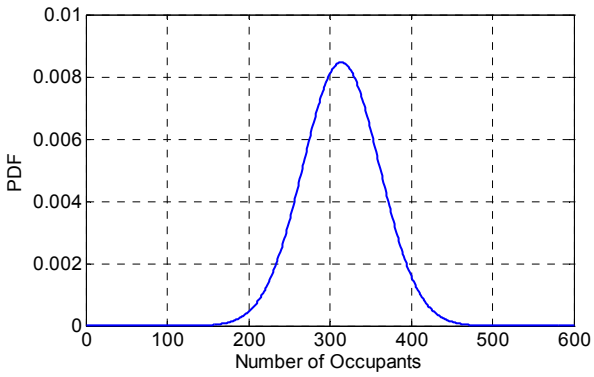

(b) Probability distribution describing the number of occupants in the building.

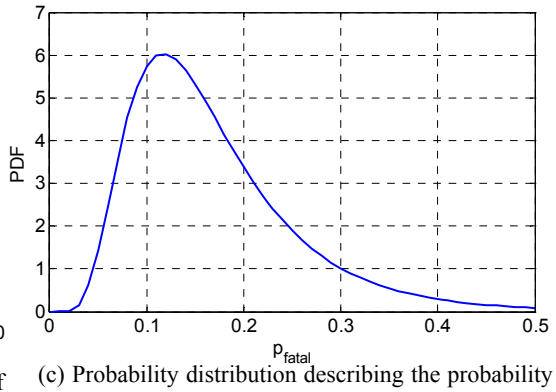

(c) Probability distribution describing the probability of an occupant dying, given that they are trapped in the building.

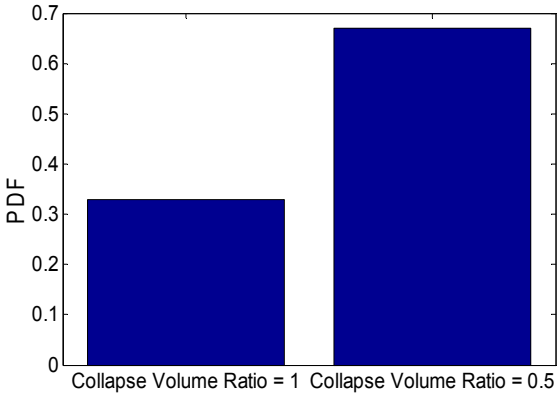

(d) Assumed probability distribution of the collapse volume ratio of this structure.

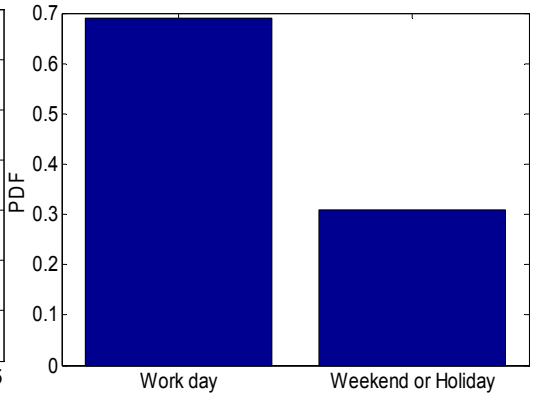

(e) Distribution describing the probability of a future earthquake occurring on work day.

Figure 6.20 Probability distributions for random variables associated with prediction of earthquake-related fatalities.

Monte Carlo Study

Monte Carlo simulation is used to quantify the effects of each of these sources of uncertainty on the fatality predictions, illustrating the variability in the number of fatalities that may occur. In this study, at each spectral acceleration level of interest, 2000 sets of independent realizations of the random variables of interest are generated from the probability distributions defined in Table 6.13 and Figure 6.20. The number of fatalities is then predicted from each set of realizations of the random variables, resulting in 2000 different simulations of the number of fatalities at each spectral acceleration level, as illustrated in Figure 6.21a. Statistics such as the 20^{th} and 80^{th} percentile of the fatality predictions at each intensity level can help to reasonably bound the prediction of fatalities.

The results of Monte Carlo simulation when each random variable is perturbed individually are illustrated in Figure 6.21. The occupancy random variable, defined with a small coefficient of variation, has a small effect on the predictions. Collapse, collapse volume and epistemic uncertainty in p_f lead to greater variation in the results. These random

variables all have an element of epistemic uncertainty, such that if we could improve our understanding of these parameters it would be possible to reduce the overall uncertainty in fatality predictions.

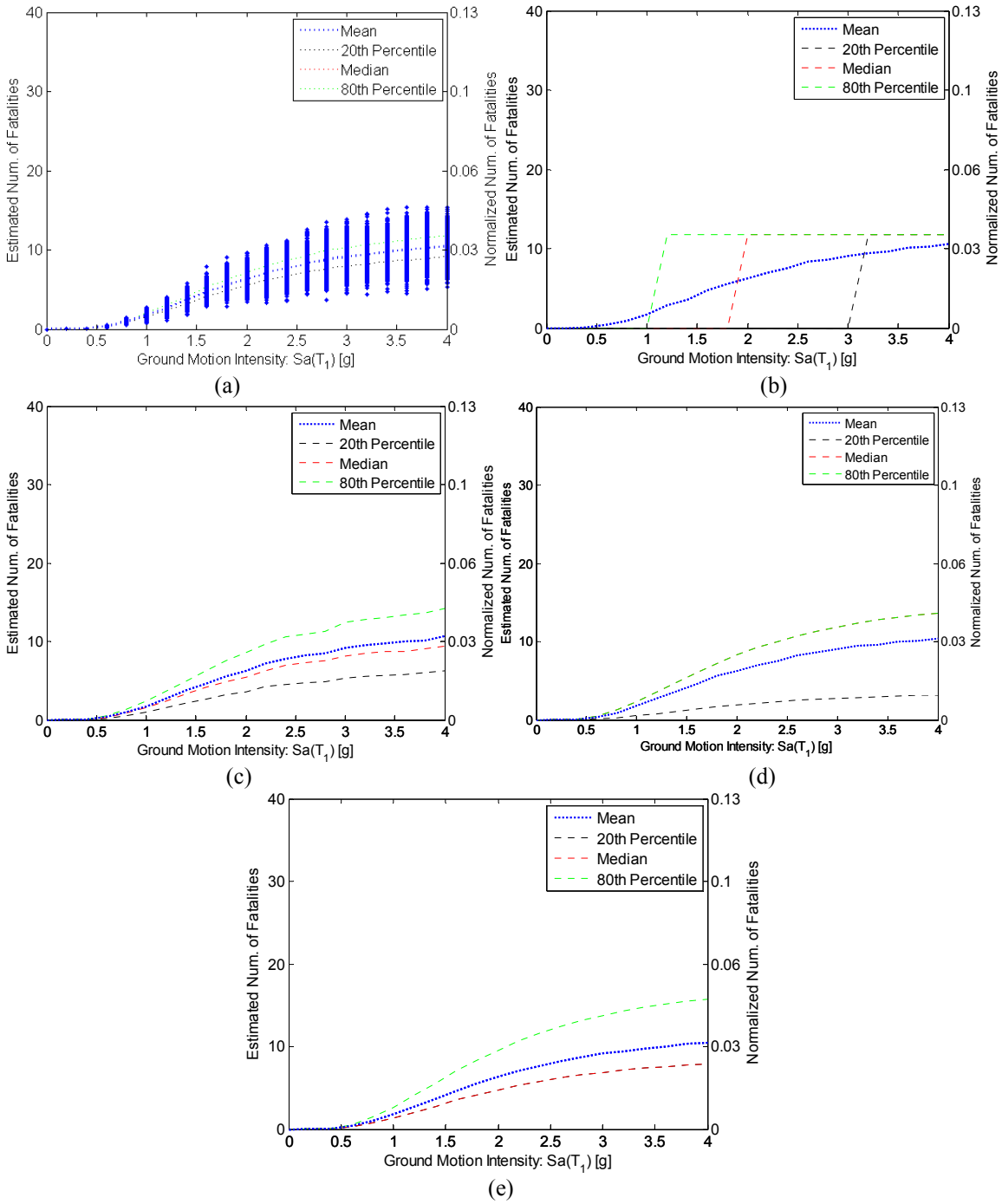

Figure 6.21 Effect of uncertainty in (a) number of building occupants; (b) collapse capacity of the building; (c) prediction of the probability of fatality given entrapment (p_{fatal}); (d) whether the earthquake will occur on a work day or holiday; and (e) the volume of structure that collapses.

The collapse random variable has a bifurcated effect, as shown in Figure 6.21b. Although collapse occurs on average x % of the time at a specified level of ground motion intensity, the Monte Carlo simulation predicts either "collapse" or "no collapse" for each simulation, based on the binary distribution defined, such that of the 2000 realizations x % have collapsed. For those realizations that have not collapsed, zero fatalities occur, based on the assumptions above. When collapse occurs, the number of fatalities that occur depend on the collapse volume ratio and other parameters (held constant in Figure 6.21b). Therefore, as shown in Figure 6.21b, at very low spectral acceleration levels, the mean value is non-zero because a small number of realizations predicted collapse, but the counted percentiles (20^{th} percentile, median and 80^{th} percentile) all predict zero fatalities.

The combined effect of these sources of uncertainty on the fatality predictions are shown in Figure 6.22. At high spectral acceleration levels there is significant variability in the results such that, depending on the collapse mode and then number of people in the building and other factors, between 1 and 6 % of the occupants may be killed. As observed with the collapse random variable alone, at low spectral acceleration levels the expected or mean values are driven by a few realizations with high predictions of fatalities, whereas most of the simulations predict zero fatalities, hence, the counted percentiles are consistently below the mean.

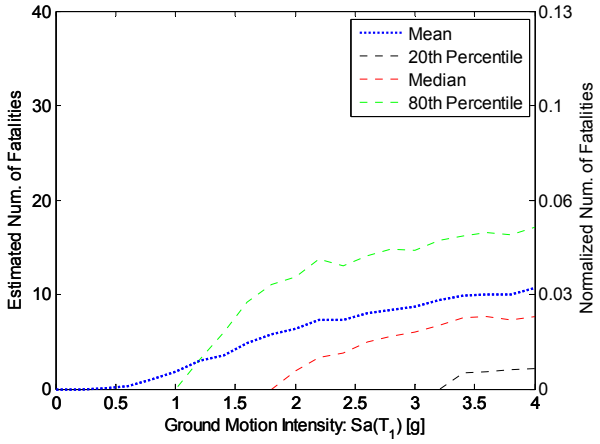

Figure 6.22 Effect of all sources of uncertainty on the predicted number of fatalities.

6.3.8 Summary and Future Research Needs

This section provided estimates of the number of earthquake-related fatalities and injuries that may be expected in RC frame office buildings in high seismic areas of California. As

protecting life safety remains the primary motivation for mandating or encouraging retrofit of existing non-ductile RC frame buildings, assessments of earthquake-induced fatalities and injuries are useful for identifying risky structures and justifying (or not) retrofit regulations motivated by life safety concern. Estimates of the number that could be killed or injured in future earthquakes are also needed by emergency responders and public health officials, who can better plan mitigation and response efforts to ensure that sufficient post-earthquake medical care is provided and to target search and rescue operations that focus on vulnerable buildings or parts of the urban area. Expected values of fatalities, like those presented here, provide consistent metrics for comparing life-safety performance of different structures, provided that the underlying sources of uncertainty are the same. In other applications, such as emergency preparedness planning, it may be useful to know the range of possible fatalities. With future research and improved data gathering, it will be possible to obtain more precise estimates of earthquake-induced fatalities.

The fatality estimations provided here are hampered by available data. To improve the predictions obtained by the methodology described above, data on earthquake casualties needs to be collected together with data on building type, level of building damage, and the level of severity of injuries. Statistics relating victim behavior to survivability, such as whether they took any preventative action during the earthquake, could also benefit the models. Ideally, this information would be systematically collected and reported in a global database. There is also insufficient data relating to injuries that may occur during earthquakes, and injuries are crudely accounted for in this study. Shoaf (2007) proposes that a consistent taxonomy is needed for gathering and classifying data on the type and frequency of earthquake-related injuries such that these can be more accurately predicted in the future. This research neglects deaths and injuries due to damage in nonstructural components; systematic data on the mechanism by which people are injured in earthquakes could help to establish the ways in which nonstructural components endanger life safety. In collecting data, collaboration between engineering and public health professionals is needed.

6.4 Conclusions

In this chapter, the archetypical non-ductile RC frame structures are reexamined to evaluate the earthquake-related economic losses, fatalities and injuries. Economic losses are predicted on a component-by-component basis following Mitrani-Reiser (2007), where

structural response is used to predict damage in non-structural and structural components of the structure, and this damage is used to estimate needed repair costs. Owners of non-ductile RC frame structures can expect to lose (on average) 2.2% of the replacement value annually due to earthquake-induced damage and repairs. These predictions of losses may be used to evaluate investments in seismic strengthening or earthquake insurance. Expected annual losses in non-ductile RC frame structures are expected to be approximately double those expected in a comparable modern code-conforming RC office building. Predicted losses would be even more significant if indirect losses associated with downtime and building closure were included.

Fatalities are predicted based on structural damage and the predicted collapse volume of the structure. This method provides a consistent approach for evaluating earthquake-related fatalities in RC frame structures, but would benefit from systematic data collection in future earthquakes. On average, expected annual fatalities in non-ductile RC frame structures are 0.02% of building occupants. In terms of the annualized fatality rate, 1967-era structures in highly seismic areas in California may be 20 times deadlier than the 2003 modern RC frame structures.

Economic losses and fatalities provide additional measures of structural performance, in addition to the collapse performance metrics described in Chapter 5. Data related to earthquake-induced economic losses and fatalities serves as input to Chapter 7, which examines the cost-effectiveness of retrofitting or replacing the non-ductile RC frame structures. Estimations of fatalities are used to quantify the discrepancies in safety between modern and existing RC frame structures. An additional benefit to retrofit or replacement is reduced financial losses in future earthquakes.

Appendix 6.1 Prediction of Fatalities in Modern RC Frame Structures

Table A6.1 Fatality predictions for complete set of modern RC frame structures, including all code-conforming structures designed by Haselton (2006).

Design ID	Num. of Stories	Framing System	Total Num of Occupants[1]	EANF ($x10^{-3}$)	Normalized EANF (%)
2061	1	S	88	0.48	0.0005
2062			88	0.31	0.0003
2063			88	0.47	0.0005
2069		P	88	1.28	0.0014
1001	2	S	173	0.41	0.0002
1001a			173	0.40	0.0002
1002			173	0.83	0.0005
2064		P	173	1.73	0.0010
1003	4	P	346	2.70	0.0008
1004			346	2.03	0.0006
1008		S	346	1.28	0.0004
1009		P	346	1.80	0.0005
1010		S	346	0.54	0.0002
1011	8	P	461	8.33	0.0018
1012		S	461	3.08	0.0007
1022			461	3.15	0.0007
2065			461	2.85	0.0006
2066			461	2.03	0.0004
1023			461	5.70	0.0012
1024			461	5.78	0.0013
1013	12	P	692	9.90	0.0014
1014		S	692	9.38	0.0014
1015			692	5.78	0.0008
2067			692	5.63	0.0008
2068			692	5.70	0.0008
1017			692	8.48	0.0012
1018			692	9.30	0.0013
1019			692	3.75	0.0005
1020	20	P	1152	12.08	0.0010
1021		S	1152	6.23	0.0005
			Average	4.0	0.0008

[1]Weekday, daytime occupancy. These values reflect a 120 ft. x 180 ft. footprint for the shorter buildings and a 120 ft. x 120 ft. footprint for the taller buildings (≥ 8 stories).

Appendix 6.2 Photo Database of Collapsed or Nearly Collapsed RC Structures

Database of 84 photos of collapsed or partially collapsed multi-story RC frames, assembled from field reconnaissance studies of 11 deadly earthquakes: Alaska (1964), San Fernando, CA (1971), Mexico City, Mexico (1985), Costa Rica (1991), Northridge, CA (1994), Kobe, Japan (1995), Izmit, Turkey (1999), Gujarat, India (2001), Bingol, Turkey (2003) and Pakistan (2005). Sources included the Earthquake Engineering Research Center's EQIIS database (EERC 2007), U.S. Geological Survey damage photos (USGS 2006), and published journal articles including Mitchell and Tinawi (1992), Mitchell et al. (1995), Mitchell et al. (1996), Su (2001) and Dogangun (2004), and are listed for each photo at the end of the photos.

Earthquake: Alaska (1964)

Earthquake: San Fernando, California (1971)

Earthquake: Mexico City (1985)


(5)


(6)


(7)


(8)


(9)


(10)


(11)


(12)

Earthquake: Costa Rica (1991)


(13)


(14)


(15)

Earthquake: Northridge, California (1994)


(16)


(17)


(18)


(19)

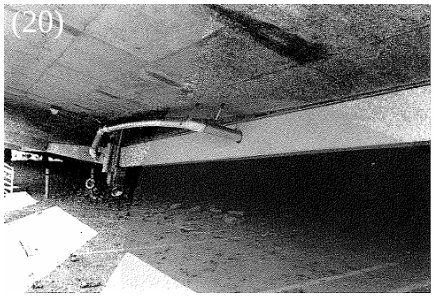
(20)


(21)


(22)


(23)


(24)


(25)


(26)


(27)


(28)


(29)


(30)


(32)


(33)

Earthquake: Kobe, Japan (1995)


(34)


(35)


(36)


(37)

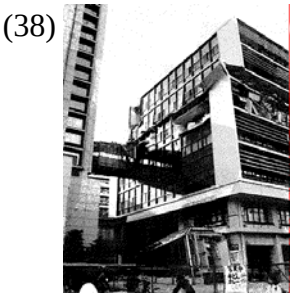
(38)

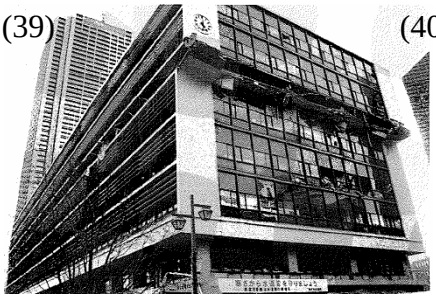
(39)

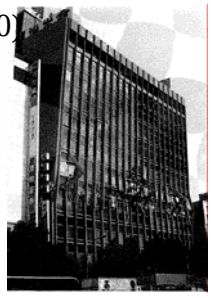
(40)

(41)

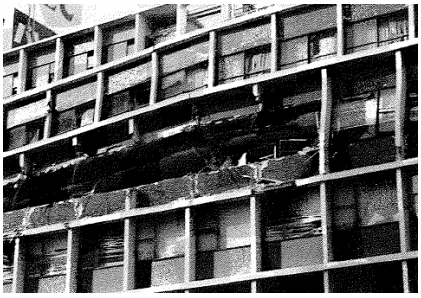

(42)

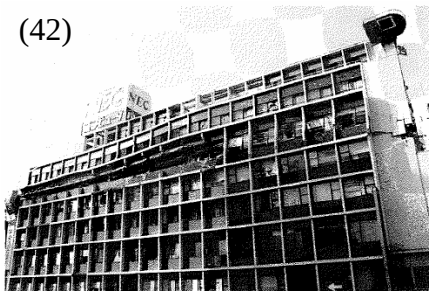

(43)

(44)

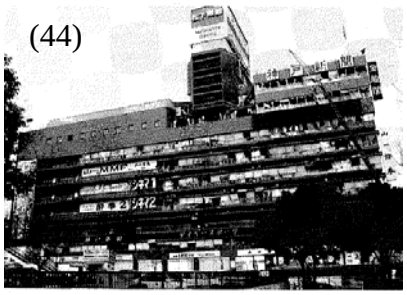

(45)

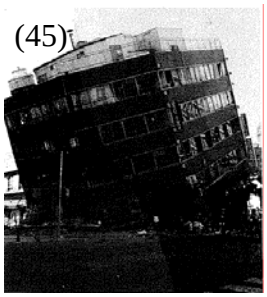

(46)

(47)

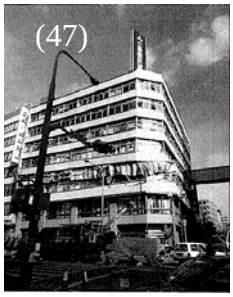

Earthquake: Duzce, Turkey (1999)

(48)

(49)

(50)

(51)

(52)

(53)

(54)

(55)

(56)


(57)


(58)


(59)


(60)


(61)


(62)


(63)

Earthquake: Bingol, Turkey (2003)


(64)


(65)


(66)


(67)

Earthquake: Chi Chi, Taiwan (1999)

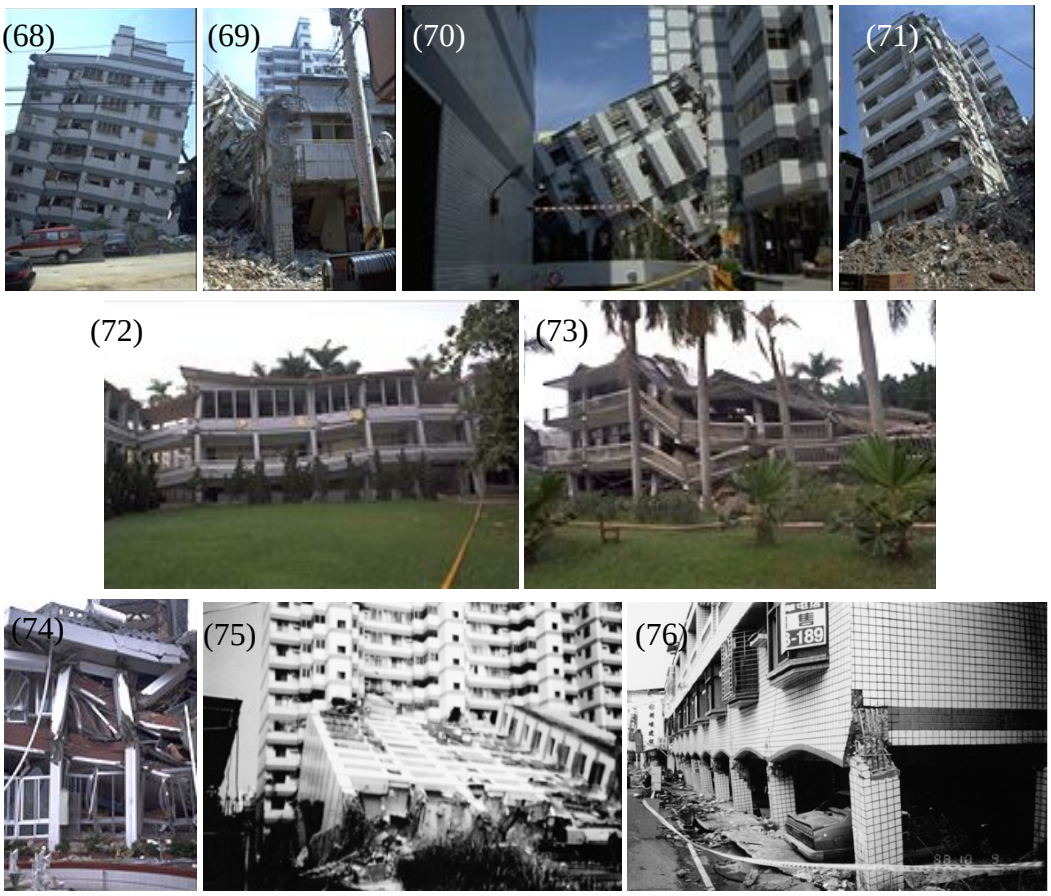

Earthquake: Gujarat, India (2001)

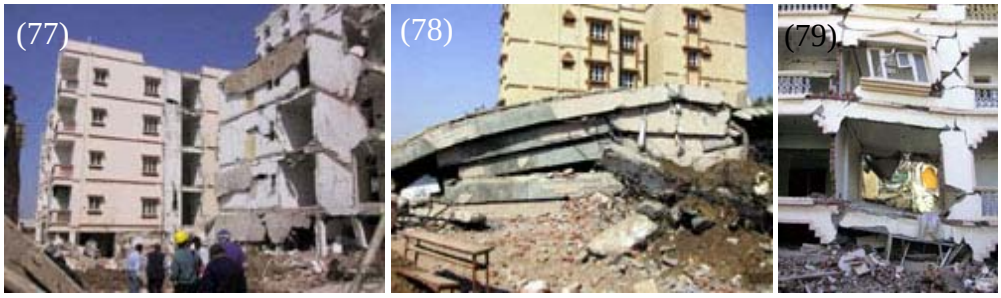

Earthquake: Pakistan (2005)

Sources

Photos 1 – 10. EQIIS Database. (EERC 2007). 11. USGS Database (USGS 2006). 12. Unknown 13 – 15. (Mitchell and Tinawi 1992). 16 – 18. EQIIS Database. 19 - 20. (Mitchell et al. 1995). 21 - 22. EQIIS Database. 23. (Mitchell et al. 1995). 24 – 30. EQIIS Database. 31 - 33. (Mitchell et al. 1995) 34 – 37. EQIIS Database. 38 – 47. (Mitchell et al. 1996). 48. USGS Database. 49 – 63. EQIIS Database. 64 – 67. (Dogangun 2004) 68 – 74. EQIIS Database (EERC 2007) 75 – 76. (Su 2001) 77 – 84. Unknown.

Chapter 7

Cost-Benefit Assessment of Replacing or Retrofitting Non-Ductile Reinforced Concrete Frame Structures

7.1 Overview

Evidence from previous chapters shows that non-ductile (1967) reinforced concrete (RC) moment frames in California have significantly higher collapse rates than modern (2003) reinforced concrete structures and, as a result, pose a more significant threat to life safety. Their owners can also expect to pay substantially more to repair seismic damage in future earthquakes. These seismic deficiencies could be mitigated by either retrofitting or replacing deficient existing RC moment frames. In this chapter, the costs and benefits of either (a) replacing these structures or (b) retrofitting these structures are quantified in dollar terms. Several retrofit strategies are considered, including fiber-wrapping RC columns, jacketing columns with well-confined reinforced concrete or constructing shear walls to provide additional lateral resistance. Cost-benefit analysis is used to assess the economic efficiency of retrofit or replacement of vulnerable structures, accounting for the benefits of improved safety, the benefits of reduced repair costs and the costs of implementing these seismic improvements. The cost-benefit assessment does not account for business interruption due to closure or repairs.

These evaluations of retrofit and replacement of non-ductile RC frame structures are valuable for examining the effectiveness of policy alternatives for reducing the seismic risk associated with these structures. In the latter part of this chapter, several examples of policies that could be implemented by state or local government are investigated. Results from performance-based engineering analysis are used to quantify potential improvements in safety resulting from mandatory or voluntary programs for retrofit or replacement of vulnerable non-ductile RC frame structures. Seismic performance data also provide meaningful insights into the policy implementation process, by calling attention to the importance of providing financial and other incentives to building owners, of establishing a

procedure through which the most vulnerable structures can be identified, and of developing quantifiable requirements for seismic performance of retrofitted structures. Societal goals for seismic safety are the topic of the final section of the chapter.

7.2 Replacement of Non-Ductile Reinforced Concrete Frame Structures

7.2.1 Design of Modern Reinforced Concrete Frame Structures

One option for mitigating the seismic hazard posed by non-ductile RC moment frames in California is to replace these structures with modern RC frames that comply fully with current building code requirements. Code-conforming special moment frames have demonstrated superior seismic performance to existing non-ductile moment frames due to more stringent design and detailing requirements. Brittle shear failure in columns and joints is prevented by capacity design provisions, strong column-weak beam ratios delay collapse by spreading damage and deformations over the height of the structure, and closely spaced transverse stirrups and anchorage on stirrup hooks improve the confinement of plastic hinge regions.

The archetypical code-conforming (2003) special moment frames that could be used to replace 2, 4, 8 and 12-story existing (1967) RC moment frames are listed in Table 7.1. Each of these structures has been designed by Haselton (2006) according to the relevant building standards in the International Building Code (ICC 2003), including ASCE 7 (2002) and ACI (2002). The structures are designed for a Los Angeles site with a maximum considered earthquake S_1 = 0.90g. Nonlinear analyses use the same archetype analysis models described in Chapter 5, but with modifications to material model parameters to account for differences in strength and ductility from the non-ductile RC frame structures, as described in Chapter 3. For details on design and modeling of these structures, see Chapter 5 and Haselton (2006).

7.2.2 Replacement Costs

The costs of replacing an older RC frame office building with one that is constructed to meet the requirements of modern building codes are estimated in Table 7.2 (repeated from Table 6.2). As described in Chapter 6, these replacement costs are given in 2006 dollars and obtained using RS Means Building Construction Costs (Waier 2005). These estimates account for construction costs in Los Angeles associated with all significant structural and nonstructural components, including HVAC systems, partitions and interior finishes, exterior

enclosures, services, and basements (for 8- and 12-story buildings). The new structures are assumed to have typical quality of finishes. The estimates include a 25% contractor fee, but no additional fees related to permitting, administrative/management costs, and financing, which can increase construction costs by 25 to 100% (Reis 2007/2008). The costs associated with demolishing the existing structure and of interrupting business or tenants while construction is carried out are also excluded. It is therefore expected that the replacement costs used here provide a lower bound on the true cost of replacement.

Table 7.1 Design parameters for archetype modern (2003) RC frame structures.

Design ID	Num. of Stories	Bay Width (ft)	Framing System
1001	2	20	Space
2064		20	Perimeter
1008	4	20	Space
1003		20	Perimeter
1012	8	20	Space
1011		20	Perimeter
1014	12	20	Space
1013		20	Perimeter

Table 7.2 Estimated replacement costs for non-ductile RC archetype buildings.

Num. of Stories	Framing System	Total Cost ($, millions)	Cost per sq. foot ($)
2	space	6.1	140.4
	perimeter	6.5	150.7
4	space	12.5	144.4
	perimeter	12.0	138.3
8	space	19.9	172.7
	perimeter	19.4	168.4
12	space	29.1	168.4
	perimeter	28.1	162.6

7.2.3 Performance Metrics for Modern Reinforced Concrete Frame Structures

Probabilistic assessments of earthquake-induced collapse, economic losses and fatalities for modern RC frame structures are conducted following the procedures described in Chapters 5 and 6 and follow all of the same assumptions regarding treatment of spectral shape, modeling uncertainties, and non-simulated failure modes. Table 7.3 summarizes the seismic performance of modern RC frame structures in terms of the mean annual frequency of collapse ($\lambda_{collapse}$), expected annual losses (EAL) and expected annualized number of fatalities (EANF). All performance metrics are based on the ground motion hazard predicted for a specified non-near fault site in Los Angeles for which probabilistic seismic hazard analysis has been conducted by Goulet et al. (2007). Compared to existing non-ductile

frames (for which performance metrics are reported in Table 7.4), the modern code-conforming structures are less likely to be damaged in future earthquakes, reducing economic losses due to seismic damage incurred by the owner, and less likely to collapse, lessening the life safety threat to building occupants. Interested readers should refer to Haselton (2006) and Chapters 5 and 6 for details on the collapse assessment and loss and fatality estimation.

Table 7.3 Metrics for earthquake-induced collapse, economic losses and fatalities in modern (2003) RC frame structures.

Building Design			Collapse[1]	Economic Losses[2]	Fatalities[3]
Design ID	Num. of Stories	Framing System	$\lambda_{collapse}$ x 10^{-4}	EAL (% of replacement costs)	EANF x 10^{-3}
1001	2	Space	1.0	1.04%	0.4
2064		Perimeter	3.4	0.96%	1.7
1008	4	Space	1.7	1.09%	1.3
1003		Perimeter	3.6	1.18%	2.7
1012	8	Space	2.4	1.26%	3.1
1011		Perimeter	6.3	1.01%	8.3
1014	12	Space	4.7	1.05%	9.4
1013		Perimeter	5.2	0.77%	9.9

[1] $\lambda_{collapse}$ is the mean annual frequency of collapse, defined in Chapter 5. It can be interpreted as a collapse rate, ie. collapses per year.

[2] EAL are expected annual losses, defined in Chapter 6. The losses are normalized by the replacement cost of the structure.

[3] EANF are expected annual fatalities, defined in Chapter 6.

Table 7.4 Metrics for earthquake-induced collapse, economic losses and fatalities in existing (1967) RC frame structures.

Building Design			Collapse	Economic Losses	Fatalities
Design ID	Num. of Stories	Framing System	$\lambda_{collapse}$ x 10^{-4}	EAL (% of replacement costs)	EANF x 10^{-3}
3001	2	Space	109	5.20%	41
3002		Perimeter	47	3.16%	24
3004	4	Space	107	2.29%	62
3003		Perimeter	100	2.30%	97
3016	8	Space	64	1.79%	77
3015		Perimeter	135	2.07%	141
3023	12	Space	50	1.62%	75
3022		Perimeter	119	1.64%	192

7.2.4 Cost-Benefit Assessment of Replacing Non-Ductile Reinforced Concrete Frame Structures

Cost-benefit assessment is used to evaluate the tradeoffs involved in replacing or seismically strengthening non-ductile RC frame structures, by comparing the costs of retrofit or replacement with the benefits of improved seismic performance. Benefits are measured in terms of reduced economic losses and fatalities in future earthquakes. The outcome of the cost-benefit assessment is the cost-benefit ratio, a ratio of the costs of retrofitting or replacing

a hazardous older RC frame structure to the benefits (also given in dollars). Cost-benefit ratios less than 1 indicate that mitigation action is cost-effective. All costs and benefits reported in this study are expected values.[1] This assessment assumes a risk-neutral decision maker whose risk attitude is constant regardless of the magnitude of losses, though our society may be risk averse due to the potentially catastrophic nature of the earthquake risk.

The use of cost-benefit assessment presumes that the risks imposed by seismic collapse of RC frame structures fall within the range in which economic analysis is appropriate (Pate-Cornell 1994). Below some threshold level of risk, known as the *de minimis* criterion, risks are small enough that they do not matter. Above another threshold risk value, potential consequences are intolerably high, justifying extreme precaution. Cost-benefit analysis is most applicable in the intermediate region, where significant constraints on resources exist, forcing prioritization of mitigation strategies (Pate-Cornell 1994; Pate-Cornell 2002). The use of cost-benefit analysis here is consistent with previous efforts as a society to mitigate seismic hazards in California, which have occurred either where the risks were perceived to be particularly high, the case with unreinforced masonry construction, or where mitigation is relatively inexpensive, as in the various parapet ordinances throughout the state. Language in the California Multi-Hazard Mitigation Plan explicitly encourages "cost-effective mitigation" (California Office of Emergency Services 2004).

The benefits of replacing existing non-ductile RC frame structures are the seismic performance improvements gained, as summarized in Table 7.5. These benefits include reduced mean annual frequency of collapse, reduced expected annual losses and reduced expected annual number of fatalities. In Table 7.5, the performance improvements are couched in terms of the remaining life span of the structure, assumed to be 50 years. Replacing a non-ductile reinforced concrete frame structure is predicted to save an owner (in avoided losses) between 2.7 and 6.5 million dollars in reduced seismic repair costs alone. Likewise, between 2 and 9 fatalities are avoided over the lifetime of the structure. There is significant variability in the benefits predicted for different structures, with bigger increases in performance between older and replaced structures for some heights and framing systems than others. Due to the high predicted percentage of economic losses in the non-ductile 2-story RC space frame structure, for example, the potential savings from reducing earthquake-

[1] Cost-benefit analysis is sometimes referred to as benefit-cost analysis. The formulations are identical, except that one presents the ratio of costs to benefits and the other uses the ratio of benefits to cost.

induced damage are significantly higher than for the other structures (4.2% of replacement cost, compared to 0.5 to 2.2% for the other structures).

Table 7.5 Expected value of benefits from replacing non-ductile RC frame structures.

Num. of Stories	Framing System	Reduction in $\lambda_{collapse}$ (x 10^{-4})	Reduction in EAL[2] (% of replacement costs)	Reduction in EANF (x 10^{-3})	Present Value of Losses Avoided in 50 years[1] ($ millions)	Lives Saved in 50 years[3]
2	Space	108	4.16%	40	6.5	2.0
	Perimeter	44	2.20%	22	3.7	1.1
4	Space	105	1.20%	61	3.9	3.1
	Perimeter	96	1.12%	95	3.5	4.7
8	Space	62	0.53%	74	2.7	3.7
	Perimeter	129	1.06%	133	5.3	6.6
12	Space	45	0.57%	66	4.2	3.3
	Perimeter	114	0.87%	182	6.3	9.1

[1] Assuming a real interest rate of 3%, as in Chapter 6.

[2] Includes direct economic losses only.

[3] Lives not discounted here (see discussion below).

In order to compare costs and benefits, the benefits of retrofit or replacement of older structures must be quantified in economic terms. To account for the benefits of saving lives, a value per life is assigned, which can be interpreted as the amount our society is willing pay to save a life. Assigning dollar values to lives is controversial because it commodifies human life, but our society has limited resources to invest in public safety and evaluation of the economic efficiencies of various policies and regulations is needed to prioritize spending. Acceptable risks and the willingness of industries to pay to prevent life safety threats vary significantly depending on the type of risk, but in engineering cost-benefit assessment human life is typically valued between $2 and $5 million dollars (Pate-Cornell 1994; Porter et al. 2006b). The Federal Highway Administration's Technical Advisory on Motor Vehicle Accident Costs uses a value of $2.6 million per life (in 1994 dollars) (Mitrani-Reiser 2007). Another approach computes the value of life or the implied cost of averting a fatality based on the life quality index, which is related to a country's per capital gross domestic product and life expectancy. These analyses result in a value of $0.5 - $0.6 million per life saved (Rackwitz 2004). More recently, the September 11th victim compensation fund awarded an average of $2 million dollars to relatives of the deceased in the 9/11 terrorist attacks (Feinberg et al.). For the purposes of this study, it is assumed that human life is valued at $2 million dollars per life, implying that our society is willing to spend $2 million dollars to prevent one future death. This valuation is assumed to be constant for all people, and is not dependent on a victim's remaining life span, future earnings or other factors.

The dollar losses associated with fatalities must5 be appropriately discounted to account for the time value of money. This discounting implies that we are willing to invest more to

prevent loss of life today than to prevent a life being lost some time in the more distant future. Although controversial, discounting the 'value of life' is needed to ensure that individuals exposed to the same level of risk at different points of time have the same protection, provided that one assumes that there is investment such that improved life-saving technologies are available in the future. For consistency, the same discount rate used for economic losses is applied to the 'value of life' (Pate-Cornell 1984; Pate-Cornell 1985; Pate-Cornell 2004). A discount rate of 3% is used in this study. Values between 2 and 7% are frequently used for public safety projects, though Rackwitz (2004) suggests that a lower value (1.6% to 2.3%) is likely more appropriate given observed economic growth rates.

The costs and benefits of replacing non-ductile RC frame structures in high seismic areas of California are reported in Table 7.6. As mentioned above, the analysis summarized in Table 7.6 assumes each life saved is worth $2 million dollars and applies a discount rate of 3% to all losses. The benefits of replacing non-ductile RC frames are calculated assuming that structures have a remaining usable lifespan of 50 years and are computed in three different ways: (i) accounting only for reduction in seismically induced repair costs ("economic losses"), (ii) accounting for both the reduction in economic losses and the lives saved, and (iii) accounting for reduced economic losses, lives saved and reduced downtime. Downtime losses are included for illustration purposes only and approximated based on data from computed downtime losses in 4-story RC frame structures by Mitrani-Reiser (2007).[2] This approach to estimating downtime is simplistic, but is used to obtain an initial estimate of the effect of including building interruption modeling in cost-benefit assessments.

The cost-benefit ratio is highly dependent on the definition of benefits used in the assessment. Accounting only for savings related to repairing damage, and neglecting the benefits of saving lives, replacing non-ductile RC frame structures is not cost-effective, as shown in the top section of Table 7.6. The potential savings in earthquake-related repair costs are sufficient to warrant investment in replacing only the 2-story space frame structure. The cost-benefit assessment in the top section of Table 7.6 is shown primarily for illustration purposes, as benefits should account for saving lives. When savings due to repair costs and

[2] Mitrani-Reiser's estimates of downtime include the time needed to complete the repair effort and account also for the effects of financial, economic and regulatory uncertainty. Taking Mitrani-Reiser's results, Table 7.6 assumes that estimated annual losses due to downtime in both existing and replaced reinforced concrete frame structures are approximately 30% of expected annual losses due to repair costs. These estimations should not be taken as actual predictions of downtime losses, and are included in Table 7.6 for illustration only.

fatalities are considered, in the middle section of Table 7.6, cost-benefit ratios decrease, but still only the 2-story space frame structure has a cost-benefit ratio less than 1. For the other structures, the cost of replacement exceeds the computed benefits of replacement, implying that the cost per life saved exceeds the assumed $2 million dollars. Approximately 40% to 60% of the computed benefits reported in the middle section of Table 7.6 results from improved safety, i.e. reduction in fatalities. The cost-benefit ratios are even lower in the bottom section of Table 7.6, where benefits are increased by accounting for downtime in the assessment. However, even considering all three benefits, the economic assessment only justifies replacement of the two two-story buildings. The downtime estimates provided here are approximate, since they are based on a previous study of a 4-story modern RC frame structure (Mitrani-Reiser 2007). Research is ongoing to improve models of downtime prediction, e.g. (ATC 2007). Since the downtime estimates are approximate, benefits are computed due to reduced earthquake-related repairs costs and fatalities for the remainder of this chapter.

Table 7.6 Comparison of costs and benefits of replacing non-ductile RC frame structures.

Num. of Stories	Framing System	Cost of Replacement ($, millions)	Benefits of Replacement ($, millions)	Cost-Benefit Ratio
Benefits: Reduction in economic losses only				
2	Space	6.1	6.5	0.9
	Perimeter	6.5	3.7	1.8
4	Space	12.5	3.9	3.2
	Perimeter	12.0	3.5	3.5
8	Space	19.9	2.7	7.3
	Perimeter	19.4	5.3	3.7
12	Space	29.1	4.2	6.9
	Perimeter	28.1	6.3	4.5
Benefits: Reduction in economic losses and fatalities				
2	Space	6.1	8.6	0.7
	Perimeter	6.5	4.8	1.4
4	Space	12.5	7.0	1.8
	Perimeter	12.0	8.3	1.4
8	Space	19.9	6.5	3.1
	Perimeter	19.4	12.1	1.6
12	Space	29.1	7.6	3.8
	Perimeter	28.1	15.6	1.8
Benefits: Reduction in economic losses, fatalities and downtime				
2	Space	6.1	10.5	0.6
	Perimeter	6.5	5.9	1.1
4	Space	12.5	8.2	1.5
	Perimeter	12.0	9.4	1.3
8	Space	19.9	7.3	2.7
	Perimeter	19.4	13.7	1.4
12	Space	29.1	8.9	3.3
	Perimeter	28.1	17.5	1.6

The calculated cost-benefit ratios vary significantly among the different heights and framing systems considered. Ranked in terms of economic efficiency, the 12-story space frame shows the least benefits from replacement. Due to design characteristics that make the 2-story non-ductile space frame likely to incur particularly high economic losses, replacement of that structure is the most cost-effective. In general, the cost-effectiveness of replacement decreases with height. For taller buildings, normalized losses tend to be smaller, as damage concentrates primarily in lower stories. This damage concentration is particularly apparent in non-ductile RC frame structures, which lack design provisions that spread deformations over the height of the structure. Therefore, as the number of stories in a building increases, losses in non-ductile RC frame structures decrease more quickly than losses in ductile RC frame structures, reducing the relative differences in predicted economic losses. However, the economic losses neglect the costs associated with building closure if a structure is red-tagged. Where taller non-ductile buildings have large residual drifts, the building closure may exceed other contributors to economic losses and the trend with height may be less apparent.

An alternate presentation of the results of cost-benefit assessment is provided in Figure 7.1, which illustrates the relationship between the projected replacement cost and the computed cost-benefit ratio. Logically, the cost-benefit ratio increases as the projected cost of replacement increases. The replacement cost that results in a cost-benefit ratio equal to 1 can be interpreted as the maximum amount we would be willing to pay for replacement to achieve the quantified benefits in seismic performance. According to this analysis, benefits associated with replacement of the 2-story structure are worth spending approximately $200 per square foot to replace the structure, whereas for the 4-story structure they are worth spending only $80 per square foot. Figuring a typical replacement cost on the order of $200 per square foot, only the 2-story building is a viable replacement candidate.

If a $2 million value of life is insufficient to warrant replacement of most of these non-ductile RC frame structures, it is possible to evaluate how much we would need to be willing to pay per life saved in order to make these replacements neutral from a cost-benefit standpoint. Cost-benefit ratios for replacing the buildings are illustrated in Figure 7.2, as a function of the assumed 'value of life'. As the 'value per life' increases and we are willing to pay more for each life saved, replacement becomes increasingly economically feasible. Of the space frames (Figure 7.2a), replacement of the 2-story space frame is a good economic investment, even without accounting for the improvements in life safety. Neutral cost-benefit

assessment of the 4-story and 8-story space frames requires spending $5.5 and $9.5 million dollars per life saved, respectively. In contrast, the 12-story space frame is not an economically efficient investment, even when human life is valued at $10 million. There is considerably less variability in the results for perimeter frames (Figure 7.2b), which generally have high risks of collapse and hence lower economic thresholds to achieve a cost-benefit ratio less than 1. As shown, replacing the non-ductile perimeter frames would imply costs of between $4 and $5 million dollars per life saved.

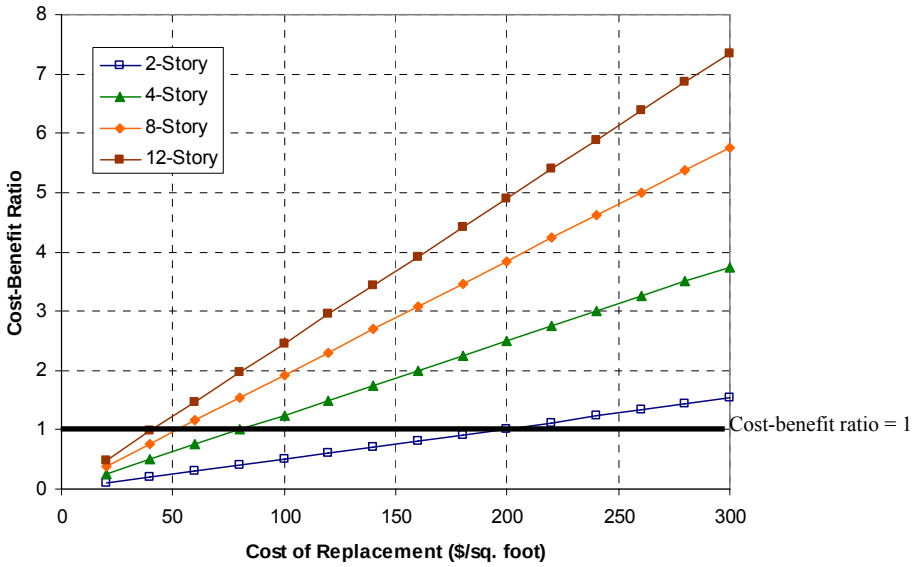

Figure 7.1 Cost-benefit ratio for RC space frame structures as a function of the projected cost of replacing the structure. Benefits include reduction in fatalities and economic losses.

The results shown in Figure 7.2 reflect typical characteristics of non-ductile RC moment frames designed in accordance with the 1967 Uniform Building Code. Even among these regular archetypical buildings, there is significant variation in the outcome of cost-benefit assessment. In reality, of the non-ductile RC moment frames existing in California, these archetype structures probably represent a subset of average or above average seismic performance, since they are all regular structures that are designed in accordance with the building code and are assumed to be constructed to high quality standards. Real buildings may have irregularities in plan or elevation due to architectural constraints, construction deficiencies, or age related deterioration that are likely to have lead to higher predictions of seismic-related losses and fatalities.

This variation in the design and construction of older RC frame structures impacts the outcome of cost-benefit assessment. To examine the effects of design variability it is assumed that the archetypical perimeter frame structures result in average (μ) cost-benefit assessment,

and that variation in design features in the existing building stock leads to a coefficient of variation of 0.50 in the computed cost-benefit ratio. This coefficient of variation is based on previous studies of the effect of uncertainties in design, construction, and modeling on collapse. Looking at a 4-story modern RC frame structure, Haselton (2006) used FOSM reliability methods to determine that design variability in that structure was associated with a logarithmic standard deviation (σ_{ln}) of 0.26. The ATC-63 project assumes that the logarithmic standard deviation associated with modeling and design varies between 0.28 and 0.64 (ATC 2007). In ATC-63, design uncertainty accounts for variability in the design of a particular structure and in the archetype design space. These results are extended to obtain the assumed coefficient of variation of 0.50 in cost-benefit ratios for this study.[3]

The effect of design and construction variability on cost-benefit assessment is illustrated in Figure 7.3. The results for the average plus or minus one standard deviation ($\mu \pm \sigma$) therefore represent worse-case (i.e., $\mu - \sigma$) and better-case designs (i.e., $\mu + \sigma$). The conclusion regarding the cost-effectiveness of replacing non-ductile RC frame structures alters dramatically depending on whether the structure of interest is a 'worse', 'average' or 'better' building. Assuming that human life is valued at $2 million dollars, the resulting cost-benefit ratio is 0.8 for a worse-case building, suggesting that replacement is a worthwhile investment. For the average structures, as discussed previously, closer to $5 million dollars needs to be expended per life saved. This evidence points to the importance of targeting mitigation efforts at the most dangerous non-ductile RC moment frames.

Identifying the worst of California's non-ductile RC frame structures as candidates for replacement remains a challenge. Some of the poorest performing structures can be identified on the basis of an archetype study such as the one considered here, e.g. the 2-story space frame structure shown in Figure 7.2a. Other structures, such as T- and L-shaped structures, are vulnerable due to configuration issues in plan and elevation. Creation of simulation models to develop criteria for identifying these buildings is a topic for future research. The worst performing non-ductile RC frame structures may be the result of human error in design and construction. These buildings will be difficult to locate without a building-specific examination of design drawings and as-built conditions. Other non-ductile RC frame structures may be particularly vulnerable because of their location. The

[3]The coefficient of variation of a lognormally distributed random variable is approximately equal to the logarithmic standard deviation.

assessments conducted here assume that the structures is located at a typical high seismic, but not near-field site with stiff soil/rock (Goulet et al. 2007). Structures near to faults or on soft soils are also likely to be riskier - and hence better candidates for replacement.

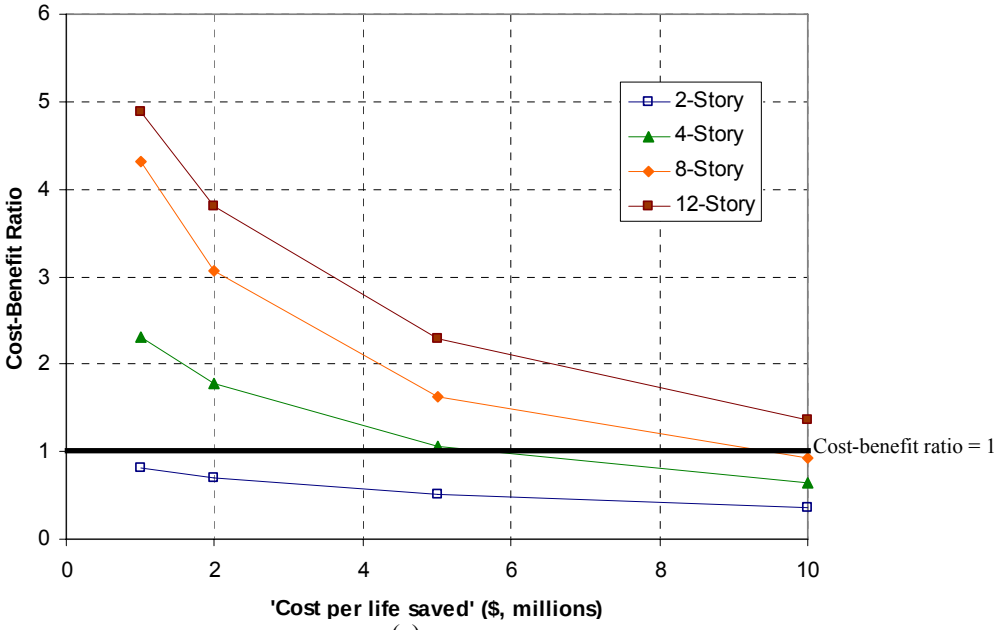

(a)

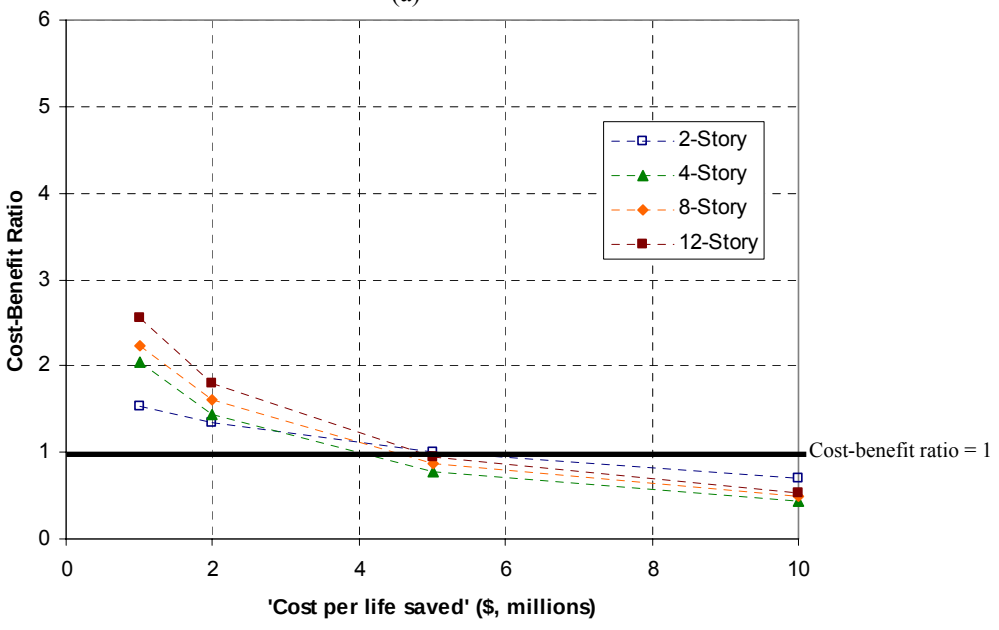

(b)

Figure 7.2 Effect of value of human life on cost-benefit assessment of replacing (a) non-ductile RC space frame structures of different heights and (b) non-ductile RC perimeter frame structures of different heights.

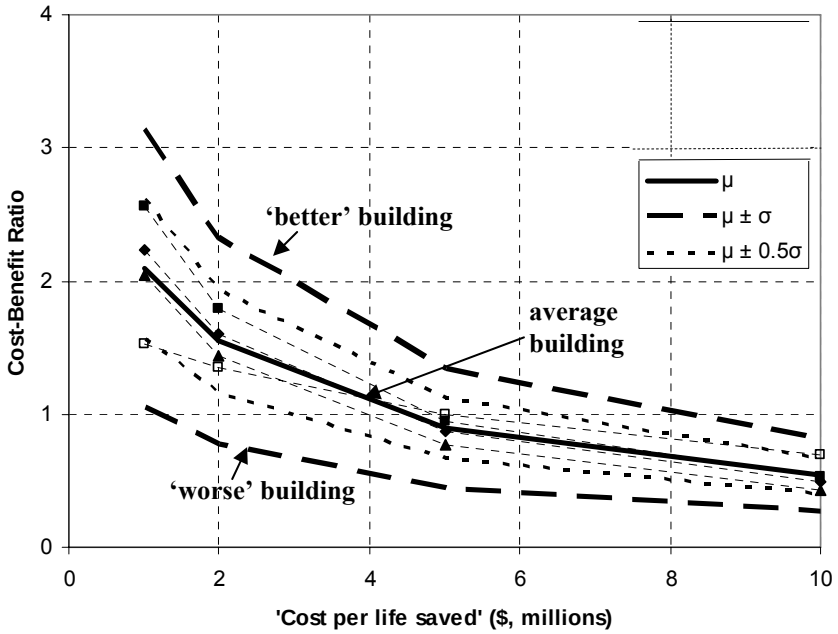

Figure 7.3 Effect of design variability on cost-benefit assessment of replacing non-ductile RC frame structures. Original data is for perimeter RC frames of 2, 4, 8 and 12 stories. Average, better and worse buildings are based on assumptions given in the paragraph above.

Figure 7.4 and Figure 7.5 examine how other underlying assumptions related to interest rates and the useful life expectancy of the building affect the outcome of the cost-benefit assessments. As real interest rates increase, shown in Figure 7.4, replacing existing non-ductile RC frame structures becomes less cost-effective. With higher interest rates, investments gain in value more quickly, reducing the present value of future losses. The actual interest rate fluctuates, and depends on the health of the U.S. economy and other factors. The proposed discount rate of 3% is based on historical values of inflation and interest rates on corporate bonds in the U.S. (Nuti and Vanzi 2003).

If the structure is expected have a longer remaining service life, as shown in Figure 7.5, the cost-benefit ratio decreases. Conversely, it decreases for a shorter life. However, the curve flattens as the assumed time horizon increases due to compounding effects of investments, so that in most cases time alone will not make these investments in seismic improvement pay off. After about 50 years, the present value of future benefits saturates (Figure 7.5). Some existing structures may be reaching the end of their useful life span and be slated for replacement in 5 or 10 years. For these structures, a shorter time horizon is justified in cost-benefit assessment. Owners who plan to quickly resell a structure may also be interested in a different time period for assessment unless resale values reflect the safety

(or perceived safety) of the structure. New owners may be willing to pay more if they benefit from improved financing and insurance options associated with a safer structure.

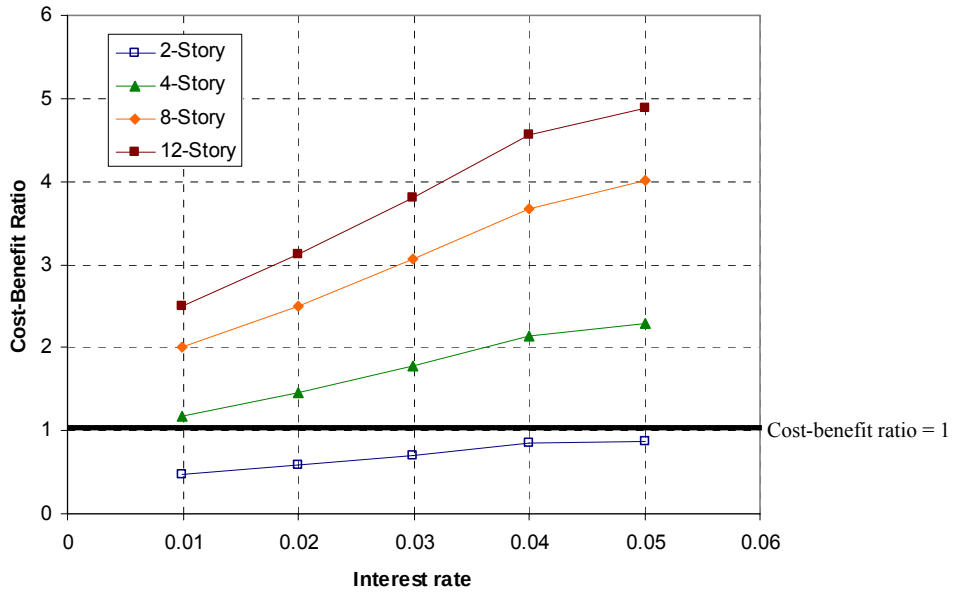

Figure 7.4 Effect of assumed interest rate on cost-benefit assessment of RC space frame structures of different heights.

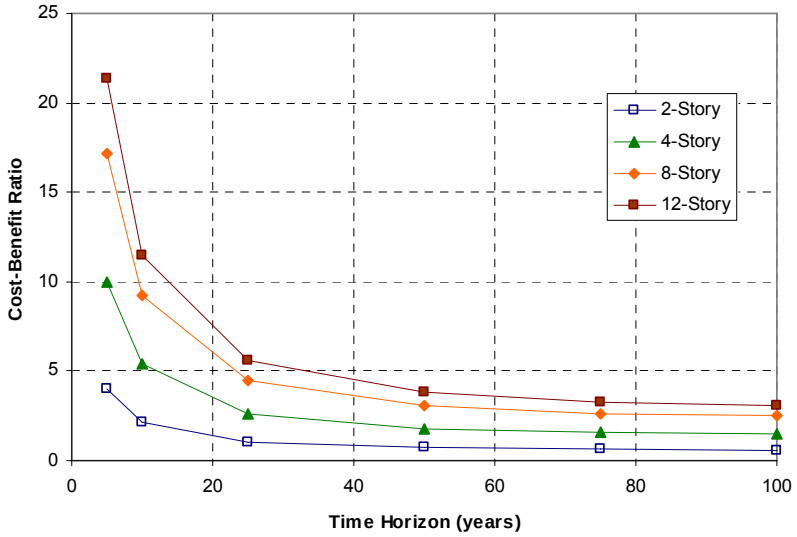

Figure 7.5 Effect of assumed time horizon on cost-benefit assessment of replacing RC space frame structures of different heights.

As demonstrated in the tables and figures above, there is a marked difference in seismic performance between existing non-ductile structures and the performance of these structures if they were replaced by modern, code-conforming structures. However, in all except one case the potential savings to the owner is less than the cost of replacing the building. Justifying these investments economically, therefore, requires some willingness to pay to save lives. The cost per life saved depends on the building, but the typical values of cost per life saved are on the order of $4 to $5 million. These results reflect the costliness of

construction and the expected frequency of earthquakes in California. It is further noted that while costs and benefits are directly compared here, the benefits and costs are not necessarily borne by the same person or organization. The costs of replacing the existing structure are likely to be incurred by the owner, and while reduction in future seismic repair costs benefits the owner, the reduced life safety hazard of the structure is of broader benefit to society. As a result of the high costs and the inequitable distribution of costs and benefits, either governmental financial assistance or rigid regulations are likely needed to encourage building owners to replace their structures.

This type of cost-benefit assessment provides a valuable tool for examining the advantages and disadvantages of *replacing* existing non-ductile RC frame structures in order to prioritize seismic safety decisions and to enumerate the costs associated with protecting human life. The same procedure is utilized for evaluating the costs and benefits of *retrofitting* non-ductile frame structures in Section 7.3.

The evaluation of cost-effectiveness depends on the underlying assumptions used in generating the assessments. In this study, the costs do not include the cost of demolition[4], the administration project costs, or the cost of disrupting business while construction activity is ongoing, leading to an underestimation of replacement costs. Benefits are also underestimated where the effect of downtime is neglected, which may make a significant contribution to overall savings, as shown in Table 7.6 and by Comerio (2006) and Mitrani-Reiser (2007). In certain cases, a building may be 'red-tagged' and closed while inspections and repairs are made. Building closure may occur even if significant portions of the structure are not damaged if residual drifts are large or egress is blocked. Reduction in building closure time is another possible benefit from replacing non-ductile RC frame structures. Additionally, the assessment neglects the many significant non-seismic motivations that owners may have for renovating buildings. For example, hospital owners may choose to upgrade their structures to provide state-of-the-art facilities and keep up with new technologies. These are benefits due to replacement that are not directly related to seismic performance, and are excluded from the analysis in this study. Nonfatal injuries are not included, and reduction in these injuries may contribute to benefits of replacement, depending on the assessed decrease in the number of injuries and the dollar value associated

[4] Demolition costs are also not included in the earthquake losses on the benefits side of the calculations so their inclusion is not expected to significantly alter the results.

with avoiding injuries (ranging perhaps from 0.25% to 100% of the value of human life, depending on the severity of injuries) (Porter et al. 2006). Also not quantified in the cost-benefit assessment here are indirect economic impacts and the broader benefit to public well-being resulting from protecting buildings and infrastructure, making our communities, cities and economic systems more seismically resilient.

7.3 Retrofit of Non-Ductile Reinforced Concrete Frame Structures

7.3.1 Overview and Approach

Retrofit or seismic upgrading of non-ductile reinforced concrete frame structures can also mitigate the seismic hazard posed by these structures. In this section, the effect of retrofitting on the seismic performance of non-ductile RC frames is examined. Depending on the extent of the retrofit effort, retrofitted frames are expected to have an intermediate level of seismic performance, between the unretrofitted existing non-ductile RC frame structures and code-conforming RC frames, as illustrated in Figure 7.6. The benefits of retrofitting existing non-ductile RC frame structures are quantified in terms of seismic collapse performance, economic losses and fatalities. By comparing these benefits with typical costs of retrofit, the cost-effectiveness of retrofitting vulnerable non-ductile RC frame structures as a seismic hazard mitigation strategy is evaluated.

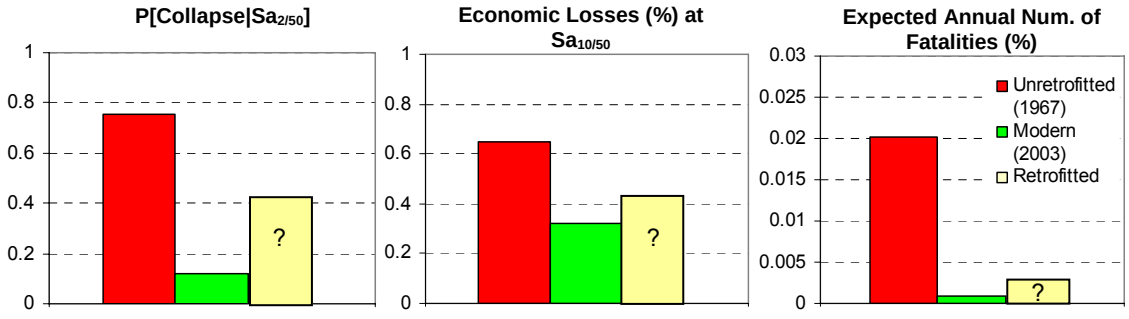

Figure 7.6 Relative seismic performance of unretrofitted non-ductile RC frame structures, modern RC frame structures and retrofitted non-ductile RC frame structures. Data for older and modern RC frame structures is based on Chapter 5 and 6. The seismic performance of retrofitted structures is shown for illustration, and the topic of Section 7.3.

The effect of retrofit on seismic performance is evaluated by selecting a number of retrofit techniques that have been frequently used in practice to improve the performance of non-ductile RC frame structures (Bai 2003; Maffei 2007; Reis 2007): carbon fiber wrapping of columns, jacketing of columns with reinforced concrete and construction of shear walls around some existing columns to provide an alternative lateral load path. These techniques

are used to design multiple retrofit alternatives for each of four case study structures, which are then modeled and analyzed following the procedures described in Chapters 5 and 6 to quantify the collapse performance and earthquake-induced economic losses and fatalities. The case study structures are 4 and 8-story space and perimeter frame systems. Cost-benefit assessment is carried out in Section 7.3.6.

7.3.2 Techniques for Retrofitting Non-Ductile Reinforced Concrete Frames

The design of a seismic retrofit for a particular building typically depends on the ground motion hazard of the site of interest, structural characteristics of the building, the structure's use and occupancy, the target building performance level, as well as any specific seismic deficiencies of the existing structure. The ASCE Standard for *Seismic Rehabilitation of Buildings* (ASCE/SEI 41) identifies four target building performance levels: (i) immediate occupancy, in which the structure is safe to occupy, (ii) damage control, in which damage and downtime are minimized to the extent possible, (iii) life safe, in which the structure may have significant damage, but retains a margin against the onset of partial or total collapse, and (iv) collapse prevention, in which the structure continues to support gravity loads, but retains no margin against collapse (ASCE 2000; ASCE 2007). Retrofit designs typically ensure that the global performance criteria are met at either the MCE, occurring with 2% likelihood in 50 years, or the design level earthquake, occurring with 10% likelihood in 50 years. In practice, retrofits tend to be primarily aimed at meeting life safety or collapse prevention performance goals in extreme earthquakes, like the maximum considered earthquake (MCE) (Maffei 2007). Since the choice of the retrofit performance criteria is project-specific and generally not specified by regulations, seismic upgrades may be designed to provide from marginal to significant improvements in seismic performance in comparison to the unretrofitted structure.

A variety of methods can be used to retrofit non-ductile RC frames, including addition of concrete shear walls or steel braces to the lateral resisting system and jacketing of RC columns with steel, reinforced concrete or fiber polymer products. These techniques aim to enhance seismic performance by preventing brittle failure modes and/or improving the ductility of the structural system at the member and system level (ASCE 2000; Bai 2003). Shear walls can be created as either infill panels, constructed between existing frame elements, or around an existing column to create a 'supercolumn', using the existing column as the wall's core. The effect of retrofitting non-ductile RC frames with RC shear walls is to

increase the lateral strength and stiffness of the existing RC frame, controlling lateral drifts and drift-sensitive damage in non-ductile elements and non-structural systems (ASCE 2000; Bai 2003; Maffei 2007). Another standard retrofit technique involves wrapping vulnerable elements with fiber polymer sheets (ASCE 2000; Bai 2003; Maffei 2007; Reis 2007). This fiber wrapping may be used to prevent column shear failure, to increase the flexural capacity of columns or to improvement confinement. Carbon and glass fiber products are most commonly used, and may be applied to either the lateral or gravity resisting system. RC elements may also be jacketed with either additional concrete and reinforcement or steel plates. RC jacketing is typically employed to increase the flexural and shear strength of a column, and improves member ductility, by adding confinement around the existing column (Bai 2003). Likewise, steel jackets have been shown to improve the strength and deformability by enhancing confinement of RC columns (Xiao and Wu 2003). Another retrofit approach uses concentric or eccentrically configured steel braces to increase structural strength and stiffness (Bai 2003). However, this technique is not evaluated in this study. Similarly, there are many alternative techniques, such as ones employing buckling restrained braces and damping and isolation systems, which are not specifically addressed in this study.

7.3.3 Retrofitted Archetypes, Designs, and Models

Three retrofit techniques are selected for inclusion in this study as illustrations of the types of retrofit possible in non-ductile RC frame structures: jacketing of RC columns with reinforced concrete, carbon fiber-wrapping of RC columns and construction of supercolumn shear walls around existing columns. For each type of retrofit both ‘modest’ and ‘significant’ retrofits are designed, to capture the range of possible improvements in performance obtained from seismic rehabilitation. Descriptions of the performance goals associated with modest and significant retrofits of each type are provided in Table 7.7. The selected seismic upgrade methods are easily incorporated in existing archetype analysis models for RC frames. All retrofitted archetype structures are listed in Table 7.11.

Retrofits are designed and evaluated for the 4 and 8-story non-ductile RC space and perimeter frame structures. All retrofit strategies are applied to each of the case study structures without particular regard to the seismic deficiencies of an individual building. It is therefore expected that all strategies will not be equally effective for all structures. Retrofit designs are deliberately generic, and are used to define changes in member and system level performance to modify archetype analysis models of the non-ductile archetype structures.

For example, the design of the carbon-fiber retrofit does not directly specify the number of plies and arrangement of CFRP needed. Rather, data on carbon-fiber wrapped columns are used to predict the effect of typical application of carbon-fiber wrapping on behavior of RC columns. In practice, the retrofit designs would be fully specified on the basis of detailed design calculations and as-built structural data and are likely to be more effective than the general archetypes considered here. Comparisons between various retrofit techniques for non-ductile RC frame structures are made in this study with the caveat that the performance guidelines differed in each case.

Table 7.7 Description of retrofit design variants.

Retrofit Variant	Description
F1	*Modest* carbon fiber retrofit. RC columns are wrapped with CFRP to eliminate likelihood of column shear failure and improve confinement.
F2	*Significant* carbon fiber retrofit. RC columns are wrapped with CFRP to eliminate likelihood of column shear failure and substanially improve confinement.
CJ1	*Modest* retrofit by jacketing RC columns. Columns are increased in strength, size and deformation capacity by surrounding the existing column with a RC jacket.
CJ2	*Significant* retrofit by jacketing RC columns. Columns are increased in strength, size and deformation capacity by surrounding the existing column with a RC jacket. Column strength is increased sufficiently to ensure that all joints have a ratio of column strength to beam strength greater than 1.2.
CJ3	*Modest* retrofit by jacketing RC columns. Same as CJ1, except that only columns in stories 1-4 are jacketed. Applies only to 8-story retrofit archetypes.
SC1	*Modest* shearwall retrofit. Shearwalls are constructed around existing interior columns to increase the lateral strength of the structure by 25%.
SC2	*Modest* shearwall retrofit. Shearwalls are constructed around existing exterior columns to increase the lateral strength of the structure by 25%.
SC3	*Signficant* shearwall retrofit. Shearwalls are constructed around existing interior columns to increase the lateral strength of the structure by 40%.
SC4	*Modest* shearwall retrofit. Shearwalls are constructed around existing exterior columns to increase the lateral strength of the structure by 40%.

Reinforced Concrete Jacketing

Reinforced concrete jacketing is a retrofit technique in which structural elements, typically columns, are surrounded by new concrete and reinforcement, thereby increasing the strength, stiffness and ductility of these members. In non-ductile RC moment frames, jacketing of RC columns also improves structures' strong column-weak beam ratios and, since it is often continuous from story to story, increases strength and confinement of beam-column joints (Bousias et al. 2007). These jackets can be designed to minimize the impact of other aspects of poor detailing in non-ductile frames, such as inadequately lapped splices. This method of retrofit is appealing because of its compatibility with the original concrete elements and the versatility of cast-in-place concrete (Ong et al. 2004; Bousias et al. 2007). In practice, however, jacketing with RC tends to be expensive due to the disruption of

pouring concrete around a large number columns, the quantity of formwork required and because it is labor intensive (Rodriguez and Park 1994; Ong et al. 2004; Maffei 2007).

For the non-ductile frame structures retrofitted with RC jacketing in this study, it is assumed that every column in the frame is jacketed. Column specimens reported by Bousias et al (2007; 2007), Rodriguez and Park (1994) and Julio et al. (2005) were used to determine typical jacket thicknesses, jacket transverse reinforcement ratios and reinforcement ratios for longitudinal reinforcement. The modest retrofit designs provide the minimum feasible jacket size to provide the necessary reinforcement and concrete cover. This corresponds to an increase of 3 inches of concrete on each face of space frame columns. The width of perimeter frame columns is increased by only 2 inches on each face. These retrofits are labeled 'CJ1'. Significant retrofit designs further increase the flexural strength of columns sufficiently to ensure that the strong column-weak beam ratio is at least 1.2 at every joint in the frame. These retrofits are labeled 'CJ2'. Since the modest retrofit satisfies the strong column-weak beam requirement in the perimeter frame structures, the modest and significant retrofits are identical for the perimeter frame archetypes. All jackets are constructed with 4 ksi concrete.

Descriptions of the 4-story non-ductile RC perimeter and space frame structures retrofitted with RC jackets provided in Table 7.8. Column strength and stiffness is increased from the addition of the concrete jacket and additional reinforcement, increasing the strength of each column by 60% to 130% as shown in Table 7.8. Stiffening of columns increases the stiffness of the structure, as the first mode period (obtained from eigenvalue analysis of the modeled structures) in Table 7.8 shows. The transverse reinforcement in jackets is provided such that spacing and reinforcement ratios are similar to those in code-conforming ductile RC frame structures. The jacketed columns therefore have larger deformation capacities than the unretrofitted columns, as indicated by the typical modeling parameters in Table 7.9. Composite action of the original column and jacket is accounted for in the model following Bousias et al. (2007), which provides simple rules for estimating strength, stiffness and deformation capacity of jacketed members. It is assumed that axial loads in the original column can be transferred to the jacket. The jacketing retrofits are also expected to provide additional strength and confinement to the beam-column joint region. Models of the joint panel region are strengthened to account for additional concrete and reinforcement in this region. In addition, the confinement is assumed to improve joint deformation capacity by 20%. Details for the retrofits of the 8-story non-ductile RC frame structures are similar to

those shown in Table 7.8. Complete documentation of all retrofit designs are provided in Appendix C.

Table 7.8 Description of retrofit designs for RC jacket retrofits of 4-story space and perimeter frame structures.

Design ID	Num. of Stories	Framing System	Description	Column Size[1]	Column Strength (kip-in) [1,2]	Column Transverse Reinf. Ratio, ρ_{sh} [3]	T_1(sec)
3003	4	perimeter	1967 Frame	24 in. x 28 in.	18000	0.0015 to 0.005	1.96
3053		perimeter	Retrofit of 3003 - CJ2	28 in. x 34 in.	29000	0.006	1.48
3004		space	1967 Frame	20 in. x 20 in.	8200	0.0015 to 0.003	1.98
3063		space	Retrofit of 3004 - CJ1	26 in. x 26 in.	16000	0.006	1.45
3064		space	Retrofit of 3004 - CJ2	28 in. x 28 in.	19000	0.006	1.32

[1]Including reinforced concrete jacket.

[2]Column strength of typical interior 1st story column. Other columns show similar increases in strength.

[3]For jacketed columns, this value represents the transverse reinforcement in the jacket. There is additional reinforcement in the original column.

Table 7.9 Typical material model parameters for jacketed RC columns.

Design ID	Num. of Stories	Framing System	Description	$\theta_{cap,pl}$ (rad)[1]	θ_{pc} (rad)	λ[2]
3003	4	perimeter	1967 Frame	0.018 to 0.031	0.053 to 0.100	45
3053		perimeter	Retrofit of 3003 - CJ2	0.063 to 0.072	0.100	110
3004		space	1967 Frame	0.021 to 0.035	0.033 to 0.076	40
3063		space	Retrofit of 3004 - CJ1	0.054 to 0.069	0.100	90
3064		space	Retrofit of 3004 - CJ2	0.056 to 0.070	0.100	100

[1]Notation follows Notation List and Chapter 3.

[2]Typical values.

Supercolumn Shear Walls

The second retrofit technique is the addition of shear walls. The shear walls considered in this study are 'supercolumns', large columns with ductile detailing that surround an original column. Infill panel shear walls are also common, but are not considered here. The supercolumn configuration may be preferable to infill panel shear walls for architectural considerations, with a smaller intrusion on office windows, and because the walls surround the non-ductile frame elements, rather than incorporating existing elements in the boundary region of the wall (Maffei 2007). For the retrofits in this study, it is assumed that these supercolumn shear walls are either provided on the two exterior columns, as illustrated in Figure 7.7b, or on the two interior columns, as in Figure 7.7a. The modest shear wall retrofits are designed to increase the static pushover strength of the structure by 25%. These retrofits are labeled 'SC1' and 'SC2', depending on the configuration location of the added supercolumns. Significant retrofits are designed to achieve a 40% improvement in static pushover strength. These retrofits are labeled 'SC3' and 'SC4'.

The supercolumns are designed such that they have sufficient strength and stiffness to provide the required increase in base shear. Unlike the RC jacket retrofits, these shear walls are only provided around some of the existing columns and in some cases may significantly change the aspect ratio of the column/wall. Supercolumn shear wall retrofits for the 4-story

non-ductile RC frame structures are summarized in Table 7.10. As with the RC jacketed columns, the shearwalls provide significant transverse reinforcement with ductile detailing that meets current code requirements. It is noted that fairly small 'supercolumns' are sufficient to achieve the desired increase in lateral strength for the modest retrofits. It would have been possible to add a much larger supercolumn shear wall, contributing more strength and stiffness to the structure. Retrofit designs for the 8-story structures are similar, except that only the interior-configured supercolumn shear walls are considered for the taller structures. See Appendix C for more details.

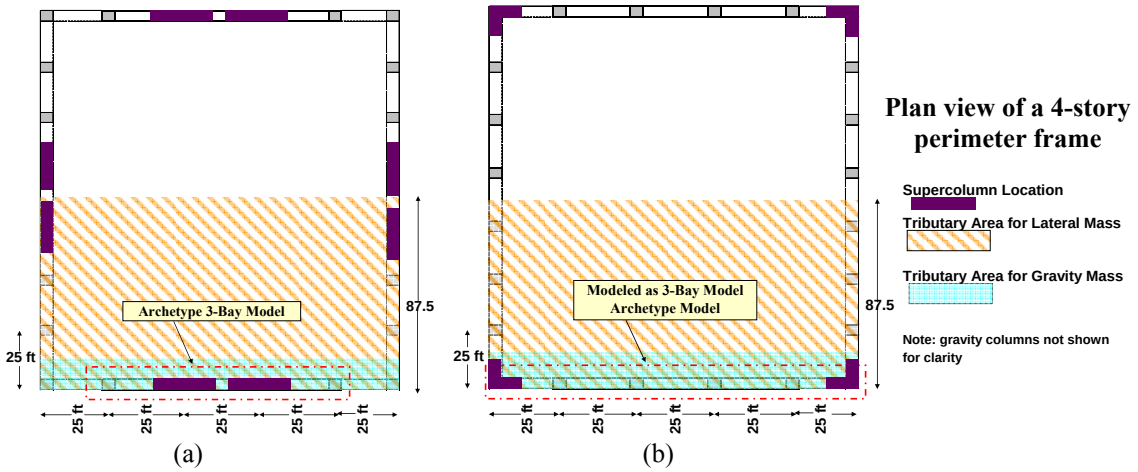

Figure 7.7 Possible configurations of 'supercolumn shear wall' retrofit, showing (a) construction of supercolumns around existing interior columns and (b) construction of supercolumns around existing exterior columns. Supercolumns not to scale.

Table 7.10 Description of retrofit designs for 'supercolumn shear wall' retrofits of 4-story space and perimeter frame structures.

Design ID	Num. of Stories	Framing System	Description	Column Size[1]	Supercolumn Size[2]	Supercolumn Placement	T_1 (sec)
3003	4	perimeter	1967 Frame	24 in. x 28 in.	n/a	n/a	1.96
3056		perimeter	Retrofit of 3003 - SC1	24 in. x 28 in.	28 in. x 34 in.	interior	1.63
3057		perimeter	Retrofit of 3003 - SC2	24 in. x 28 in.	28 in. x 50 in.	exterior	1.44
3058		perimeter	Retrofit of 3003 - SC3	24 in. x 28 in.	28 in x. 40 in.	interior	1.44
3059		perimeter	Retrofit of 3003 - SC4	24 in. x 28 in.	28 in. x 96 in.	exterior	1.10
3004		space	1967 Frame	20 in. x 20 in.	n/a	n/a	1.98
3066		space	Retrofit of 3004 - SC1	20 in. x 20 in.	24 in. x 24 in.	interior	1.74
3067		space	Retrofit of 3004 - SC2	20 in. x 20 in.	24 in. x 26 in.	exterior	1.72
3068		space	Retrofit of 3004 - SC3	20 in. x 20 in.	24 in. x 26 in.	interior	1.66
3069		space	Retrofit of 3004 - SC4	20 in. x 20 in.	24 in. x 30 in.	exterior	1.60

[1]For retrofitted structures, includes only those columns not surrounded supercolumn by shear walls

[2]Supercolumns surround the existing column (i.e. for 3056, the 28 in. x 34 in. supercolumn includes the original 24 in. x 28 in. column)

Modeling parameters for supercolumn wall elements are computed based on predictive equations for modeling RC columns developed by Haselton et al. (2007) and discussed in Chapter 3. Typical modeling parameters for supercolumns are similar to those reported in Table 7.9, i.e. new supercolumns are modeled with substantial more ductility than existing

RC columns. The joints affected by the shearwalls also increase in strength. There is no change in modeling for existing beams and columns and joints not forming part of the new supercolumn shear wall.

Carbon Fiber Wrapping of Columns

In the final retrofit application considered here, columns are wrapped with a carbon-fiber polymer product (CFRP), consisting of sheets of long carbon fibers saturated with a thermosetting polymer that bonds the laminate to the concrete (Seible et al. 1997; Bakis et al. 2002; Bank 2006; Bousias et al. 2007). Depending on the orientation of the fiber sheets, CFRP can be used to improve confinement, increase shear strength or increase flexural strength of a non-ductile RC element. The hinge regions, the center of the column or the entire column can be wrapped. Design equations are used to determine the orientation and number of layers of FRP, as a function of the application and properties of the FRP used. In gravity columns, CFRP is typically used to improve confinement, thereby increasing the axial load carrying capacity of the column and increasing the lateral deformation capacity. Retrofit of beams with CFRP is much less common. Compared to RC jacketing, fiber wrapping of non-ductile RC columns can be advantageous where open floor area is a priority. Retrofit construction also typically leads to less disruption of building occupants. However, care must be taken to prevent undesirable brittle failure modes such as FRP fracture or debonding.

In this study, CFRP is used to improve the strength and ductility of all lateral-resisting columns[5] in the retrofitted structures and is not applied to beams and joints, reflecting common practice (Reis 2007). CFRP is provided in the transverse direction, with fibers running perpendicular to the length of the column, in order to increase column shear strength and deformation capacity. It is assumed that both modest and significant retrofits eliminate the possibility of column shear failure. The significant retrofit consists of more layers of CFRP in the plastic hinge region, leading to a more significant improvement in column deformation capacity, as described below. The flexural strength of the columns is assumed to remain unchanged from the existing columns, as any significant improvement would require additional plies of CFRP with fibers running parallel to the direction of the column. Experimental data from FRP-retrofitted columns in research validate these assumptions

[5] Gravity columns in perimeter frames are not modeled, but these would likely also be wrapped with CFRP to ensure deformation compatibility with the lateral resisting system.

(Iacobucci et al. 2003; Chang and Tsai 2004; Sause et al. 2004; Galal et al. 2005; Harries et al. 2006). While the CFRP retrofits improve flexural behavior by increasing deformation capacity, the relative strength of columns, beams and joints is not altered in these retrofits, and therefore large improvements in sidesway collapse capacity are not expected. Flexure-shear failure is infrequent in the archetype perimeter frame structures, so only the archetype space frame structures are retrofitted with this technique.

Improvements in column deformation capacity are modeled by modifying the parameters used to define the Ibarra inelastic spring model for columns. For more detail, see Chapter 5 or Ibarra et al. (2005). Based on the previously referenced experimental studies, it is assumed that applying CFRP to plastic hinge regions improves the plastic rotation capacity ($\theta_{cap,pl}$), post-capping rotation capacity (θ_{pc}) and energy dissipation (λ) parameters of the model as illustrated for a typical column in Figure 7.8. Experimental data for full-scale CFRP-retrofitted columns showed a 58% to 250% improvement in deformation capacity of flexurally dominated columns. Therefore, the modest retrofit assumes a 75% improvement in plastic rotation capacity and the significant retrofit assumes a 150% increase. For both modest and significant retrofits, it is assumed that θ_{pc} is comparable to the modeling parameters for a ductile-detailed RC column with similar axial loads. λ is based on the level of column confinement provided by CFRP, and is higher for the significant retrofits than the modest retrofits. Since the retrofits prevent column shear failure and subsequent loss of gravity load carrying capacity, the check on non-simulated failure modes is no longer needed. In the discussion that follows, the modest CFRP retrofits are labeled 'F1' and the significant CFRP retrofits are labeled 'F2'.

Possible fracture or debonding of fiber-wrapping is not incorporated into the analysis models. These failure modes are very brittle, and are typically prevented through capacity design provisions that ensure that ductile sidesway failure modes occur first (Bank 2006). It is assumed that the sidesway collapse mode will continue to dominate the collapse assessment of the CFRP retrofitted structures.

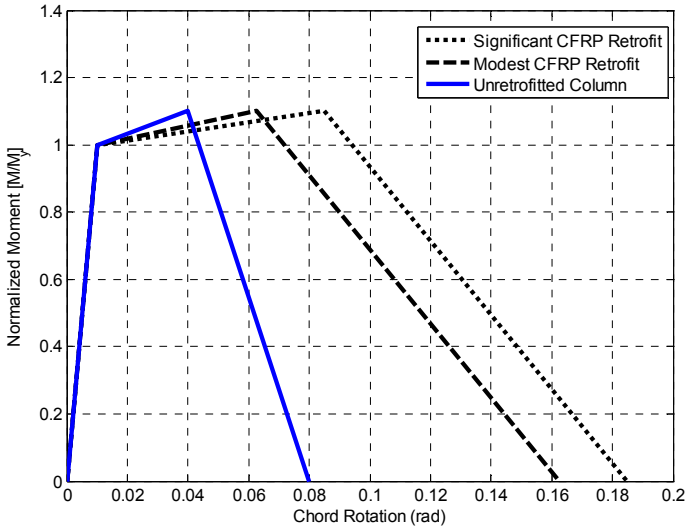

Figure 7.8 Modified column material model for a typical column, when retrofitted with modest and significant CFRP retrofits.

7.3.4 Estimated Costs for Seismic Retrofit

Estimates of the cost of seismic retrofit are needed for cost-benefit assessment. The cost of seismic retrofit varies widely, depending on the desired level of improvement in seismic performance and other characteristics of the existing structure. Buildings with historic value tend to be very expensive to retrofit and seismic upgrading costs may exceed the cost of replacing the structure. For conventional structures, various retrofit alternatives may differ significantly in cost as a function of the types of materials and labor needed, and the disruption of working space and time needed to carry out the retrofit. Another important factor is the degree of architectural renovation that will accompany the seismic rehabilitation work, as many owners take the opportunity to remodel while the building is disrupted for seismic upgrading. As a result of these complexities, it is outside the scope of this study to estimate retrofit costs on a case-by-case basis for the retrofit archetypes described in Table 7.11. Instead, published data on retrofit costs from FEMA (1994) and anecdotal evidence from earthquake engineering professionals is used to estimate a reasonable range of retrofit costs for non-ductile RC frame structures that can be used in cost-benefit assessments of retrofit techniques later in this chapter.

FEMA 156 provides a general method of predicting typical costs of seismic rehabilitation, depending on the structural system, size of structure, location, seismic hazard at the site and the retrofit performance goal (FEMA 1994). These predictions are based on a database of seismic retrofit costs from real projects throughout the country. Retrofit costs in

FEMA 156 represent mean structural costs, including contractor overhead and related fees, but not architectural finishes. For the purposes of this study, the generic structural type of interest is C1, concrete moment frame, and the structure is assumed to be located in Los Angeles on a site of "very high" seismicity. Dollar values are converted to 2006 dollars, accounting for inflation. The values reported here include modifications made to the underlying database by engineers in San Francisco in 2002 to account for changes in construction costs (Heintz 2007). Following this procedure, it is estimated that seismic upgrade of the 4-story non-ductile RC moment frames would cost between $40 and $70 per square foot, depending on the target performance level for the retrofit (immediate occupancy, damage control or life safety). Costs of retrofit for the 8-story non-ductile RC frame structures are estimated to range from $35 to $60 per square foot.

These appraisals from FEMA 156 are relatively consistent with anecdotal evidence on retrofit costs of RC frames obtained from practicing engineers, which range from $20 to $100 per square foot (Conrad 2004; Maffei 2007). These costs will be used in examining the cost-effectiveness of seismic rehabilitation of non-ductile RC frame structures in Section 7.3.6.

7.3.5 Performance Metrics for Retrofitted Reinforced Concrete Frame Structures

Collapse Assessment

The collapse assessment of the retrofit archetype structures listed in Table 7.11 followed the procedure described in detail in Chapters 3 and 5. For each structure, a nonlinear analysis model was created, based on the assumptions for retrofit behavior described above, and subjected to incremental dynamic analysis to determine when sidesway collapse occurs. Where applicable, post-processing of dynamic analysis results was used to account for possible vertical collapse due to column shear failure. These collapse results are appropriately adjusted to account for three-dimensional effects, modeling uncertainties and spectral shape, following the same assumptions described in Chapter 3, such that the collapse metrics reported here are directly comparable to those reported in Chapter 5. Key results obtained from static pushover analysis and collapse assessment of the retrofitted structures are reported in Table 7.11.[6]

[6] As described in Chapter 5, a target spectral shape of $\varepsilon = 1.2$ is used for the non-ductile RC frames because they collapse, on average, close to the 2% in 50 year ground motion. Since some of these retrofit structures

Table 7.11 Results of collapse performance assessment for unretrofitted and retrofitted non-ductile RC frame structures. Collapse performance metrics for modern RC frames are included for comparison.

Design ID	Num. of Stories	Framing System	Description	T(s)	Overstrength (Ω)	Median Collapse Sa [g]	$\sigma_{ln,RTR}$	Margin	P[Collapse| $Sa_{2/50}$]	$\lambda_{collapse}$ x 10^{-4}
3003	4	Perimeter	1967 Frame	1.96	1.1	0.32	0.39	0.66	0.75	100
3053			Retrofit - CJ1	1.48	1.7	0.65	0.42	1.06	0.46	32
3056			Retrofit - SC1	1.63	1.5	0.43	0.42	0.74	0.68	79
3057			Retrofit - SC2	1.44	1.5	0.51	0.34	0.80	0.64	54
3058			Retrofit - SC3	1.44	1.7	0.59	0.45	0.94	0.54	57
3059			Retrofit - SC4	1.10	1.7	0.69	0.37	0.89	0.58	48
1003			2003 Frame	1.12	1.6	1.56	0.37	2.04	0.13	4
3004		Space	1967 Frame	1.98	1.4	0.25	0.38	0.53	0.91	107
3061			Retrofit - F1	1.98	1.4	0.37	0.37	0.78	0.65	64
3062			Retrofit - F2	1.98	1.4	0.35	0.37	0.74	0.69	75
3063			Retrofit - CJ1	1.45	2.9	0.89	0.42	1.40	0.30	14
3064			Retrofit - CJ2	1.33	3.5	1.19	0.42	1.75	0.20	7
3066			Retrofit - SC1	1.74	1.8	0.43	0.36	0.78	0.65	61
3067			Retrofit - SC2	1.72	1.8	0.48	0.35	0.84	0.61	46
3068			Retrofit - SC3	1.66	2.0	0.59	0.37	1.03	0.48	30
3069			Retrofit - SC4	1.60	2.1	0.70	0.37	1.20	0.38	20
1008			2003 Frame	0.94	2.7	2.22	0.38	2.56	0.07	2
3015	8	Perimeter	1967 Frame	2.36	1.1	0.23	0.36	0.58	0.82	135
3073			Retrofit - CJ1	1.91	1.7	0.38	0.37	0.76	0.67	67
3076			Retrofit - CJ3	1.94	1.7	0.39	0.36	0.79	0.65	59
3077			Retrofit - SC1	2.11	1.4	0.27	0.38	0.61	0.79	121
3078			Retrofit - SC3	1.93	1.6	0.35	0.39	0.71	0.70	84
1011			2003 Frame	1.71	1.6	1.00	0.40	1.77	0.19	6
3016		Space	1967 Frame	2.20	1.6	0.32	0.39	0.75	0.68	64
3081			Retrofit - F1	2.20	1.6	0.34	0.39	0.79	0.64	62
3082			Retrofit - F2	2.20	1.6	0.34	0.38	0.79	0.64	60
3083			Retrofit - CJ1	1.87	2.2	0.84	0.37	1.65	0.21	7
3084			Retrofit - CJ2	1.86	2.2	0.92	0.40	1.74	0.19	6
3086			Retrofit - CJ3	1.89	2.1	0.94	0.41	1.81	0.18	6
3087			Retrofit - SC1	1.81	2.0	0.77	0.41	1.44	0.29	12
3088			Retrofit - SC3	1.62	2.2	1.02	0.41	1.75	0.19	7
1013			2003 Frame	1.8	2.3	1.23	0.37	2.29	0.09	2

Figure 7.9 and Figure 7.10 illustrate the improvements in collapse capacity obtained when existing non-ductile RC frame structures are retrofitted by jacketing columns with additional reinforced concrete. Collapse performance metrics are reported in Table 7.11 (and also in Table 7.12). Recall that these retrofits jacketed every column in the structure. Design criteria for the modest jacket retrofit (CJ1) related to construction considerations, i.e. minimum feasible jacket size. The significant retrofits (CJ2) are designed to increase the strong column-weak beam ratios at each joint to current code levels.

The predicted median collapse capacity of the modest RC jacket retrofitted space frame structures are 2.2 to 2.7 times larger than the unretrofitted non-ductile reinforced concrete space frame structures. The significantly retrofitted space frame structures had slightly higher collapse capacities, between 2.3 and 3.3 times the unretrofitted structures. Since the

have higher collapse capacities, $\varepsilon > 1.2$ is probably warranted in some cases. However, $\varepsilon = 1.2$ is conservative and used in all the results presented in Table 7.8.

modest retrofit for the perimeter frame structures already had strong column-weak beam ratios greater than 1.2, no distinction is made between modest and significant retrofits for these structures. For perimeter frames, the RC jacket retrofit increased the collapse capacity by a factor of approximately 1.5.

These increases in the collapse capacity are the result of improvements in both member and system ductility as the result of jacketing of non-ductile RC columns. Greater column (and joint) strength allows the damage to spread more over the height of the structure. Transverse reinforcement provided in the jackets is closely spaced, increasing column and joint shear strength, and properly detailed, improving confinement, and member level deformation capacity. As a result, the retrofitted structures have significantly less hinging in columns and more hinging in beams, leading to significantly higher roof drift ratios collapse (increasing 1.3 to 1.5 times for perimeter frames and 2.1 to 2.2 times for space frames). Interstory drift ratios at collapse also increased with retrofit. Typical collapse mechanisms are illustrated in Figure 7.11. Taller, perimeter frame structures benefit the least from the retrofit, because columns are still not strong enough to spread damage over many stories. There is no advantage in the 8-story structure from continuing the jacketing above the 4th story because most of the damage is at the base of the structure, as illustrated in Figure 7.10. In fact, there is a benefit from curtailing the jacketing at the 4th story, allowing the weaker upper stories not involved in the collapse mechanism to yield, dissipating energy. The effectiveness of jacketing columns would be increased if more concrete was added, making the new columns stronger and stiffer, compared to the unretrofitted columns.

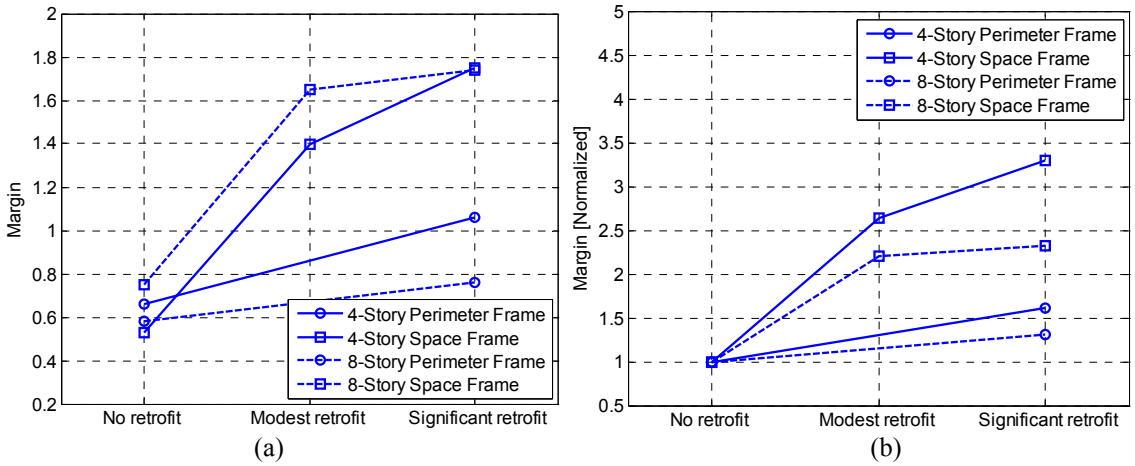

Figure 7.9 Effect of RC jacket retrofits on the predicted collapse margin ratio for non-ductile RC frame structures, showing (a) collapse margin and (b) collapse margin normalized with respect to the collapse margin of the unretrofitted structures.

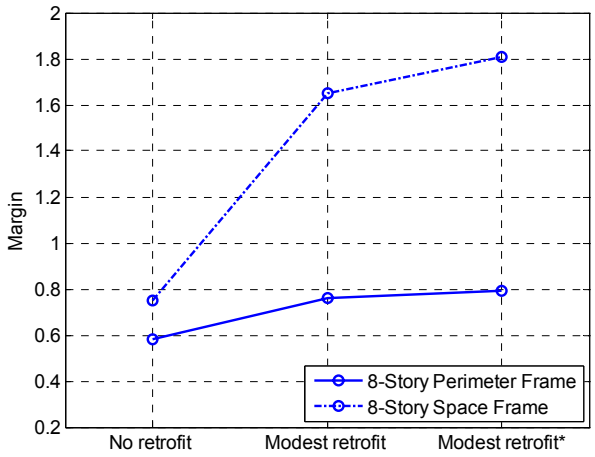

Figure 7.10 Effect of RC jacket retrofits on the predicted collapse margin ratio of 8-story non-ductile RC frame structures, exploring the effect of the jacketing only the columns in stories 1-4 (labeled modest retrofit*). The significant retrofit (not shown) achieves a collapse margin of 1.74 for the 8-story space frame structure. For the 8-story perimeter frame structure, the modest and significant retrofits are the same.

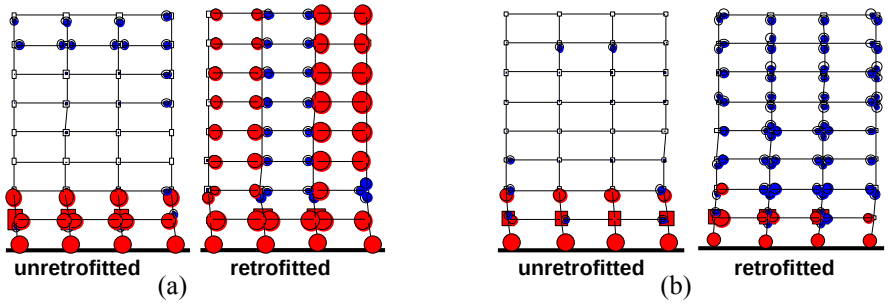

Figure 7.11 Collapse mechanisms in unretrofitted and RC jacket retrofitted (a) 8-story perimeter frame structures and (Design IDs 3015 and 3073) (b) 8-story space frame structures (Design IDs 3016 and 3083). For consistency, collapse mechanisms are shown for the same ground motion for the unretrofitted and retrofitted case.

The collapse performance of non-ductile RC frame structures retrofitted with supercolumn shear walls is illustrated in Figure 7.12. The modest retrofits, which were designed to increase the lateral strength of the structure by 20% (obtained from pushover analysis), increased the collapse margin by 10% to 100%. The significant retrofit designs increased the lateral strength by 40% compared to the unretrofitted structure, and led to a 25% to 130% increase in the collapse margin. It is expected that had a more ambitious performance goal been considered, such as an 80% increase in lateral strength, the corresponding improvement in collapse performance would have been even larger. The effect of the supercolumn retrofit is to improve the strong column-weak beam ratio in the structure, causing deformations to spread over a larger portion of the structure and increasing its energy dissipation capacity before collapse, as illustrated in Figure 7.13. However, because supercolumn structures are stiffer (Table 7.10), the structure is subjected to higher earthquake-induced forces.

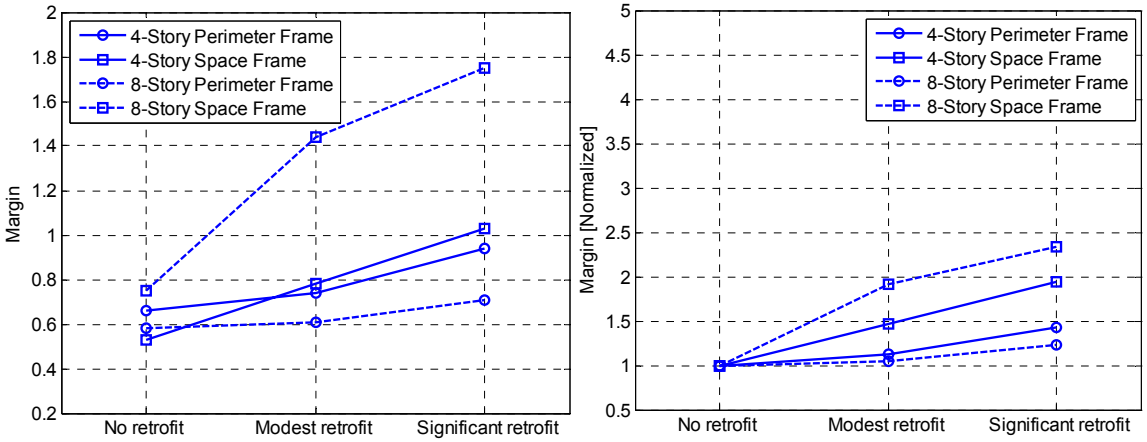

Figure 7.12 Effect of supercolumn retrofits on non-ductile RC frames (SC1 and SC3), illustrating (a) collapse margin and (b) collapse margin normalized with respect to the collapse margin of the unretrofitted structures.

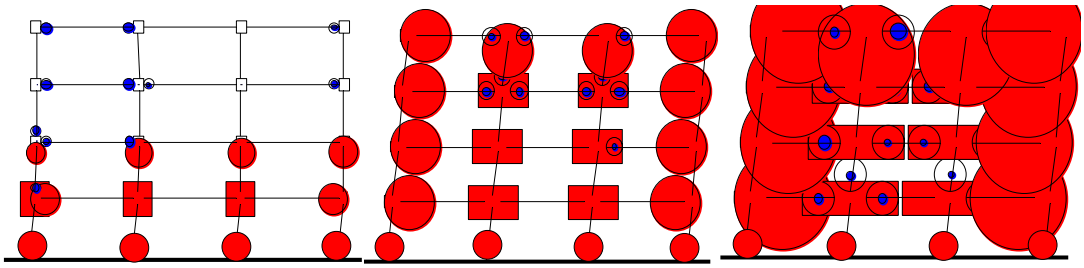

Figure 7.13 Predicted collapse mechanisms for a selected earthquake record in (a) unretrofitted, (b) modestly retrofitted, and (c) significantly retrofitted 4-story perimeter frame structure. Both of the retrofits are from the construction of supercolumns on exterior columns (SC2 and SC4). In the retrofitted structures, there is no damage to joints or columns in the exterior supercolumns. The larger circles in (b) and (c) indicate that the structure is able to undergo more significant deformations (plastic rotations) before collapse.

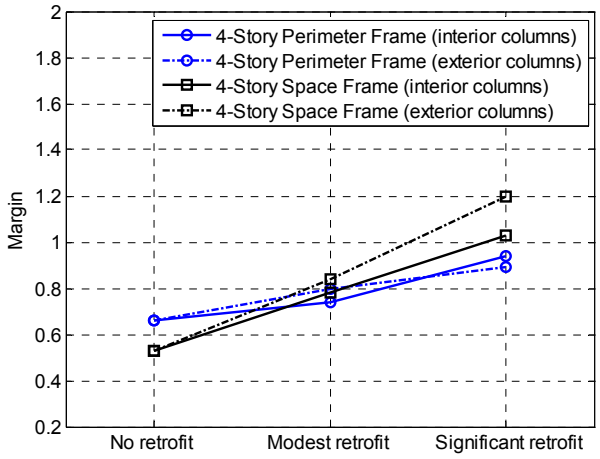

Figure 7.14 Assessed collapse margins for interior and exterior configurations of supercolumn retrofits for 4-story non-ductile RC frame structure.

The largest improvement in collapse capacity due to supercolumn retrofits is in the 8-story space frame. When retrofitted with a supercolumn shear wall this structure frequently fails in 3+ stories, rather than the 2-story mechanism that is common in the unretrofitted structure. On average, the roof drift ratio at collapse is doubled. As with the RC jacket retrofits, the supercolumn shear wall retrofits led to a larger improvement in the collapse performance of the space frame structures, compared to the perimeter frame structures. The space frame retrofits are more effective in part because they have higher overstrength to begin with than the perimeter frame structures. Therefore, the retrofit performance criteria, based on a percent increase in the ultimate base shear, leads to a larger improvement in these structures. As noted above, P-Δ effects are more significant on the perimeter frames because they are more flexible and larger increases in column strength would be needed to spread damage over multiple stories. As shown in Figure 7.14, the exterior column configurations (labeled SC2 and SC4 in Table 7.11) tend to have a slightly bigger effect on the collapse capacity than the interior column configurations shown in Figure 7.12 (SC1 and SC3). In order to achieve the same increase in static overstrength to meet the modest and significant retrofit criteria, the exterior configured supercolumns are larger and stiffer and the exterior configuration is better able to spread deformations over the structure (Figure 7.13).

The carbon fiber retrofits were only applied to the space frame structures, obtaining the predicted collapse margins shown in Figure 7.15. The collapse capacity of the retrofitted structures increased due to the prevention of column shear failure such that columns were not subject to a local collapse and loss of vertical carrying capacity. For these structures, improvements in member ductility alone are insufficient to significantly improve the collapse capacity of the system, because the relative strengths of columns, beams and joints are unaltered and strength deterioration simply moves form one component to another. The retrofits do not alter the hysteretic behavior of beams or joints. The minor decrease in collapse margin between the modest and significant retrofits of the 4-story space frame occurs because strength degradation moves from the now more-ductile CFRP-wrapped columns to the non-ductile unretrofitted joints. These results suggest that it may be beneficial to use carbon-fiber wrap to improve column flexural strength, as well as shear strength and confinement. This retrofit strategy would require additional plies of carbon-fiber running along the longitudinal axis of the column. The use of CFRP to improve flexural strength was not considered in this study.

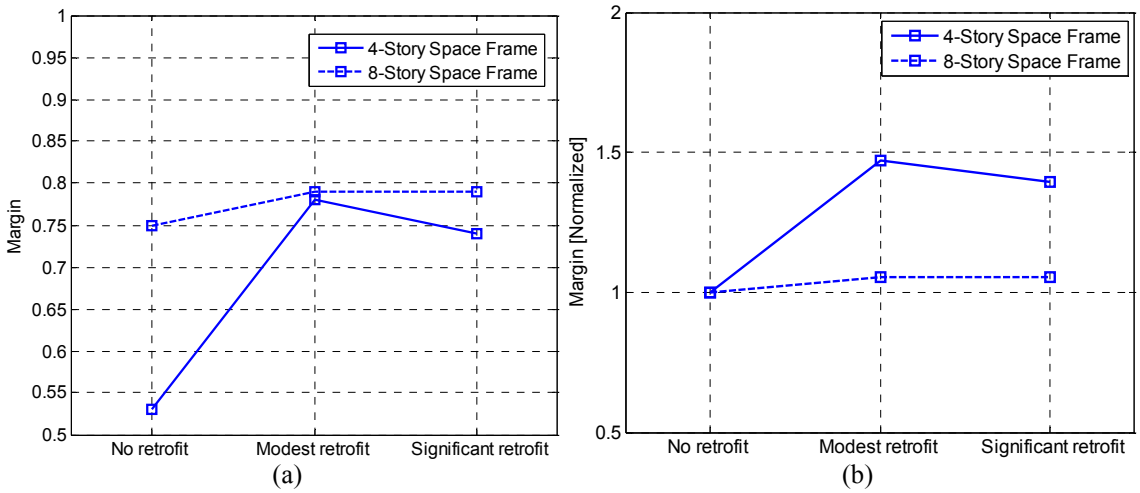

Figure 7.15 Effect of CFRP retrofits on non-ductile RC frame structures, illustrating (a) collapse margin and (b) collapse margin normalized with respect to the collapse margin of the unretrofitted structures.

Collapse performance assessments for all retrofitted non-ductile RC frame structures are shown together in Figure 7.16, and compared to collapse assessments for unretrofitted and modern RC frames. Table 7.12 assesses the effectiveness of each of the retrofit strategies considered. Figure 7.17 shows the computed collapse fragilities for all the 4-story perimeter and space RC frame structures considered in this thesis: unretrofitted, retrofitted and replaced (code-conforming)[7].

As Figure 7.16, Figure 7.17 and Table 7.12 make evident, there is significant variability in the collapse performance of the retrofitted structures depending on the existing structure and the type and ambitiousness of the seismic retrofit. This result is consistent with seismic upgrades that occur in practice. Without regulations precisely defining the performance level, the effectiveness of the retrofit is highly variable. In fact, some of the retrofitted structures have only slightly improved seismic performance from the unretrofitted structures. None of the retrofit strategies considered in this study successfully mitigated all the deficiencies in the structure to obtain collapse capacities comparable to the code-conforming structures. Of the retrofit strategies considered, jacketing the columns with reinforced concrete proved to be the most effective (Table 7.12). Supercolumn retrofits were also quite effective in some cases, and could have led to a bigger improvement in collapse performance if larger shear walls had been provided, leading to a more significant increase in lateral strength and stiffness relative to the unretrofitted structure. The collapse performance of the fiber-retrofits illustrates that, by itself, increasing ductility may not provide an improvement

[7] Code-conforming modern RC frame results are taken from Haselton (2006) for the 4-story RC frame structures with 20 ft. and 30 ft. bay widths. Previously, only the 20 ft. bay width results were given.

in collapse performance if the strength degradation simply moves from one component to another. These retrofits could be improved by adding carbon fibers to improve flexural strength as well.

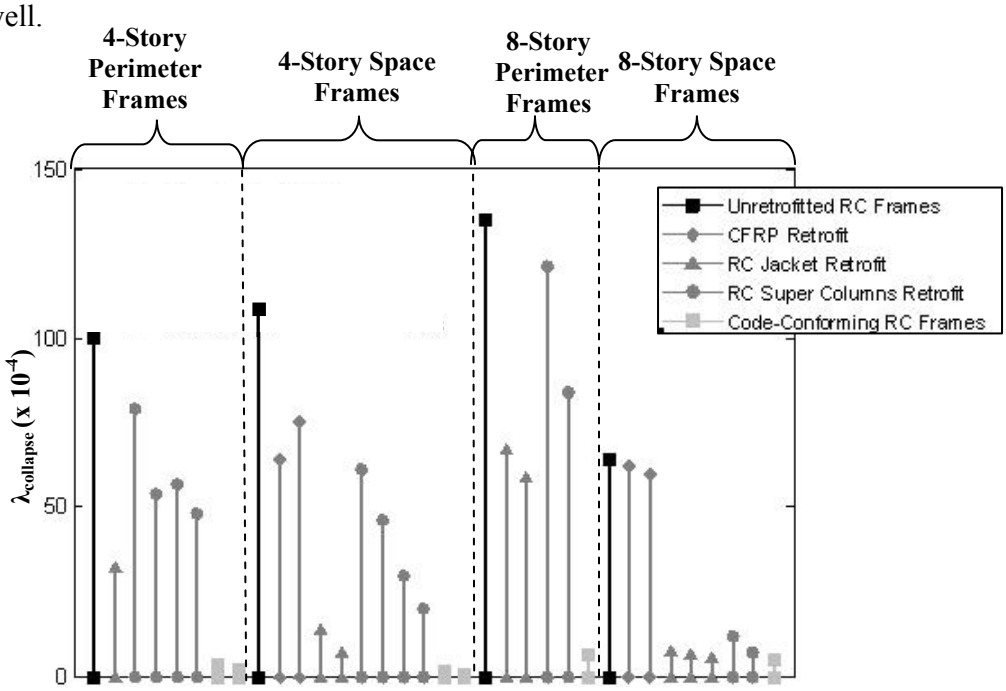

Figure 7.16 Comparison of mean annual frequency of collapse for archetype unretrofitted, retrofitted and modern RC moment frames.

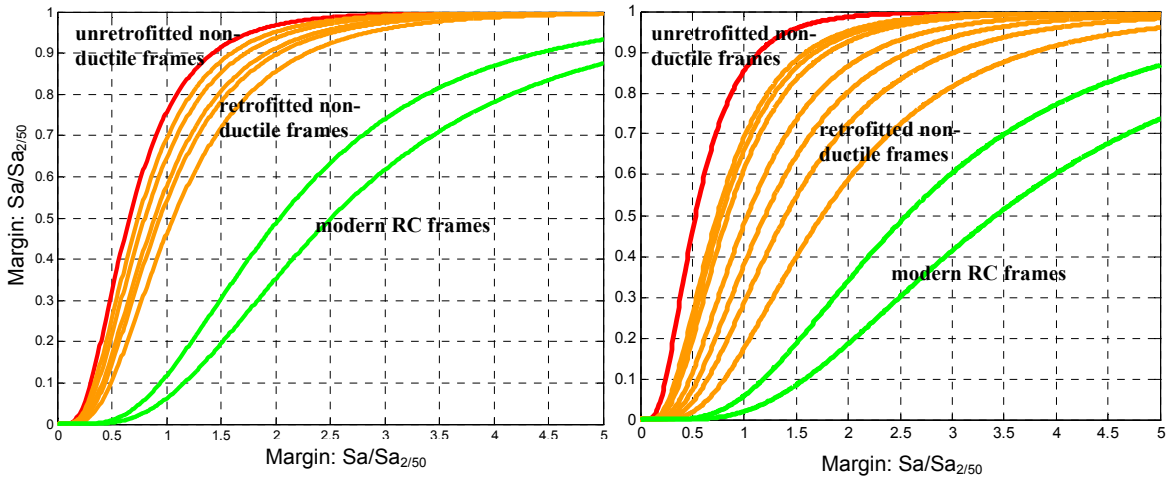

Figure 7.17 Collapse fragility functions for (a) 4-story perimeter frames and (b) 4-story space frames.

Each of the performance metrics considered here depends on the choice of retrofit method and performance goals used in developing retrofit designs. The generic retrofit strategies and designs proposed in this study are inherently limited, as they do not fully take advantage of advancements in retrofit technologies and design that can be achieved in design of retrofit for an individual building. Thus, these measures of seismic performance, including predictions of collapse, economic losses and fatalities, are intended to be illustrative of the

range of retrofit techniques that are possible, rather than representative of the benefits of alternative mitigation strategies.

Table 7.12 Collapse performance ratings for retrofitted non-ductile RC structures.

Num. of Stories	Framing System	Retrofit Strategy	Collapse Performance Rating[1]
4	perimeter	CJ1	3
		SC1	1
		SC2	2
		SC3	2
		SC4	2
	space	F1	2
		F2	1
		CJ1	4
		CJ2	4
		SC1	2
		SC2	2
		SC3	3
		SC4	3
8	perimeter	CJ1	2
		CJ3	2
		SC1	1
		SC3	2
	space	F1	0
		F2	1
		CJ1	3
		CJ2	3
		CJ3	3
		SC1	3
		SC3	3

[1]Collapse Performance Rating: 0 -- Ineffective to 4 -- Very Effective
Very effective collapse performance is equivalent to modern RC frames

Fatalities

One of the primary motivations to retrofit non-ductile RC frame structure is the improvement of the life safety of the structure. Prediction of seismically induced fatalities in retrofitted RC frame structures follows the same procedure used to predict fatalities in unretrofitted RC frames in Chapter 6. The primary differences between the unretrofitted and retrofitted frames, insofar as affecting computation of fatalities, are the collapse capacity and the predicted collapse volume ratios. Since some of the retrofit strategies increase the number of stories in the collapse mechanism, these structures typically have higher collapsed volumes such that, if the structure collapses, may trap a larger percentage of its occupants. Assumptions related to collapsed volumes are described in detail in Chapter 6.

The earthquake-related fatalities predicted for retrofitted non-ductile RC frame structures are reported in Table 7.13 and Figure 7.18. As with the collapse results, the fatalities for retrofitted structures are typically less than those predicted for unretrofitted structures and larger than those expected in code-conforming structures. Though the retrofitted structures

are safer than the unretrofitted structures, in most cases they do not reach code levels of safety as modern codes have been very effective at reducing earthquake-related fatalities. . The RC jacket retrofits and significant supercolumn retrofits are particularly effective at reducing the life safety risk, i.e. reducing the probability of collapse and, hence, the predicted number of earthquake-related fatalities. An apparent exception is the modest supercolumn retrofit of the 8-story non-ductile perimeter frame structure, which leads to a predicted minor increase in the predicted number of fatalities despite a 5% improvement in the collapse margin. This increase is the result of assumptions about collapsed-volumes made in the fatality prediction method. The unretrofitted 8-story perimeter frame typically fails in the bottom two stories, as illustrated in Figure 7.11a. The retrofitted structure typically fails in the bottom three stories, increasing the number of occupants at risk of entrapment by 50%. Thus, the retrofitted structure collapses slightly less frequently, but may endanger more of its inhabitants. This unfavorable result is the product of performance goals used to define retrofit designs in this study.

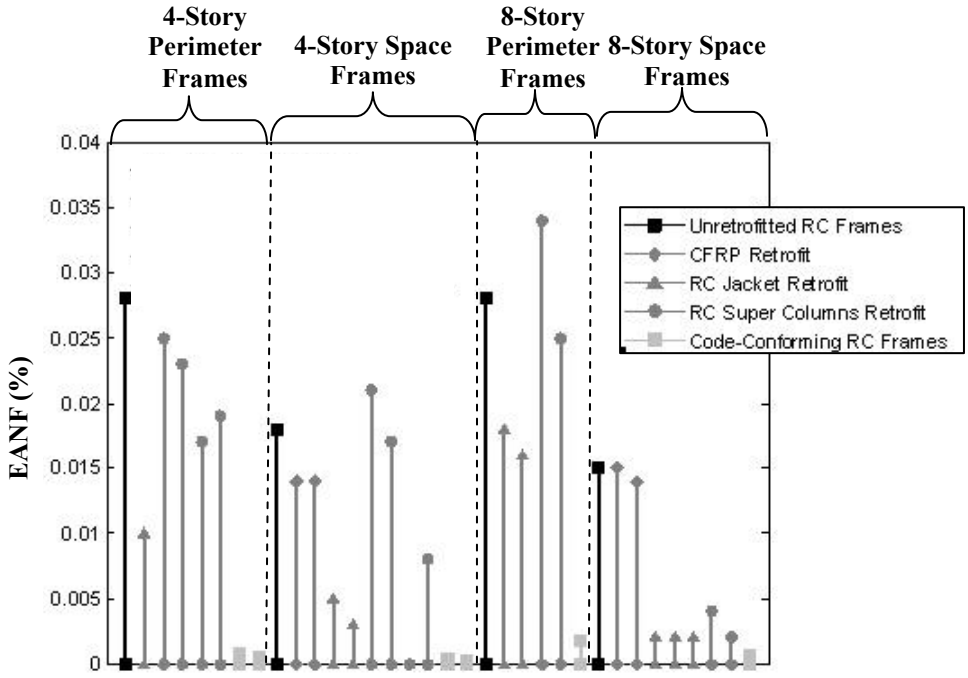

Figure 7.18 Comparison of normalized annual fatalities (% of building occupants) predicted in non-ductile, retrofitted and modern RC moment frames.

Table 7.13 Predicted fatalities and economic losses for retrofitted archetype non-ductile RC frame structures.

Design Description				Fatalities		Economic Losses	
Design ID	Num. of Stories	Framing System	Design Variant	EANF x 10^{-3}	Normalized EANF (% of occupants)	EAL (% of replacement costs)	Normalized Losses over 50 years (%, Present Value)
3003	4	Perimeter	A	97	0.028	2.3	7.1
3053			CJ1	35	0.010	1.8	5.6
3056			SC1	87	0.025	2.1	6.4
3057			SC2	80	0.023	2.3	7.1
3058			SC3	60	0.017	2.0	6.3
3059			SC4	66	0.019	2.0	6.3
3004		Space	A	62	0.018	2.3	7.4
3061			F1	50	0.014	2.2	7.1
3062			F2	50	0.014	2.1	6.9
3063			CJ1	17	0.005	1.2	4.0
3064			CJ2	9	0.003	1.2	3.7
3066			SC1	73	0.021	1.9	6.0
3067			SC2	59	0.017	2.0	6.5
3068			SC3	2	0.0005	1.6	5.1
3069			SC4	27	0.008	1.8	5.7
3015	8	Perimeter	A	141	0.028	2.1	10.4
3073			CJ1	91	0.018	1.5	7.5
3076			CJ3	79	0.016	1.5	7.7
3077			SC1	170	0.034	1.9	9.3
3078			SC3	126	0.025	1.7	8.5
3016		Space	A	77	0.015	1.8	9.2
3081			F1	68	0.014	1.6	8.4
3082			F2	68	0.014	1.6	8.1
3083			CJ1	10	0.002	1.5	7.6
3084			CJ2	9	0.002	1.3	6.6
3086			CJ3	9	0.002	1.4	7.1
3087			SC1	20	0.004	1.6	8.0
3088			SC3	11	0.002	1.5	7.9

Economic Losses

In addition to improving life safety, retrofitting non-ductile RC structures may decrease the repair costs incurred in future earthquakes. For a small number of owners with high value building contents or buildings, reduction in earthquake-related losses may be the stated purpose of the retrofit. For others, reduction of seismic losses is a favorable byproduct of choices to retrofit to improve life safety. To quantify the reduction in economic losses resulting from the retrofit methods considered here, the loss toolbox described in Chapter 6 is used to predict economic losses in the retrofitted RC frame structures. As before, the computed losses are based on the cost of repairing earthquake-induced damage and do not account for the costs of business interruption while the structure is repaired or building closure.

As reported in Table 7.13 and illustrated in Figure 7.19, retrofitting the 4-story non-ductile RC frame structures decreases the expected annual losses from 2.3% of the

replacement cost of the structure to a range between 1.2 and 2.3%, depending on the retrofit strategy. The results are comparable for 8-story structures. There is significant variability in the effect of retrofit on loss reduction. Of the generic retrofit techniques evaluated in this study, concrete jacketing results in the most significant reduction in estimated losses, decreasing annualized losses by 20 to 50%, depending on the retrofit variant and case study structure. Concrete jacketing reduces losses by increasing stiffness of the structures, reducing damage and losses in drift-sensitive structural and non-structural components. For the same reason, significant supercolumn retrofits reduce estimated losses from 13% to 27% for the structures of interest. Relatively speaking, as illustrated by comparing Figure 7.19, with Figure 7.16 and Figure 7.18, retrofit and replacement are less effective at reducing estimated losses than collapse and fatalities. In Figure 7.16, retrofits may decrease the mean annual frequency of collapse by as much as a factor of 10 compared to the unretrofitted structures; losses in Figure 7.19 are reduced by a factor of 2, at most. These differences serve to underscore the life safety emphasis of building code modifications and seismic rehabilitation guidelines. If loss prevention is a priority for a particular structure, a retrofit design can be carefully tailored to maximize the reduction of reduced earthquake-related losses.

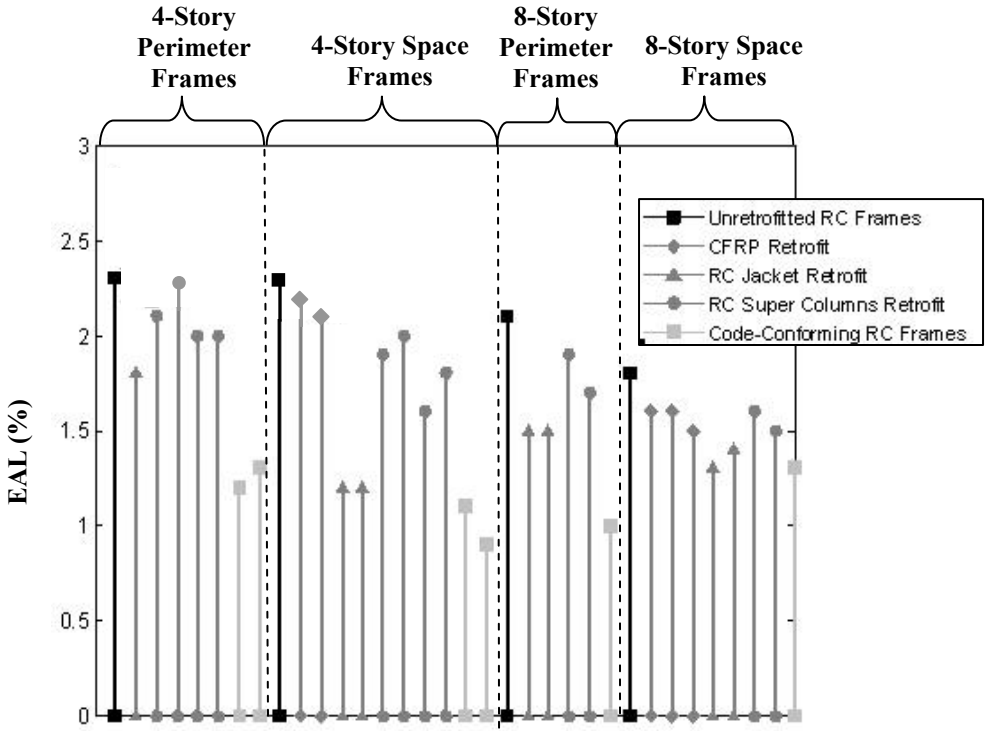

Figure 7.19 Comparison of expected annual losses (% of building replacement cost) in non-ductile, retrofitted and modern RC moment frames.

Both retrofit and replacement tend to reduce economic losses, as shown in Figure 7.19. The estimation of economic losses in this study excludes important contributors to the loss, especially that related to building downtime and closure (red-tagging). Had economic losses been computed using a model that accounts for these factors, the difference in predicted losses between the code-conforming and existing non-ductile RC frame structures would be even greater. The economic losses predicted in retrofitted structures likely also would show bigger improvement relative to the unretrofitted non-ductile RC frame structures.

7.3.6 Cost-Benefit Assessment of Retrofitting Non-Ductile Reinforced Concrete Frame Structures

The cost of retrofitting non-ductile RC frame structures is expected to vary between $20 and $100 per square foot, depending on the structure and retrofit approach, as described in Section 7.3.4. The benefits of retrofitting, represented in dollar-terms, result from reduction in seismic-related repair costs and lives saved. The cost-benefit assessment follows the same assumptions as Section 7.2.4: human life is valued at $2 million per life saved, each building has a remaining 50 year life span, and the discount rate is 3%. Other aspects of the assessment procedure were discussed in detail in the cost-benefit assessment of replacing non-ductile RC frame structures.

The results of cost-benefit assessment for retrofitted structures are reported in Table 7.14. Since estimates of retrofit costs are uncertain, Table 7.14 presents the cost-benefit assessment in terms of the maximum price we would be willing to pay per square foot to achieve the desired performance benefits. If the true costs of the retrofit method exceed this value, the cost-benefit assessment concludes that retrofit is not economically viable (cost-benefit ratio >1).[8] According to the estimates of retrofit costs collected (Section 7.3.4), the minimum retrofit cost in today's construction market is approximately $20 per square foot. Accordingly, the fiber-wrapped retrofits and modest supercolumn retrofits cannot be justified from a cost-benefit standpoint. Several of the other retrofits are worth $80 to $100 per square foot according to this analysis, including the concrete jacketed and the significant supercolumn retrofits. Provided that the retrofit can actually be achieved for the price shown

[8] The surprising negative benefits reported for the 8-story perimeter frame with modest supercolumn retrofit design (Design ID 3077) occur because the predicted earthquake-related fatalities increase post-retrofit. The reduction in annualized losses with retrofit was insufficient to counterbalance this effect. This result could have been avoided with a better-designed retrofit. This finding illustrates some of the limitations of the generic retrofit designs used in this study.

in the final column of Table 7.14, these retrofits are economically feasible. As with the cost-benefit assessment associated with replacing non-ductile RC moment frames, increased value of life would increase the economically justified maximum retrofit price.

On average, approximately half of the computed benefits results from saving lives and the other half results from reducing seismic damage in future earthquakes. Without including the benefits to public safety, most of these retrofits would be economically infeasible. An early study by Pate-Cornell (1985) examining the cost-effectiveness of seismic strengthening of unreinforced masonry warehouses and RC manufacturing buildings in Boston reached the same conclusion. Smyth et al. (2004) also found that loss of life was the dominant contributor to benefits of retrofitting or replacing apartment buildings in Turkey. In contrast, Porter et al. (2006) found that seismic retrofit of some wood frame buildings in California was cost-effective without considering the benefits due to live saved, especially for fairly inexpensive upgrading of small, single family homes.

Table 7.14 Cost-benefit assessment of retrofitting non-ductile RC frame structures.

Num. of Stories	Framing System	Retrofit Design	Reduction in $\lambda_{collapse}$ (x 10^{-4})	Reduction in EAL (% of replacement costs)	Reduction in EANF (x 10^{-3})	Benefits of Retrofit[1] ($, millions)	Max. Retrofit Cost for Neutral Cost-Benefit Assessment ($/ft^2)
4	Space	F1	43	0.1%	13	0.9	15
		F2	32	0.2%	13	1.1	18
		CJ1	93	1.0%	46	5.6	90
		CJ2	100	1.1%	54	6.2	100
		SC1	46	0.4%	-10	0.7	12
		SC2	61	0.3%	4	1.1	17
		SC3	77	0.7%	61	5.4	86
		SC4	87	0.5%	36	3.5	57
	Perimeter	CJ1	68	0.5%	63	4.8	76
		SC1	21	0.2%	11	1.3	21
		SC2	46	0.0%	18	0.9	14
		SC3	43	0.3%	38	2.7	44
		SC4	52	0.3%	31	2.4	39
8	Space	F1	2	0.1%	9	1.2	19
		F2	4	0.2%	9	1.5	24
		CJ1	57	0.3%	66	4.9	79
		CJ2	58	0.5%	68	6.0	97
		CJ3	58	0.4%	68	5.6	89
		SC1	52	0.2%	57	4.1	66
		SC3	57	0.3%	65	4.7	75
	Perimeter	CJ1	68	0.6%	50	5.5	88
		CJ3	76	0.5%	62	6.0	95
		SC1	14	0.2%	-29	-0.5	-7
		SC3	51	0.4%	15	2.6	42

[1]Includes benefits due to reduction of economic losses and fatalities

Cost-benefit assessment permits comparison of different risk mitigation strategies such as retrofit or replacement. Depending on the costs of retrofit, it may be much cheaper to save lives through retrofit than replacement. Recall that replacing non-ductile structures costs between $4 and $5 million per life saved (to achieve a neutral cost-benefit ratio equal to 1). If columns can be jacketed with reinforced concrete for $80 per square foot, for example, this

retrofit strategy costs between $2 and $3 million dollars per life saved. If the retrofit can be achieved more cheaply, at $40 per square foot, the seismic upgrade costs approximately $0.1 million dollars per life saved because the reductions in seismic repair make up for the cost of the retrofit.

Overall, the cost-benefit assessment of retrofit conducted in this study is probably pessimistic. The generic retrofit strategies and designs proposed in this study are inherently limited, as they do not fully take advantage of advancements in retrofit technologies and design that can be achieved in design of retrofit for an individual building. Building-specific retrofits, designed by a practicing engineer specifically targeting a structure's identified deficiencies, would likely exhibit better seismic performance than the more generic retrofit designs considered here.

7.4 Policy Choices, Consequences, and Considerations

7.4.1 Engineering Implications of Seismic Safety Policies

The assessment of earthquake-related collapse risks, casualties and economic losses in unretrofitted (non-ductile), retrofitted and modern RC frame structures provides an infusion of data that can be used to evaluate the implications of various seismic safety policies for non-ductile RC frame structures. In this section, several possible policy alternatives for mitigating risks in vulnerable RC frame structures in California are identified, and their consequences, in terms of seismic performance, are examined using metrics from this and previous chapters.

Policy alternatives for reducing the threat of collapse of existing non-ductile RC frame structures are considered in Table 7.15. Any of these could in concept be implemented at either the state or local government level. The first option, maintaining the status quo, provides no specific regulation regarding retrofit or replacement of non-ductile RC frame structures, except in a few special cases, such as hospitals and schools, which are already governed by seismic safety legislation. Under the status quo, building owners may choose to seismically upgrade their structures, but they are not required or encouraged to do so. The second policy alternative in Table 7.15 is termed "comprehensive retrofit or replacement." Under regulations of this type, all pre-1975 non-ductile RC frame structures would be required to be evaluated, replaced or retrofitted by a specified date. Financial incentives may or may not be provided to owners to help mitigate costs. A program of "targeted retrofit or

replacement" is similar, except that it would require only that certain, particularly vulnerable, pre-1975 RC frames be upgraded or replaced. The final option listed in Table 7.15 is a voluntary mitigation policy, which provides owners with incentives to retrofit or replace their structures, but does not mandate action. Incentives for upgrading could be financial in nature, but do not necessarily need to be. The existing Hospital Safety Act is an example of targeted retrofit or replacement, in which hospitals are required to evaluate their structures and seismically upgrade if certain performance criteria are not met. Examples of the other types of policies can be found in different local government responses to California's Unreinforced Masonry Building Act, which mandated that local governments mitigate risks associated with unreinforced masonry construction, but left choices regarding policy implementation to the municipality.

The seismic performance metrics in Table 7.15 summarize data from this study regarding the earthquake performance of existing RC frame structures, and those that have been replaced or retrofitted. If no policy changes are made, the status quo alternative, few existing non-ductile RC frame structures are likely to be retrofitted or replaced due to high cost-benefit ratios described previously. The status quo alternative is therefore associated with a collapse rate of 45 to 135 x 10^{-4} collapses/year, and estimations of expected annual economic losses and fatalities that reflect the expected performance of non-ductile 1967-era RC frames. Under a mandatory retrofit or replacement program ("comprehensive retrofit or replacement"), those structures that are replaced will have much improved seismic performance: lower collapse rates, reduced earthquake-related fatalities and decreased seismic repair costs. The effectiveness of retrofitting under such a program depends on the standards used to regulate the design and performance of retrofitted buildings. As shown in Section 7.3.5, retrofits lead to a wide spectrum of performance depending on the cost and quality of the retrofit. With well-defined performance standards for retrofitted buildings the upper bound on the collapse rate, fatalities and losses associated with the retrofit or replacement alternatives (reported in Table 7.15) could likely be reduced. The targeted program of retrofit or replacement achieves the same level of performance as the comprehensive retrofit or replacement program in the buildings that are slated for seismic upgrading. The performance of the non-upgraded structures depends on how the rules are developed to select buildings for upgrading. If the policy appropriately targets the most vulnerable structures, the remaining existing non-ductile structures should have better than average performance, possibly reducing the collapses, fatalities and losses reported in these

structures in Table 7.15 for the targeted retrofit and replacement alternative. Fatalities reported in Table 7.15 reflect the large uncertainty in fatality prediction, associated with the number of occupants in a particular collapsed building, the void space in the collapsed structure, and the time of day of the earthquakes.

Table 7.15 Policy alternatives for mitigating seismic risks associated with non-ductile RC frame structures.

Policy Alternative	Seismic Performance Metrics[1]			Earthquake Scenarios[4]		
	Collapse Rate (λ)[3]	Economic Losses[2] (EAL)	Fatalities (EANF)	Moderate	Rare	Very Rare
Status Quo	45 to 135 x 10^{-4} collapses/year	1.6 to 5.2% of building replacement cost	0.01 to 0.03% of building occupants	1 to 6 collapses of RC frame buildings <1 to 10 fatalities in RC frame buildings	15 to 35 collapses of RC frame buildings 2 to 200 fatalities in RC frame buildings	30 to 45 collapses of RC frame buildings 10 to 500 fatalities in RC frame buildings
Comprehensive Retrofit or Replacement	Replaced Structures: 1.0 to 6.5 x 10^{-4} collapses/year	0.77 to 1.26% of building replacement cost	0.0002 to 0.002% of building occupants	<<1 to 6 collapses of RC frame buildings	<1 to 30 collapses of RC frame buildings	2 to 40 collapses of RC frame buildings
	Retrofitted Structures: 10 to 120 x 10^{-4} collapses/year	1.2 to 2.3 % of building replacement cost	0.001 to 0.03 % of building occupants	<<1 to 2 fatalities in RC frame buildings	<1 to 30 fatalities in RC frame buildings	1 to 90 fatalities in RC frame buildings
Targeted Retrofit or Replacement	Replaced Structures: 1.0 to 6.5 x 10^{-4} collapses/year	0.77 to 1.26% of building replacement cost	0.0002 to 0.002% of building occupants	<<1 to 6 collapses of RC frame buildings	<1 to 35 collapses of RC frame buildings	2 to 45 collapses of RC frame buildings
	Retrofitted Structures: 10 to 120 x 10^{-4} collapses/year	1.2 to 2.3 % of building replacement cost	0.001 to 0.03 % of building occupants			
	Remaining Existing Structures: 45 to 135 x 10^{-4} collapses/year	1.6 to 5.2 % of building replacement cost	0.01 to 0.03 % of building occupants	<<1 to 10 fatalities in RC frame buildings	<1 to 200 fatalities in RC frame buildings	1 to 500 fatalities in RC frame buildings
Voluntary Retrofit or Replacement	Replaced Structures: 1.0 to 6.5 x 10^{-4} collapses/year	0.77 to 1.26% of building replacement cost	0.0002 to 0.002% of building occupants	<<1 to 6 collapses of RC frame buildings	<1 to 35 collapses of RC frame buildings	2 to 45 collapses of RC frame buildings
	Retrofitted Structures: 10 to 120 x 10^{-4} collapses/year	1.2 to 2.3 % of building replacement cost	0.001 to 0.03 % of building occupants			
	Remaining Existing Structures: 45 to 135 x 10^{-4} collapses/year	1.6 to 5.2 % of building replacement cost	0.01 to 0.03 % of building occupants	<<1 to 10 fatalities in RC frame buildings	<1 to 200 fatalities in RC frame buildings	1 to 500 fatalities in RC frame buildings

[1] As reported in Chapters 5, 6 and 7.

[2] Losses due to repair of earthquake-induced damage only.

[3] λ - mean annual frequency of collapse; EAL - expected annual losses; EANF - expected annual number of fatalities

[4] Among 100,000 typical buildings, of which 500 are non-ductile reinforced concrete moment frame structures. See text for more details. Each building is assumed to have 200 occupants during working hours

Table 7.15 extends these predictions of seismic performance to examine the consequences of each policy alternative for some general earthquake scenarios, including a 'moderate' earthquake, a 'rare' earthquake and a 'very rare' earthquake. These scenarios provide a broad illustration of how these policy alternatives could impact a collection of buildings. In the absence of detailed maps of ground-shaking and building inventory data,

these results are very generally and based on several key assumptions. First, it is assumed that the earthquake affected area consists of 100,000 buildings, approximately the same number of total buildings found in the City of San Francisco (ATC 2003). Of these 100,000 buildings approximately 500, or 0.5%, are non-ductile RC frame structures constructed between 1950 and 1975.[9] It is further assumed that only 10% of buildings in the selected region are subject to the highest level of ground-shaking, where 'moderate', 'rare' and 'very rare' earthquake events correspond to service-level, design-level and MCE-level ground motions, respectively.[10] The fatality predictions in Table 7.15 assume that a non-ductile RC frame office building has on average 200 occupants during working hours. As Table 7.15 shows, the number of collapses in RC frame structures that may occur varies significantly depending on the scenario earthquake level and policy alternative. Those policy alternatives that eliminate the most vulnerable structures have fewer collapses and endanger fewer lives. If the retrofit structures are required to meet high standards, the upper limit on collapses reported for retrofitted structures would be further reduced. For a given earthquake scenario, uncertainty in the number of collapses that are predicted reflects the variability in the building stock and performance of unretrofitted, retrofitted and replaced structures. Though obviously very general, Table 7.15 illustrates the type of data that seismic risk analysis contributes to policy makers concerned with seismic safety. Communities with a particularly high number of non-ductile RC structures or in a region of more significant seismicity are at higher risk of collapse, threatening life safety.

7.4.2 Lessons for Implementing Seismic Safety Policy

The analysis of seismic performance conducted here also reveals some of the barriers and opportunities related to costs, compliance and performance standards that are critically important in designing and implementing seismic safety policies for mitigating seismic risks associated with non-ductile RC frame structures. In identifying characteristics of successful seismic safety policy, evidence from previous experience with seismic safety regulations in California is also considered (see Chapter 2).

---

[9] See Chapter 2.

[10] Service-level ground motions are defined as those that occur with 50% likelihood in 50 years. Design-level ground motions occur with 10% likelihood every 50 years, while MCE ground motions have 2% likelihood of being exceeded in 50 years.

As shown in the cost-benefit assessment of Sections 7.2.4 and 7.3.6, the significant costs of retrofit or replacement present a significant barrier to regulations to improve the seismic safety of non-ductile RC frame structures. This study found that though retrofitting or replacing these structures significantly reduces the life safety threat associated with non-ductile RC frame structures, these benefits imply spending millions of dollars per life saved (see Figure 7.2, for example). Therefore, any policy requiring retrofit or replacement of all non-ductile RC structures will be expensive. Costs are an even more significant deterrent to policy success, considering that past legislation has tended to place the responsibility of paying for seismic safety primarily on building owners. Owners are often asset rich and cash poor, and may not have the financial wherewithal to comply with regulations. Some building owners may also challenge the equity of a program that primarily benefits the general public, as made evident in Table 7.6 and Table 7.14, at the expense of a few. In current real estate markets, owners may find that they cannot recoup investments in seismic safety through rent, resale or reduced insurance premiums. These observations are supported by data from California's experience with implementing other seismic safety legislation. Costs have significantly delayed compliance with the Hospital Safety Act (1994), which is estimated to cost the health care industry as much as 40 billion dollars to achieve the necessary improvements in seismic safety (Alesch and Petak 2004). Many hospital owners have side-stepped regulations by closing facilities or requested waivers for delayed compliance, citing financial difficulties, forcing Governor Schwarzenegger to defer the 2008 deadline for hospitals to meet 'life safety' requirements.

The reality of the cost-benefit assessment described in Sections 7.2 and 7.3, which indicates that much of the benefits of retrofitting or replacing older RC frame structures are associated with improved safety, emphasizes the ineffectiveness of seismic safety regulations without incentives for building owner participation. The importance of regulatory or financial incentives is further illustrated by the success of the varied policies for unreinforced masonry buildings implemented by local governments in California. On average, voluntary strengthening programs with financial or other incentives for building owner participation achieved double the retrofit rates of those in programs without incentives and, statewide, mandatory programs have achieved much higher levels of compliance than in voluntary programs (Turner 2006).

Several types of incentives can make the cost-benefit ratio more agreeable for building owners. One approach is to provide financial assistance to building owners, either in the form

of grants or beneficial loan conditions to help finance the necessary seismic upgrades, as in some of the unreinforced masonry policies throughout the state (Comerio 1992). Another incentive could involve modification of other development regulations for owners that comply with seismic retrofit or replacement. For example, in Palo Alto, California, owners of unreinforced masonry structures who agreed to retrofit were allowed modification to the standard floor area ratios and parking requirements, essentially increasing the value (benefits) of the investment in seismic strengthening (Beatley and Berke 1990). Non-financial incentives of this type are relatively cheap to provide, a significant advantage due to the limited financial resources of state and local governments. Other policies provide indirect incentives for owner participation, by invoking fears of litigation or loss of property values. Requiring public notification of seismic risks, through posting of building placards or inclusion in tenants' lease and rental agreements, as required for all unreinforced masonry structures in California, seems to provide a strong incentive to retrofit as building owners become concerned about possible liabilities, and fear losing insurance or rental income, see e.g. (Beatley and Berke 1990). The threat of litigation has been shown to be a powerful motivator for recall of defective products in automobile and airplane industries, and may significantly alter an owner's cost-benefit calculations (Bates et al. 2007). Resale values may be affected by safety (or perceived safety) of a structure, as the new owner may expect to pay less for earthquake insurance and obtain better financing options. Due to the short time horizon for real estate investments and the general lack of concern for seismic risks, though, it is difficult to know whether the differential in rent or property values associated with seismic performance could be realized (Porter et al. 2004).

The results in this chapter also demonstrate that a targeted policy that selects particularly vulnerable structures for retrofit or replacement is appealing because it would improve the performance of the worst non-ductile RC frame structures. This type of policy is motivated by the highly variable performance of existing RC frame structures, some of which may not warrant seismic strengthening, as shown in Figure 7.2, and the established cost-efficiencies in mitigating the poorest performing structures first, illustrated in Figure 7.3. These policies, however, require developing a set of criteria to be used for identifying candidate structures for retrofit or replacement, which may include factors besides structural assessment, such as the number of building occupants or the expected remaining service life of the structure. In the past, a variety of approaches have been used to identify vulnerable buildings. This thesis illustrates the usefulness of performance-based methods for quantifying seismic performance

metrics and differentiating between structures. Depending on the level of detail required for the assessment, though, even evaluating whether performance requirements are met can represent a financial burden for building owners.

Without explicit definition of performance criteria for retrofitted structures, seismic safety policies may have inconsistent results, as discussed in Section 7.3 and illustrated by Figure 7.17. The establishment of standards for retrofitted buildings can be contentious, and have important impacts on costs and compliance. If performance goals are not ambitious, retrofitting may be inexpensive but ineffective in leading to significant improvement in life safety of structures. Well-known California engineer Henry Degenkolb alleged that the Los Angeles ordinance for unreinforced masonry construction was made ineffective by lax performance requirements (Degenkolb 1994). However, performance standards for seismic upgrade that are too stringent may serve as a deterrent to participation in voluntary retrofit programs or lead to unnecessary demolition of structures. Performance-based engineering assessments of the type described in this thesis provide an opportunity to improve consistency by evaluating better metrics of seismic performance.

7.4.3 Decision Making Needed for Seismic Safety

The contribution of performance-based engineering studies, such as the assessment of earthquake-induced collapse, fatalities and economic losses in existing buildings, is to quantify risks for prioritizing risk mitigation and recovery choices such that seismic safety goals can be met (Nathe 2000; May 2001; Pate-Cornell 2002; May 2004). Evaluation of seismic performance metrics provides clarity in societal decision making, by exposing the consequences and distributional aspects of various policy approaches, as detailed in the results presented in this chapter. What is missing in the policy process is a transparent discussion of desired safety goals or acceptable risks, given the nature of the earthquake hazard in California, available information about earthquake risks, and the economic implications of the considered regulations. Although an objective of zero-risk or absolute safety is political appealing, it is unattainable where resources are limited, there are alternative risk mitigation strategies and other risks (e.g. AIDs, traffic accidents etc.) compete for public funds. In the past, safety goals have tended to be the byproduct of other choices, especially those related to tolerable costs. Risk-informed decision-making, supported by engineering risk analysis, enables more explicit consideration of acceptable risks.

Safety goals depend on a variety of circumstances, including the level of available resources, the current safety and health situation in society, and factors related to risk control, exposure and immediacy that affect our perception of risks (Reid 2000; Pate-Cornell 2002). As a result of differing risk perception, acceptable risks can vary significantly depending on the characteristics of the risk. These differences are evident in the large variability in the amount societies are willing to pay to save lives. In a 1980 study, for example, Okrent (1980) found that the French paid approximately $30,000 per life saved for car accidents, a frequent, low consequence event, and up to $1 million per life saved to prevent aviation accidents, which are much more infrequent, but of higher consequence and visibility due to the number of casualties involved. Because earthquakes are catastrophic and uncontrollable, societies tend to be risk averse in the face of this hazard. Yet, because earthquakes are a natural phenomenon that will occur at an undetermined time and place, earthquakes are also treated fatalistically, as "Acts of God" that cannot be prevented.

In the past, acceptable failure rates for buildings have been largely determined implicitly based on decisions by engineers on building code committees. For new buildings, provisions for load and resistance factor design for steel and ultimate strength design for concrete have been calibrated to provide consistent reliability in an overall or average sense (Ellingwood et al. 1982; Ellingwood and Corotis 1991; Ellingwood and Tekie 1999). In calibrating these codes a higher factor of safety was provided for gravity, compared to wind and earthquake loading. This reliability is implicitly taken to be acceptable, though there has been little discussion outside the engineering community about what constitutes acceptable risks.

A comparison of predicted failure rates for building structures is reported in Table 7.16. In presenting this comparison, it is acknowledged that comparison of risks can be problematic, even when all risks relate to building failure, as in Table 7.16. Difficulties in comparison arise from use of different definitions for failure rates and perceptions that differ depending on the hazard phenomena. Nevertheless, data in Table 7.16 are included to summarize available data on collapse rates of buildings. Under current code design, gravity load failures are infrequent, with collapse rates below 10^{-5} per year. Collapse risks associated with structural fires in office buildings appear to be even lower, indicating the low incidence of flashover fires and the effectiveness of thermal insulation and other aspects of fire resistant design. Compared to the predicted failure rates associated with structural fire or gravity loading, the risk of seismic collapse is much higher, even for modern code-conforming structures. The high risk associated with seismic collapse is due in part to high levels of

seismicity in California (and particularly the Los Angeles site in this study), but more importantly it reflects the large degree of uncertainty in designing buildings to resist earthquakes. The higher rate of earthquake-related failures is the outcome of decisions for provisions for seismic design, rather than discussions of desired safety. Until recently, there was little data on failure rates to cite in discussions of acceptable risks.

It is apparent from Table 7.16 that older construction has higher collapse rates, especially when it comes to seismic risks. This observation may also be valid for other types of structural failure, but there is little data available. Because of higher costs of mitigating risks, time constraints and the age of structures, existing buildings tend to be held to a lower standard. Diamantidis and Bazzurro (2007) suggest that acceptable failure rates for new and existing construction may reasonably differ by a factor of 10.

Table 7.16 Comparison of probabilities of structural failure for earthquake, wind, fire and gravity loading.

Type of Structural Failure	Annual probability of failure (p_f)	Source
Gravity loading (yielding)[1]	6 to 8 x 10^{-4}	Ellingwood and Tekie (1999)
Gravity loading (collapse)[2]	<6 to 8 x 10^{-5}	assumed, based on Ellingwood and Tekie (1999)
Structural fires[3]	1 x 10^{-6}	Ellingwood and Corotis (1991)
Earthquakes - modern construction	1 to 6.5 x 10^{-4}	this study
Earthquakes - older construction	45 to 135 x 10^{-4}	this study

[1] Gravity load failure is defined in Ellingwood and Tekie's study as yielding of structural members.

[2] Yielding, of course, is not collapse. Collapse will occur much less frequently than yielding. There is little data to suggest what is the probability of gravity load collapse. Here, it is assumed that 10% of gravity load failures, defined as yielding, lead to collapse. This assumption is made for illustration purposes. The probability of gravity-related collapse may be substantially lower.

[3] Structurally significant flashover fire.

The failure rates shown in Table 7.16 have been implicitly accepted for new construction. Regulation of seismic safety, especially for existing construction, would benefit from explicit consideration of acceptable risks. F-N diagrams, developed for use by government and planning agencies provide one framework for evaluating low probability, high consequence events (Christian 2004). F-N diagrams relate the frequency (F) of accidents with fatalities with the number (N) of fatalities, and identify accidents that are acceptable – infrequent, small consequence events, unacceptable – frequent or high consequence events, and an intermediate region where cost-benefit assessment and other methods should be used to ensure that risk as are as low as reasonably practical (ALARP). Figure 7.20 superimposes data from this study on seismic risks associated with collapse of RC frame structures on an F-N diagram adopted by the Hong Kong Planning Department. According to the guidelines of this diagram, the data for unretrofitted 1967-era RC frames is unacceptable, whereas retrofitted and code-conforming structures lie in the cost-benefit or acceptable region. Other

F-N diagrams may give different results depending on the location and shape of the acceptable and unacceptable regions. Likewise, if a particular community had a very large number of non-ductile RC structures, the acceptability assessment would differ with higher expected number of fatalities. Figure 7.20 is not meant to imply that unretrofitted existing non-ductile RC frame structures do or do not pose an unacceptable collapse risk, but rather to illustrate how data on seismic risks can be deliberately examined in the context of societal safety goals.

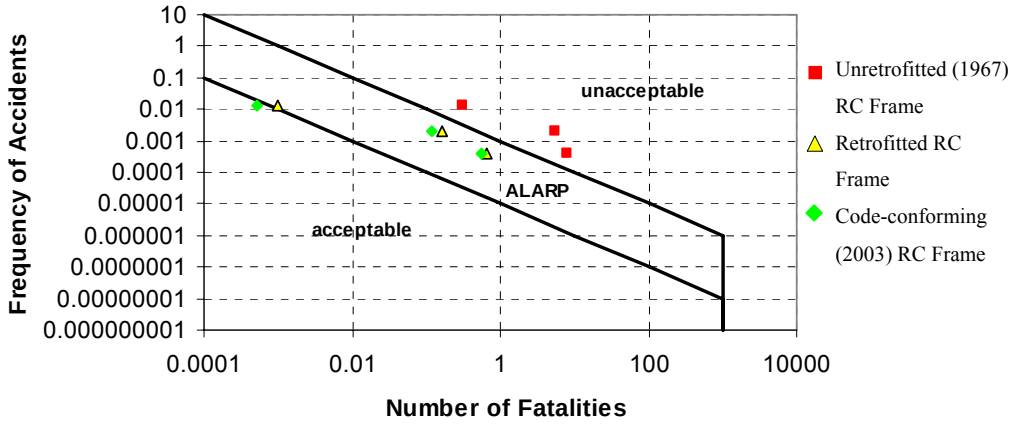

Figure 7.20 Example F-N diagram for risk acceptance, showing the risk of seismically-induced collapse of RC frame structures, modified from (Christian 2004).

7.5 Conclusions

In this chapter, strategies for mitigating the seismic risks posed by non-ductile RC frame structures are evaluated by comparing the costs of retrofitting or replacing vulnerable structures with the benefits, measured in terms of reduced seismic risks. Policy choices range from the status quo, with no specific policy for non-ductile RC frame structures, to a mandatory program of retrofit or replacement.

In Sections 7.2 and 7.3, these policy alternatives are evaluated in terms of their cost-effectiveness in mitigating seismic risks, using data on earthquake-induced collapse, related fatalities, and repair costs presented in Chapters 5 and 6. Replacing non-ductile RC frames with modern code-conforming structures has the effect of significantly reducing the risk associated with loss of life in these structures, as well as reducing costs incurred by owners in repairing future earthquake damage. However, this improvement comes at a large price, on the order of $4 to $5 million dollars per life saved for many of the archetype buildings investigated in this study. The study does show, however, that some of the archetype non-ductile RC frame structures are cost-effective candidates for replacement. Retrofit provides

an intermediate level of seismic performance, between existing non-ductile RC structures and new, code-conforming structures. Performance-based collapse assessment using nonlinear time history analysis is an effective tool for evaluating the effectiveness of various retrofit strategies. The cost-effectiveness of retrofitting non-ductile RC frames is highly dependent on the cost of retrofitting, which is difficult to estimate. The most effective of the retrofit designs considered in this study are estimated to be worth approximately $85 to $100 per square foot and, if they can be achieved for this price, the retrofit is cost-effective. The cost of saving lives by seismic retrofitting is clearly dependent on the true cost of retrofit. If all the retrofits considered in this study can be achieved for $80 per square foot, costs per life saved are as low as $2 to $3 million. It is expected that building-specific retrofits designed by engineering practitioners would be even more effective at reducing losses and lives lost, increasing the cost-effectiveness of seismic upgrading.

Decisions regarding seismic safety policy alternatives for non-ductile RC frames are difficult. The older non-ductile RC frame structures are clearly more likely to collapse than code-conforming RC frame structures in earthquakes, but are they too unsafe? Answers to this type of question beg explicit consideration of public safety goals for engineered structures, and the amount of public resources, financial and institutional, that are available to support reaching these goals. Safety goals are often the unintended consequence of available resources. Engineering data on collapse risks, economic losses and fatalities can provide transparency in this decision-making process. Depending on decision criteria established, a variety of policy mechanisms exist to achieve the desired objectives for safety of non-ductile RC frame structures in California. Important considerations include whether a policy should be mandatory or voluntary, criteria for identifying vulnerable structures, required performance standards for strengthened structures, and incentives for building owner compliance and participation.

Chapter 8

Conclusions

8.1 Summary

Reinforced concrete frame structures constructed in California prior to the mid-1970s may lack important features of good seismic design, such as strong columns and ductile detailing of reinforcement, making them potentially vulnerable to earthquake-induced collapse. In contrast, designs for modern code-conforming special moment frames for high seismic regions employ a variety of detailing and capacity design provisions that prevent or delay unfavorable failure modes such as column shear failure and soft-story collapses. As a result of deficiencies in pre-1975 seismic design, some of California's approximately 40,000 older non-ductile RC structures may present a significant hazard to life safety. The primary objective of this study is to apply performance-based earthquake engineering methods to quantify collapse performance and life safety of existing non-ductile RC frames in comparison to modern code-conforming RC frame structures, generating needed data for use in developing mitigation strategies for non-ductile RC buildings.

An integral component of this work is the evaluation of the risk of earthquake-induced collapse in non-ductile RC frame structures, where collapse risk is used as a measure of life safety. Design characteristics of these buildings, and their deficiencies, are described in Chapter 2. Assessment of collapse risk is conducted by identifying a set of archetypical structures, selected to be representative of typical RC frame structures designed and constructed between approximately 1950 and 1975, and predicting structural collapse using nonlinear time history analysis. The collapse assessment process, described in Chapter 3, is deliberately systematized to provide comparable results for structures with different characteristics. Results of performance-based collapse assessment (Chapter 5) show that existing non-ductile RC moment frames are approximately 40 times more likely to collapse (in any given year) than corresponding code-conforming structures (in terms of mean annual frequency of collapse).

Several aspects of the probabilistic collapse assessment procedure are considered in detail: nonlinear modeling of non-ductile RC frame structures (Chapter 3), treatment of non-simulated failure modes (Chapter 3) and methods for incorporating uncertainties in structural modeling (Chapter 4). To capture component and system-level degradation of strength and stiffness as the structure collapses, models for beams and columns are calibrated to available experimental data, such that model parameters can be predicted as a function of design and detailing parameters. Failure modes that cannot be directly simulated by analysis models are identified by post-processing of dynamic analysis results to determine if component limit states for these failure modes have been exceeded. These models are calibrated to expected values to obtain a mean, rather than lower bound, estimate of collapse capacity. In addition to the mean prediction, uncertainties in ground motion prediction and structural modeling are reflected in the probabilistic assessments of collapse. Structural modeling uncertainties are propagated through the collapse assessment using both simplified and Monte Carlo reliability-based methods.

The seismic performance predictions are extended to include probabilistic estimates of economic losses and fatalities in non-ductile RC frame structures and, again, these results are compared to ductile code-conforming structures (Chapter 6). Data on fatalities and economic losses are used to evaluate the costs and benefits associated with retrofitting and replacing vulnerable non-ductile RC frame structures in Chapter 7. Lessons learned from cost-benefit assessment can help inform development of policies that mitigate collapse risk in the most dangerous buildings in as cost-effective and equitable a manner as possible.

8.2 Findings

8.2.1 Seismic Performance of California's Non-Ductile Reinforced Concrete Frame Structures

A primary objective of this study is the quantitative assessment of the seismic performance of California's existing non-ductile RC frame structures. These assessments are based on a group of archetypical pre-1975 RC frame structures, designed according to the seismic provisions of the 1967 Uniform Building Code and varying in height (2 to 12 stories) and framing system (space and perimeter frames). These buildings are selected such that the group includes variations in structural design that may affect collapse performance and reflects contemporary design practice. Collapse performance is systematically evaluated

through nonlinear dynamic analysis. Sidesway collapse performance is obtained directly from collapse simulation, and then results are post-processed to detect non-simulated vertical collapse modes. Seismic collapse safety is evaluated with reference to the seismic hazard at a typical high seismic non near-field stiff soil site in Los Angeles. Of particular interest is the susceptibility of non-ductile RC frames to collapse in earthquakes and the extent to which the risk of collapse is related to specific building features such as building height and framing system.

- Non-ductile RC frame structures are predicted to have mean annual frequencies of collapse between 20 and 220 x 10^{-4} (collapses per year). The average collapse rate for the baseline space and perimeter frame systems is 91 x 10^{-4} collapses per year, corresponding to a collapse return period of 110 years. When subjected to strong, rare ground motions with mean recurrence intervals of 2500 years ($Sa_{2/50}$), the non-ductile RC frames have a high conditional probability of collapse (60 – 90%). Note that these collapse assessments depend on the seismic hazard at the Los Angeles site of interest, and results will differ at areas of different seismicity or site soil conditions.
- The sidesway collapse capacity of non-ductile RC frame structures tends to decrease with the number of stories in the structure, indicating that collapse safety deteriorates with increasing building height. Collapse margin ratios (of the median collapse capacity divided by $Sa_{2/50}$) are 0.85 and 0.56 for the 2- and 12-story perimeter frame structures, representing a 35% decrease in collapse resistance. Taller structures are more flexible and tend to be more susceptible to P-Δ effects. Column strength is insufficient to distribute demands over many floors in the structure.
- Non-ductile perimeter frames are more vulnerable to sidesway collapse than space frames due to these structures' lack of strength and stiffness. For taller mid-rise buildings (8 and 12 stories) in which the sidesway collapse mode dominates, perimeter frame structures have higher collapse rates than comparable space frame structures. The 12-story perimeter and space frame structures have mean annual frequencies of collapse of 119 x 10^{-4} and 50 x 10^{-4} (collapses per year), respectively. However, the analysis model's exclusion of the contribution of the flat-plate gravity system to strength and stiffness accounts for at least some of the difference between space and perimeter frame structures.
- Columns in non-ductile RC space frame structures have higher axial loads than those in perimeter frame structures (compare an axial load ratio of approximately 0.3 in 1st floor interior columns of the 8-story space frame structure, to an axial load ratio of

approximately 0.1 in the 1st-floor interior columns of the 8-story perimeter frame structure). More heavily loaded columns are more likely to experience a loss of gravity-load carrying capacity in columns induced by column shear failure. For shorter buildings (2 and 4 stories), space frames have higher probabilities of collapse (lower collapse capacities) than perimeter frames, due to the significant effect of the vertical collapse mode.

- Modest improvements in collapse capacity on the order of 10 to 60% are observed for structures that exceed the 1967 UBC's code-minimum detailing requirements in beams and columns (reduced spacing of transverse reinforcement) or joints (provision of transverse reinforcement in joints). Structures with overstrength in beams, which can result from a variety of possible design decisions such as neglecting slab contribution in design, have below average collapse performance (with collapse capacities 10 to 25% lower than other structures).

Collapse predictions for non-ductile RC frame structures are extended to examine the consequences for building owners and occupants in terms of direct economic losses and fatalities. Economic losses in these office buildings are predicted on a component-by-component basis, and depend on the seismic demands on the building, contents and non-structural elements in the building and estimated repair costs. Economic losses are of concern to building owners, who will need to repair damage to structural and non-structural components in their structure following a damaging earthquake or insurance providers who will expect to pay out to repair damage. Several observations can be made regarding predictions of economic losses for older RC frame structures:

- Owners of older non-ductile RC frame structures located in highly seismic regions in California can expect to lose 2.2% of the replacement value (on average) of the structure annually due to earthquake-induced damage and repairs. Over the 50 year building life-span, this corresponds to approximately 60% of the value of the structure. It is noted that though high, these losses do not account for business interruption, a potentially significant contributor.
- 8 and 12-story space frame structures tend to incur smaller economic losses than 8 and 12- perimeter frame structures, because they are stiffer, reducing demands to drift-sensitive components, and have higher collapse capacities, reducing collapse losses.
- As a percentage of replacement cost, estimated economic losses predicted in this study decrease with building height. Since damage tends to concentrate in the lower stories of

tall buildings, repairs to upper stories are expected to be small in the most frequent (smaller) earthquakes. The component-based loss estimation approach used in this study misses appreciation of system damage effects such as residual drift that may trigger additional damage states not captured by the floor-to-floor assessment, particularly in taller buildings.

Quantification of fatalities requires additional information about the collapsed volume, the occupancy of the structure, and the lethality of reinforced concrete in order to predict how many lives are threatened in non-ductile RC frame buildings. Primary findings from the fatality assessments are as follows:

- The annualized fatality rate from seismic collapse of non-ductile RC frames is 0.02% (% of building occupants).
- The fatality estimation process finds that space frames are typically safer than perimeter frames structures, with an average fatality rate for the baseline structures of 0.016%, compared to 0.024% in the space frame structures. Space frames have higher sidesway collapse capacities, and although they can be more susceptible to vertical failure modes than perimeter frames, fewer people are at risk from localized collapses.

8.2.2 Comparisons to Seismic Performance of Modern Reinforced Concrete Frame Structures

Evaluations of seismic performance of potentially vulnerable non-ductile RC frame structures are particularly meaningful when compared to the seismic performance of modern code-conforming RC frame structures. Modern special moment frame structures are evaluated following the same procedure of collapse assessment, loss prediction and fatality estimation used in assessing the seismic performance of non-ductile RC frame structures. Comparison of collapse safety, economic losses, and fatalities among new ductile structures and existing non-ductile structures illustrates the improvement in building code seismic provisions for reinforced concrete over the last 40 years in California. The seismic performance of modern structures also serves as a yardstick by which the safety of older RC frame structures can be judged and shows the seismic performance gain that could be realized by replacing a non-ductile RC frame structure with a new one.

- This study shows that modifications to building code seismic requirements for RC moment frames in California between 1967 and 2003 have lead to:
  - a 40% increase in lateral overstrength obtained from static pushover analysis,

  - a 75% increase in component deformation capacity (measured in terms of column plastic rotation capacity),
  - an increase in system deformation capacity by 2.5 times, accounting for both improvements in component deformation capacity and system-level ductility effects,
  - a tripling of the structure's median collapse capacity (measured in terms of ground motion spectral intensity), and
  - a decrease in the collapse rate (mean annual frequency of collapse, collapses per year) by a factor of 40.
- As a consequence of their worse collapse performance, non-ductile RC frame structures have a seismic fatality rate that is 20 times higher than modern RC frame structures. (While the seismic fatality rate in non-ductile RC frame structures is 20 times higher than modern structures, the collapse rate is 40 times higher. The difference in fatality rate is smaller because the non-ductile RC frames are more likely to collapse in story mechanisms, endangering a smaller percentage of their occupants when collapse occurs.)
- Economic losses (repair costs) are significantly larger in older RC frame structures than modern, code-conforming RC frame structures. In terms of expected annualized losses, economic losses predicted in older RC frames are double those in modern RC frames (2.2% vs. 1.0% of replacement cost). For a typical structure, this difference may represent savings to a structure's owner of 50% of the value of the structure (on average) over 50 years. While significant, this percentage reduction in losses is smaller than the percentage reductions in fatalities or collapse between older and modern RC frame structures.
- Modern building code requirements for RC frame structures provide more consistent collapse safety than older non-ductile RC frame structures. Conditional probabilities of collapse under $Sa_{2/50}$ for the modern ductile RC buildings vary between 0.05 and 0.20. The range of conditional collapse probabilities is twice as large ($0.6 < P[\text{Collapse} \mid Sa_{2/50}] < 0.9$) in the non-ductile buildings, indicating wider variability in collapse performance.

8.2.3 Cost-Benefit Assessment of Replacing or Retrofitting Non-Ductile Reinforced Concrete Frame Structures

These assessments of the likelihood of earthquake-induced collapse, fatalities and economic losses in non-ductile RC frame structures can inform efforts to mitigate the hazard posed by non-ductile RC buildings through seismic retrofit or replacement. Cost-benefit

analysis is used as a tool for examining and comparing the cost-effectiveness of policies requiring replacement or retrofit of vulnerable non-ductile RC frame structures. The benefits of seismic retrofit or replacement are quantified in terms of reduced collapse risk, decreased economic losses and decreased life-safety threat to building occupants. Three different retrofit techniques were considered: jacketing non-ductile RC columns with additional concrete and reinforcement, fiber-wrapping non-ductile RC columns, and surrounding selecting existing columns with 'supercolumn' shear walls. The cost-benefit assessment results in several findings:

- The benefits associated with retrofitting or replacing non-ductile RC frame structures includes reduced repair costs and fatalities. The benefit associated with improvements in public safety, i.e. reduced fatalities, accounts for 40 to 60% of computed benefits of replacing vulnerable non-ductile RC frame structures (assuming a nominal value of $2 million for human life). Ideally, the benefits would also include the contribution of reductions in business interruption, which is not currently incorporated into the cost assessment in this study.
- Cost-benefit assessment of demolishing and replacing non-ductile RC frame structures shows that the resulting cost per life saved is on the order of 4 to 5 million dollars.
- Retrofit of non-ductile RC frames may be more or less cost-effective than replacing these structures, depending on the cost and effectiveness of the retrofit strategy. Given the improvements in loss-reduction and reduced fatalities, the most effective retrofit designs in this study are estimated to be worth approximately $85 to $100 per square foot (again, assuming a $2 million value of human life).
- The most cost-effective candidates for retrofit or replacement are the worst existing non-ductile RC frame structures. Of the archetype structures considered, the 2-story space frame structure is the best candidate for mitigation, and replacement of this structure costs as little as $1 million per life saved. Other structures, such as those with configuration irregularities or deficiencies in design or construction, may also be particularly cost-effective.

8.2.4 Technical Aspects of Seismic Performance Assessment

The findings described above relied on development of a systematic procedure for assessing earthquake performance of different buildings, which is used to compare structures of different heights and framing systems and structures designed according to different

building code provisions. This procedure for seismic performance assessment is probabilistic, utilizing dynamic analysis of nonlinear structural simulation models of RC frame structures, and accounting for uncertainties in both future ground motions and structural modeling. Critical aspects of the performance assessment procedure include quantification and propagation of modeling uncertainties, procedures for incorporating non-simulated failure modes, and detailed nonlinear analysis models capable of capturing important aspects of structural behavior.

Simulation of the behavior of RC frame structures up to the onset of structural collapse required the calibration and validation of element models for modeling the degradation of strength and stiffness in RC columns, beams and joints. Observations regarding the modeling of RC beams and columns are listed below:

- Important aspects of flexure and flexure-shear strength and stiffness deterioration in non-ductile RC beams and columns can be captured using an appropriately calibrated concentrated plasticity model. A typical interior column at the 1st-story of an 8-story non-ductile space frame structure is modeled with an initial stiffness of $0.5EI_g$, a plastic rotation capacity of 0.013 radians and a post-capping rotation capacity (to zero remaining strength) of 0.028 radians. Beams and columns with smaller axial loads are predicted to be more ductile.
- Non-ductile RC beams and columns are modeled with smaller plastic rotation capacity, smaller post-capping rotation capacity and faster cyclic deterioration than comparable ductile RC components. Plastic rotation capacity and post-capping rotation capacity are between one-quarter and one-half those predicted for well-detailed ductile RC elements, depending on the properties of the beam-column. These differences result primarily from smaller amounts of transverse reinforcement and confinement provided in hinge regions of RC beam-columns in non-ductile structures.

The effect of loss of gravity-load carrying capacity and possible progressive collapse induced by column shear failure is indirectly incorporated by post-processing dynamic analysis results, using component limit-state criteria.

- This procedure is potentially conservative, since it assumes that collapse has occurred if any column in the structure loses its ability to carry gravity loads, but prevents the underestimation of the occurrence of collapse if difficult-to-simulate failure modes were excluded entirely.

- For the non-ductile RC frame structures, inclusion of the non-simulated vertical collapse mode has a greater effect on space frame structures, whose columns carry higher axial load levels in columns and therefore are more susceptible to loss of gravity-load carrying capacity at lower levels of interstory drift. Inclusion of the non-simulated failure modes decreases the median collapse capacity by 2 to 30% depending on the structure.
- Component-based limit state checks that treat column shear failure as collapse are very conservative, and would reduce the collapse margin by one-third and triple the predicted mean annual frequency of collapse.

A study of uncertainties in the structural modeling process, and how these uncertainties propagate through the analysis to affect structural response predictions yielded a number of findings:

- Neglecting uncertainties in structural modeling in structural performance assessment is non-conservative in almost all cases. These modeling uncertainties have a more significant effect when the relationship between model parameters and structural response is highly nonlinear, as in predicting collapse.
- Incorporating modeling uncertainties tends to increase the dispersion and shift the median in the response parameter of interest. The shift in the median associated with modeling uncertainties is particularly important in predicting collapse of structures with multiple failure modes.
- Depending on the performance metric and type of analysis needed, modeling uncertainties may be accounted for using Monte Carlo sampling and response surfaces, FOSM, or ASOSM, a procedure developed for improving FOSM predictions. The Monte Carlo and response surface approach is able to predict changes in the median and variance of structural response associated with modeling uncertainties. ASOSM is an approximate technique that mimics these results.

Other lessons learned during systematization of the assessment procedure relate to ground motion scaling and selection.

- Results of collapse assessment of non-ductile RC frames corroborate previous studies, showing that the spectral shape of rare ground motions in California has an important impact on the predicted collapse capacity of the structure, even for less-ductile structures. Properly accounting for the shape of rare spectra (ε) increases the median predicted collapse capacity of the structures by approximately 25% for these structures.

8.3 Future Research

There are several possible avenues for future research that could either improve the study of seismic performance of non-ductile RC frame structures or extend these results. These future research directions can be broadly organized into several categories, including model validation and improvement, treatment of sources of uncertainty, loss and fatality estimation, and inventory, archetype and cost-benefit data needed for policy development.

8.3.1 Model Validation and Improvement

Performance-based earthquake engineering requires development of computational simulation models that accurately characterize structural behavior. Several aspects of modeling of non-ductile RC frames provide opportunities for future study:

- Models in this study do not account for the contribution of the gravity designed flat-plate system to the seismic resistance of the structure. These gravity frames should be incorporated into the analysis model to improve predictions of collapse performance in perimeter frame structures.
- Models of non-ductile RC frames used here neglect several possible failure modes, including pull-out of lap-splices and beam bottom bars and punching shear failure in flat-plate type construction. Three-dimensional torsional failure modes are also excluded. Future research is needed to further development and validation of models for these failure mechanisms, and to incorporate these in the seismic performance assessment.
- Models could also be advanced by accounting for varying axial load in columns and the effect of non-structural components in contributing strength and stiffness to the structure.
- Calibrated lumped plasticity models for RC beams and columns would benefit from additional data from experimental tests. For the purpose of model validation, these tests should include columns tested at large deformations to quantify plastic-rotation capacity and post-capping rotation. In addition, pairs of identical columns tested under monotonic and cyclic loading are needed to advance predictions of cyclic deterioration.
- More experimental data is needed to create analysis models capable of simulating the loss of gravity load carrying capacity following column shear failure. This failure mode is currently incorporated using component limit state checks.

More broadly, the performance-based earthquake engineering approach to predicting collapse, economic losses and fatalities in California's non-ductile RC frame structures

requires validation in comparison to the observed long-term performance of California's building stock. This validation effort would require documentation of structural response, losses and fatalities in non-ductile RC structures in past (and future) earthquakes in California to identify discrepancies between the seismic performance prediction methodology and evidence from experience.

8.3.2 Treatment of Sources of Uncertainty

The investigation of propagation of uncertainties here focused on characterizing the effects of structural modeling uncertainties on collapse performance assessment. This study could be expanded in various ways:

- The modeling uncertainty study in this thesis is limited to frame structures. Examination of different types of structural systems with less redundancy and fewer failure modes would help to generalize the results.
- Correlation assumptions at the element and building level are worthy of future study. Future research can continue to investigate how correlations may affect the results, and quantify the extent to which correlation assumptions are valid.
- Other sources of uncertainty, including those related to construction and human error in design, could be investigated in a similar manner as modeling and design uncertainties, and may reduce the median collapse capacity.
- Performance assessments could also be improved by modeling the possible deterioration and aging of properties of reinforced concrete that may have occurred since these non-ductile RC frame structures were constructed 40 years ago, accounting for variations in maintenance, site conditions and past earthquakes.

8.3.3 Loss and Fatality Estimation

Certain aspects of the performance evaluation could be improved when additional data about quantifying losses and fatalities becomes available. Possible directions for future research include the following:

- Downtime losses and other indirect losses are a significant contributor to building owners' financial losses. Accounting for downtime losses would likely show that retrofit has a much higher financial benefit than shown in this study. An interesting extension of the loss estimation results presented in this study would be a comparison of predicted downtime in existing non-ductile and modern ductile RC frame structures.

- In addition to downtime, building closure due to residual drifts or other hazards may significantly increase a building owner's losses. Criteria for red-tagging are a logical extension of the loss estimation framework.
- Data regarding damage to structural and non-structural components can be improved by future research, testing and post-earthquake observations (especially in instrumented buildings), decreasing uncertainty in damage predictions and facilitating incorporation of more types of repair and damage directly in the loss estimation process. Due to the modular nature of the loss estimation process, the predicted losses can be easily updated when additional data becomes available.
- Investigation of correlation between damage states in components for loss estimation is needed. Current research tends to either assume full or zero correlation. Unfortunately, available data on correlations is very limited.
- Fatalities prediction is hampered by the paucity of data on earthquake-related fatalities that relates deaths and injuries to building type, level of building damage (collapsed volume) and damage in non-structural components and contents. To ensure that better data is gathered in subsequent earthquake disasters, it is suggested that a global database for collecting this data is established, providing a framework for information gathering and classification of damage and injuries.

8.3.4 Inventory and Archetype Data Needed for Policy Development

This thesis aims to apply data from performance-based earthquake engineering studies to inform decisions related to seismic safety policy at the state and local government level. This application provides the motivation for a number of topics for future research:

- The usefulness of seismic performance data of archetype structures in this study would be enhanced if combined with more detailed inventory data on RC frames in highly seismic regions of California. This inventory data could be used to characterize the distribution of buildings of different heights and framing systems, typical design and detailing features, and the type of irregularities frequently found in structures for the purpose of including these irregular structures in the archetype assessment process. Since many engineers may have exceeded code-minimum requirements in design, understanding typical design and detailing features is important to ensure the study is representative of California design.

- A more general consideration of different California sites with varying seismicity is needed. Several "typical" California hazard curves are needed to conduct a comprehensive assessment of the risk of collapse, economic losses and fatalities in non-ductile RC frame structures. Variation in hazard may have a significant effect on cost-benefit assessment.
- Other types of RC frame structures, such as those with infill walls, irregularities in plan creating torsional effects, or shear critical structures, exist in California's building stock. These structures should be analyzed and incorporated into the collapse assessment, comparisons and cost-benefit assessment.
- A perennial challenge in cost-benefit assessment is complete and accurate quantification of benefits. Estimates of benefits in this study should include reductions in downtime, building closure and non-fatal injuries when existing non-ductile RC frame structures are retrofitted or replaced, providing a more accurate representation of cost-effectiveness.

8.4 Concluding Remarks

Results of this study serve to quantify the debate over seismic safety of California's existing non-ductile RC moment frames, providing data on collapse rates, direct economic losses, fatalities and the cost-effectiveness of retrofit and replacement mitigation strategies. This information may be used to make transparent and well-informed choices related to identification and prioritization of particularly vulnerable non-ductile RC frame structures in California, evaluation of policies and performance requirements for seismic strengthening, and developing incentives for building owner investment in seismic safety. Still lacking is a frank discussion of societal seismic safety goals and available resources for seismic hazard mitigation.

Notation List

A_g	gross cross-sectional area of reinforced concrete column
a_{sl}	flag variable; asl = 0 if bond-slip is prevent from occurring in reinforced concrete column due to experimental test configuration
A_{st}	transverse steel provided in reinforced concrete column
BD	beam ductility meta model random variable
b_j	width of reinforced concrete joint
BS	beam strength meta model random variable
c	cyclic deterioration parameter for Ibarra element model; describes the change in the rate of cyclic deterioration as the energy dissipation capacity is exhausted
c_{units}	factor for converting psi to MPa
d	depth of column section, measured from extreme compression fiber to centerline of tension reinforcement
d_c	depth of column section, measured as centerline-to-centerline distance between stirrups
C	design base shear coefficient
CD	column ductility meta model random variable
CDR	column drift ratio
CMR	collapse margin ratio, equal to $Sa(T_1)/Sa(T_1)_{2/50}$
CS	column strength meta model random variable variable
DM	damage measure
DV	decision variable, eg. dollars, deaths or downtime
EAL	expected annual losses, usually represented as a % of the building replacement cost
EANF	expected annual number of fatalities, usually represented as % of the total number of occupants in the building
EI_g	uncracked stiffness of reinforced concrete column where E - Young's modulus of concrete, I_g – gross moment of inertia of reinforced concrete column
EI_{stf}	secant stiffness to 40% of yield of reinforced concrete column
EI_y	secant stiffness to yield of reinforced concrete column
EDP	engineering demand parameter, measures of structural response
f'_c	concrete compressive strength
f_{yt}	yield strength of transverse steel
h	height of column section or height of reinforced concrete joint
IDA	incremental dynamic analysis
IDR	interstory drift ratio

IM intensity measure, measure of ground motion intensity

K ductility factor existing in 1967 Uniform Building Code; reduces design base shear for ductile structures

K_s hardening stiffness for use in Ibarra element model, ie. stiffness between θ_y and $\theta_{cap,pl}$

K_e secant stiffness through the yield point, for use in Ibarra element model

K_c post-capping stiffness for use in Ibarra element model

L_s shear span

$\hat{m}$ median of lognormal probability distribution

$\hat{m}_{mod}$ median of collapse probability distribution when modeling uncertainties are accounted for

MCE maximum considered earthquake

M_c ultimate moment capacity (at capping point) of a reinforced concrete column, for input in Ibarra material model

M_w earthquake magnitude (moment magnitude)

M_y nominal moment capacity of a reinforced concrete column, for input in Ibarra material model

p_d probability that building occupant will die in earthquake

p_e probability of entrapment in building by earthquake

$p_{f|e}$ probability of fatality, given that the victim is trapped by the earthquake

p_o fraction of building occupants in the building at a given time

P axial load, typically on a column

PFA peak floor acceleration

PGA peak ground acceleration

PV present value of losses

RC_i cost of repairing i^{th} component in the building, following earthquake damage

RDR_{ult} ultimate roof drift ratio, defined as the roof drift ratio corresponding to 20% strength loss

s stirrup spacing

Sa spectral acceleration

$Sa_{2/50}$ the spectral acceleration that has a 2% likelihood of being exceeded in 50 years at the site of interest; depends on the natural period of interest

$Sa_{10/50}$ the spectral acceleration that has a 10% likelihood of being exceeded in 50 years at the site of interest; depends on the natural period of interest; also denoted as S_D

SC sidesway collapse

SMF special moment frame designed according to requirements in ACI 318

s_n rebar buckling coefficient; $sn = (s/d_b)(f_y/100)^{0.5}$, where f_y is the yield strength of the longitudinal rebar in MPa, s is the spacing of transverse reinforcement, and d_b is the diameter of the longitudinal bars.

T_1 a structure's fundamental (first mode) period

TC total cost of repairs to earthquake-induced damage

X_i i^{th} model random variable
V design base shear for equivalent seismic loading
VC vertical collapse
V_n shear strength of reinforced concrete joint
W weight of structure

Δ^+/Δ^- measure of response asymmetry for purpose of computing effect of modeling uncertainty (Chapter 4)
ε a measure of spectral shape, defined as the number of logarithmic standard deviations between the observed spectral value and the median prediction from an attenuation function; depends on the period of interest
γ factor accounting for confinement in joint
λ mean annual frequency of exceedance, either λ(IM) or λ(DV), which describes the mean annual frequency of exceeding a ground motion of specified intensity or of exceeding a particular consequence (eg. dollars, deaths, downtime)
λ normalized energy dissipation parameter for Ibarra element model, defined as the normalized value defined by the total energy dissipation capacity
μ_{ln} logarithmic mean of lognormal probability distribution
σ_{ln} logarithmic standard deviation, associated with a lognormal probability distribution
θ_y chord rotation at yield, for input into the Ibarra element model (radians)
$\theta_{cap,pl}$ plastic chord rotation from yielding to capping (radians)
θ_{cap} plastic chord rotation to capping (radians)
θ_{pc} post-capping rotation capacity (radians)
ρ longitudinal reinforcement ratio in reinforced concrete column
ρ correlation coefficient between two random variables
ρ_{sh} transverse reinforcement ratio in reinforced concrete column
Ω static overstrength of a structure, defined as the ratio of the ultimate base shear to the design base shear
ν axial load ratio: $P/A_g f'_c$

References

ABAG (2005). Taming Natural Disasters: Multi-Jurisdictional Local Government Hazard Mitigation Plan for the San Francisco Bay Area.

Abrahamson, N. A. and W. J. Silva (1997). "Empirical response spectral attenuation relations for shallow crustal earthquakes." Seismological Research Letters 68(1): 94 - 126.

Abrahamson, N. A. and W. J. Silva (2008). Abrahamson and Silva NGA Ground Motion Relations for the Geometric Mean Horizonal Component of Peak and Spectral Ground Motion Parameteres, Pacific Earthquake Engineering Research Center 2008/xx (in draft form), University of California at Berkeley.

ACI (2002). Building Code Requirements for Structural Concrete (ACI 318).

Alesch, D. and W. Petak (2004). "Seismic Retrofit of California Hospitals: Implementing Regulatory Policy in a Complex and Dynamic Context." Natural Hazards Review 5(2): 89-96.

Aleskerov, F., A. I. Say, A. Toker, H. L. Akin and G. Altay (2005). "A cluster-based decision support system for estimating earthquake damage and casualties." Disasters 29(3): 255-276.

Alexander, D. (1996). "The Health Effects of Earthquakes in the Mid-1990s." Disasters 20(3): 231 - 247.

Altoontash, A. (2004). Simulation and Damage Models for Performance Assessment of Reinforced Concrete Beam-Column Joints, Doctoral Dissertation, Stanford University.

Armenian, H. K., A. Melkonian, E. K. Noji and A. P. Hovanesian (1997). "Deaths and Injuries due to the Earthquake in Armenia: A Cohort Approach." International Journal of Epidemiology 26(4): 806-813.

ASCE (2000). Prestandard and Commentary for the Seismic Rehabilitation of Buildings (FEMA 356). Washington DC, Federal Emergency Management Agency.

ASCE (2002). Minimum Design Loads for Buildings and Other Structures (ASCE 7-02), American Society of Civil Engineers.

ASCE (2005). Minimum Design Loads for Buildings and Other Structures (ASCE 7-05), American Society of Civil Engineers.

ASCE (2007). Seismic Rehabilitation of Existing Buildings (ASCE/SEI 41-06). Reston, American Society of Civil Engineers.

Aschheim, M., P. Gulkan, H. Sezen, M. Bruneau, A. Elnashai, M. Halling, J. Love and M. Rahnama (2000). "Performance of Buildings in 1999 Marmara Earthquake." Earthquake Spectra 16(S1): 237 - 279.

Aslani, H. (2005). Probabilistic Earthquake Loss Estimation and Loss Disaggregation in Buildings, Doctoral Dissertation, Stanford University.

ATC (1985). Earthquake Damage Evaluation Data for California (ATC 13). Redwood City Federal Emergency Management Agency.

ATC (1996). Seismic Evaluation and Retrofit of Concrete Buildings (ATC 40), California Seismic Safety Commission.

ATC (2003). San Francisco's Earthquake Risk: Report on Potential Earthquake Impacts in San Francisco, San Francisco Department of Building Inspection: Community Action Plan for Seismic Safety, Draft.

ATC (2005). Improvement of Nonlinear Static Analysis Procedures (FEMA 440). Washington D.C., Federal Emergency Management Agency.

ATC (2007). Guidelines for Seismic Performance Assessment of Buildings, ATC-58 35% Draft. Redwood City, CA, FEMA.

ATC (2007). Recommended Methodology for Quantification of Building System Performance and Response Parameters, ATC-63 75% Draft. Redwood City, CA, FEMA.

Aycardi, L. E., J. Mander and A. Reinhorn (1994). "Seismic Resistance of Reinforced Concrete Frame Structures Designed Only for Gravity Loads: Experimental Performance of Subassemblages." ACI Structural Journal 91(5): 552-563.

Bai, J.-W. (2003). Seismic Retrofit of Reinforced Concrete Building Structures, Mid-America Earthquake Center, CM-4.

Baker, J. W. (2005). Vector-Valued Ground Motion Intensity Measures for Probabilistic Seismic Demand Analysis, Doctoral Dissertation, Stanford University.

Baker, J. W. (2008). Intensity Measures, Personal Communication to A. Liel on March 31, 2008.

Baker, J. W. and C. A. Cornell (2005). "A Vector-Valued Ground Motion Intensity Measure Consisting of Spectral Acceleration and Epsilon." Earthquake Engineering and Structural Dynamics 34(10): 1193-1217.

Baker, J. W. and C. A. Cornell (2005). "Which Spectral Acceleration are you Using?" Earthquake Spectra 22(2): 293-312.

Baker, J. W. and C. A. Cornell (2007). "Uncertainty propagation in seismic loss estimation." Structural Safety 30(3): 236-252.

Bakis, C. D., L. C. Bank, V. L. Brown, E. Cosenza, J. F. Davalos, J. J. Lesko, A. Machida, S. H. Rizkalla and T. C. Triantafillou (2002). "Fiber-Reinforced Polymer Composites for Construction - State-of-the-Art Review." Journal of Composites for Construction 6(2): 73-87.

Bank, L. C. (2006). Composites for Construction: Structural Design with FRP Materials. Hoboken, NJ, John Wiley & Sons.

Bates, H., M. Holweg, M. Lewis and N. Oliver (2007). "Motor vehicle recalls: Trends, patterns, and emerging issues." Omega: The International Journal of Management Science 35: 202- 210.

Bazzurro, P. and C. A. Cornell (2004). "Nonlinear Soil-Site Effects in Probabilistic Seismic Hazard Analysis." Bulletin of the Seismological Society of America 94(6): 2110-2123.

Beatley, T. and P. Berke (1990). "Seismic Safety Through Public Incentives: The Palo Alto Seismic Hazard Identification Program." Earthquake Spectra 6(1): 57-79.

Beck, J. L., K. A. Porter, R. Shaikhutdinov, S. K. Au, T. Moroi, Y. Tsukada and M. Masuda (2002). Impact of Seismic Risk on Lifetime Property Values. Richmond, CA, Consortium of Universities for Research in Earthquake Engineering.

Benjamin, J. R. and C. A. Cornell (1970). Probability, Statistics and Decision for Civil Engineers. New York, McGraw-Hill.

Benuska, L., Ed. (1990). "Loma Prieta Earthquake Reconnaissance Report." Earthquake Spectra 6 (Supplement).

Beres, A., S. Pessiki, R. White and P. Gergely (1996). "Implications of Experiments on the Seismic Behavior of Gravity Load Designed RC Beam-to-Column Connections." Earthquake Spectra 12(2): 185-198.

Berg, G. (1983). Seismic Design Codes and Procedures, Earthquake Engineering Research Institute.

Bernstein, S. (2005). How Risky Are Older Concrete Buildings?, Los Angeles Times, Oct. 11, 2005.

Berry, M. and M. Eberhard (2003). Performance Models for Flexural Damage in Reinforced Concrete Columns, PEER.

Berry, M. and M. Eberhard (2005). "Practical Performance Model for Bar Buckling." Journal of Structural Engineering 131(7): 1060 - 1070.

Berry, M., M. Parrish and M. Eberhard (2004). PEER Structural Performance Database, User's Manual, Pacific Earthquake Engineering Research Center.

Biddah, A. and A. Ghobarah (1999). "Modeling of shear deformation and bond slip in reinforced concrete joints." Structural Engineering and Mechanics 7(4): 413-432.

Blume, J. (1994). Connections (Interview by Stanley Scott). Oakland, Earthquake Engineering Research Institute.

Blume, J., N. Newmark and L. M. Corning (1961). Design of Multi-story Reinforced Concrete for Earthquake Motions. Chicago, Portland Cement Association.

Bonacci, J. and S. Pantazopoulou (1993). "Parametric Investigation of Joint Mechanics." ACI Journal 90(1): 61-71.

Bonneville, D. R. and R. H. Lanning (1996). "Development of an Industrial Corporate Seismic Program." Cascadia Region Earthquake Workgroup.

Boore, D. M. and G. M. Atkinson (2007). Boore-Atkinson NGA Ground Motion Relations for Geometric Mean Horizontal Component of Peak and Spectral Ground Motion Parameters, Pacific Earthquake Engineering Research Center 2007/01, University of California at Berkeley.

Boore, D. M., W. B. Joyner and T. E. Fumal (1997). "Equations for estimating horizontal response spectra and peak accelerations from western North America earthquakes: A summary of recent work " Seismological Research Letters 68(1): 128 - 153.

Bousias, S., A.-L. Spathis and M. N. Fardis (2007). "Seismic Retrofitting of Columns with Lap Spliced Smooth Bars through FRP or Concrete Jackets." Journal of Earthquake Engineering 11: 653-674.

Bousias, S. N., D. E. Biskinis, M. N. Fardis and A.-L. Spathis (2007). "Strength, Stiffness and Cyclic Deformation Capacity of Concrete Jacketed Members." ACI Structural Journal 104(5): 521-531.

Browning, J., Y. R. Li, A. Lynn and J. Moehle (2000). "Performance Assessment for a Reinforced Concrete Frame Building." Earthquake Spectra 16(3): 541-555.

CA Office of Emergency Services (2003). Guide and Checklist for Nonstructural Earthquake Hazards in California Schools, Department of General Services.

California Dept. of General Services (2002). Seismic Safety Inventory of California Public Schools.

California Office of Emergency Services (2003). Guide and Checklist for Nonstructural Earthquake Hazards in California Schools, Department of General Services.

California Office of Emergency Services (2004). State of California Multi-Hazard Mitigation Plan.

California Seismic Safety Commission (1985). Earthquake Safety: Potentially Hazardous Buildings [SSC 85-04].

California Seismic Safety Commission (1995). Northridge Earthquake: Turning Loss to Gain (Report to the Governor's Office after the Northridge Earthquake) [SSC 95-01].

California Seismic Safety Commission (1999). Earthquake Risk Management: A Toolkit for Decision Makers.

California Seismic Safety Commission (2003). Status of the Unreinforced Masonry Building Law.

Campbell, K. W. and Y. Bozorgnia (2006). Campbell-Bozorgnia NGA Empirical Ground Motion Model for the Average Horizontal Component of PGA, PGV, PGD and SA at Selected Spectral Periods Ranging from 0.01 - 10.0 seconds (version 1.0), Pacific Earthquake Engineering Research Center.

Charlet, A. Y., A. Schellenberg, K. J. Elwood, T. Haukaas and S. A. Mahin (2008). "Hybrid Simulation of the Gravity Load Collapse of Reinforced Concrete Frames." 2008 ASCE Structures Congress (Vancouver, Canada).

Cheong, H. K. and N. MacAlevey (2000). "Experimental Behavior of Jacketed Reinforced Concrete Beams." Journal of Structural Engineering 126(6): 692-699.

Chopra, A. K. and R. K. Goel (2000). "Building Period Formulas for Estimating Seismic Displacement." Earthquake Spectra 16(2).

Chou, Y.-J., N. Huang, C.-H. Lee, S.-L. Tsai, L.-S. Chen and H.-J. Chang (2004). "Who Is at Risk of Death In an Earthquake." American Journal of Epidemiology 160(7): 688- 695.

Christian, J. T. (2004). "Geotechnical Engineering Reliability: How Well Do We Know What We Are Doing?" Journal of Geotechnical and Geoenvironmental Engineering 130(10): 985-1003.

Coburn, A., R. Spence and A. Pomonos (1992). "Factors determining human casualty levels in earthquakes: mortality prediction in building collapse." 10th World Conference on Earthquake Engineering.

Comerio, M. C. (1992). "Impacts of the Los Angeles Retrofit Ordinance on Residential Buildings." Earthquake Spectra 8(1): 79 - 94.

Comerio, M. C. (2000). The Economic Benefits of a Disaster Resistant University: Earthquake Loss Estimation at UC Berkeley.

Comerio, M. C. (2006). "Estimating Downtime in Loss Modeling." Earthquake Spectra 22(2): 349 - 365.

Comerio, M. C. and J. C. Stallmeyer (2003). "Laboratory Equipment: Estimating Losses and Mitigating Costs." Earthquake Spectra 19(4): 779 - 797.

Comerio, M. C., S. Tobriner and A. Fehrenkamp (2006). Bracing Berkeley: A Guide to Seismic Safety on the UC Berkeley Campus, Pacific Earthquake Engineering Research Center.

Comité Euro-International du Béton (1996). RC Frames Under Earthquake Loading – State of the Art Report. London, Thomas Telford.

Concrete Reinforcing Steel Institute (1970). Manual of Standard Practice.

Conrad, K. (2004). Analysis: Seismic retrofit may reduce bomb damage, Sacramento Business Journal.

Cornell, C. A., F. Jalayer, R. Hamburger and D. A. Foutch (2002). "Probabilistic Basis for 2000 SAC Federal Emergency Management Agency Steel Moment Frame Guidelines." Journal of Structural Engineering 128 (4): 525 - 533.

Degenkolb, H. (1994). Connections (Interview by Stanley Scott). Oakland, EERI Oral History Series, EERI.

Degenkolb, H. J., T. D. Wosser, L. A. J. Wyllie, C. D. Poland, D. R. Bonneville, R. A. Bruce, T. J. Canon, G. E. Greenwood and R. J. Love (1987). The Whittier Narrows Earthquake October 1, 1987. San Francisco, Degenkolb Engineers.

Deierlein, G. G. (2004). "Overview of a Comprehensive Framework for Earthquake Performance Assessment." Proceedings of International Workshop on Performance-Based Seismic Design Concepts and Implementation (Bled, Slovenia).

Deierlein, G. G., A. B. Liel, C. B. Haselton and C. A. Kircher (2007). "Assessing Building System Collapse Performance and Associated Requirements for Seismic Design." SEAOC Convention (Tahoe, CA).

DerKiureghian, A. (2005). "Non-ergodicity and PEER's framework formula." Earthquake Engineering and Structural Dynamics 34: 1643 - 1652.

DerKiureghian, A. and O. Ditlevsen (2007). "Aleatory or Epistemic? Does it matter?" Stanford Workshop on Risk Acceptance and Risk Communication (Stanford, CA).

Dhakal, R. P. and K. Maekawa (2002). "Modeling of Post-yielding Buckling of Reinforcement." Journal of Structural Engineering 128(9): 1139 - 1147.

Diamantidis, D. and P. Bazzurro (2007). "Safety acceptance criteria for existing structures." Stanford Workshop on Risk Acceptance and Risk Communication (Stanford, CA).

Dogangun, A. (2004). "Performance of reinforced concrete buildings during the May 1, 2003 Bingol Earthquake in Turkey." Engineering Structures 26(6): 841-856.

Durkin, M. E. (1987). "The San Salvador Earthquake of October 10, 1986 - Casualties, Search and Rescue, and Response of the Health Care System." Earthquake Spectra 3(3): 621 - 634.

Durkin, M. E. (1992). "Improving Measures to Reduce Earthquake Casualties." Earthquake Spectra 8(1): 95 - 113.

Durkin, M. E. and H. O. Murakami (1988). "Casualties, Survival and Entrapment in Heavily Damaged Buildings." 9th World Conference in Earthquake Engineering.

EERC. (2007). "The Earthquake Engineering Online Archive." Retrieved Mar. 2008, from http://nisee.berkeley.edu/elibrary/index.html.

El-Attar, A. G., R. N. White and P. Gergely (1997). "Behavior of Gravity Load Designed Reinforced Concrete Buildings Subjected to Earthquakes." ACI Structural Journal 94(2): 133 - 145.

Ellingwood, B. (2007). "Quantifying and Communicating Uncertainty in Seismic Risk Assessment." Risk Acceptance and Risk Communication (Stanford, CA).

Ellingwood, B. and R. B. Corotis (1991). "Load combinations for building exposed to fires." Engineering Journal of the American Institute of Steel Construction 28(1): 37-44.

Ellingwood, B., T. V. Galambos, J. G. MacGregor and C. A. Cornell (1980). Development of a Probability Based Load Criterion for American National Standard A58: Building Code Requirements for Minimum Design Loads in Buildings and Other Structures, National Bureau of Standards, U.S. Department of Commerce.

Ellingwood, B., J. G. MacGregor, T. V. Galambos and C. A. Cornell (1982). "Probability Based Load Criteria: Load Factors and Load Combinations." Journal of the Structural Division 108(ST5): 978 - 997.

Ellingwood, B. R. and P. B. Tekie (1999). "Wind Load Statistics for Probability-Based Structural Design." Journal of Structural Engineering 125(4): 453 - 463.

Elwood, K. (2004). "Modeling failures in existing reinforced concrete columns." Canadian Journal of Civil Engineering 31(5): 846-859.

Elwood, K. and J. Moehle (2005). "Axial Capacity Model for Shear-Damaged Columns." ACI Structural Journal 102(4): 578-587.

Elwood, K. J. and M. O. Eberhard (2006). "Effective Stiffness of Reinforced Concrete Columns." PEER Research Digest(2006-1): 1- 5.

Elwood, K. J., A. B. Matamoros, J. W. Wallace, D. E. Lehman, J. A. Heintz, A. D. Mitchell, M. A. Moore, M. T. Valley, L. N. Lowes, C. D. Comartin and J. P. Moehle (2007). "Update to ASCE/SEI 41 Concrete Provisions." Earthquake Spectra 23(2): 493-523.

Elwood, K. J. and J. P. Moehle (2005). "Drift Capacity of Reinforced Concrete Columns with Light Transverse Reinforcement." Earthquake Spectra 21(1): 71 - 89.

Engindeniz, M., L. F. Kahn and A.-H. Zureick (2005). "Repair and Strengthening of Reinforced Concrete Beam-Column Joints: State of the Art " ACI Structural Journal 102(2): 187 - 197.

EQE Incorporated (1987). Summary of the October 1, 1987 Whittier, California Earthquake: An EQE Quick Look Report, EQE.

Esteva, L. and S. E. Ruiz (1989). "Seismic Failure Rates of Multistory Frames." Journal of Structural Engineering 115(2): 268 - 283.

Fardis, M. N. and D. E. Biskinis (2003). "Deformation Capacity of RC Members, as Controlled by Flexure or Shear." Otani Symposium.

FEMA (1994). Typical Costs for Seismic Rehabilitation of Existing Buildings, Second Edition, Earthquake Hazards Reduction Series 39, FEMA.

FEMA (2003). HAZUS-MH MR1 Technical Manual. Washington D.C., FEMA.

Filiatrault, A., E. Lachapelle and P. Lamontagne (1998). "Seismic performance of ductile and nominally ductile reinforced concrete moment resisting frames I. Experimental Study." Canadian Journal of Civil Engineering 25(2): 331-341.

Filiatrault, A., E. Lachapelle and P. Lamontagne (1998). "Seismic performance of ductile and nominally ductile reinforced concrete moment resisting frames II. Analytical Study." Canadian Journal of Civil Engineering 25(2): 342-352.

Frankel, A. D., M. D. Petersen, C. S. Mueller, K. M. Haller, R. L. Wheeler, E. V. Leyendecker, R. L. Wesson, S. C. Harmsen, C. H. Cramer, D. M. Perkins and K. S. Rukstales (2002). Documentation for the 2002 Update of the National Seismic Hazard Maps, U.S. Department of the Interior, U.S. Geological Survey.

Frazier, G. A., J. H. Wood and G. W. Housner (1971). "Earthquake Damage to Buildings." Engineering Features of the San Fernando Earthquake of February 9, 1971. P. C. Jennings, Ed. Pasadena, California Institute of Technology.

Galal, K., A. Arafa and A. Ghobarah (2005). "Retrofit of RC Square Short Columns." Engineering Structures 27(5): 801 - 813.

Geschwind, C.-H. (2001). California Earthquakes: Science, Risk and the Politics of Hazard Mitigation. Baltimore, Johns Hopkins University Press.

Goulet, C., C. Haselton, J. Mitrani-Reiser, J. Stewart, E. Taciroglu and G. Deierlein (2006). "Evaluation of Seismic Performance of a Code-Conforming Reinforced-Concrete Frame Buildings- Part I. Ground Motion Selection and Structural Collapse Simulation." 8th National Conference on Earthquake Engineering.

Goulet, C. A., C. B. Haselton, J. Mitrani-Reiser, J. L. Beck, G. G. Deierlein, K. A. Porter and J. P. Stewart (2007). "Evaluation of the Seismic Performance of a Code-Conforming Reinforced-Concrete Frame Building - from Seismic Hazard to Collapse Safety and Economic Losses." Earthquake Engineering and Structural Dynamics 36(13): 1973 - 1997.

Goulet, C. A., J. Watson-Lamprey, J. W. Baker, C. B. Haselton and N. Luco (2008). "Assessment of Ground Motion Selection and Modification (GMSM) Methods for Non-Linear Dynamic Analyses of Structures." Geotechnical Earthquake Engineering and Soil Dynamics IV (Sacramento, CA).

Green, M. (1993). "Code Provisions for Unreinforced Masonry Bearing Walls in California." Structures Congress: Structural Engineering in Natural Hazards Mitigation.

Gutierrez, E., F. Taucer, T. D. Groeve, D. H. A. Al-Khudhairy and J. M. Zaldivar (2005). "Analysis of Worldwide Earthquake Mortality using Multivariate Demographic and Seismic Data." American Journal of Epidemiology 161: 1151 - 1158.

Harries, K. A., J. R. Ricles, S. Pessiki and R. Sause (2006). "Seismic Retrofit of Lap Splices in Nonductile Square Columns Using Carbon Fiber-Reinforced Jackets." ACI Structural Journal 103(6): 874-884.

Haselton, C., A. Liel, S. Taylor Lange and G. G. Deierlein (2007). Beam-Column Element Model Calibrated for Predicting Flexural Response Leading to Global Collapse of RC Frame Buildings, Pacific Earthquake Engineering Research Center 2007/xx (In Preparation), University of California at Berkeley.

Haselton, C. B. (2006). Assessing Seismic Collapse Safety of Modern Reinforced Concrete Frame Buildings, Doctoral Dissertation, Stanford University.

Haselton, C. B. and J. W. Baker (2006). "Ground Motion Intensity Measures for Structural Collapse Capacity Prediction: Choice of Optimal Spectral Period and Effect of Spectral Shape." 8th National Conference of Earthquake Engineering.

Haselton, C. B., J. W. Baker, A. B. Liel, C. A. Kircher and G. G. Deierlein (2008). "Accounting for Expected Spectral Shape (Epsilon) in Collapse Performance Assessment " Earthquake Spectra Submitted.

Haselton, C. B., A. B. Liel and G. G. Deierlein (2007). "Significance of Various Design and Assessment Parameters on Seismic Collapse Safety Assessment of Reinforced Concrete Frame Buildings." Asian-Pacific Network of Centers for Earthquake Engineering Research (ANCER), 2007 Meeting.

Haselton, C. B., J. Mitrani-Reiser, C. Goulet, G. G. Deierlein, J. Beck, K. A. Porter, J. Stewart and E. Taciroglu (2008). An Assessment to Benchmark the Seismic Performance of a Code-Conforming Reinforced-Concrete Moment-Frame Building, Pacific Earthquake Engineering Research Center 2008/xx (In Preparation), University of California at Berkeley.

Hegger, J., A. Sherif and W. Roeser (2003). "Nonseismic Design of Beam-Column Joints." ACI Structural Journal 100(5): 654 - 664.

Heintz, J. (2007). Typical retrofit costs, Personal Communication. to A. Liel.

Helton, J. C. and F. J. Davis (2001). Latin Hypercube Sampling and the Propagation of Uncertainty in Analyses of Complex Systems, Sandia National Laboratories.

Hengjian, L., M. Kohiyama, K. Horie, N. Maki, H. Hayashi and S. Tanaka (2003). "Building Damage and Casualties after an Earthquake." Natural Hazards 29: 387 - 403.

Hueste, M. B. D. and J. K. Wight (1999). "Nonlinear Punching Shear Failure for Interior Slab-Column Connections." Journal of Structural Engineering 125(9): 997-1008.

Iacobucci, R. D., S. A. Sheikh and O. Bayrak (2003). "Retrofit of Square Concrete Columns with Carbon Fiber-Reinforced Polymer for Seismic Resistance." ACI Structural Journal 100(6): 785-794.

Ibarra, L. (2003). Global Collapse of Frame Structures under Seismic Excitations, Doctoral Dissertation (Blume Center TR 152), Stanford University.

Ibarra, L. F., R. A. Medina and H. Krawinkler (2005). "Hysteretic Models that Incorporate Strength and Stiffness Deterioration." Earthquake Engineering and Structural Dynamics 34: 1489- 1511.

ICBO (1967). Uniform Building Code. Pasadena, CA.

ICBO (1973). Uniform Building Code. Pasadena, CA.

ICC (2003). International Building Code. Falls Church, VA.

Ikuta, E., M. Miyano, F. Nagashima, A. Nishimura, H. Tanaka, Y. Nakamori, K. Kajiwara and Y. Kumagai (2004). "Measurement of the Human Body Damage Caused by Collapse Building." 13th World Conference on Earthquake Engineering

Jennings, P., Ed. (1971). Engineering Features of the San Fernando Earthquake of February 9, 1971. Pasadena, CA.

Jephcott, D. K. (1986). "50-year Record of Field Act Seismic Building Standards for California Schools." Earthquake Spectra 2(3): 621-629.

Johnson, C. B. (1972). "Structural Engineering." The San Fernando Earthquake of February 9, 1971 and Public Policy. G. O. Gates, Special Subcommittee of the Joint Committee on Seismic Safety, California Legislature.

Kabeyasawa, T., T. Matsumori, H. Katsumata and K. Shirai (2005). "Design of the Full-Scale Six-Story Reinforced Concrete Wall-Frame Building for Testing at E-Defense." US-Japan Workshop.

Kaul, R. (2004). Object Oriented Development of Strength and Stiffness Degrading Models for Reinforced Concrete Structures, Doctoral Dissertation, Stanford University.

Kircher, C. A. (2007). Loss Results, Personal Communication to C. Haselton.

Kircher, C. A., H. A. Seligson, J. Bouabid and G. C. Morrow (2006). "When the Big One Strikes Again - Estimated Losses due to a Repeat of the 1906 San Francisco Earthquake." Earthquake Spectra 22(S2): S297 - S339.

Krawinkler, H., Ed. (2005). Van Nuys Hotel Building Testbed Report: Exercising Seismic Performance Assessment, Pacific Earthquake Engineering Research Center 2005/11, University of California at Berkeley.

Krawinkler, H. and E. Miranda (2004). "Performance-Based Earthquake Engineering." Earthquake Engineering: From Engineering Seismology to Performance-Based Engineering. Y. Bozorgnia and V. V. Bertero, Ed. Boca Raton, CRC Press.

Krawinkler, H. and F. Zareian (2007). "Prediction of Collapse - How Realistic and Practical Is It-And What Can We Learn From It." Structural Design of Tall Buildings 15: 633 - 653.

Kunnath, S. K., G. Hoffmann, A. M. Reinhorn and J. B. Mander (1995). "Gravity-Load-Designed Reinforced Concrete Buildings -Part I: Seismic Evaluation of Existing Construction." ACI Structural Journal 92(3): 343-354.

Kunnath, S. K., G. Hoffmann, A. M. Reinhorn and J. B. Mander (1995). "Gravity Load-Designed Reinforced Concrete Buildings- Part II: Evaluation of Detailing Enhancements." ACI Structural Journal 92(3): 355-366.

Kurama, Y. C., S. P. Pessiki, R. Sause and S. Wu (1994). "Seismic Behavior of Non-Ductile Concrete Frame Structures." ASCE Structures Congress.

Lee, T. H. and K. M. Mosalam (2005). "Seismic Demand Sensitivity of Reinforced Concrete Shear-Wall Building Using FOSM Method." Earthquake Engineering and Structural Dynamics 34: 1719 - 1736.

Lew, H. S., E. V. Leyendecker and R. D. Dikkers (1971). Engineering Aspects of the 1971 San Fernando Earthquake. Washington, D.C., U.S. Government Printing Office.

Liao, Y.-H., L.-C. Hwang, C.-C. Chang, Y.-J. Hong, I.-N. Lee, J.-H. Huang, S.-f. Lin, M. Shen, C.-H. Lin, Y.-Y. Gau and C.-T. Ynag (2003). "Building Collapse and Human Deaths Resulting from the Chi-Chi Earthquake in Taiwan, September 1999." Archives of Environmental Health 58(9): 572 - 578.

Liel, A. B., C. B. Haselton and G. G. Deierlein (2006). "The Effectiveness of Seismic Building Code Provisions on Reducing the Collapse Risk of Reinforced Concrete Moment Frame Buildings." 4th International Conference in Earthquake Engineering (Taiwan).

Liel, A. B., C. B. Haselton, G. G. Deierlein and J. W. Baker (2007). "Incorporating Modeling Uncertainties in the Assessment of Seismic Collapse Risk of Buildings." Structural Safety (in press).

Lignos, D. G. and H. Krawinkler (2007). "A Database in Support of Modeling of Component Deterioration for Collapse Prediction of Steel Frame Structures." ASCE Structures Congress (Long Beach, CA).

Lowes, L. (2005). Modeling Beam-Column Joints, Personal Communication to A. Liel.

Lowes, L. N. and A. Altoontash (2003). "Modeling of Reinforced-Concrete Beam-Column Joints Subjected to Cyclic Loading." Journal of Structural Engineering 129(12): 1686-1697.

Lowes, L. N., N. Mitra and A. Altoontash (2004). A Beam-Column Joint Model for Simulating the Earthquake Response of Reinforced Concrete Frames, PEER.

Lynn, A., J. Moehle, S. Mahin and W. Holmes (1996). "Seismic Evaluation of Existing Reinforced Concrete Building Columns." Earthquake Spectra 12(4): 715-739.

MacGregor, J. G., J. E. Breen and E. O. Pfrang (1970). "Design of Slender Concrete Columns." ACI Journal 67(1): 6-28.

Macleod, J. D. and S. Scott (1987). "Earthquake Safety: California's Comprehensive New Program." Earthquake Spectra 3(4): 811-819.

Maffei, J. (2007). Retrofit of Reinforced Concrete Frames, Personal Communication to A. Liel on October 17, 2007.

Marusic, D. and P. Fajfar (2005). "On the inelastic seismic response of asymmetric buildings under bi-axial excitation." Earthquake Engineering and Structural Dynamics 34: 943 - 963.

May, P. J. (2001). Organizational and Societal Considerations for Performance-Based Earthquake Engineering, Pacific Earthquake Engineering Research Center 2001/04, University of California at Berkeley.

May, P. J. (2001). "Societal Perspectives about Earthquake Performance: The Fallacy of 'Acceptable Risk'." Earthquake Spectra 17(4).

May, P. J. (2002). Barriers to Adoption and Implementation of PBEE Innovation.

May, P. J. (2004). "Making Choices about Earthquake Performance." Natural Hazards Review 5(2): 64-70.

Meehan, J. F. and E. E. Cole, Eds. (1991). Reflections on the Loma Prieta Earthquake, October 17, 1989. Ad Hoc Earthquake Reconnaissance Committee, Structural Engineers Association of California.

Meinheit, D. F. and J. O. Jirsa (1981). "Shear strength of R/C beam-column connections." ASCE Journal of Structural Division 107(11): 2227-2244.

Melchers, R. E. (1999). Structural Reliability Analysis and Prediction. Chichester, England, John Wiley & Sons.

Melek, M. and J. W. Wallace (2004). "Cyclic Behavior of Columns with Short Lap Splices." ACI Structural Journal 101(6): 802-811.

Melek, M., J. W. Wallace and J. P. Conte (2003). Experimental Assessment of Columns with Short Lap Splices Subjected to Cyclic Loads, Pacific Earthquake Engineering Research Center 2003/04, University of California at Berkeley.

Messinger, D. L., H. S. Kellam, L. W. Graham, H. W. Martin and D. S. Ellifritt (1984). "Survey of 'Engineered Buildings' After the Coalinga Earthquake." Coalinga, California, Earthquake of May 2, 1983: Reconnaissance Report. R. E. Scholl and J. L. Stratta, EERI.

Miranda, E. (1991). Seismic evaluation and upgrading of existing buildings. Doctoral Dissertation, University of California, Berkeley.

Miranda, E., H. Aslani and S. Taghavi (2006). "Damage and Loss Estimation of a Nonductile RC Building - A PEER Testbed Study." 8th National Conference on Earthquake Engineering.

Miranda, E. and V. V. Bertero (1996). "Seismic Performance of an Instrumented Ten-Storey Reinforced Concrete Building." Earthquake Engineering and Structural Dynamics 25: 1041 - 1059.

Mitchell, D., R. H. DeVall, M. Saatcioglu, R. Simpson, R. Tinawi and R. Tremblay (1995). "Damage to concrete structures due to the Northridge earthquake." Canadian Journal of Civil Engineering 22: 361-377.

Mitchell, D. and R. Tinawi (1992). "Structural damage due to the April 22, 1991, Costa Rican earthquake." Canadian Journal of Civil Engineering 19: 586-605.

Mitchell, D. D., Ronald H., K. Kobayashi, R. Tinawi and W. Tso (1996). "Damage to concrete structures due to the January 17, 1995, Hyogo-ken Nanbu (Kobe) earthquake " Canadian Journal of Civil Engineering 23: 757-770.

Mitra, N. and L. N. Lowes (2007). "Evaluation, calibration and verification of a reinforced concrete beam-column joint model." Journal of Structural Engineering 133(1): 105 - 120.

Mitrani-Reiser, J. (2007). An Ounce of Prevention: Probabilistic Loss Estimation for Performance Based Earthquake Engineering, Doctoral Dissertation, California Institute of Technology.

Moehle, J. (1998). "Existing Reinforced Concrete Building Construction." SEAONC Fall Seminar.

Moehle, J., D. Lehman and L. Lowes (2006). "Beam-Column Connections." New Information on the Seismic Performance of Existing Buildings, EERI Technical Seminar.

Murakami, H., Y. Ohta, Y. Kuwata and M. Koyama (2004). "Factor Analysis of Human Entrapment and Casualty Occurrence due to Dwelling Collapses in the 1995 Hanshin-Awaji Earthquake." 13th World Conference on Earthquake Engineering.

Murakami, H. O. (1992). "A simulation model to estimate human loss for occupants of collapsed buildings in an earthquake." Tenth World Conference on Earthquake Engineering.

Murphy, L. M., Ed. (1973). San Fernando, California, Earthquake of February 9, 1971. Washington DC, US Government Printing Office.

Nathe, S. K. (2000). "Public Education for Earthquake Hazards." Natural Hazards Review 1(4): 191-196.

NGDC (2007). Earthquake Data at NGDC, National Geophysical Data Center, NOAA.

Nichols, J. M. and J. E. Beavers (2003). "Development and Calibration of an Earthquake Fatality Function." Earthquake Spectra 19(3): 605 - 633.

NOAA (1972). A Study of Earthquake Losses in the San Francisco Bay Area: Data and Analysis. Boulder, U.S. Department of Commerce.

NOAA (1993). Earthquake damage, the Cape Mendocino earthquakes, April 25 and 26, 1992. Boulder, U.S. Department of Commerce.

NOAA (1993). Earthquake damage, the Landers and Big Bear earthquakes, June 28, 1992. Boulder, U.S. Department of Commerce.

Nuti, C. and I. Vanzi (2003). "To retrofit or not to retrofit." Engineering Structures 25: 701-711.

Okrent, D. (1980). "Comment on Societal Risk." Science 208(4442): 372-375.

Olson, R. (2003). "Legislative Politics and Seismic Safety: California's Early Years and the 'Field Act': 1925 - 1933." Earthquake Spectra 19(1): 111-131.

Ong, K. C. G., Y. C. Kog, C. H. Yu and A. P. V. Sreekanth (2004). "Jacketing of reinforced concrete columns subjected to axial load." Magazine of Concrete Research 56(2): 89 - 98.

Pagni, C. A. (2003). Modeling of Structural Damage of Older Reinforced Concrete Components, MSc. Thesis, University of Washington**:** 124.

Pagni, C. A. and L. N. Lowes (2006). "Fragility Functions for Older Reinforced Concrete Beam-Column Joints." Earthquake Spectra 22(1): 215-238.

Panagiotakos, T. B. and M. N. Fardis (2001). "Deformations of Reinforced Concrete Members at Yielding and Ultimate." ACI Structural Journal 98(2): 135 - 148.

Pandey, M. D., J. S. Nathwani and N. C. Lind (2006). "The derivation and calibration of the life-quality index (LQI) from economic principles." Structural Safety 28(341-360).

Pantelides, C. P., C. Clyde and L. D. Reaveley (2002). "Performance-Based Evaluation of Reinforced Concrete Building Exterior Joints for Seismic Excitation." Earthquake Spectra 18(3): 449 - 480.

Park, R. (1997). "A Static Force-Based Procedure for Seismic Assessment of Existing Reinforced Concrete Moment Resisting Frames " Bulletin of the New Zealand Society for Earthquake Engineering 30(3): 213 - 226.

Pate-Cornell, E. (1985). "Costs and Benefits of Seismic Upgrading of Some Buildings in the Boston Area." Earthquake Spectra 1(4): 721-740.

Pate-Cornell, E. (2002). "Risk and Uncertainty Analysis in Government Safety Decisions." Risk Analysis 22(3).

Pate-Cornell, M. E. (1984). "Discounting in Risk Analysis: Capital vs. Human Safety " Proceedings of Symposium on Structural Technology and Risk (Waterloo, Ontario).

Pate-Cornell, M. E. (1994). "Quantitative safety goals for risk management of industrial facilities." Structural Safety 13(3): 145-157.

Pate-Cornell, M. E. (2004). Engineering Risk Analysis (Course Materials for MS&E 250A), Stanford University.

PEER. (2006). "NGA Database " Retrieved June, 2006, from peer.berkeley.edu/nga.

PEER. (2006). "OpenSees (Open System for Earthquake Engineering Simulation)." May, 2007, from opensees.berkeley.edu.

Pincheira, J. A. (2005). "A Nonlinear Model for the Seismic Assessment of RC Columns with Short Lap Splices." US-Japan Workshop.

Pincheira, J. A., F. S. Dotiwala and J. T. D'Souza (1999). "Seismic analysis of older reinforced concrete columns." Earthquake Spectra 15(2): 245-272.

Pinto, P., R. Giannini and P. Franchin (2005). Seismic Reliability Analysis of Structures. Pavia, Italy, IUSS Press.

Poland, C. D., J. F. Silva and J. O. Malley (1983). "Observations on the Structural Damage Caused by the Coalinga Earthquake of May 2, 1983." The 1983 Coalinga, California Earthquakes. J. H. Bennett and R. W. Sherburne, Ed. Sacramento, California Department of Conservation, Division of Mines and Geology.

Porter, K., C. Cornell and J. Baker (2005). "Propagation of Uncertainties from IM to DV." Van Nuys Hotel Building Testbed Report: Exercising Seismic Performance Assessment. H. Krawinkler, Pacific Earthquake Engineering Research Center (PEER 2005/11).

Porter, K., D. Wald, T. Allen and K. Jaiswal (2007). "An Empirical Relationship Between Fatalities and Instrumental MMI." 1st International Workshop on Disaster Casualties (Kyoto, Japan).

Porter, K. A. (2007). "Fragility of Hydraulic Elevators for Use in Performance-Based Earthquake Engineering." Earthquake Spectra 23(2): 459 - 469.

Porter, K. A., J. L. Beck and R. V. Shaikhutdinov (2002). "Sensitivity of Building Loss Estimates to Major Uncertain Variables." Earthquake Spectra 18(4): 719- 743.

Porter, K. A., C. R. Scawthorn and J. L. Beck (2006). "Cost-Effectiveness of Stronger Woodframe Buildings." Earthquake Spectra 22(1): 239 - 266.

Porter, K. A., K. Shoaf and H. Seligson (2006). "Value of Injuries in the Northridge Earthquake, Technical Note." Earthquake Spectra 22(2): 553 - 563.

Rackwitz, R. (2004). "Optimal and Acceptable Technical Facilities Involving Risks." Risk Analysis 24(3): 675 - 695.

Ramirez, C. M. (2008). Building-Specific Loss Estimation Methods & Tools for Simplified Performance-Based Earthquake Engineering, Doctoral Dissertation, Stanford University.

Ramirez, C. M., A. B. Liel, J. Mitrani-Reiser, C. B. Haselton, A. D. Spear, J. Steiner, G. G. Deierlein and E. Miranda (2008). "Performance-Based Predictions of Earthquake-Induced Economic Losses in Reinforced Concrete Frame Structures." Unpublished.

Reid, S. G. (2000). "Acceptable Risk Criteria." Progress in Structural Engineering and Materials 2: 254 - 262.

Reis, E. (2007). Retrofit of Reinforced Concrete Frame Structures, Personal Communication to A. Liel on July 26, 2007.

Reis, E. (2008). Retrofit of Reinforced Concrete Frame Structures, Personal Communication to A. Liel on March 25, 2008.

Reyes, O. (1999). Modeling of Reinforced Concrete Columns with Short Lap Splices Subjected to Earthquakes, MSc. Thesis, University of Wisconsin- Madison.

Robertson, I. (2002). "RC Floor Systems." PEER Annual Meeting.

Rodriguez, M. and R. Park (1994). "Seismic Load Tests On Reinforced Concrete Columns Strengthened by Jacketing." ACI Structural Journal 91(2): 150-159.

Rubinstein, R. Y. (1981). Simulation and the Monte Carlo Method. New York, John Wiley and Sons.

Russell, S. (2001). Hospitals at Risk in Big Quakes, San Francisco Chronicle.

Sause, R. H., Kent A., S. L. Walkup, S. Pessiki and J. M. Ricles (2004). "Flexural Behavior of Concrete Columns Retrofitted with Carbon Fiber-Reinforced Polymer Jackets." ACI Structural Journal 101(5): 708 -716.

SEAONC (1955). 1952 Earthquakes of Kern County California. San Francisco, Structural Engineers Association of Northern California.

Seible, F., M. J. N. Priestley, G. A. Hegemier and D. Innamorato (1997). "Seismic Retrofit of RC Columns with Continuous Carbon Fiber Jackets." Journal of Composites for Construction 1(2): 52 - 62.

Sezen, H. and J. Moehle (2004). "Shear Strength Model for Lightly Reinforced Concrete Columns." Journal of Structural Engineering 130(11): 1692-1703.

Shiohara, H. (2001). "New Model for Shear Failure of RC Interior Beam-Column Connections." Journal of Structural Engineering 127(2): 152 - 160.

Shoaf, K. (2007). "Classifying, Quantifying and Valuing Injuries in Disaster." 1st International Workshop on Disaster Casualties (Kyoto, Japan).

Shoaf, K., H. Seligson, M. Ramirez and M. Kano (2005). "Fatality Model for Non-Ductile Concrete Frame Structures Developed From Golcuk Population Survey Data." Van Nuys Hotel Building Test Bed Report: Exercising Seismic Performance Assessment. H. Krawinkler, Ed. PEER 2005/11.

Shoaf, K. I., H. A. Seligson and S. J. Rottman (2006). "Hazard Risk Assessment for Earthquakes from a Public Health Perspective." 8th National Conference on Earthquake Engineering.

Smyth, A. W., G. Altay, G. Deodatis, M. Erdik, G. Franco, P. Gulkan, H. Kunreuther, H. Lus, E. Mete, N. Seeter and O. Yuzugullu (2004). "Probabilistic Benefit-Cost Analysis for Earthquake Damage Mitigation: Evaluating Measures for Apartment Houses in Turkey." Earthquake Spectra 20(1): 171-203.

Stanford University (2002). Seismic Performance Guidelines.

Steinbrugge, K. F., W. K. Cloud and N. H. Scott (1970). The Santa Rosa, California Earthquakes of October 1, 1969. Washington, D.C., U.S. Department of Commerce.

Steinbrugge, K. F. and D. F. Moran (1954). "An Engineering Study of the Southern California Earthquake of July 21, 1952 and Its Aftershocks." Bulletin of the Seismological Society of America 44(2B): 199-462.

Steinbrugge, K. V., E. E. Schader and D. F. Moran (1975). "Building Damage in San Fernando Valley." San Fernando, California, Earthquake of 9 February 1971. G. B. Oakeshot, Ed. Sacramento, California Department of Conservation, Division of Mines and Geology.

Stevens, N. J., S. M. Uzumeri and M. P. Collins (2001). "Reinforced Concrete Subjected to Reversed Cyclic Shear." ACI Structural Journal 88(2): 135-146.

Stewart, J. P., Y. Choi and R. W. Graves (2005). Empirical Characterization of Site Conditions of Strong Ground Motion Pacific Earthquake Engineering Research Center 2005/01 (In Preparation), University of California at Berkeley.

Stojanovski, P. and W. Dong (1994). "Simulation Model for Earthquake Casualty Estimation." 5th National Conference on Earthquake Engineering.

Su, N. (2001). "Structural Evaluations of Reinforced Concrete Buildings Damaged by Chi-Chi Earthquake in Taiwan." Practice Periodical on Structural Design and Construction 6(3): 119 - 128.

Tabata, N., N. Takai and S. Okada (2004). "Casualty Estimation Model Based on the Mechanisms of Human Injury in Damaged Buildings." 13th World Conference on Earthquake Engineering

Thiel, C. C., F. J. Willsea and J. P. Singh (1991). Breaking the Pattern: a research and development plan to improve seismic retrofit practices for government buildings, California Seismic Safety Commission.

Tien, Y.-M., D.-S. Juang, C.-H. Pai, C.-P. Hisao and C.-J. Chen (2002). "Statistical Analyses of Relation Between Mortality and Building Type in the 1999 Chi-Chi Earthquake." Journal of the Chinese Institute of Engineers 25(5): 577-590.

Tothong, P. and C. A. Cornell (2006). "An Empirical Ground Motion Attenuation Relation for Inelastic Spectral Displacement." Bulletin of the Seismological Society of America 96(6): 2146- 2164.

Tothong, P., C. A. Cornell and J. W. Baker (2007). "Explicity directivity-pulse inclusion in probabilistic seismic hazard analysis." Earthquake Spectra 23(4): 867-891.

Tsai, Y.-B., T.-M. Yu, H.-L. Chao and C.-P. Lee (2001). "Spatial Distribution and Age Dependence of Human-Fatality Rates from the Chi-Chi, Taiwan, Earthquake of 21 September 1999." Bulletin of the Seismological Society of America 91(5): 1298 - 1309.

Turner, F. (2006). "Unreinforced Masonry Building Collapse Mitigation in California." 8th National Conference on Earthquake Engineering.

U.S. General Services Administration (2005). Facilities Standards for the Public Building Service. Washington D.C., GSA.

USGS. (2006). "Damage Photos." Retrieved Aug. 2007, from www.usgs.gov.

USGS. (2008). "Historic United States Earthquakes." Retrieved Mar. 2008, from http://earthquake.usgs.gov/regional/states/historical_state.php.

Val, D., F. Bljuger and D. Yankelevsky (1997). "Reliability Evaluation in Nonlinear Analysis of Reinforced Concrete Structures." Structural Safety 19(2): 203 - 217.

Vamvatsikos, D. and C. A. Cornell (2002). "Incremental Dynamic Analysis." Earthquake Engineering and Structural Dynamics 31: 491-514.

Vecchio, F. J. and M. P. Collins (1986). "Modified Compression-Field Theory for Reinforced Concrete Elements Subjected to Shear." ACI Journal 83(2): 219-231.

Waier, P. R., Ed. (2005). Building Construction Costs Data 2006. Kingston, RS Means Company.

Wood, S. L., R. Stark and S. A. Greer (1990). "Collapse of Eight-Story RC Building during 1985 Chile Earthquake." Journal of Structural Engineering 177(2): 600- 619.

Wosser, T. D., D. E. Campi, M. A. Fovinci and W. H. Smith (1982). "Damage to Engineered Structures in California." The Imperial Valley, California, Earthquake of October 15, 1979. Ed. Washington, D.C., US GPO.

Xiao, Y. and H. Wu (2003). "Retrofit of Reinforced Concrete Columns Using Partially Stiffened Steel Jackets." Journal of Structural Engineering 129(6): 725 - 732.

Yeo, G. and C. Cornell (2003). "Building-specific Seismic Fatality Estimation Methodology " Ninth International Conference on Applications of Statistics and Probability in Civil Engineering (ICASP9).

Youssef, N. (1995). "Behavior Characteristics of Reinforced Concrete Structures in Northridge Earthquake, California 1994." ASCE Structures Congress.

Zareian, F. (2006). Simplified Performance-Based Earthquake Engineering, Doctoral Dissertation, Stanford University.

Zareian, F. and H. Krawinkler (2007). "Assessmnet of probability of collapse and design for collapse safety." Earthquake Engineering and Structural Dynamics 36: 1901 - 1914.

Zhang, J. and B. Ellingwood (1995). "Effects of Uncertain Material Properties on Structural Stability." Journal of Structural Engineering 121(4): 705 - 716.

Zhu, L., K. J. Elwood and T. Haukaas (2007). "Classification and Seismic Safety Evaluation of Existing Reinforced Concrete Columns." Journal of Structural Engineering 133(9): 1316-1330.